Romanian Journal of
MINERAL DEPOSITS

continuation of

VOL. 85
No. 1

CONTENT

SUBVOLCANIC INTRUSIONS WITH REGARD TO SOME NEOGENE MAGMATITES OF METALIFERI MTS. – ROMANIA

Radu JUDE

University of Bucharest, Faculty of Geology and Geophysics, Department of Mineralogy

Abstract The paper deals with the characteristic features of subvolcanic intrusions necessary to distinguish them from hypabyssic facies or relatively to the volcanic rocks. The examples concern especially three interesting Neogene subvolcanic structures from the "Golden Quadrangle" of the Metaliferi Mts. A special attention is given to the connected eruptive breccias and related mineral deposits; some subvolcanic bodies carry "porphyry copper ore" (Roşia Poieni), others epithermal Au, Ag ± Te ore veins (Săcărâmb, Baia de Arieş), with theirs specific hydrothermal alterations. Some ideas on the mechanism of genesis of the collapse breccias suggest analogy to the collapse of underground working (Baia de Arieş).

Key words: Neogene magmatites, subvolcanic intrusions; hypabyssic facies, eruptive breccias; mineral deposits.

1. Introduction

In the last century of the geologic and geochemical researches, as well as the exploration practices reveal new and interesting data concerning the Alpine magmatites of Romania, inclusively about the related igneous intrusions.

At the Liverpool Symposium, devoted to "Mechanism of the Igneous Intrusions", Rast (1970) distinguishes five categories of igneous intrusions according to the depth of their position: 1 – Inner crater side (partially intrusive and partially as extrusive cupolas of viscous magma and necks). 2 – Intruded into volcanites (sills, stocks and complex networks). 3 – Subvolcanic intrusions (sills, dikes, stocks etc.). 4 – Hypabyssic intrusions (frequently dikes, sills, laccoliths especially in regions devoid of volcanic activity or where the volcanic products are insignificant). 5 – Plutonic intrusions (lopolyths, stocks, great sills and batholiths).

The present paper deals with the subvolcanic intrusions in order to distinguish them from the plutonic and volcanic rocks, a problem of petrologic significance and, on the other hand, of practical interest in the geological exploration.

The **subvolcanic intrusion** is a magmatic body, frequently of tens to hundreds meters, rarely exceeding these dimensions, situated in a volcanic environment, near surface, up to more than 2 km depth.

The subvolcanic facies distinguishes from volcanic one by the presence of hornblende, biotite and, eventually, hypersthene stable at high pressure of gases (volatiles) and by lacking of glass in the groundmass of the porphyritic structure of the magmatic rocks (Rittmann, 1973, p. 169). Frequently, the subvolcanic bodies have an andesitic and dacitic composition, which pass to microdioritic varieties, often propylitized in the mineralized terranes.

Generally, the subvolcanic intrusions mark the cease of the volcanic activity. The field evidences reveal that the subvolcanic bodies and related mineralizations are subsequent to the volcanic products. The radiometric data point out differences up to 1 Ma. The subvolcanic intrusions come from the resurgence of magmas in a postvolcanic or postcalderian state of evolution. The exsolved vapors from the rising magmas promote the genesis of varied kind of eruptive breccias, as stockworks, collapse breccias, breccia pipes etc. (Norton, Cathles, 1973).

Mechanical ($P\Delta V$) energy involved in the formation of these breccias is released from hydrous magmas, in subvolcanic environment, by second boiling and subsequent decompression. This energy, according to Burnham, is dependent of some parameters, as: depth of emplacement of the magma bodies (2-3 km), $Pt = 0.6$ Kb, tensile strength of the wall rocks (3.77×10^{10} ergs.kg) etc., but the mass fraction of H_2O in the initial melt (2.7 %) is regarded as the most important factor in the formation of the breccia bodies, in typical porphyry system (Burnham, 1985, p. 1515).

Some examples of subvolcanic intrusions and related ore deposits may be mentioned in the areas of the Neogene magmatism from the Eastern Carpathians (Oaş, Gutâi, Călimani-Gurghiu, etc.) as well as in South Apuseni Mountains (S.A.M.).

The **hypabyssic intrusions** mark the transition zone between the plutonic and shallow level subvolcanic facies of magmatic rocks, estimated at 1.5 and 3, even 5 km below surface (Smirnov, 1976, p. 81). Often at this domain, the magmatic rocks occur as a complex – multistage intrusions, characterized by a porphyritic holocrystalline medium to micrograined structure of the groundmass. An evolved contact

aureole is also characteristic to the hypabyssic domain of intrusion. The cupola cover may be partially or complete preserved.

2. Examples of subvolcanic intrusions from South Apuseni Mountains

In the S.A.M. – Metaliferi Mts. – the principal volcanic events, regarded in the geotectonic framework and according to the radiometric data (Roşu et al. 2004), cover the interval between Badenian and Pannonian. The volcanic products: dacites – rhyodacites, quartz-andesites, andesites, even basalt-andesites (Detunata) and related intrusive bodies, belong to the calc-alkaline series of rocks, with some affinity to the adakite type (Roşu et al. 2004).

Varied types of eruptive breccias accompany the subvolcanic intrusions: Deva, Baia de Arieş, Troiţa, Brad, Măgura Ţebei – Caraci etc. They constitute an excellent medium to focus the hydrothermal solutions and to concentrate the ore minerals.

Characteristic to the Neogene metallogenesis from the Metaliferi Mts. there are the epithermal Au-Ag-Te mineralizations, subordinate base metals sulfide ores. Modern geologic and geophysical investigations reveal the presence of the "porphyry Cu-Au type" of mineralizations, related to the Sarmatian subvolcanic intrusions (Deva, Roşia Poieni – Muşca, Troiţa – Bolcana, Brad). Important today, the Roşia Poieni porphyry copper deposit is mined in open pit.

2.1 The Roşia Poieni Structure

The Poieni volcanic edifice of amphibole andesite traverses the basement of crystalline schists and Cretaceous sedimentary cover. This former structure is pierced by Fundoia subvolcanic intrusion of andesites and porphyry – microdiorites, the host of the "porphyry mineralization". This may be seen as an example of "inner crater intrusion".

2.2 Săcărâmb volcano-subvolcanic entity

Previous opinions on the Săcărâmb volcanic architecture are due to Palfy (1912); Ghiţulescu and Socolescu (1941); Rădulescu (1956); Jude (1962, unpublished data) and Udubaşa et al. (1992).

It represents the southern corner of the "Golden Quadrangle" of the Metaliferi Mts. and is composed by a group of Sarmatian volcanic edifices of hornblende adesite (Calvaria), quartz-hornblende, biotite-andesites (Haitău, Frăsinata, Sarcău, Gurguiata) and quartz-andesites to dacites ("Zuckerhuţ" − Rădulescu, 1956) accompanied by subvolcanic intrusions (Jude, 1962, unpublished data); Scarce monoclinic pyroxenes occur in some volcanites. The disposition of the Frăsinata, Haităul Mare and Haităul Mic seem to describe a segment of crater rim in the terrain morphology.

In this idea, the Haitău subvolcanic body may represent an "inner crater intrusion". There is a quartz-andesite to dacite with phenocryst of quartz, andesine, hornblende and biotite within a micrograined felsitic groundmass; apatite and Fe, Ti oxides, as accessory minerals.

The subvolcanic body traverses a tectonized basement of Paleozoic crystalline schists with theirs Tertiary sedimentary cover (Fig. 1). The effect of thermal metamorphism over the wall rocks may be recognized as a band of brown-red "hard rock" up to 10-15 cm wide in the argillitic sequences of Tertiary sedimentary formations.

Many fissures, ore veins and faults of centimeters and decimeters in width crosscut the subvolcanic body and neighbouring formations. Some of these fractures contain detritic quartz grains, fragments of crystalline schists and andesites into a fluidized sedimentary matter (mud) with an aspect of "pebble breccias" or "glauch" (a mining idiom). Two principal trends of the structural elements may be discerned: one with NW-SE direction, another NNE-SSW, the main positions, of the ore veins (Ghitulescu and Socolescu, 1942; Jude 1962, unpublished data). A pervasive, pre-ore, propylitic alteration affects almost whole Haitău subvolcanic intrusion, the host of the majority of the ore veins. Hydromicas (illite) and kaolin minerals, with relics of adularia in the wall rocks of the veins mark the argillitic alteration.

The Săcărâmb epithermal ore veins are (were) famous due to their richness in Au-Ag telluride minerals, the mineralization have many characteristics of the "low sulphidic epithermal ore deposits" (Alderton, Fallik 2000).

2.3 Caraci – Măgura Ţebei Structure

The Caraci – Măgura Ţebei volcano –subvolcanic structure near Brad town marks the western corner of the "Golden Quadrangle" (Papp, 1906). The principal volcanic phenomena produced important volumes of lava flow and pyroclastic rocks of hornblende ± pyroxene andesites that constitute the volcanic cone, with the neck in the Caraci summit (838 m).

The second stage of evolution is marked by an extrusive cupola and by subvolcanic intrusions of hornblende ± biotite quartz-andesite in the Măgura Țebei hill and Steampuri valley, accompanied by breccia pipes and stockworks. The principal breccia pipe of approx. 300 m diameter, at Emilia gallery penetrates a subvolcanic stock of quartz-andesites; there is a polymictic breccias with a matrix of "tuffisitic" matter and by a massive, more felsic rock (Jude et al. 1973, Jude, 2000) (Fig. 2).

The gold mineralization with sulphides and some tellurides constitute thin ore veins and stockworks in Măgura Țebei and Caraci hill. There is a "low sulphidic epithermal type" of gold mineralization with some features of the "high sulphidation style" for the Caraci ore veins (Fig. 2).

2.4 Baia de Arieş igneous entity

Together with the related mineral deposits, Baia de Arieş Neogene magmatites represent the NE corner of the "Golden Quadrangle" of the Metaliferi Mts. The geologic framework consist of metamorphic formations with garnet, staurolite ± cyanite micaschists, paragneisses, amphibolites, manganiferous quartzites and crystalline limestones belonging to the Precambrian, Baia de Arieş Series (Ianovici et al. 1976), in tectonic relations with epimetamorphic chlorite-sericitic schists and Cretaceous sedimentary formations. A group of Sarmatian extrusive cupolas and subvolcanic intrusions traverses a dome-like structure of metamorphic formations. There are varieties of amphibole andesites (Ambrului, Lacului andesites), amphibole, biotite quartz-andesites (Afiniş type) and amphibole, pyroxene andesites (Pleşului type). Some subvolcanic intrusions are crosscut at the principal mining horizon by Pacea gallery (507 m alt.). The limits of the magmatic bodies with the surrounding formations are marked sometimes by faults and (or) by intrusion breccias (Lacului Valley; Baia Roşie in SW part)(Fig. 3 – a).
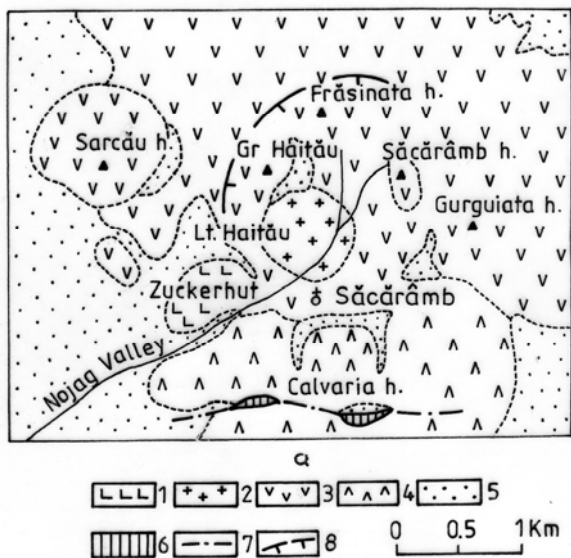
Fig. 1. a. Geologic sketch of the Săcărâmb volcanic structure, acc. to Ghiţulescu and Socolescu (1941), Rădulescu (1956) and Jude (1962, unpubl. data): 1. Zuckerhut quartz-andesite to dacite; 2. Quartz-andesite, subvolcanic intrusion; 3. Quartz-andesite, Săcărâmb type; 4. Hornblende andesite, Calvaria type; 5. Tertiary sedimentary formations; 6. Paleozoic crystalline schists; 7. Fault; 8. Segment of the hypothetical crater rim.

b. Geological section in the Săcărâmb volcano – subvolcanic structure.

c. The image of the Haitău subvolcanic intrusion at the Nicolae horizon of the Săcărâmb mine acc. to Jude (1962, unpubl. data): 1. Hornblende, biotite quartz-andesite of Haitău subvolcanic intrusion; 2. Hornblende ± pyroxene andesite of volcanic facies; 3. Tertiary sedimentary formations; 4. Paleozoic crystalline schists; 5. Ore veins; 6. Fault; 7. Stratification, position of the veins, contacts of the rocks; 8. Plunge of the beds; 9. Gallery.
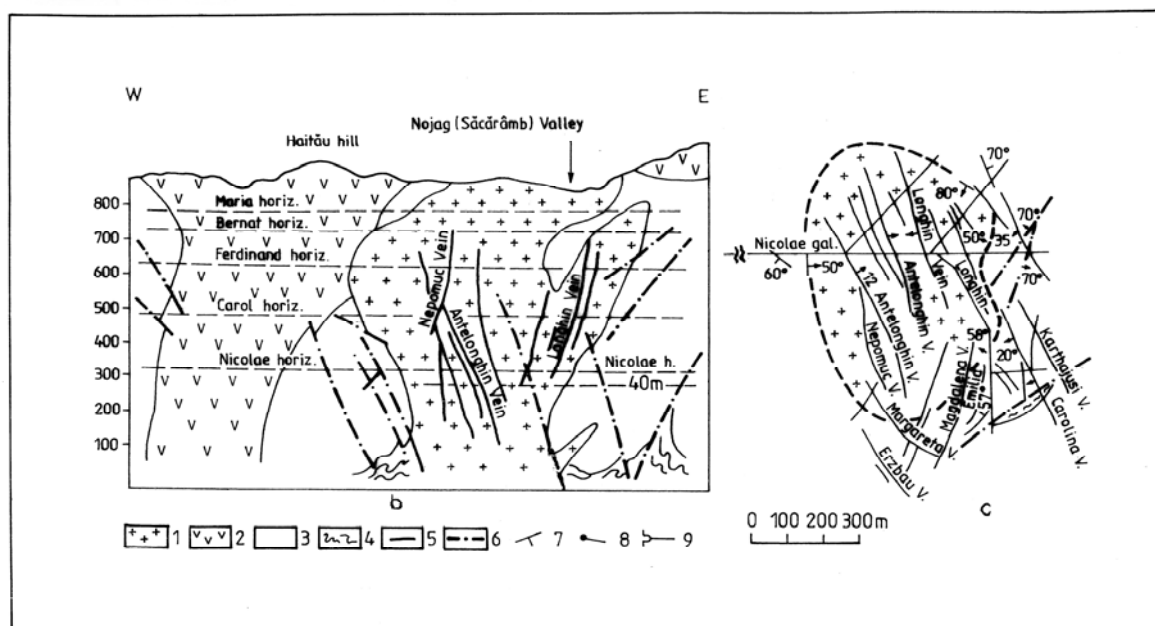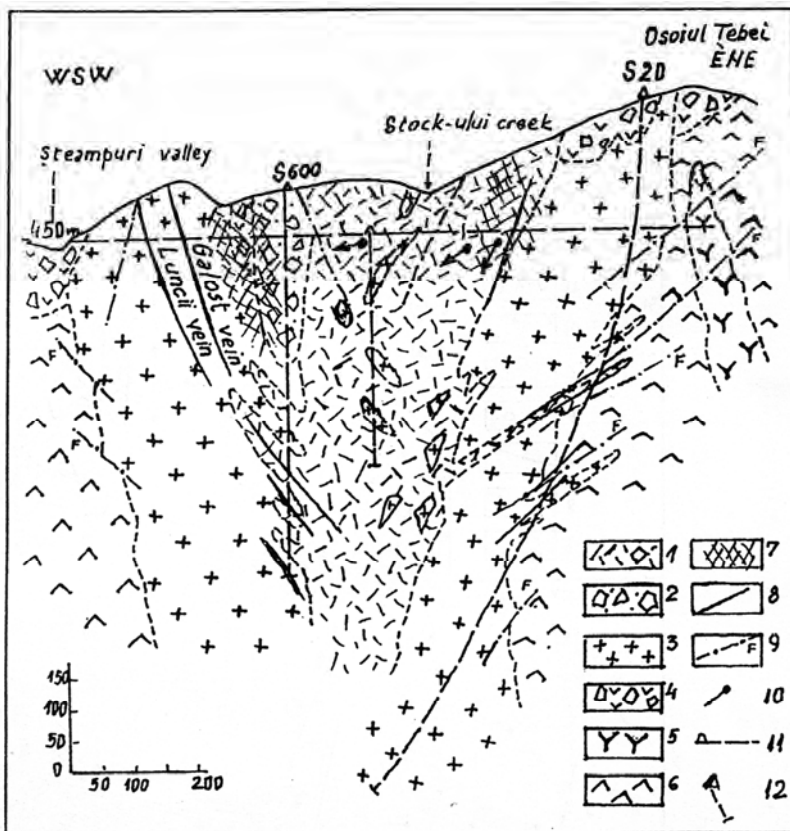
Fig.2. Geological cross section in the subvolcanic structure of Măgura Ţebei (Jude, 2000): 1. Eruptive breccias with massive – felsic matrix; 2. Eruptive brecia with polymictic matrix; 3. Quartz andesite of subvolcanic facies; 4. Pyroclastic rocks of Caraci hornblende andesite type; 5. Laramic "banatitic" intrusions of quartz-diorites; 6. Mesozoic ophiolitic rocks; 7. Stockworks; 8. Ore veins; 9. Fault; 10. Foliation of the breccia matrix; 11. Gallery; 12. Boreholes.

A remarkable feature is also the uncommon spread of eruptive breccias, with a ring disposal, that suggest their connection to a magmatic intrusion, probable of hypabyssic facies. Most of the breccia bodies are hosted by the Afiniş quartz-andesites. Enclaves of microdiorite porphyry in andesites and as deep-seated drill-hole samples are mentioned by Cioflica et al. (1999).

The Afiniş andesite consists of plagioclase, green hornblende, biotite and quartz into felsitic or micrograined groundmass; frequent apatite, zircon, magnetite, ilmenite and, occasionally garnet, occur as accessory minerals. Flow banded textures may be seen at the border of the some subvolcanic intrusions.

Ghiţulescu (1958, 1979) postulated that the "volcanic breccia pipes have been formed by the percussive blast of some punctiform volcanic eruptions, ejecting gases with volcanic ash without lavas", that preceded the hydrothermal process.

Another original hypothesis (Cochet, 1957) explains the genesis of the breccia pipes by collapse of the andesitic matter due to the withdrawal of the magma within volcanic channels (laccoliths, necks) (Fig. 3 – b).

In similar cases, Norton and Cathles (1973) say that the "pre-breccia – void was formed by magmatic water which resolved as a pluton rose to shallower depths"; the hydrous bubble was trapped for a time beneath the cooled rim in the apical region of the pluton.

Lack of the pyroclastic products of these "volcanic pipes" should be considered veritable diatribes. Some breccia pipes represent blind breccia bodies, another are opened in notable outcrops (Afiniş, Frantz) (Fig. 3 – a).

A fissured zone surrounds some breccia pipes which, if is mineralized, receives the character of the "stockwork ore bodies".

Except for the collapse breccias no. 1 – "Concordia stock" and no. 2 – "Combinat stock", the Baia de Arieş breccia pipes have a polymictic composition of neighbouring rocks: andesites, metamorphic rocks, even exotic ones as gneisses and granitic clasts from the deepest levels (Ghiţulescu et al., 1979), with various proportion of rock flour matrix. They have the characteristics of the "phreato-magmatic type" of breccia pipes (Sillitoe, 1985).

The collapse breccias, in the upper part of the no. 1 and no. 2 breccia pipes, consist of clasts of andesites of cm. and dm. size and blocks that may exceed 1 m size, devoid of matrix, into "sheet fracture boundaries" of andesite. The clasts are enveloped by mineralized dark grey silica shells and white scoria like silica crusts. These crusts of quartz and chalcedony, with a "foam structure" resulted by losing vapors and silica polymerization from the ascending hydrothermal solutions (Fig. 3 – c).

4

Fig. 3. a. Geological map of the Baia de Arieş Neogene metallogenetic field (modified from Cioflica et al., 1999): 1-4. Various types of Sarmatian andesites (1. Quartz-andesite of Pleşu; 2. Quartz-andesite of Ambru; 3. Quartz-andesite of Lacului Valley; 4. Quartz-andesite of Afiniş); 5. Crystalline limestone; 6. Precambrian crystalline schists; 7. Ore veins with sulphides ± free gold; 8. The boundary of the area with Au-Ag tellurides ± free gold ore veins; 9. Breccia pipes with gold mineralization; 10. Intrusion and tectonic breccias; 11. Non-mineralized breccia pipes; 12. Hydrothermal – metasomatic polymetallic ore bodies; 13. Fault; 14. Direction of cross section.

b. Cross section from A-A' modified from Cioflica et al (1999): 1. Poprhyry microdiorite; 2. Quartz-andesite of Lacului valley type; 3. Quartz-andesite of Afiniş type; 4. Crystalline schists; 5. Non-mineralized breccia pipe; 6. Breccia pipe with gold mineralization; 7. Mineralized collapse breccia into sheet-fracture boundary andesite (at the top of no.2 breccia pipe); 8. Ore veins; 9. Principal mining horizon, Pacea gallery; 10. Drill hole; 11, 12. Projected drill holes. BP_2; BP_4 – breccia pipes no. 2 and no.4; F_{1004} – drill hole no. 1004.

c. A clast of quartz-andesite from collapse breccia no. 1 with a zonal disposition of the gold mineralization. Simplified, from Cochet (1957). A – outer, mineralized silica shell; B, C – intermediate zones with attenuated ore grade; D – unmineralized core.

The hydrothermal metallogenesis related to the Neogene magmatism of Baia de Arieş region generated hydrothermal metasomatic concentrations of Pb, Zn, Cu and pyrite in crystalline limestones and breccias, nearby the andesitic intrusions from Ambrului hill and Lacului valley and, on the other hand, Au, Ag ± Te epithermal ore veins and breccia pipes, mainly in the Afiniş quartz-andesites (Ghiţulescu, Socolescu, 1941; Cochet, 1957; Cioflica et al. 1999).

A widespread propylitic alteration of the andesitic rocks in chlorite, calcite, albite ± epidote, actinolite facies precedes the hydrothermal metallogenesis. The neoformations of adularia, sericite, argillitic and silica minerals accompany the Au, Ag ± Te ore veins and the breccia pipes mineralisations.

Characteristic of the epithermal gold mineralization is that there are two types of mineral parageneses. The former constitutes gold bearing ore veins with sulphides and sulphosalts ± free gold in NW part of the Baia de Arieş Ore field (Noroc Nesperat, Ecaterina, Ion ore veins etc.) in dark grey quartz, calcite and rhodocrosite; the "auriferous arsenopyrite type of ore veins" (Cochet, 1957), or "the invisible gold in arsenian pyrite and arsenopyrite" (Cioflica et al. 1999). The same mineral paragenesis may be

found in the no. 1 and no. 2 – breccia pipes. An ore with low content in Ag and with a copper-rich gold is present (Cioflica et al. 1999).

The second mineral paragenesis represents the gold mineralization with tellurides (sylvanite, nagyagite, altaite etc.) Ag minerals and free gold, from SE of the Ore field; the Goldkluft, Silverkluft, Neuekluft, Sylvanit ore veins etc., that succeed the former parageneses. They belong to "low sulphidation type of epithermal gold mineralization" (ore deposits).

3. Conclusions

The above examples reveal the different mode of occurrence of the Neogene magmatic intrusions in Metaliferi Mts. The morphology of the intrusive bodies depends on the composition of the magmatic melt and, on the other hand, on the physico-mechanical characteristics of the host rocks; when intruded into plastic sedimentary formations the intermediate and felsic intrusions receive often a diapir shape (Săcărâmb, Coranda – Hondol, Roşia Montană). Nearby contact may be seen as flow band textures (Măgura Ţebei, Baia de Arieş etc.).

Often, the subvolcanic intrusions display a deuteric, preore, propylitic alteration in chlorite, calcite, albite ± epidote, zoisite facies, eventually with a fine dissemination of pyrite. In such intrusions frequently may be found crystals of accessory apatite (Săcărâmb, Măgura Ţebei, Baia de Arieş etc.). In the "porphyry systems" the alkaline, potassic metasomatosis occupy the deepest zone of the column of hydrothermal alteration; above them it follows the phyllic and/or argillitic facies (Roşia Poieni, Rovina – Brad, Bolcana – Troiţa).

The eruptive breccias connected to the subvolcanic intrusions may be formed in two or more steps, with eventually flow textures that suggests the fluidization of the breccia matter (Măgura Ţebei, Baia de Arieş). They may occur in the inner side of the subvolcanic bodies (Măgura Ţebei) or at the boundary of the magmatic intrusions. Some breccia pipes exhibit the features of the "blind" breccia pipes (Baia de Arieş). The genesis of the collapse breccias into "sheet fracture boundary" andesites (no. 1, no. 2 breccia pipes, Baia de Arieş) supposes some analogies to the collapse of the underground working.

References

Burnham C.W., 1985. Energy release in subvolcanic environment: implication for breccia formation. Economic Geology, vol. 80, p. 1515-1522

Cioflica Gr., Jude R., Udubaşa G., Istrate G., Popescu G., 1968. New contributions on the Neogene volcanic products from Băiţa-Săcărâmb region. (in Romanian) St. cerc.geol.geofiz.geogr., Geologie, t. 13, no. 1, p. 77-92, Bucharest

Cioflica Gr., Jude R., Berbeleac I., Lupulescu M., Costea D., Costea A., 1999. Epithermal gold mineralizations of low-sulphidation type from Baia de Arieş Mine, Southern Apuseni Mts., Romania. Revue Roumaine de Géologie, I. 43, p. 3-18, Bucharest

Cochet R., 1957. Geological contributions on the golden ore deposits from Baia de Arieş. (in Romanian) Rev. Minelor, 10, p. 466-475, Bucharest

Ghiţulescu P., Socolescu M., 1941. Étude géologique et minière des Monts Metallifères (Quadrilatère aurifère et régions environnantes). Anuarul Institutului Geologic al României, XXI

Ghiţulescu T.P., Pitulea G., Ghiţulescu I., 1979. Petrogenesis of the volcanic breccia pipes at Baia de Arieş (Metaliferi Mts.). Revue Roumaine de Géologie, Géophysique et de Géographie, t. 23, no. 2, p. 271-281

Jude R., Tabacu M., Inescu O., 1973. The geologic and petrographic studies of the magmatic rocks from the Neogene Caraci volcanic area (Metaliferi Mts.). Anuarul Institutului Geologic, XL, p. 7-69

Jude R., 2000. Gold mineralization with tellurides related to the Neogene volcanic edifices of Caraci – Măgura Ţebei (Metaliferi Mts. Romania). Revue Roumaine de Géologie, t. 44, p. 3-14, Bucharest

Norton D., Cathles L., 1973. Breccia pipes – products of exsolved vapor from magmas. Economic Geology, vol. 68, p. 540-546

Rast N., 1970. Origin, ascend and genesis of the magmas (in Russian), Mechanism of the Magma Intrusion. Gallery Press, Liverpool, Izd. "MIR", p. 285-310, Moskva

Rădulescu D, 1956. Geologic observations on the structure of the volcanic apparatus from Săcărâmb. (in Romanian). Analele Universităţii Bucureşti, Seria Ştiinţele Naturii, 10, p. 137-145

Roşu E., Udubaşa G., Peczkay Z., Panaiotu C., Panaiotu C., 2004. Timing of Miocene – Quaternary magmatism and metallogeny in the South Apuseni Mts., Romania. Journal of Mineral Deposits, vol. 81, p. 33-38

Smirnov V.I., 1976. Geology of Mineral Deposits, Mir. Publisher, Moskva.

Jude R., 1961. Geological prospections for gold in the Hondol, Măgura, Troiţa region (Metaliferi Mts.). (in Romanian). Geological report, "Prospecţiuni" S.A., Bucharest.

Jude R., 1962. Geological researches in the Săcărâmb Neogene volcanic area. (in Romanian). Geological report, "Prospecţiuni" S.A., Bucharest.

MODELING OF EPITHERMAL GOLD AND PORPHYRY COPPER DEPOSITS FROM METALIFERI MOUNTAINS (ROMANIA)

Gheorghe C. POPESCU, Antonela NEACŞU

Dept of Mineralogy, Faculty of Geology and Geophysics, University of Bucharest, 1, N. Bălcescu Blvd., 010041 Bucharest, ghpop@geo.edu.ro, antonela.neacsu@gmail.com

Abstract. In the last decades 14 porphyry copper systems were discovered in the Metaliferi Mountains, Romania. For explaining disseminated copper mineralization and vein gold-silver accumulations within the same metallogenic field, some metallogenic models have been elaborated.

Keywords: Apuseni Mountains, porphyry copper systems, gold content, metallogenic regeneration, paleocaldera, metallogenic model.

1. Introduction

The Metaliferi Mountains represent an anomaly of the European gold metallogeny and constitute one of the most productive gold areas in Europe and worldwide, especially due to the number of ore deposits, mined and discovered gold reserves *vs.* the surface of the metallogenic province (Popescu, 1986). According to recent estimates (Tămaş-Bădescu, 2010), this ratio exceeds 1.87 t/km^2. Based on the amount of reserves discovered through recent exploration programs carried out by private companies and on the data concerning the resources discovered by state-owned companies before 1989, the unexploited gold resources in the so called "Gold Quadrilateral" (Fig. 1) exceed 1000 t. Gold reserves that can be exploited on present-day economic circumstances are only about 305 t.
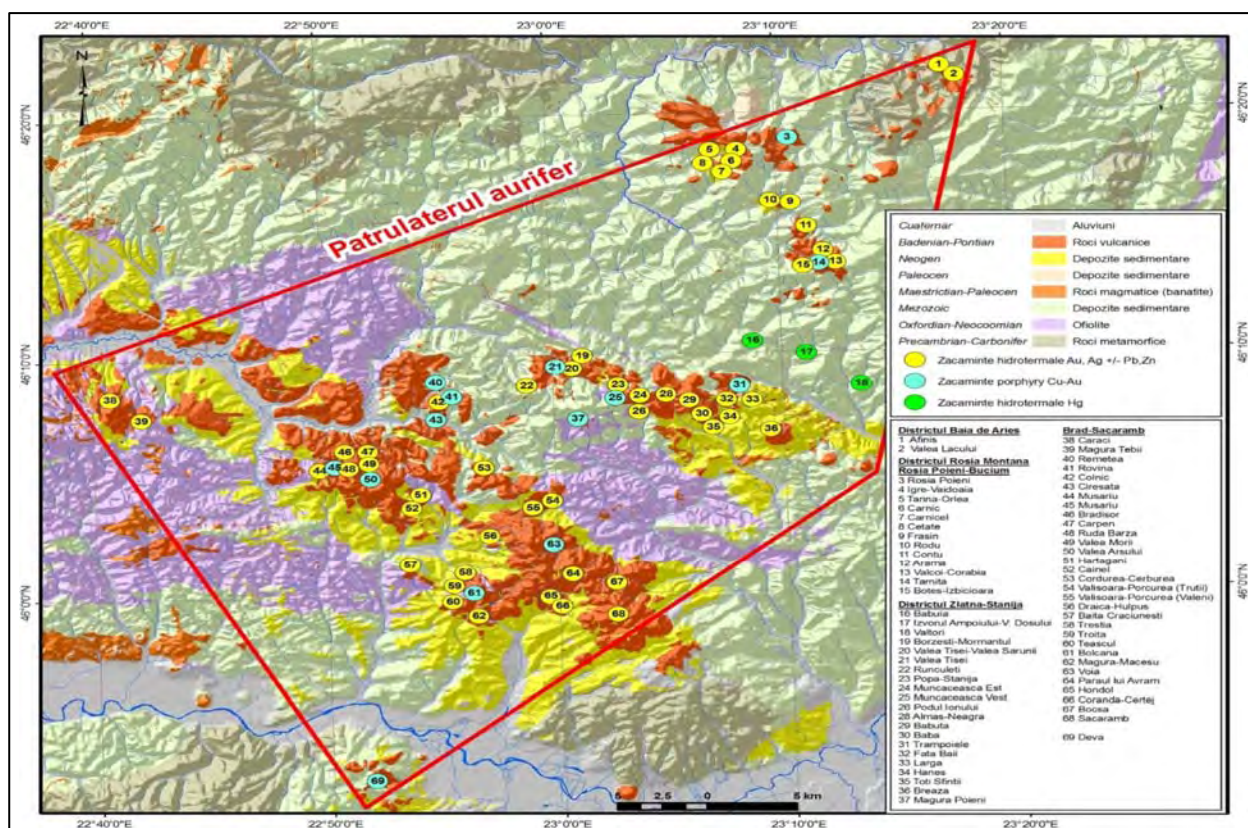

Fig. 1. Ore deposits and occurrences of mineralization in the Gold Quadrilateral, Apuseni Mountains (Tămaş-Bădescu, 2010).

The exceptional metallogenic novelty of the last decades was the discovery of 14 porphyry copper systems in the Metaliferi Mountains, Romania. As a rule, such systems are spatially associated with epithermal gold deposits, excepting the Deva ore deposit. Gold is present in porphyry copper deposits, sometimes reaching up to 1 g/t. The specificity of such deposits is the direct correlation between copper and gold contents. The Cu:Au ratio varies however, from one deposit to another.

2. The individual (singular) models

These are characteristic to the initial and classic period of gold ore deposits study in the Metaliferi Mountains. These models are related to the empirical concept in accordance with which every object has its own specificity. The most important representations of these models belong to von Inkey, von Palfy, Ghitulescu and Socolescu, Udubaşa, Berbeleac, etc, for the Săcăramb ore deposit (Fig. 2), and also Ghitulescu for the Valea Morii Nouă ore deposit (Fig. 3).
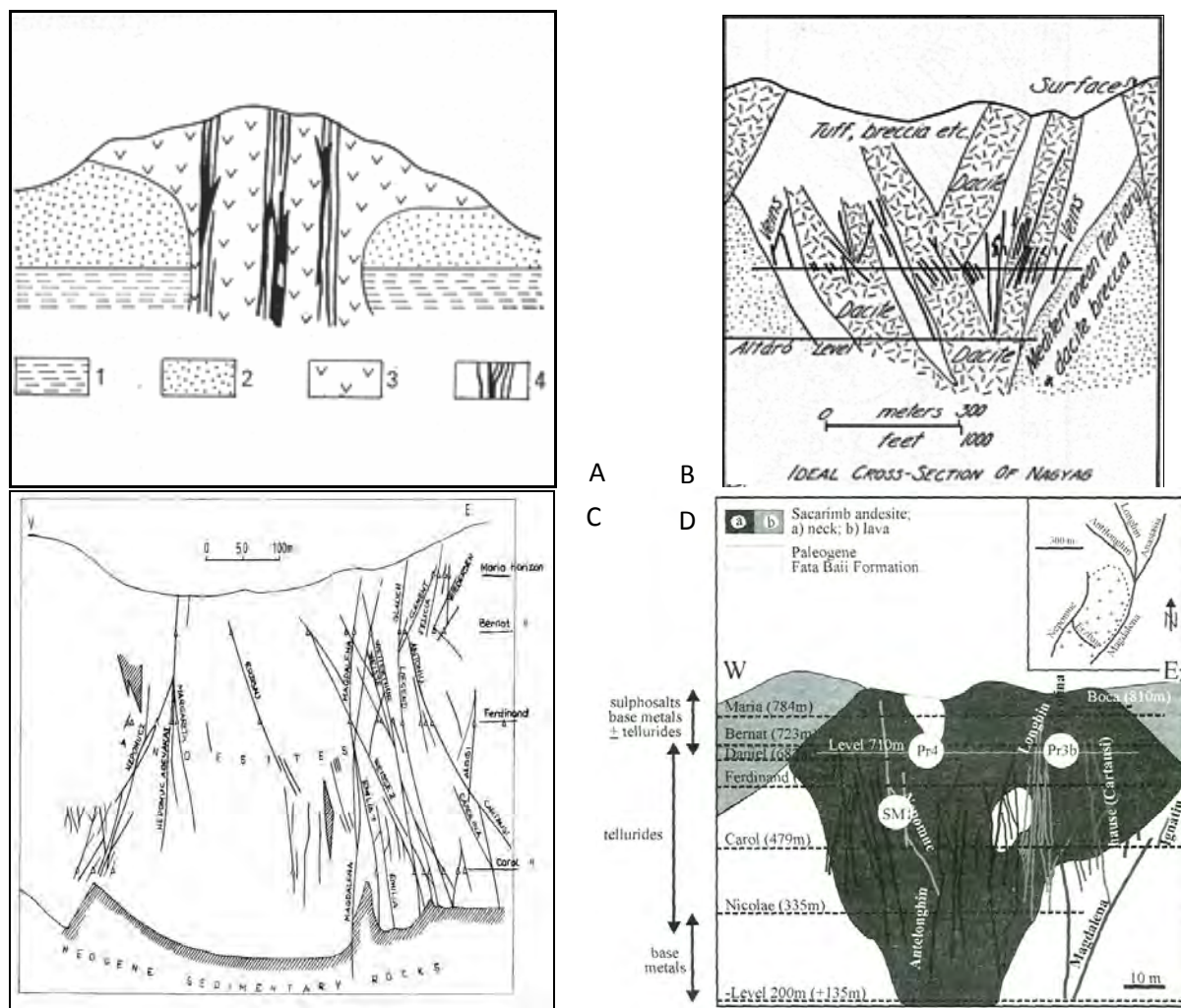

Fig. 2. Geological section through the Sacarâmb ore deposit: A) von Inkey (1883), in Smirnov, 1979; von Palfy (1907), in Emmons, 1937; C) Ghitulescu & Socolescu (1941); D) Udubasa et al., (1992) and Berbeleac et al. (1995).

2. The topogeological models

These models improve the knowledge of metallogenetic phenomenon in the Metaliferi Mts., by grouping the singular situations and creating categories of them. According to Borcos et al. (1998) the epithermal mineralized structures of the southern Apuseni Mountains are classified in the Rosia Montana type (A), with vein mineralization and breccia pipe in volcanic and sedimentary rocks and the Sacarâmb type (B), where Au-Ag-Te veins and loco base-metal mineralization are included in volcanic rocks and sedimentary siliciclastic sequences (Fig. 4).

On the other hand, Vlad & Orlandea (2004) separated two types of mineralized epithermal structures in the Apuseni Mts.: a calc-alkaline-andesitic type and a subalkaline-rhyodacite type.

Considering porphyry structures, Boştinescu (1984) mentioned two types of ore deposits through porphyry copper mineralized systems in the Metaliferi Mountains: the Deva type, related to the Lowell-Guilbert model (*e.g.*, Deva, Roşia Poieni and Bolcana) and the Tarniţa type, related to the Hollister or dioritic model (*e.g.,* Valea Tisei, Trâmpoaiele, Rovina, Musariu, Valea Morii, Voia).

Other authors (Ianovici et al., 1977, Vlad and Borcoş, 1996, Borcoş et al., 1998) related the ore deposits from the Apuseni Mountains only to the dioritic model, by separating two types: the Valea Morii

type, with a polyascendent evolution to epithermal vein halo (Valea Morii, Musariu, Bolcana, Voia, Colnic, Tălagiu, Trâmpoaiele, Muncăceasca Vest, Valea Tisei, Bucium-Tarnița), and the Roşia Poieni type, with a polyascendent evolution to pyrite halo (Fig. 5).
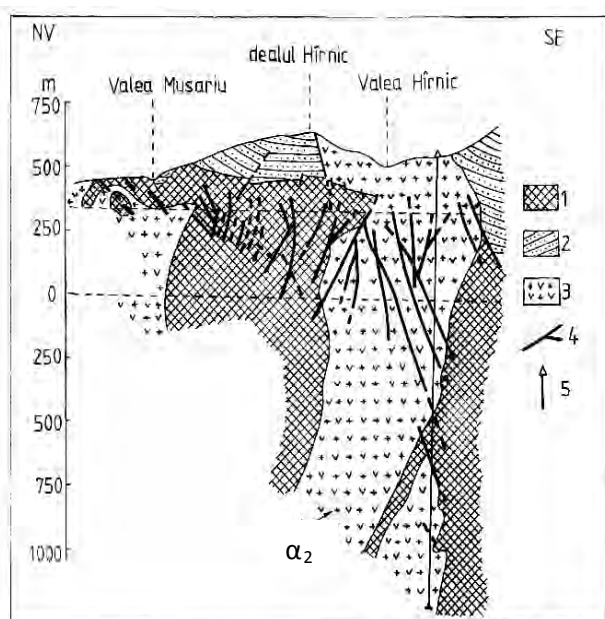

Fig. 3. Geological section through the Valea Morii Nouă ore deposit (Ghițulescu, in Ianovici et al., 1969).
1. Ophiolites ; 2. Sedimentary sequences (Badenian);
3. Andesites- Barza quartz-andesites: α1. Dealul Fetii type; α2. Barza type; 4. Faults
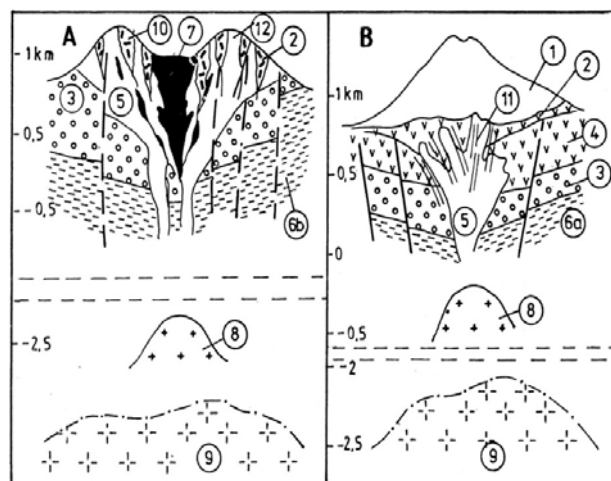
Fig. 4. Tertiary epithermal models in the South Apuseni Mts. (acc. to Borcoş and Vlad, 1997, in Borcoş et al., 1998): A. Roşia Montană Model; B. Săcărâmb Model: 1. Syn-ore palaeosurface; 2. Level of erosion; 3. Siliciclastic rocks of the Tertiary molasse; 4. Volcanic products; 5. Subvolcanic body; 6. Underlying rocks (a-Mesozoic ophiolitic and associated sedimentary rocks; b-crystalline schists and Mesozoic sedimentary rocks); 7. Phreatomagmatic explosion breccia; 8. Culmination of pluton; 9. Plutons; 10. Breccia pipe; 11. Vein; 12. Stockwork mineralization
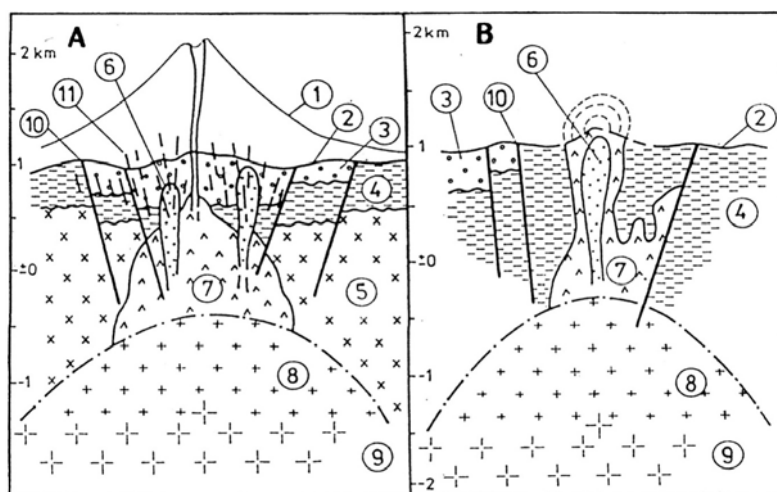

Fig. 5. Tertiary porphyry models in the South Apuseni Mts. (acc. to Vlad and Borcoş, 1996, in Borcoş et al., 1998) A. Valea Morii Model; B. Roşia Poieni Model: 1. Syn-ore palaeosurface; 2. Level of erosion; 3. Siliciclastic rocks of the Tertiary molasse; 4. Mesozoic sedimentary rocks; 5. Ophiolites; 6. Porphyry copper intrusion; 7. Composite subvolcanic structure; 8. Culmination of pluton; 9. Pluton; 10. Fracture; 11. Au-Ag and Au-Ag-Pb-Zn sets of veins.

4. The integrated models

In order to explain the presence of disseminated copper mineralization and of the gold-silver vein mineralization within the same metallogenic field – such as in the case of the mineralized structures at Brădişor, Valea Morii - Ruda, Barza, Bolcana, Troița and Trestia (Fig. 1), Popescu and Neacşu (2005) have drafted a metallogenic model which is based on the hydrothermal mineralization hypogene zoning principle (Fig. 6).

According to this model, the frequently diverse mineral content of different ore deposits is explained by remobilization of metalliferous apical zones of pre-Neogene plutons and from the gold-silver and base metal mineralization surrounding such intrusions.

A similar interpretation applies to the gold-silver metallogeny in the Metaliferi Mts., which often grades towards depth to dominant base metal and copper character, which could also result from remobilization of pre-Neogene mineralization.

A geochemical argument pleading in favor of this idea is given by Pb radiogenic isotope data (Marcoux *et al.,* 2002) from various rocks and ores in the Metaliferi Mts., suggesting higher values of the $^{206}Pb/^{204}Pb$ ratio in rocks than in hydrothermal ores. Thus, the ores are older than their host rocks and, by consequence, we deal with a metallogenetic regeneration process. Moreover, the range of $^{206}Pb/^{204}Pb$ ratios fit into that recorded for the Lower Cretaceous base-metal ores of Vorţa type. Their constant gold content may be explained by the fact that such ores represent not only the remobilization of apical copper-rich areas of pre-Neogene plutons, but also, of the later gold-silver and base metal mineralization.
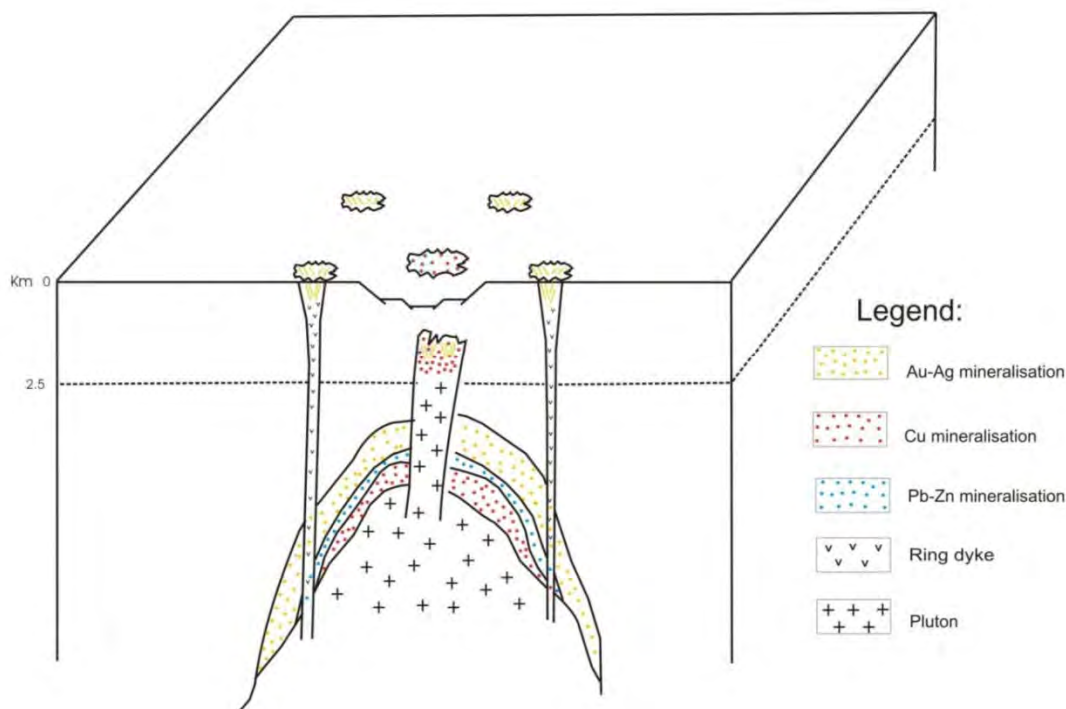

Fig. 6. The areal zoning of Au-Ag mineralization around a porphyry copper body, within a resurgent caldera structure; primary metallogenic zones around an older pluton, regenerated by Neogene hydrothermal activity, are visible in depth (Popescu and Neacşu, 2005).

However, for metallogenic units comprised of singular, heterochronous gold and porphyry copper structures – as in the case of the Roşia metallogenic sector, a different explanation should be invoked, that is one involving paleocalderas.

Popescu and Neacşu (2006) considered that in certain areas in the Southern Apuseni Mts. (Metaliferi Mts.), resurgent paleocalderas can be recognized, which functioned as complex volcanoes, probably true supervolcanoes, whose structures hosted a first event with concentric acid volcanics, followed by subvolcanic manifestations. Within such calderas, each igneous event was accompanied by a hydrothermal episode, which mobilized pre-concentrated deep mineralization.

The existence of paleocalderas in the Metaliferi Mts. was firstly mentioned by O'Connor et al. (2004), who recognized such a structure in the Roşia Montană – Bucium district (Fig. 7). This idea was further developed from a metallogenic point of view by Popescu and Neacsu (2006) in the form of a model involving a resurgent caldera, such as the one exemplified in Figure 8. According to this model, Roşia Montană and Roşia Poieni deposits belong to the same metallogenic unit.

Based on this model and in order to explain the distribution of mineralized areas in the Trestia-Măgura metallogenic node, Cioacă (2007) suggested the presence of resurgent caldera also in the Bolcana area (Fig. 1).
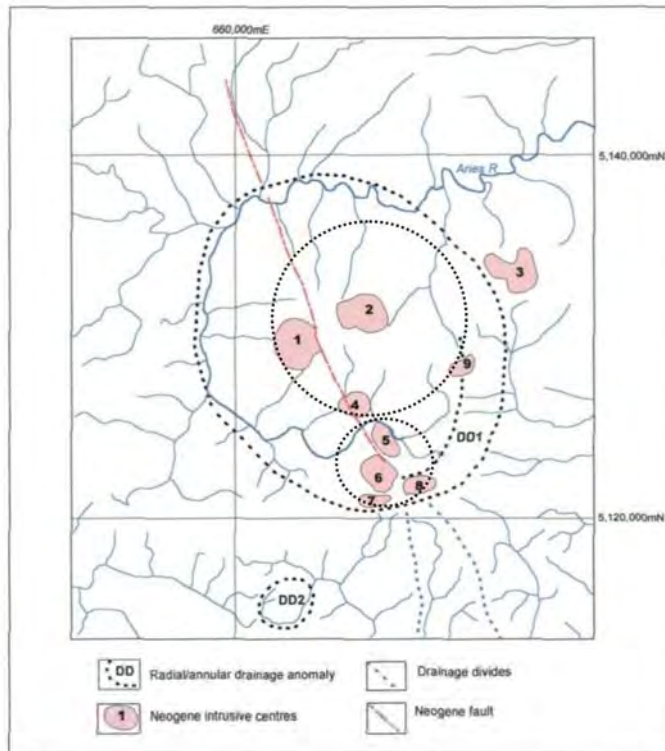
Fig. 7. Hypothetical outlining of the mineralized structures in the Roşia–Bucium district (O´Connor et al., 2004). Resurgent domes at Roşia Poieni and Bucium-Tarniţa (dotted circles) are outlined according to Popescu and Neacșu (2006), on the basis of the relationship between porphyry copper-gold-silver metallogenesis and volcanic activity: 1. Roşia Montană, 2. Roşia Poieni, 3. Baia de Arieş, 4. Rodu-Frasin, 5. Bucium-Arama, 6. Bucium-Tarniţa, 7. Boteş, 8. Vulcoi-Corabia, 9. Geamăna

Calderas and their relationship with ore deposits have been widely discussed topics in the last decades, *e.g.*, Bachman and Berganz (2008), John (2008) etc. Important scientific publications host this subject. *e.g.,* Geology, Economic Geology, Journal of Petrology, and also a special issue of Elements (v. 4, no. 1/2008), where a supervolcano with an important gold ore deposit of California is presented.
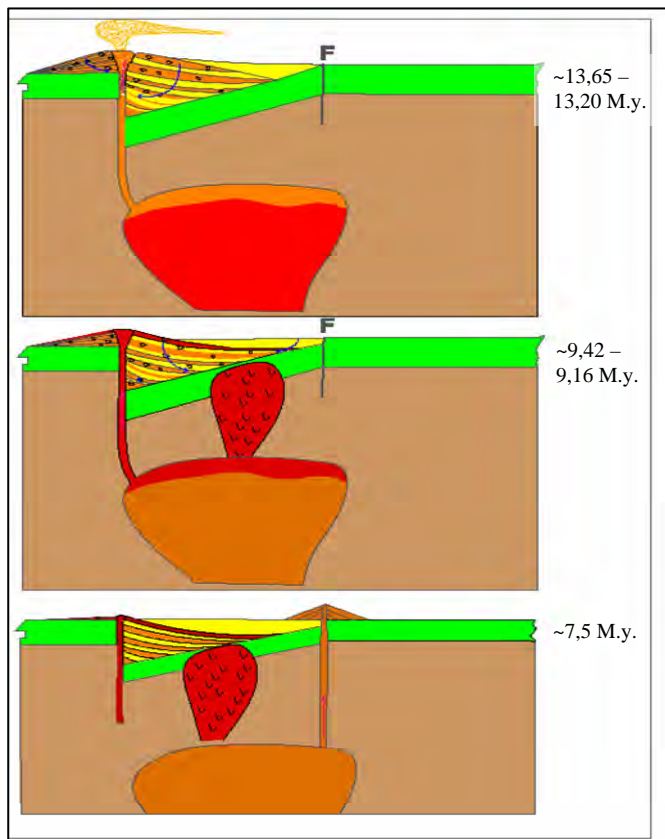
Fig. 8. The evolution of the Roşia Montană-Roşia Poieni "trap door" caldera (Popescu and Neacşu, 2008): a) the upper part of the magma chamber expands and generates an explosion only in the south-western part; magma from the deep levels of the chamber starts to rise, covering the products of the first explosion; a mixed hydrothermal fluid, with Au and Ag is formed and mineralizes the brecciated structure; b) the magma chamber segregates gravitationally – a minor volcanic and subvolcanic event is triggered and the subvolcanic areas are affected by hydrothermal alteration which generates a porphyry copper mineralization; c) magma continues to evolve towards more basic character; corresponding volcanic bodies occur in the north-eastern side of the caldera. Ages are according to Kuzmanov et al., 2007.
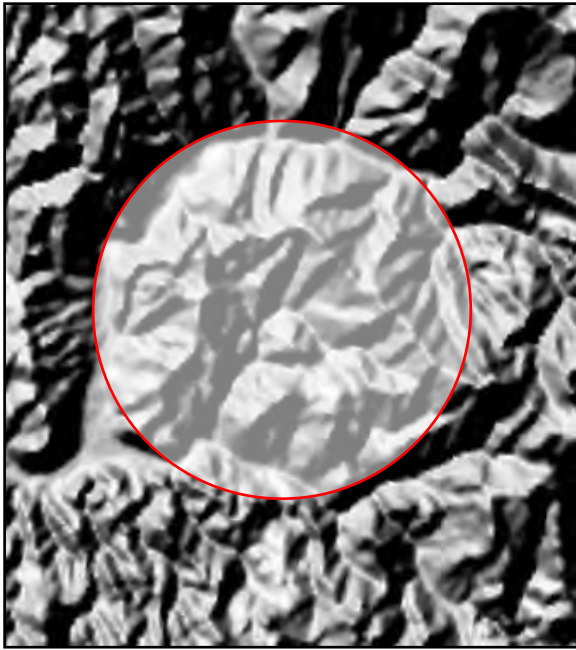
Fig. 9. Digital modeling of topographic data (DEM) in the Rovina-Colnic area, suggest a circular structure (www.edcsns17.cr.usgs.gov/) (in Tămaş-Bădescu, 2010).
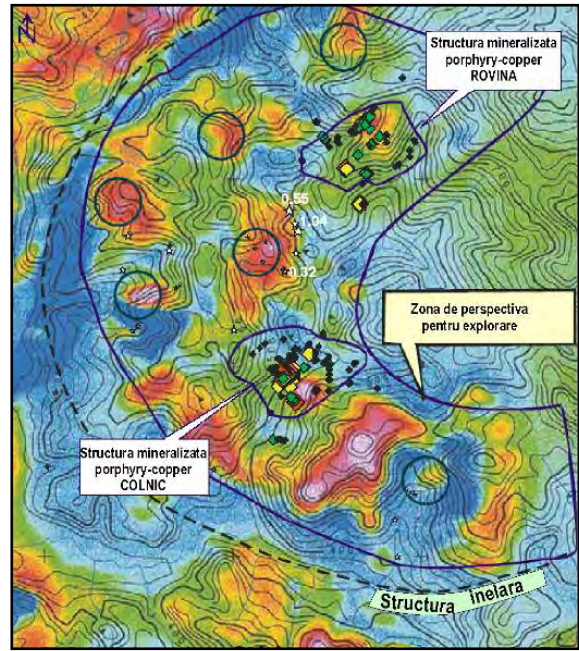
Fig. 10. Aeromagnetic map of the Rovina-Colnic area (after Carpathian Gold Inc., 2006). The image corresponds to the western rim of the supposed caldera in Fig.9.
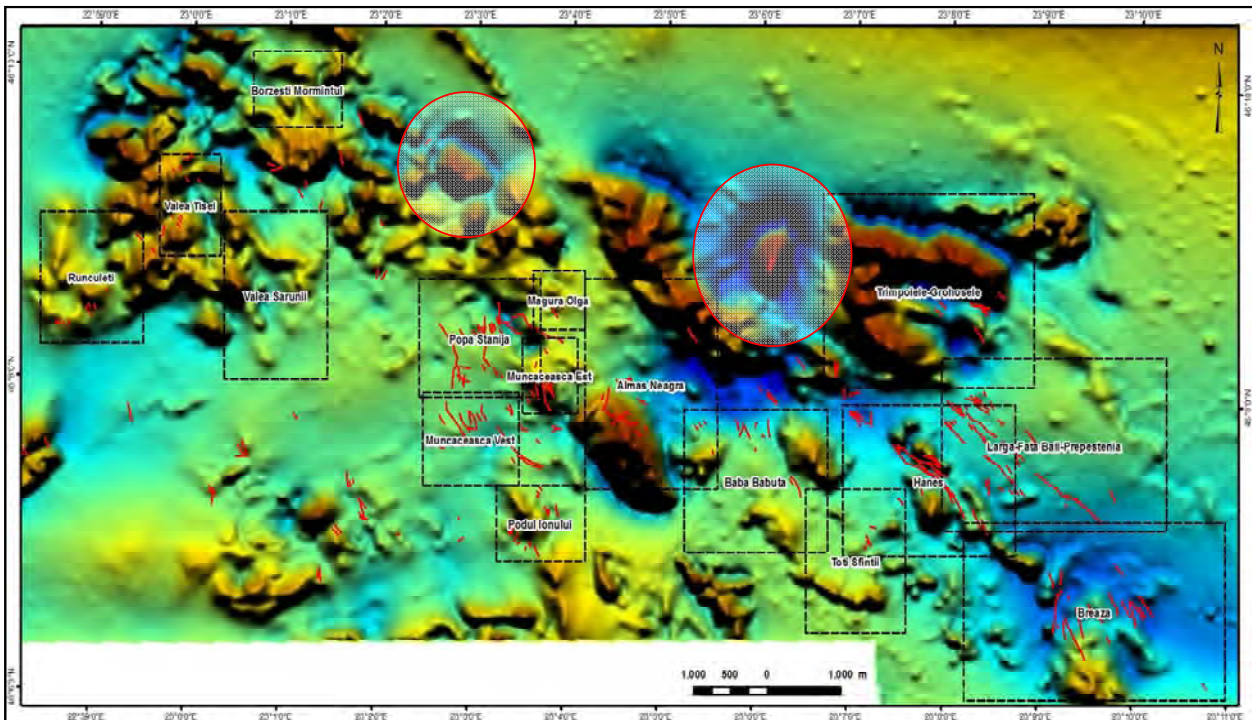
Fig. 11. Aeromagnetic map (total magnetic field) of the Zlatna-Stănija metallogenic district (after European Goldfields Ltd., 2006, with additions). Red circles indicate areas with magnetic features suggesting porphyry copper systems; red lines show vein mineralization (Tămaş-Bădescu, 2010).

The caldera model has been confirmed also by the exploration works carried out by Carpathian Gold Inc. in the Rovina-Colnic metallogenic field, in the Metaliferi Mts. A caldera-like structure was first suggested by digital processing of the topographic surface and by aeromagnetic data (Fig. 9 and Fig. 10).

Previous exploration activity in this area pointed to mineralization lacking economic significance (Ianovici et al., 1976). However, drillings executed by Carpathian Gold Inc. (2009) in the Cireşata sector have intercepted a porphyry copper system with an average 0.9 g/t Au and 0.17% Cu (Halga et al., 2010).

The aeromagnetic measurements in the Zlatna-Stănija district (Fig. 1), suggest, in their turn, the existence of porphyry copper structures outside the previously explored areas.

Figure 11 shows that along the rims of the Zlatna-Stănija district, north of the mining fields Popa-Stănija and Baba-Băbuţa, two complex anomalous magnetic areas occur (a central maximum surrounded by a marked magnetic minimum). These areas have the typical magnetic features of porphyry copper type mineralization. Thus, the porphyry copper structures in Zlatna-Stănija area are reflected in a series of complex magnetic anomalies, similar to those recorded in Rovina-Colnic.

5. Conclusions

We therefore consider that the reinterpretation of previous data concerning the geology, tectonics and metallogeny of the Metaliferi Mts. and of other areas, through new metallogenic concepts and hypotheses, modern research methods (*e.g.,* magnetic measurements, electrometry, pedo-geochemistry for comprehensive range of elements), as well as new interpretation techniques applied to exploration data, could lead to identification of new economically interesting areas within the known mineralized structures and eventually, to identification of new mineralized structures.

References
Bachmann O. and Bergantz G., 2008. The Magma Reservoirs that Feed Supereruptions. Elements, 4, 17-21.
Berbeleac I., Popa T., Ioan M., Iliescu D., Costea C., 1995. Main characteristics of Neogene-volcanic-subvolcanic structures and hosted ore deposits in Metaliferi Mts. Geol. Maced. 9, 51:60
Borcos M., Vlad S., Udubasa G. and Gabudeanu B., 1988. Qualitative and quantitative metallogenetic analysis of the ore genetic units in Romania. Romanian Journal of Mineral Deposits, Vol. 78, Special Issue.
Boştinescu S., 1984. Porphyry copper system in the South Apuseni Mountains, Romania. An. Inst. Geol. Geofiz., Vol. LXIV, p.163- 164.
Cioacă Mihaela Elena, 2007. PhD. Thesis, University of Bucharest, unpublished.
Emmons H. W., 1937. Gold Deposits of the World. McGraw-Hill Book Company, Inc. New York and London, 562.
Ghitulescu T. P. and Socolescu, M., 1941. Etude geologique et miniere des Monts Metalliferes (Quadrilatere aurifere et regions environants). An. Inst. Geol., t. 21: pp. 181-464.
Halga S., Ruff R., Stefanini Barbara, Nicolici A., 2010. The Rovina Valley project, Romania: gold – copper discoveries in a historic mining district. Rom. J. of Mineral Deposits, v. 84 Special Issue, pp. 12- 14.
Ianovici V., Borcos M., Bleahu M., Patrulius D., Lupu M., Dumitrescu R., Savu H., 1976. Geologia Muntilor Apuseni. Ed. Academiei Romane, Bucuresti, p. 631.
John D. A., 2008. Supervolcanoes and Metallic Ore Deposits, Elements, Vol.4, No. 1, p. 22.
Kuzmanov K., Wallier S., Rey R., Pettke T., Ivascanu P., Heinrich, C., 2004. Fluid processes at the porphyry to epithermal transition: Rosia Poieni copper-gold deposit, Romania. In J. Muhling et al. (Eds.), Predictive Mineral Discovery under Cover. Proceedings, SEG 2004 Conference, Perth, Western Australia, pp. 383-386.
O´Connor G. V., Nash C. R., Szentesy Cecilia, 2004. The structural setting of the Rosia Montana gold deposit, Alba, Romania", Fourth National Symposium on Economic Geology Gold in Metaliferi Mts., 3rd-5th Sept. 2004, Alba Iulia, Romania. Romanian Journal of Mineral Deposits, vol. 81, pp. 51-57.
Popescu Gh. C., 1986. Applied metallogeny and geological prognosis" (in Romanian), Part 1. Ed. Univ. of Bucharest.
Popescu Gh. C. and Neacşu Antonela, 2005. Ring zoning of the Neogene gold and copper metallogeny in the Meta-liferi Mts., Romania. Annual Meeting of GSA, SLC 2005, October 16-19, Proceedings and Abstracts, 516.
Popescu Gh. C. and Neacşu Antonela, 2007. Relationship between gold and copper metallogensis in the Metaliferi Mts., Romania", Ann. Univ. „Al. I. Cuza" Iaşi, Geologie, Tomul LIII, p. 71-78.
Tămaş–Bădescu S., 2010. PhD Thesis, University of Bucharest, unpublished.
Smirnov I., V., 1976. Geology of Mineral Deposits. Mir Publishers, Moscow, 520 p.
Udubasa G., Strusievicz R.,O., Dafin E., Verdeş Gr., 1992. Mineral Occurences in the Metaliferi Mts., Romania. Rom. J. Mineral. 75/2, 1- 35
Vlad S.N. and Borcoş M., 1996. Alpine metallogenesis of the Romanian Carpathians. In: V. Knezevic – Djordjevic, B. Kristic (eds), The formation of the geologic framework of Serbia andadjacen regions, p. 371-376.
Vlad S.N., Orlandea E. 2004. Metallogeny of the Gold Quadrilater; Style and Characteristics of Epithermal – Subvolcanic Mineralized Structures, South Apuseni Mts., Romania. Studia Geologia Babeş Bolyai Universitatis, 15-31.

REE MINERALS IN CATALÃO II, GOIAS, BRASIL

Essaid BILAL[1], Fernando Machado de MELLO[2], François SOUBIÈS[3], Moussa BOUNAKHLA[4]

1. UMR CNRS 5600 EVS-ENSMSE-Géosciences et Environnement F 42, France.bilalessaid@gmail.com
2.Universidade Federal Rural do Rio de Janeiro, Brazil (UFRRJ) - fermamll@ufrrj.br
3.IRD caixa postal 7091- Lago Sul, CEP 71619-970 Brasilia(DF), Brésil.
4. Nuclear Centre of Energies, Sciences and Nuclear Techniques (CNESTEN), B.P. 1382, R.P. 10001, Rabat, Morocco

Abstract The REE minerals pyroxenites and sövites of Catalão II show a substantial enrichment in REE from the magmatic stage. The activity of carbonate and CO_3^{2-}/PO_4^{3-} ratio have played an important role in the formation of REE-carbonate-phosphates, which are an intermediate form between REE-rich apatite and REE-rich carbonate. The magmatic enrichment in REE and Ti, favored by the presence of a carbonate phase, correlate to a high activity of CO_3^{2-} and activities of Ti and Na specially in the carbonatite. This feature explains the low enrichment in phosphate (apatite vein) in Catalão II compared to Catalão I, which is rich in apatite vein.

In the weathering stage, these minerals interact with the fluid surface and lose some of their REE and Ba. The exchange reactions between pyrochlore and ground water are generally consistent with relatively low pH, low activities of Na^+, Ca^{2+}, F^- and elevated activities of Ba^{2+} /or $Ce^{3+.}$ Significant amounts of Ba were derived from barite dissolution with some silicate contribution, whereas the Ce might come, either from dissolved REE-carbonate minerals or from the pyrochlore themselves through selective immobilisation of Ce as Ce^{4+}.

Keywords: pyrochlore, REE- carbonate phosphates, niobium, carbonatite, Brazil.

1. Introduction

The alkaline-carbonatite complex of Catalão II has been the subject of only few mineralogical studies (Machado 1983) in comparison to Catalão I, its nearest neighbor, presently under operation (Baecker, 1983, Gomes et al. 1990, Danni et al. 1991 and Pereira, 1995). This difference is probably due to the structural organization of the Catalão II complex pipes, next to the simplest Catalão I dome structure, and - until recently - to the absence of mining works on this intrusion. The surface of the bodies presents a residual metric zone with magnetite in abundant large crystals (mm-cm) and weathered white pyrochlore. However, this complex has been an attractive target for a crystallochemical study of the evolution of pyrochlore and REE-carbonate phosphate.

2. Geological setting

The Catalão II carbonatite complex (18° 02' S, 47° 52' W, 5 x 2.7 km) is located in the province of alkaline-carbonatite "Alto Paranaíba", southeast of the state of Goiás and westwards of Minas Gerais, Brazil. It outcrops at about 20 km NE of the city of Catalão, along the road connecting São Paulo and Brasilia and at 10 km NW of the better known Catalão I complex. It lies at the northern end of the tectono-magmatic lineament that controls the development of most carbonatite complexes in the region: Tapira, Araxá, Salitre, Serra Negra and Catalão I (Gomes et al. 1990). The Catalão II carbonatite complex has been dated to 83 Ma (Rb/Sr) (Machado 1983). It intrudes metasediments of the group Araxá Mesoproterozoic (Fig.1). These metasediments (quartzite, micaschists) are fenitized at the contact with intrusive bodies (sodic to potassic fenites on a south to north trend).

The structural organization of Catalão II (Fig. 1), where a tangle of veins and dykes can be divided into two "pipes" separated by a few kilometers (Machado 1983), differs from the dome of Catalão I. Geomorphic expression is also much more discreet than in the case of Catalão I: it appears only at 900-1000 m altitude, in a leveled landscape, covered by a shrub savanna (cerrado).

The most comprehensive study concerned drill-hole C3B1, located at about 175m north of the pipe). The drill first intersected several tens of meters of reddish-yellow clay soil, with frequent passages rich in agnetite. Between 30 m and 40 m, decimetric levels of red cavernous siliceous crust, with rare baryte veins. In addition, the profile becomes progressively enriched in apatite, dispersed in a yellowish-brown clay matrix.

The first not weathered carbonatite occurs only after 52 m and the completely unaltered rock at 60 m only. The six drills from 150 to 450 m (four in the northern shaft and two in the south) made by the mining company "Mineração Catalão of Goiás" and studied in great detail by Machado 1983, showed the presence of five successive magmatic facies: pyroxenites, syenites, phoscorites, carbonatites and lamprophyres.
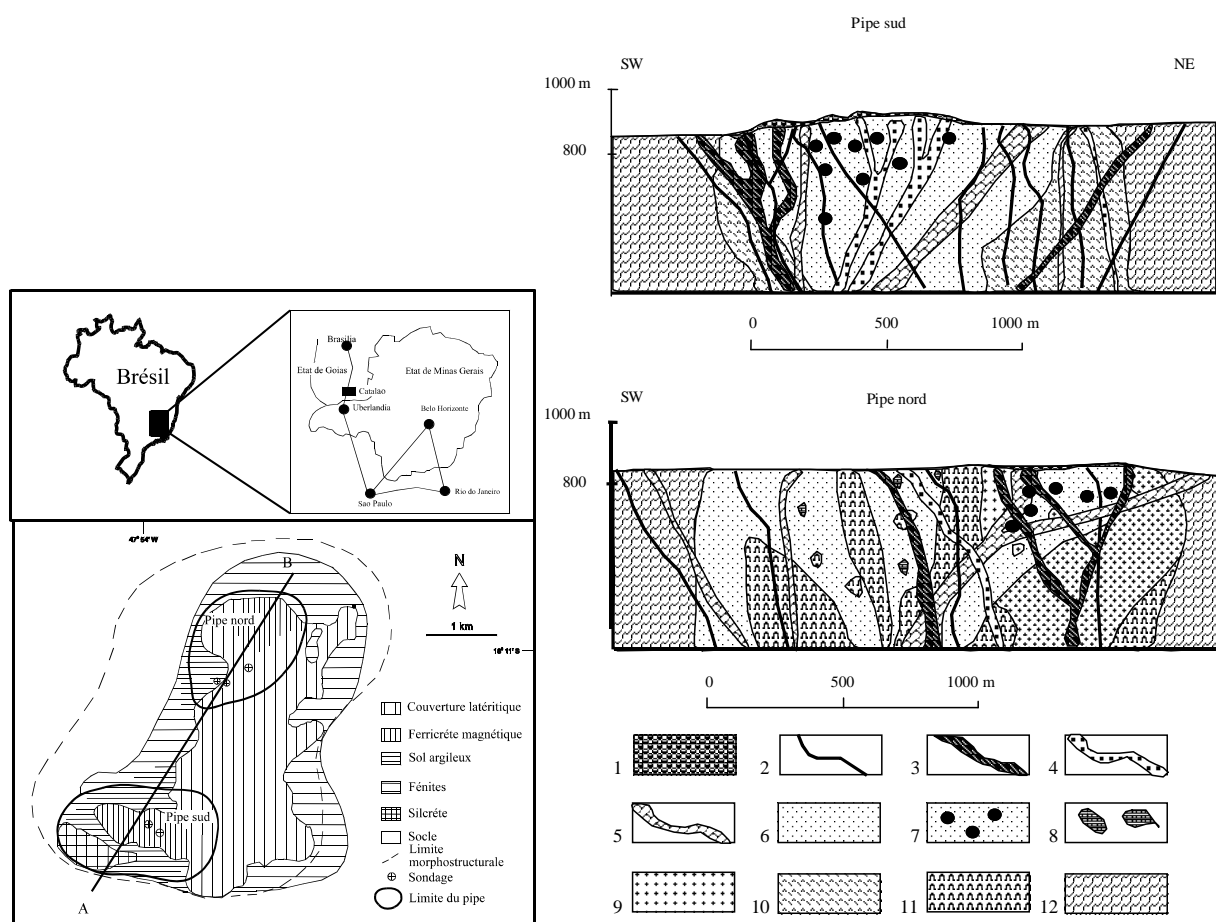
Fig. 1. The Catalão II complex localization and schematic section of the"Catalão II" Nb deposit; section drafted after drilling data and showing relationships between the different lithologic facies (Machado, 1991 and Rochas et al. 2001). 1: Blocks of residual magnetite; 2: lamprophyre dyke; 3: alvikite and béforsite dyke; 4: ankerite sövite dykes; 5: sövite; 6: silico-sövite; 7: carbonatite-rich pyrochlore; 8: phoscorite; 9: syenite; 10: altered pyroxenite glimmerite; 11: unaltered pyroxenite and 12: Mesoproterozoic host rocks (quartzite and mica schists).

3. Mineral geochemistry

3.1 Pyrochlore

The pyrochlore (in mm up to cm crystals) is associated with magnetite in carbonatites and with phlogopite, magnetite and apatite in pyroxenites. Sometimes, pyrochlore is surrounded by zirconolite, baddeleyite or columbo-tantalite. Perovskite and Nb-ilmenite surround or are included in the pyrochlore from pyroxenite or carbonatite.

The structural formula is close to the ideal formula $(Ca,Na)_2Nb_2O_6(OH, F)$. Compared to unweathered pyrochlore, structural formulas of weathered pyrochlore indicate major loss of Na, Ca, F, and major increase in Ba or Ce (Nasraoui and Bilal, 1999). These changes are correlated to an increase in the A-site vacancies and hydration, as suggested by low analytical totals (Fig. 2) Weathering involves considerable cation exchange for Ba and Ce, generating hydrated and deficient pyrochlores of B*ario* and C*erio-pyrochlore* compositions.

However, there is an unweathered rich REE pyrochlore without the A-site vacancy (Fig. 2).

The REE-rich pyrochlore associated with Ti-rich pyrochlore (Fig. 3), this association is unusual for a pyrochlore. Note that the REE plots are very similar for this phase so suggests that it is only phase but with compositional zoning in elements not including REE.

The pyrochlores from Catalão II involve coupled substitutions:

$$Na^+ + REE^{3+} = 2Ca^{2+} \qquad\qquad (1)$$
$$2Ti^{4+} + REE^{3+} = Na^+ + 2Nb^{5+} \qquad\qquad (2)$$
$$Ti^{4+} + REE^{3+} = Ca^{2+} + Nb^{5+} \qquad\qquad (3)$$
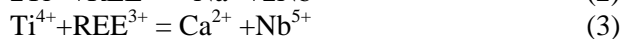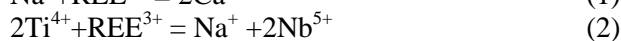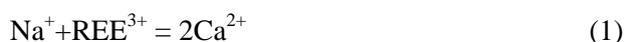
The substitutions (1) and (2) can generate REE-rich pyrochlore and the substitution (3) with Na constant is involving the Ti-rich pyrochlore.

15
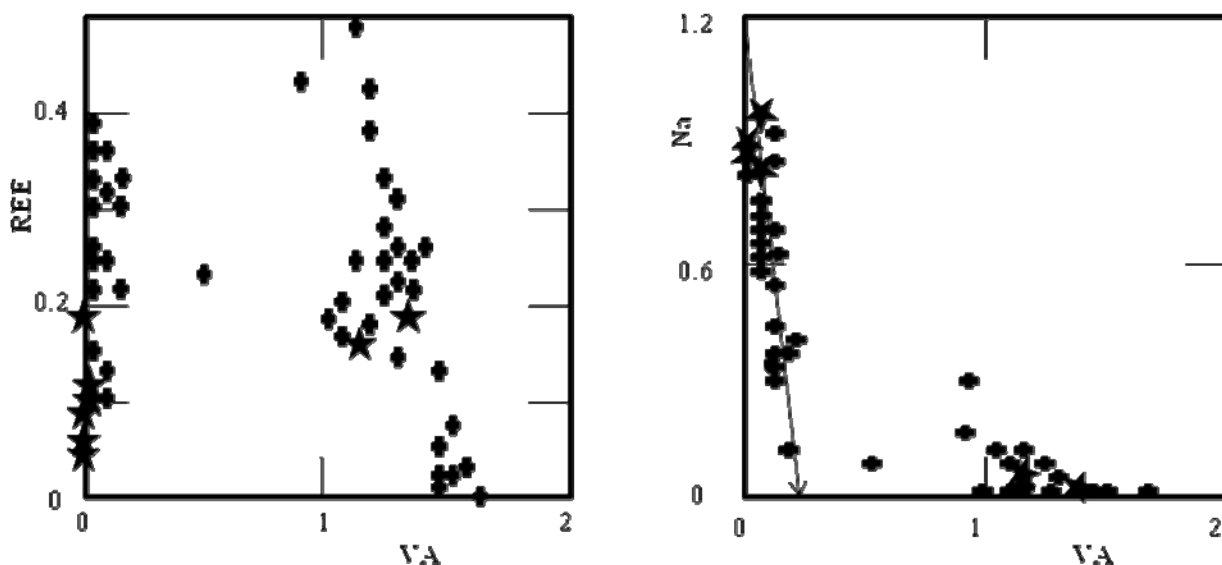
Fig. 2. Na and REE versus VA distribution in pyrochlore, in cations per unit formula. VA refers to A site vacancy.
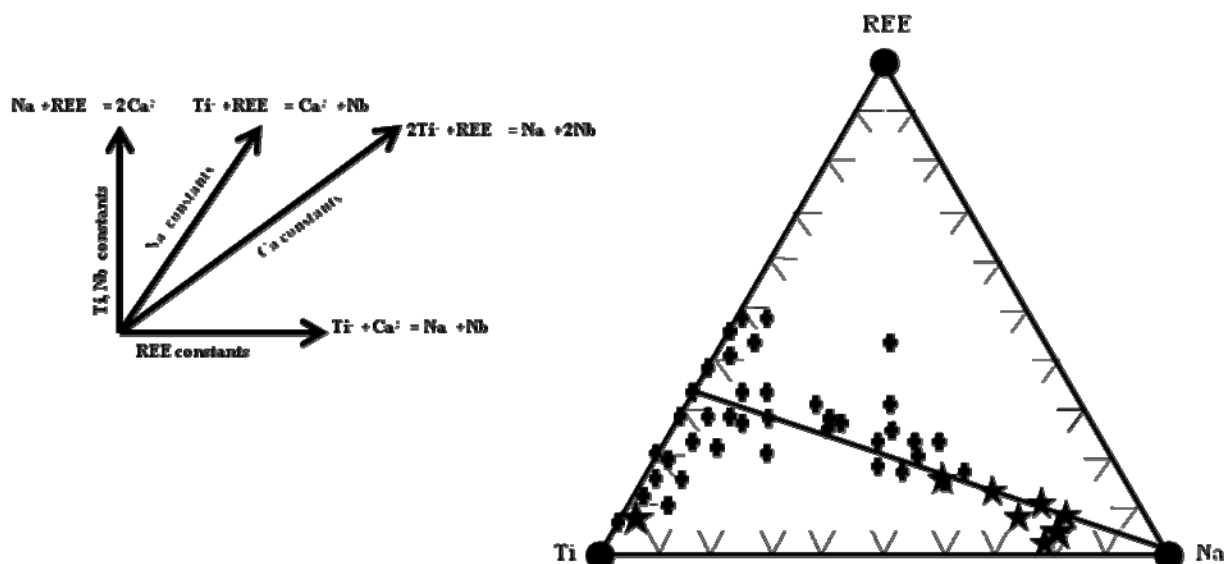
Fig. 3. Pyrochlore distribution in ternary diagram Ti-REE-Na (a/f.u.) from sövite (star) and pyroxenite (cross) of Catalão II carbonatite complex. The planar vector representation indicates different substitution mechanisms.

3.2 REE- carbonate phosphates

The infra-red (IR) study confirms the presence of carbonate ions. The peaks at 1435 cm^{-1} and 1455cm^{-1} represents the vibration of the double valence (v_3) of the C – O group and the peak at 870 cm^{-1} the vibration (v_2) of CO_3^{2-}. Elliott (1965) also showed that, compared with the free carbonate ion, the carbonate ion in apatite is distorted and although the carbonate ion of apatite type B is oriented parallel to the c axis, the carbonate ion of apatite A is approximately perpendicular to the c axis.

A site: The REEs in Ca that crystallized from H_2O bearing phosphate fluoride melts where compensated in charge by concomitant substitutions of both Si for P and Na for Ca. The distribution Nb versus Ti ions show the substitution of these two ions from the sövite. The compositional range also shows a deviation from the one recorded for pyroxenite (Fig. 4C).

B-site carbonate bearing apatite, involving replacement of the PO_4^{3-} group by CO_3^{2-} is now well established (Ivanova et al. 2001). Polarized IR studies suggested that the orientation of the CO_3^{2-} ion lies in the position of the sloping face of the replaced PO_4^{3-} tetrahedron (Elliott, 1965).

The charge compensating mechanisms have been proposed for the incorporation of CO_3^{2-} ion into the PO_4^{3-} sites:

$$CO_3^{2-} + Na^+ = PO_4^{3-} + Ca^{2+} \qquad (4)$$

$$REE^{3+} + Na^+ = 2Ca^{2+} \qquad (5)$$
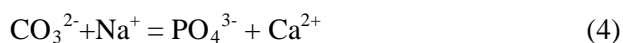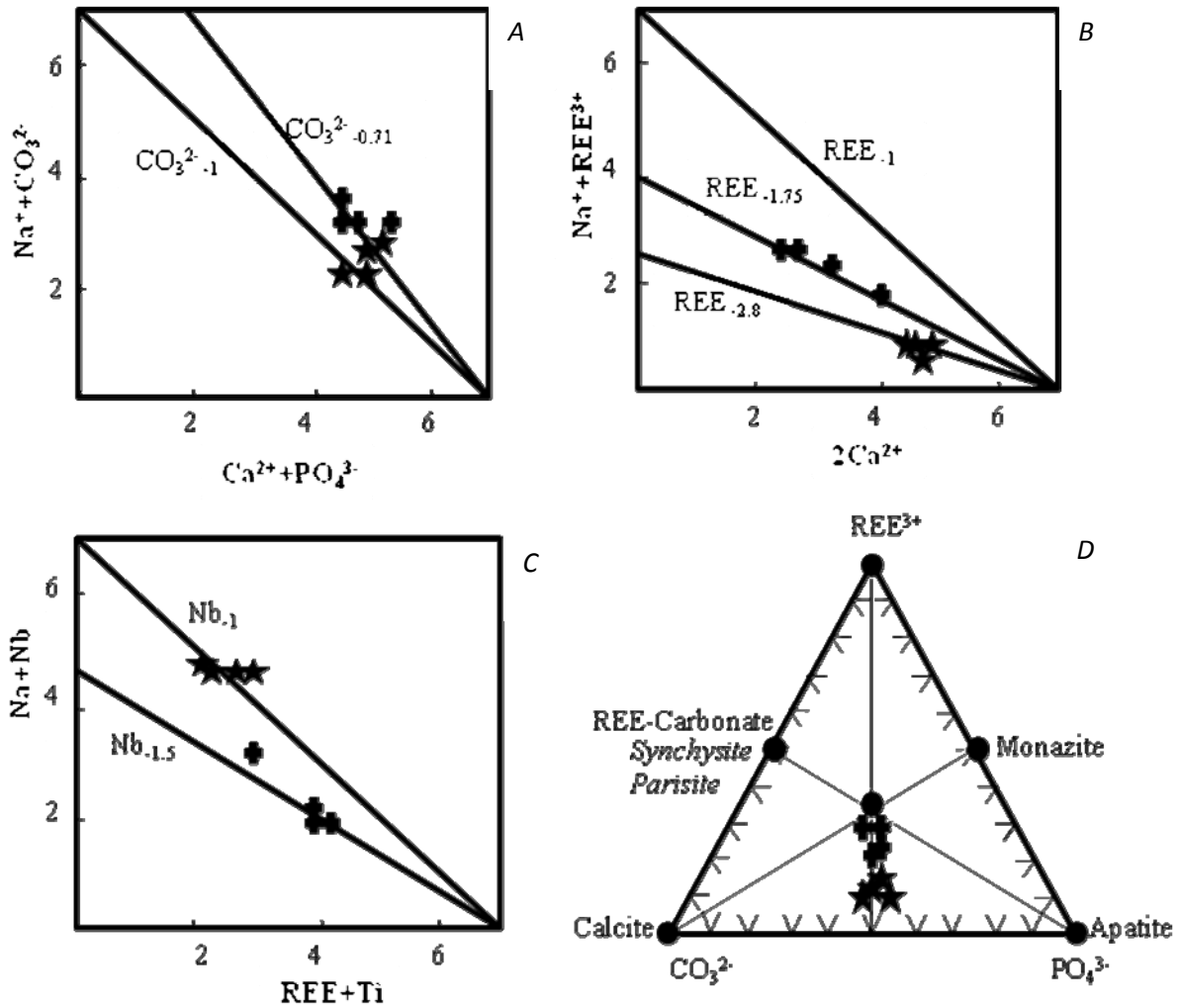
Fig. 4. Relationship between CO_3^{2-}, PO_4^{3-} and REE^{3+} and Nb-Ti in REE-carbonate-phosphate. Star symbols: sövite; cross symbols: pyroxenite.

The coupled Substitutions (4) and (5) involving simultaneous replacement of Na^+ for Ca^+ may also be proposed (Fig. 4). However, excess charge may be subsequently adjusted by CO_3OH^{3-} partly accompanied by the REE in the Ca site. The presence of F in all REE-carbonate phosphate indicated probably a substitution (6) of fluorine and carbonate.

$$CO_3^{2-} + F^- = PO_4^{3-} \qquad\qquad (6)$$

The tetravalent carbon substituted for pentavalent phosphorus and a F^- in excess has replaced one O^{2-} in structure. The substitution mechanism was found within the hydroxyapatite group (Sommerauer and Katz-Lehnert, 1985), yielding the following simplified formula:
$(Ca, Na, LREE)_{10} (F, CO_3)_x(PO_4)_{6-x}(OH, F)_2$.

4. Conclusions
We have two unaltered pyrochlore REE-rich and Ti-rich without VA vacancy site. The magmatic enrichment in REE and Ti favoured by the presence of a carbonate phase, correlate with a high activity of CO_3^{2-}, activity of Ti and activity of Na^+ specially in the carbonatite. This feature explains the low enrichment in phosphate (apatite veins) in Catalão II compared to Catalão I, which is rich in apatite veins. The activity of carbonate and ratio CO_3^{2-}/ PO_4^{3-} have played an important role in the formation of REE-carbonate phosphate, which are an intermediate form between REE-rich apatite and REE-rich carbonate.
In the weathering stage, the exchange reactions between pyrochlore and ground water are generally consistent with relatively low pH, low activities of Na^+, Ca^{2+}, F^- and elevated activities of Ba^{2+} /or of Ce^{3+}. Significant amounts of Ba derived from baryte dissolution with some silicate contribution, whereas the Ce might come, either from dissolved REE-carbonate minerals or from the pyrochlores themselves.

References

Baecker M.L., 1983. A mineralizacão de Nióbio no solo residual laterítico e a petrografía das rochas ultramáficas-alcalinas do domo de Catalão I, Goiás. *Thèse* Universidade de Brasilia (DF), Brésil, 1983, 114 p.

Danni J.C.M., Baecker M.L., Ribeiro C.C., 1991. The geology of the Catalão I carbonatite complex. In: Field Guide Book, 5th Int. Kimberlite Conf., Araxá, Brazil ; CPRM, Brasilia, Sp. Publ., 1991, pp. 25-30.

Elliott, J.e. 1965. The interpretation of the infra-red absorption spectra of some carbonate-containing apatites. In: M.V. Stack and RW. Fearnhead, Eds., Tooth enamel: Its composition, properties, and fundamental structure, p. 20-58. Wright, Bristol, U.K.

Gomes C.B., Ruberti E., Morbidelli L., 1990**.** Carbonatite complexes from Brazil: a review. J. South Amer. Earth Sc., 3-1 (1990) 51-63.

Machado D.L.,1991. Geologia e aspectos metalogenéticos do complexo alcalino-carbonatítico de Catalão II (GO). Unpublished Ph.D. Thesis, University Estadual of Campinas (SP), Brazil, 1991, 102 p..

Nasraoui, M. ; Bilal, E.1999**.** Pyrochlore of Lueshe Carbonatite complex (NE ex-Zaire) : Geochemistry memory of different alteration stages In Mineralization and alkaline magmatism. Journal of Asian Earth Science, Special Issue, 1999, 46-54

Pereira,V.P.,1995. A alteração no alcalino-carbonatitico de Catalão I (GO). Evolução mineralogica. Unpublished Ph.D. Thesis, University Federal of Rio Grande South (Brazil), 1995, 286 p.

Rocha E., Nasraoui M., Soubiès F., Bilal E., Parseval P., 2001. Evolution géochimique du pyrochlore au cours de l'altération météorique du gisement de Catalão II (Goiás, Brésil). Comptes Rendus de l'Académie des Sciences, Série II, 2001, 332(2), 91–98.

GEOLOGY AND PETROGRAPHY OF THE GOLD-RICH CIREŞATA PORPHYRY DEPOSIT, METALIFERI MOUNTAINS, ROMANIA

Randall K. RUFF*[1], Barbara STEFANINI[1], Sorin HALGA[2]

Carpathian Gold Inc.[1], SAMAX Romania SRL[2], Str. Calea Zaradului Nr. 46, 337200, Criscior, Jud. Hunedoara, Romania; rruff@carpathiangold.com , bstefanini@samax.ro , sorin@samax.ro

Abstract The gold-copper Cireşata porphyry deposit in the Metaliferi Mountains, Romania has a high gold:copper ratio with the deposit core grading 1.01 g/t gold and 0.18% copper. The Cireşata deposit is centered on a Neogene polyphase subvolcanic intrusive of porphyritic hornblende-plagioclase microdiorite. Early and late phases of this complex have similar mineralogic composition. Early-stage potassic alteration is widespread followed by a quartz-magnetite-chlorite alteration commonly associated with the ore minerals chalcopyrite and pyrite. A phyllic alteration occurs in the barren capping porphyry and locally overprints earlier potassic and magnetite-chlorite alteration.

Keywords: Metaliferi Mountains, Cireşata gold-copper porphyry deposit, alteration, lithology

1. Introduction

The Metaliferi Mountains of southwest Romania, also known as the Golden Quadrilateral mining district, is well known for its numerous epithermal and porphyry ore deposits associated with Neogene volcanics and subvolcanics. The exploration program of Carpathian Gold Inc., through its wholly owned Romanian subsidiary, SAMAX Romania SRL (SAMAX), discovered the Colnic and Cireşata gold (Au)-copper (Cu) porphyry deposits and defined a significant Au component in the previously known Rovina Cu-Au porphyry deposit. These three deposits lie in close proximity to each other along a north 20° east linear trend within the Rovina Exploration License and are collectively known as the Rovina Valley Project (RVP) (Fig. 1).

The Au grade of these porphyry deposits increases from north to south from the Rovina, Colnic, to the Cireşata deposit respectively. The RVP is presently at the Prefeasibility Study stage of development which is designing a central ore-processing plant for the three deposits.

In July 2012, SAMAX completed a Canadian National Instrument (NI) 43-101 compliant resource estimate update for the RVP based on data from 251 drill holes totaling 120,256 meters completed by SAMAX. On a consolidated basis, in the measured + indicated resource categories, this resource estimate contains 7.2 million ounces Au (224 tonnes) and 1.4 billion pounds of Cu (625,000 tonnes) within 406 million tonnes at average grade of 0.55 g/t Au and 0.16% Cu using base-case cut-off grades[1] (NI 43-101 Technical Report in-progress). Importantly, each of the three Au-Cu porphyry deposits has a higher-grade core that vectors outward toward lower grade. As an example, at the Cireşata deposit, at the higher cut-off grade of 1.0 g/t Au-equivalent[1], the measured + indicated resource includes 65 million tonnes at 1.01 g/t Au and 0.18% Cu.
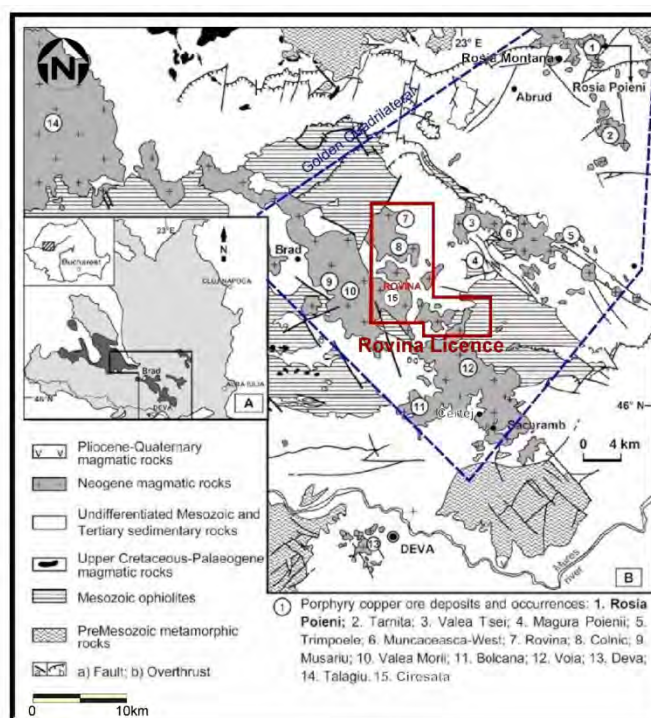

Fig. 1. Location map of the Rovina Exploration License within the Golden Quadrilateral mining district. (Modified form Milu et al., 2004).

Gold grades are locally higher in Cireşata as indicated in drill hole RGD-17 which intersected 244 meters with 1.70 g/t Au and 0.22% Cu.

The high Au grade of Cireşata makes it unique to the Golden Quadrilateral and comparable only to the Au-rich porphyry deposits of the Maricunga porphyry belt in Chile (Sillitoe, 2000). This paper presents the geology of the Cireşata deposit with emphasis on lithology and alteration.

[1] Resource estimate base case cut-off grades are 0.35 g/t Au eq. for Colnic, 0.25% Cu eq for Rovina, both of which are amenable to open-pit mining and 0.65 g/t Au eq. for the Cireşata deposit which is amenable to underground bulk mining. Gold equivalent (Au eq.) determined by using a gold price of US$1,370 per ounce and a copper price of US3.52/lb. Metallurgical recoveries are not taken into account for Au eq.

2. Geology of the Cireşata gold-copper deposit

The Cireşata Au-Cu porphyry deposit is associated with Neogene subvolcanics that intruded the middle Cretaceous "Albian Superior" siliciclastic sediments (Romania Geologic Institute, 1972). The mineralization is hosted in both a feldspar-amphibole diorite porphyry ("Early Mineral Porphyry") and in the adjacent hornfelsed siliciclastic Cretaceous sediments. Detailed core logging and observation of cross-cutting relationships of vein stockwork and intrusive contacts have identified at least three intrusive events; the Early-Mineral Porphyry (EMP), Inter-Mineral Porphyry (IMP), and the Late-Mineral Porphyry (LMP). The LMP is the last intrusive event and occurs as sub-vertical dykes, < 40 meters in width, hosting low-grade mineralization (Fig 2). The mineralization is capped by a barren litho-cap of intense phyllic-altered quartz andesite. The Au-Cu mineralization occurs as dissemination in the altered rock mass and as intensely developed quartz-magnetite-pyrite-chalcopyrite stockwork that locally comprises +80% of rock volume. The Au-Cu grades decrease from older to younger porphyry intrusive (Table 1). The lithology and alteration descriptions in this paper focus on the EMP and the LMP, representing main stage and late stage mineralization with also a description of the mineralized hornfels sediment.

Fig. 2. An E-W geology cross section through the Ciresata Au-Cu porphyry deposit.

2.1 Lithology

Descriptions of the lithology, alteration and mineralization are from detailed drill core logging, petrographic studies (including Damian, 2011), and QEMSCAN studies (section 2.3).

The EMP is the earliest and principal intrusive host rock for Au-Cu mineralization (Fig. 2). It is a hornblende-plagioclase porphyritc microdiorite with a micro-crystalline groundmass. The phenocryst assemblage consists of plagioclase, hornblende (up to 3 mm in length) and clinopyroxene. The

groundmass has a similar mineral composition as the phenocryst assemblage with rare quartz observed. The LMP is the latest mineralized intrusive with a low Au-Cu grade (Table 1) and is a hornblende-plagioclase porphyritic quartz microdiorite with an aphanitic to very-fine grained-groundmass. The phenocryst assemblage consists of plagioclase, hornblende (up to 5 mm in length) and clinopyroxene with a groundmass of similar mineral composition with the exception of a common occurrence of partly re-sorbed hexagonal quartz grains. The EMP and the LMP have a very similar mineral composition and differ principally in the intensity of alteration and mineralization.

Table 1. Average Au and Cu contents in the main lithology domains at Cireşata

Lithology unit	Avg Au ppm	Avg Cu ppm
Sediments	1.004	1957
Early Mineral porphyry (EMP)	1.146	1813
Intra Mineral porphyry (IMP)	0.877	1159
Late Mineral porphyry (LMP)	0.333	511
All lithological unit in core of the deposit (1g Au eq* envelope)		
Au eq calculated for Au price 1000USD/oz and Cu price 3USD/lb		

The Creataceous sediments (SED) are host to approximately 65% of the Au-Cu mineralization (Fig. 2 and Table 1). The SED is a very-fine grained, massive pelitic rock with increasing occurrence of bedding structures at depth consisting of fine-grained sandstone interbeds. Prior to hydrothermal alteration the SED was affected by thermal metamorphism resulting in recrystallization into a very-fine grained quartzo-feldspathic mesh + very-fine grained biotite. Locally, garnet and pyroxene are observed as part of this thermal event resulting in a hornfels. The transformation into hornfels is considered important preparation for the subsequent fracturing and stockwork mineralization.

2.2 Alteration and mineralization

The mineralization occurs as quartz-magnetite-pyrite-chalcopyrite stockwork veins and as disseminated grains in the rock mass. Alteration associated with the mineralization includes incipient biotite-potassium feldspar +/- magnetite. Amphibole is commonly observed replacing pyroxene. This is interpreted to be an early-stage potassic alteration and occurs in the EMP, SED, and weakly in the LMP. A common alteration assemblage associated with Au-Cu grades (chalcopyrite-pyrite) is quartz-magnetite-chlorite. This magnetite-chlorite alteration occurs in the EMP and in the SED and is interpreted to be associated with the main-stage mineralization. In the deeper parts of the deposit, some veins have albite alteration selvages and could represent sodic alteration.
A late-stage overprinting alteration of quartz-sericite-pyrite (Phyllic) occurs pervasively at the top of the deposit and at depth it occurs in fractures with white sericite halos. A late stage, but wide-spread occurrence of weak, incipient replacement of rock-forming minerals by carbonate and kaolinite may be related to infiltration of ground-waters during the final cooling of the system.

2.3 QEMSCAN mineral mapping

QEMSCAN (Quantitative Evaluation of Minerals by Scanning Electron Microscopy) is a mineral analysis system based on research pioneered by the CSIRO in Australia. QEMSCAN combines features found in other analytical instruments such as a Scanning Electron Microscope (SEM) or Electron Probe Micro Analyser (EPMA) into a next generation solution designed for automated analysis of minerals, rocks and materials. Several samples from the Cireşata deposit have been scanned with a high-resolution

(4 microns) QEMSCAN at the Xstrata Process Support Center in Sudbury, Canada (www.myxps.ca). Images and results of scans from the EMP, LMP, and SED are shown below (Xstrata Process Support Center, 2012) (Figs. 3, 4, 5).

MINERAL MASS	
Gold	0.00
Chalcopyrite	0.94
Pyrite	2.64
Sphalerite	0.00
Other Sulphides	0.00
Quartz	44.57
Chlorite	12.82
Muscovite	0.66
Kaolinite	3.19
Biotite	0.04
Orthoclase	0.71
Plagioclase	24.27
Epidote	0.09
Other Hard Silicates	3.39
Magnetite	3.43
Rutile/Ilmenite	1.15
Carbonates	1.68
Apatite	0.30
Other	0.12
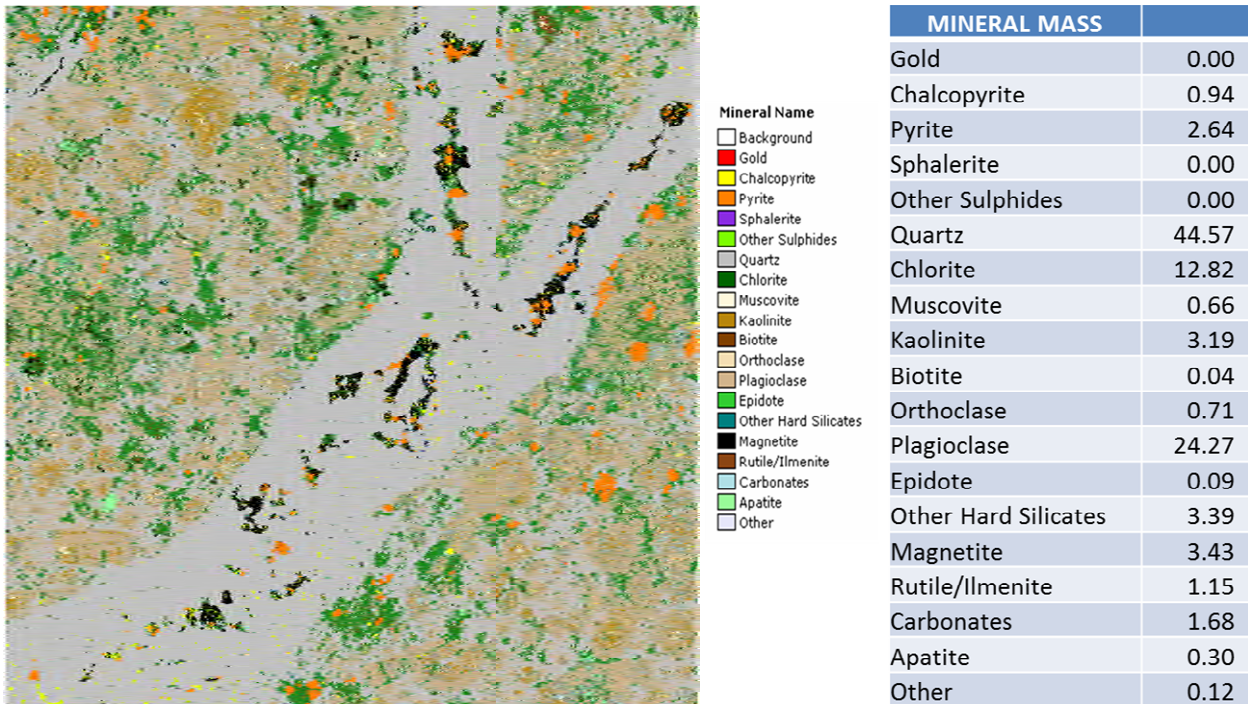
Fig. 3. QEMSCAN image of stockwork veining in the EMP affected by intense magnetite-chlorite alteration. The quartz veins contain quartz, magnetite, chlorite, pyrite and chalcopyrite. The rock is flooded with quartz and disseminated chlorite, magnetite, pyrite and chalcopyrite. Drill Hole RGD-17, 193.3 m. Picture scale is 12mm X 12 mm with a resolution of 4.4 microns.

MINERAL MASS	
Gold	0.00
Chalcopyrite	1.26
Pyrite	1.29
Sphalerite	0.00
Other Sulphides	0.00
Quartz	16.85
Chlorite	7.49
Muscovite	0.82
Kaolinite	0.54
Biotite	12.95
Orthoclase	36.87
Plagioclase	15.29
Epidote	0.14
Other Hard Silicates	0.85
Magnetite	4.19
Rutile/Ilmenite	0.36
Carbonates	0.95
Apatite	0.12
Other	0.04
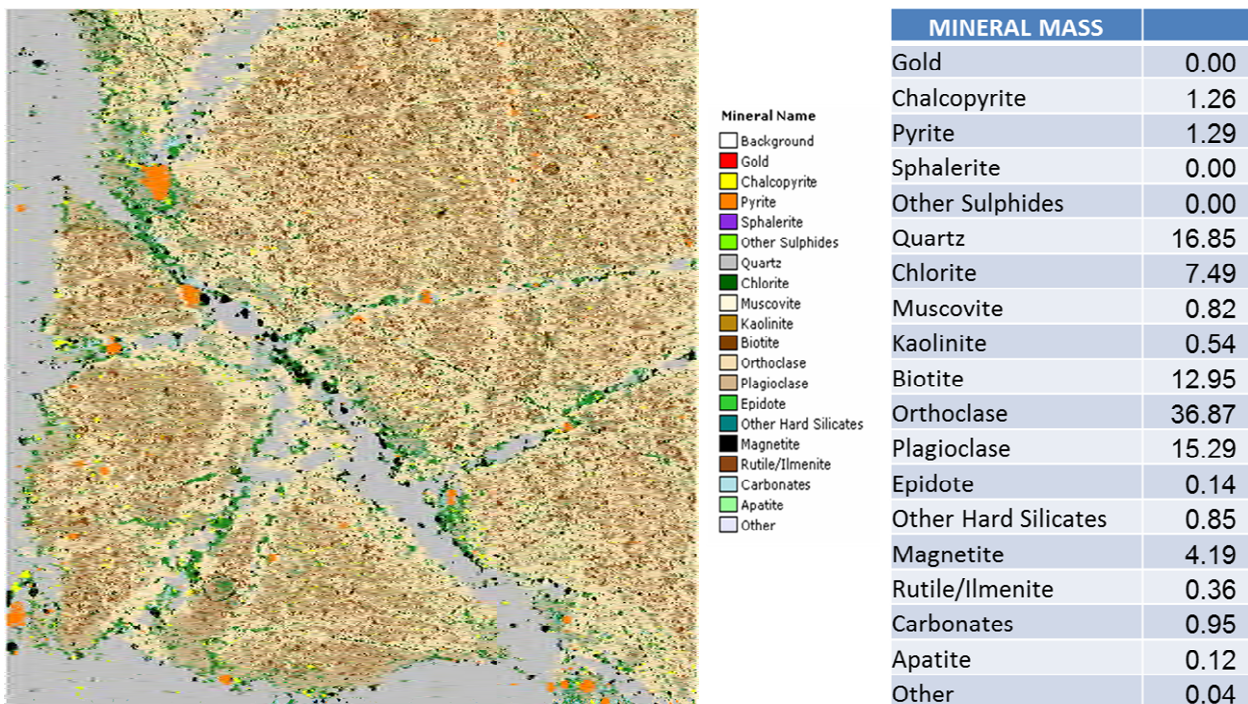
Fig. 4. QEMSCAN image of stockwork in potassic altered Cretaceous sediments (SED). The rock is affected by pervasive potassic alteration with abundant orthoclase and biotite. The quartz veins have associated magnetite-chlorite alteration. Drill Hole RGD-17, 379.5 m. Picture scale is 12mm X 12 mm with a resolution of 4.4 microns.

MINERAL MASS	
Gold	0.00
Chalcopyrite	0.00
Pyrite	3.50
Sphalerite	0.00
Other Sulphides	0.00
Quartz	24.81
Chlorite	10.22
Muscovite	7.41
Kaolinite	4.73
Biotite	2.52
Orthoclase	10.84
Plagioclase	25.69
Epidote	0.21
Other Hard Silicates	1.73
Magnetite	0.12
Rutile/Ilmenite	1.20
Carbonates	6.06
Apatite	0.62
Other	0.31
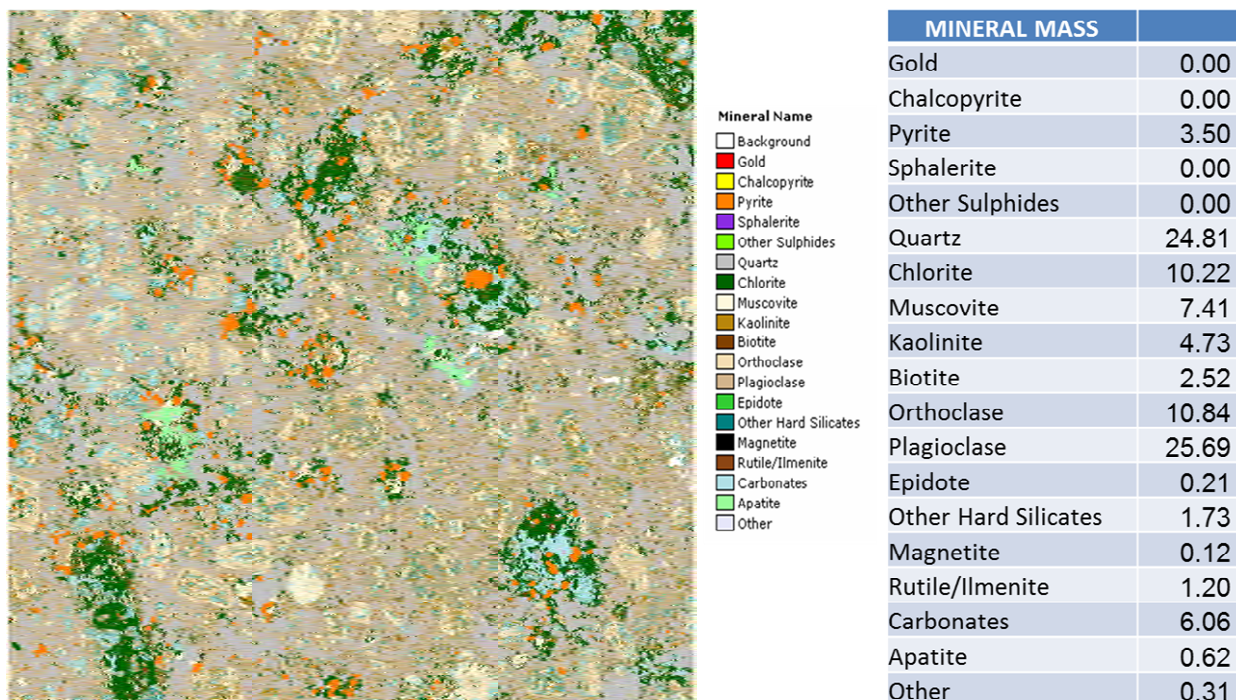
Fig. 5.. QEMSCAN image of incipient potassic altered Late Mineral porphyry (LMP). Chlorite and carbonate represent later propylitic overprint. Drill Hole RGD-12, 364.5 m. Picture scale is 12mm X 12 mm with a resolution of 4.4 microns.
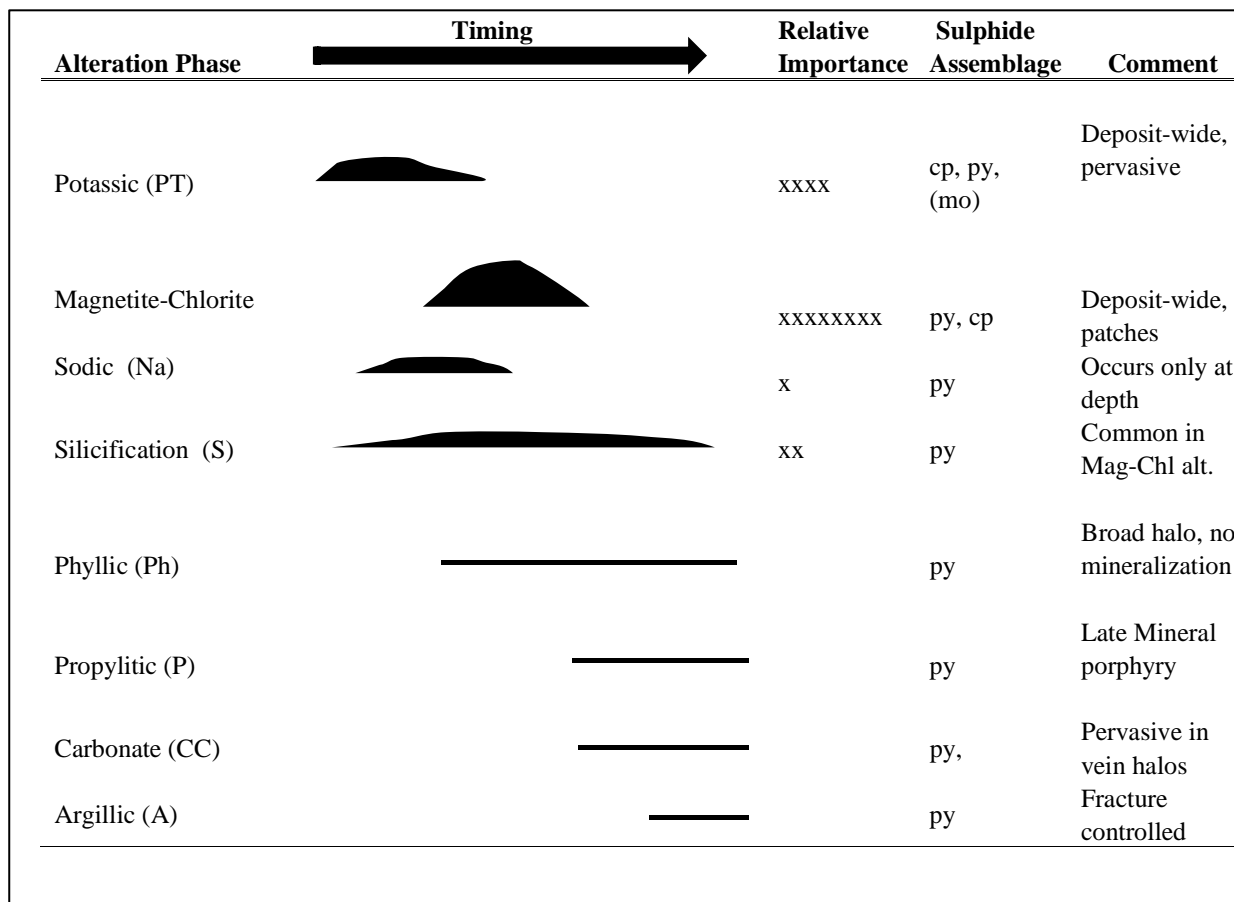
**Fig. 6.** Schematic of the alteration paragenesis and relationship with mineralization occurrence.

3. Conclusions and interpretations

The Cireşata Au-rich Cu porphyry is centered on a Neogene polyphase subvolcanic intrusive complex of hornblende-plagioclase microdiorite. The mineralogy composition of the early-mineral porphyry (EMP) and the late-mineral porphyry (LMP) are similar with only slight difference in textures. The Cretaceous sedimentary rocks (SED) underwent an early-stage thermal metamorphism that changed their rheology to a more brittle rock and enhanced their ability to host stockwork mineralization.

An early-stage potassic alteration, comprised mainly of biotite + orthoclase +/- magnetite is pervasive throughout the deposit at an incipient micro-scale. Ore-grades of Au-Cu are commonly associated with abundant magnetite related to a quartz-magnetite-chlorite alteration with pyrite-chalcopyrite occurring in stockwork veins and disseminated in the rock mass (Fig. 6).

References

Damian, G., 2011. Petrographic analyses of thin and polished section of the Cireşata porphyry deposit. Unpublished internal report from North University, Baia Mare, Romania to SAMAX SRL.

Ghitulescu, T.P. Socolescu, M., 1972. Geological Map of Romania, Sheet 73d Brad, Scale 1:50,000. Institut of Geology and Geophysics, Bucarest.

Milu, V., Milesi, J.P. and Leroy, J.L., 2004. Rosia Poieni Copper Deposit, Apuseni Mountains, Romania: Advanced Argillic Overprint of a Porphyry System: Mineralium Deposita, Volume 39: p. 173–188

Sillitoe, R.H., 2000. Gold-rich porphyry deposits: Descriptive and genetic ts/2012/80203bencini/ndx_bencini.pdf models and their role in exploration and discovery: Reviews in Economic Geology, v.13, p. 315−345.

Xstrata Process Support Center, 2012. QEMSCAN report on core samples from Colnic and Cireşata porphyry deposits. Unpublished internal report to Carpathian Gold Inc.

MINING SUBSIDENCE PREDICTION USING FINITE ELEMENT METHOD – CASE STUDY ON A SUB-LEVEL CAVING OPERATION DESIGNED FOR THE CIREŞATA-VALEA GÂRZII ORE BODY

Sorin MIHAI[1], Marius ZLĂGNEAN[1], Sorin HALGA[2]

[1] National Institute for Metals and Radioactive Resources, Bucharest, Romania.
 sorinmihai2005@yahoo.com, zlagnean_marius@yahoo.com
[2] SAMAX ROMANIA, Criscior, Hunedoara, Romania. sorin@samax.ro

1. Introduction

During the underground mining of ore deposits voids may occur, the overlaying rock could bend or fall into these voids. This results in movements and deformations at surface where a subsidence depression is formed. The size of the movements and deformations depends primarily on the geo-mechanical properties of rocks and on the general geo-mechanical situation, comprising: the geological conditions of the embedded deposit, the mined thickness and depth of the underground deposit, the mining method and other factors (Schenk, J,1999).

Sub-level caving induced subsidence may endanger the mine infrastructure and is a major concern for operational safety. Moreover, changes to surface landforms induced by sub-level caving subsidence may lead to an important environmental impact. Therefore, the ability to predict the surface subsidence associated with sub-level caving mining is critical for both mining operational hazards and environmental impact assessments.

This study may be considered an application of modern methodologies (assuming the stochastic character of the rock mass based on Knothe's theory) and time parameters, and theories based on finite element analysis of specific bi-dimensional profiles according to the different mining phases and geological rock structures.

2. Deposit description

Cave mining is typically performed when a large ore deposit is located at a certain depth below surface, making open-pit mining non-economical or environmentally feasible.

This is the case treated in the present article. Sub-level caving is an underground mining method used for steep dipping deposits. The sub-level caving method mines the deposit from various intermediate underground levels, and like other caving methods, uses gravity to help in ore extraction.

At each intermediate level, longhole drilling is performed upwards and selective blasting is used to collapse the rock. Mining then retreats towards the footwall as ore and waste rock are extracted. This mining method can be performed simultaneously on multiple levels, beginning with the lowest level and continuing upwards, extracting the entire ore.

The Ciresta-Valea Garzii deposit is considered to be one of the most important sources for gold-copper ore in the Rovina Valley Mining Project (RVP), and it is estimated to be in production for about 20 years, including three pre-production years.

The deposit is located in the Southern part of the RVP mining license, in an area positioned below the Southern part of the Bucuresci river, namely on the Valea Garzii creek.

The surface above the ore deposit is a hilly area with elevations ranging between 420m and 480m, with access through relatively gently sloped narrow valleys with moderately steep slopes.

Cireşata contains the highest average gold grades in the RVP being extensively drilled for a good knowledge of geological resources and reserves. The gold-copper mineralization is hosted by a Neogene subvolcanic neck represented by EM-P (early mineral porphyry) and IM-P (inter mineral porphyry) lithological units and adjacent Cretaceous sediments hornfelsed near the contact zone with early mineral intrusion. The subvolcanic intrusion is represented by a medium coarse-grained hornblende-plagioclase porphyry with contacts arching outward toward the surface resulting in a funnel-shaped intrusion. Mineralization occurs as a broad quartz-pyrite-chalcopyrite-stockwork zone apparently centered on the narrow deep part of the intrusive 'neck' and does not reach the present surface, occurring at 50 – 150m depth below surface. Some late-post mineral dykes cut the mineralization as shown in Fig. 1, and usually are weakly mineralized.
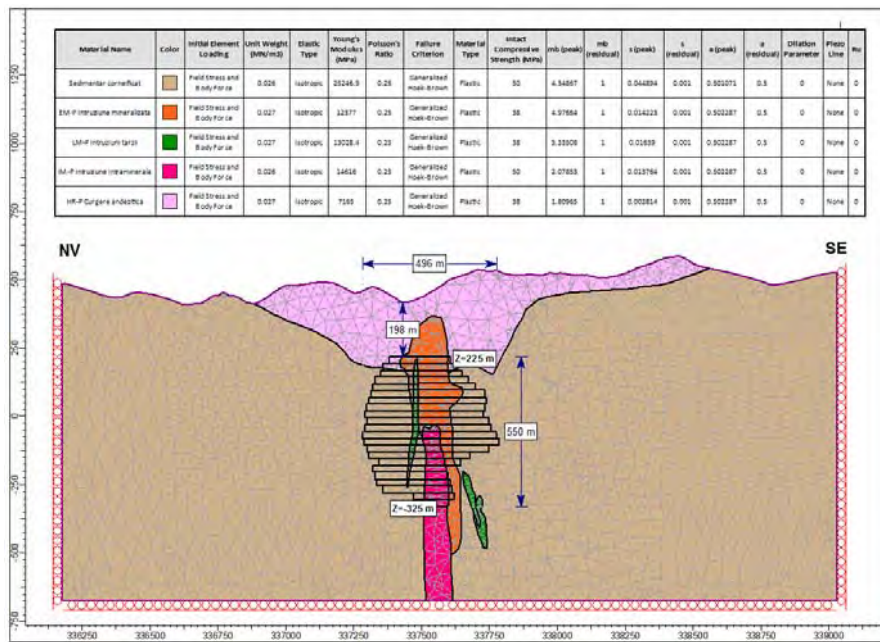
Fig. 1 A characteristic cross-section through the deposit

The main alteration types in the Cireşata-V.Garzii deposit are represented by potassic and phyllic alteration. Potassic alteration is generally represented by the biotite – quartz – K-feldspar – magnetite association with pyrite/chalcopyrite and strongly correlates with Au-Cu high grades.

It should be noted that this mineral association has a positive impact on the rock geomechanical properties.

The phyllic alteration is characterized by a dominant assemblage of sericite – quartz – pyrite +/- clay minerals that is generally consistent with the lower-grade peripheral parts of the Cireşata deposit. The presence of sericite and clay minerals has a negative impact on the rock competence.

3 Subsidence numerical modelling

Several different methods for subsidence prediction have been used in mining operations design, most of them beeing empirical and semiempirical techniques: profile function method, trigonometrical functions, influence function methods (Knothe, Keinhorst, Beyer, Litwiniszyn), but also stochastic models and numerical methods (the finite element method, the distinct element method, the finite difference method, the boundary element method). We must also mention the void-volume physical models where actions of discrete deformational and collapse mechanisms are primary modes of influencing subsidence development. Actual collapse mechanisms must be known and physical models constructed.

In our case study, the subsidence prediction (performed on 22 mining stages-sublevels) uses the finite element method (implemented on Rocscience-Phase 2 v.8 software). The Finite Element Method (FEM) can simulate non-homogeneous, non-linear material behavior and complicated mine geometries (Aston et al., 1987). The structural analysis of the overburden is made by dividing and subdividing this into individual structural elements due to the stresses in the overburden body experiencing strains and being displaced. The amount of displacement for each element depends on the stress level and material properties of each element. The modelling profile consists of two cross-section through the ore body, one aligned NW-SE and the other one SW-NE.

We used the gravity field stress option, the analysis being staged by mining the mineralized levels downward in 22 stages (from +225m to – 325m elevation).

After the mesh was generated, the external boundary conditions were applied. The left and right edges of the external boundary were fixed in the X direction only (free to move in the Y direction) and the lower edge was fixed in the Y direction only (free to move in the X direction). The surface was free of any restraint. For gravity field stress we selected the field stress and body force. The materials properties were assigned on each geological unit specifying elastic properties, strength parameters by Mohr-Coulomb or Hoek-Brown failure criteria and material type (elastic or plastic).

The subsidence main parameters were computed for each mining stage: vertical displacement, horizontal displacement and horizontal strain (first derivative of the horizontal displacement with respect to the horizontal distance). The horizontal strain is made of a tensile strain that is positive and a compression

strain that is negative. Horizontal strains cause most of the structural damage. They cause tensile or shear cracks and buckling and induce distortion, fractures, or failure. The distribution of the parameters characterizing the mining subsidence is shown on sections and diagram representation (Figs. 2, 3 & 4).
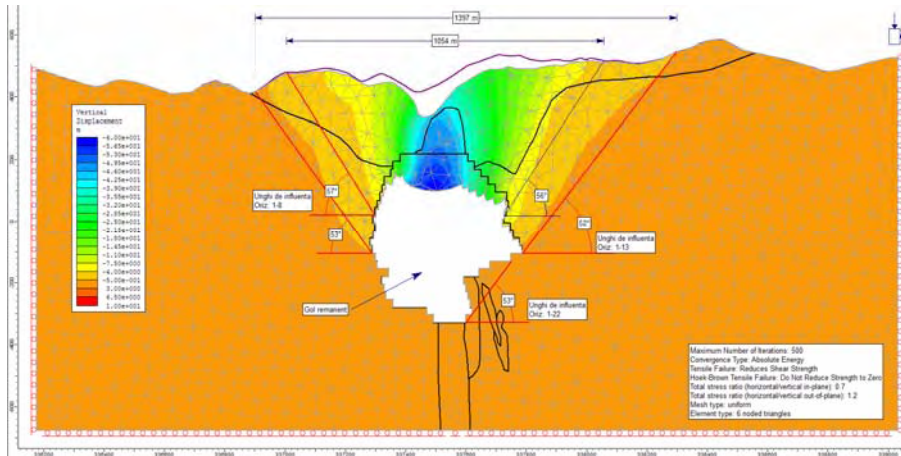

**Fig. 2** Modeling section with vertical displacement distribution
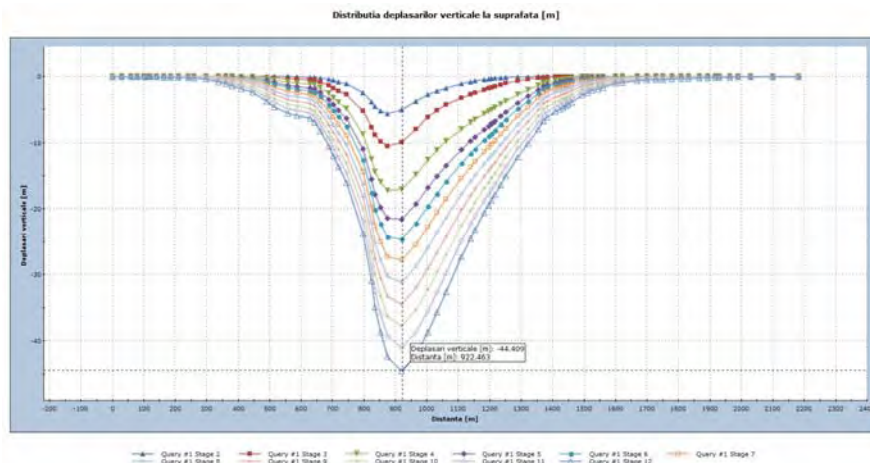
Fig. 3 Subsidence versus distance for each stage, Smax=-44.41 m
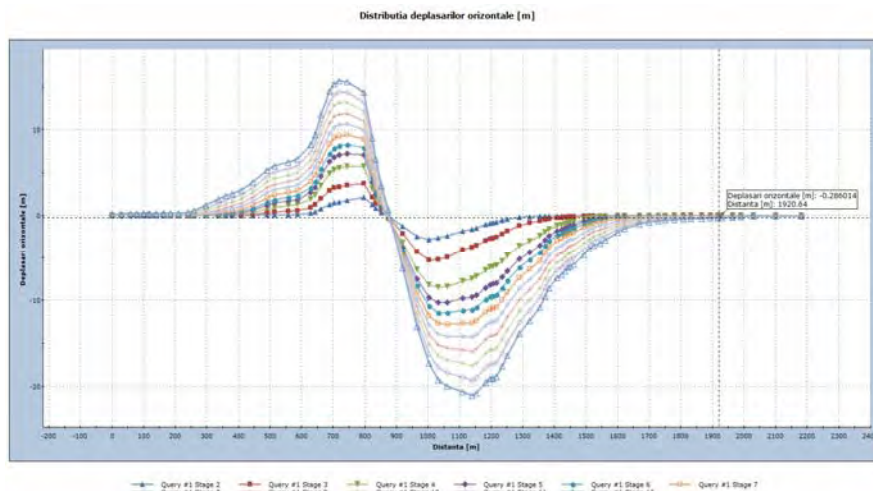

Fig. 4 Horizontal strain versus distance for each stage

27
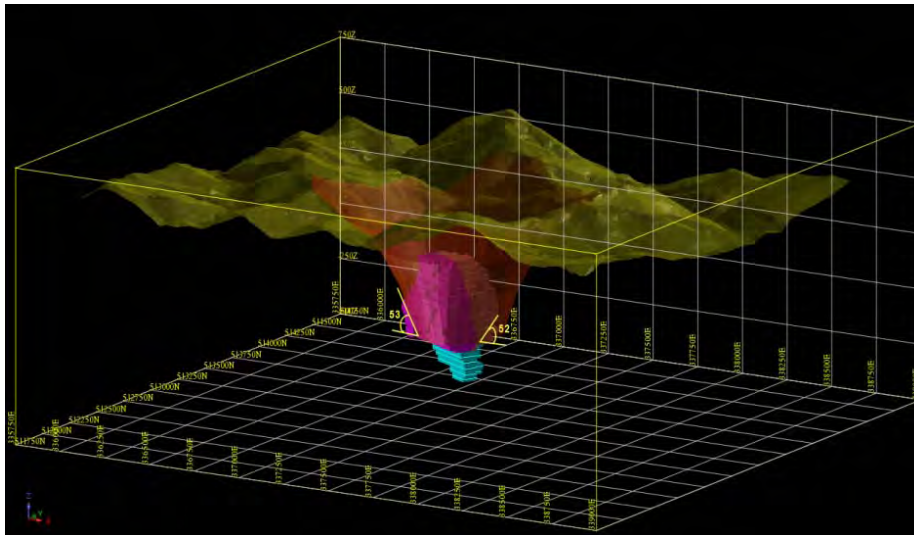
Fig. 5 The subsidence zone extension to surface due to sublevel caving

4. Conclusion

The developed methodology used in this case study has the capability to predict progressive surface subsidence at the surface points along any directions, horizontal or dipping seams, and overburden of layers with the results of subsidence, slope, curvature, horizontal displacement, and horizontal strain. The feasibility of a modern and pragmatic system that could be used for mining risk assessment and also for a more rational mining design and planning has to be verified by comparing the subsidence measured values (using local surveys or remote sensing systems) with predicted values from the numerical or stochastic methods. This will be the next step for research; the parameters sensitivity analysis should indicate the changes that could be used in designing a robust subsidence prediction system.

References

Aston T.R.C., Tammemaghi H.Y. and Poon A.W., 1987. A Review and Evaluation of empirical and Analytical Subsidence Prediction Techniques. Mining Science and Technology, vol. 5, pp. 59-69.

Braeuner G. 1973. Subsidence due to underground mining. Theory and practices in predicting surface deformation, US.IC 8571.

Cui X., Miao X., Wang J., Yang S., Liu H., Song Y., HU X.,2000. Improved prediction of differential subsidence caused by underground mining. International Journal of Rock Mechanics and Mining Sciences, 37. 615-627.

PEG, Carphatian Gold Inc., 2009. Technical report on the Rovina Valley Project Romania, Ontario Canada.

Schenk, J., 1999. Measurement of movements and deformations in subsidence depression (in Czech). Ostrava, VŠB-TUO, 144 s. ISBN 80-7078-711-2.

GEOLOGY AND ECONOMIC SIGNIFICANCE OF Cu-Pb-Zn DEPOSITS IN THE YÜCEBELEN AND SURROUNDING AREA (TORUL-GÜMÜŞHANE)

Yahya ÖZPINAR, Doğacan ÖZCAN[1], Barış SEMİZ

Pamukkale University, Department of Geological Engineering,TR-20070, Denizli-TURKEY
(*yozpinar@pau.edu.tr*, *dogacanozcan@gmail.com*, *bsemiz@pau.edu.tr*)

Abstract Study area is in the zone named "Eastern Pontide Zone" which is located in the northeastern part of Turkey. On the bottom of the study area, Cretaceous aged volcanic, pyroclastic and sedimentary rocks intercalated with pyroclastic rocks take place. All these lithologic units were intersected by Upper Cretaceous-Late Eocene aged granitoids. This pluton that generates mineralization underwent low/sub-propylitic alteration. Cu-Pb-Zn mineralization occurs in the fracture zones of a granodiorite intrusion located in the southwestern part of the study area. Same mineralization has been determined in the northeastern part of this intrusive, where intrusive contact with sedimentary rocks and also, fracture zones developed in sedimentary rocks. It is determined that quartz veins with various dimensions, generally strike N40-50°W. As a result of microscope investigation, a paragenesis including galena, sphalerite, pyrite, chalcopyrite, gold, smithsonite, malachite, azurite, covellite, goethite, lepidocrocite, hematite, and limonite was determined. This paragenesis is similar to that of the porphyry-copper deposits from the region. In this study, preliminary results of detailed geological study are given for this area, which has been never studied before.

Key Words: Torul-Gümüşhane, Eastern Pontides, Pb-Zn-Cu deposits, Ore-rich quartz veins.

1. Introduction

The study area is located in the tectono-stratigraphic zone named "Eastern Pontide Zone" from the northeastern part of Turkey (Figure 1). This is a Cu-Pb-Zn-rich zone, named "Eastern Black Sea metallogenic zone". Eastern Pontides were formed by the subduction of Tethys Ocean under the Eurasian plate, during the Early Cretaceous - Late Eocene. Eastern Pontide orogenic zone can be divided in two tectono-stratigraphic subgroups as the northern and southern zones. The northern zone consists of Senonian and Eocene volcanic and volcaniclastic rocks. Additionally, pre-Senonian rocks crop out in the southern zone, which preserves its pre-Senonian fore-arc basin location. Also, in the southern zone, due to continental collision that took place during the Early Tertiary, the deformation is stronger than in the northern zone (Okay and Şahinturk, 1997). The study area is located very close to border of these two subgroups but located in northern zone.

2. Materials and methods

In this project, the first geological map of the study area at the scale 1:5000 was made. Subsequently, detailed geological maps at the scale 1:2000 were made for the areas rich in ores. Based on these maps, the location and dispersion of the mineralization were determined. 129 samples were collected and examined under the microscope. Additionally, 10 polished sections of samples taken from the mineralized rocks were prepared in order to determine the paragenesis of the mineralization. Systematic sampling has been done from test pits opened on ore-rich zones, which are mapped in detail for this study. 46 geochemical
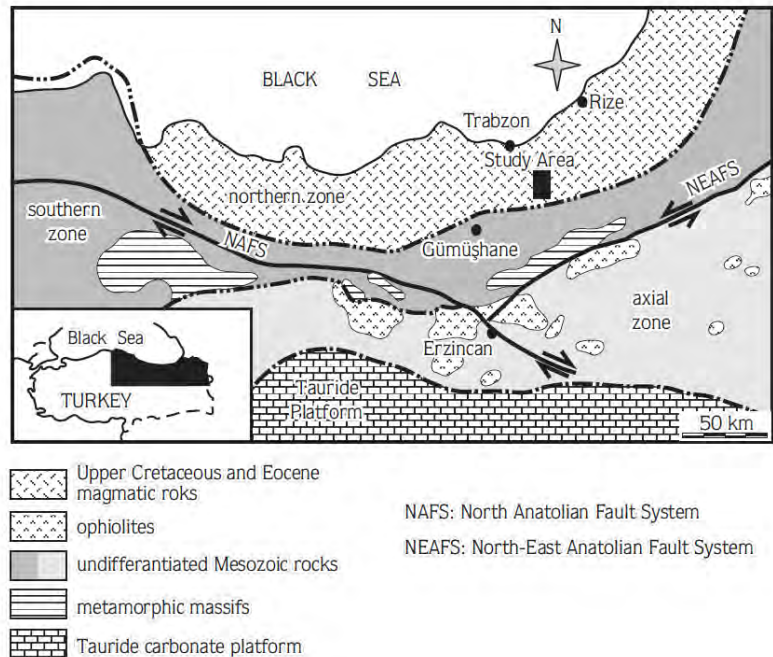

Fig. 1. Map showing the structural location of the studied area (Karslı et al., 2004).

---
[1]Corresponding author: Tel: +90-258-2963402, Fax:+90-258-2963382

samples collected from the test pits were analyzed in ACME labs (Canada) by ICP-MS device and the results were evaluated.

3. Stratigraphy and petrology

In the study area, volcanic rocks consisting of basalts and basaltic andesites take place at the bottom of the rock sequence; they are overlain by concordant pyroclastic and dacitic-rhyodacitic rocks. These rocks are overlain by sedimentary rocks intercalated with pyroclastic rocks. All those units mentioned above, were intruded by granitoids of supposed Upper Cretaceous-Eocene age. Also, all lower units are cut by Late Eocene andesitic and dacitic dykes (Fig. 2). Granitoids that crop out in the area were classified in terms of Q-ANOR parameters as granodiorites (Adile Hamlet occurrence - investigated in detail), diorites (Tuzlak Hill occurrence- eastern-part of study area) and quartz monzodiorites (İstavroma Hill occurrence- northern part of study area). It has been determined that granitoids are alkaline (Tuzlak Hill occurrence) and calc-alkaline (Adile Hamlet and Istavroma Hill occurrences) in terms of alkali-silica diagrams.

4. Mineralization

The mineralization depends on the quartz veins developed in the fracture zones of the granodiorite body. In the detailed map of the study area, nine ore-rich zones were identified (Fig. 3). Five of them developed on the fracture zones in granodiorites, one displays on intrusive contacts with the sedimentary rocks and the rest of them occur in sedimentary rocks. Hydrothermal textures were especially identified in the quartz veins and at the wall rock contacts. It is determined that quartz veins with various dimensions, generally strike N40-50°W, which is the same as that of the fracture zones developed in the mineralized granodiorite. Strikes and locations of these zones have been obtained from the strikes of the widespread quartz veins. Ore-rich zones are 4-5 m to 30 m wide and 500 m long according to the dispersion of the silicified blocks originating in the silicified zones.
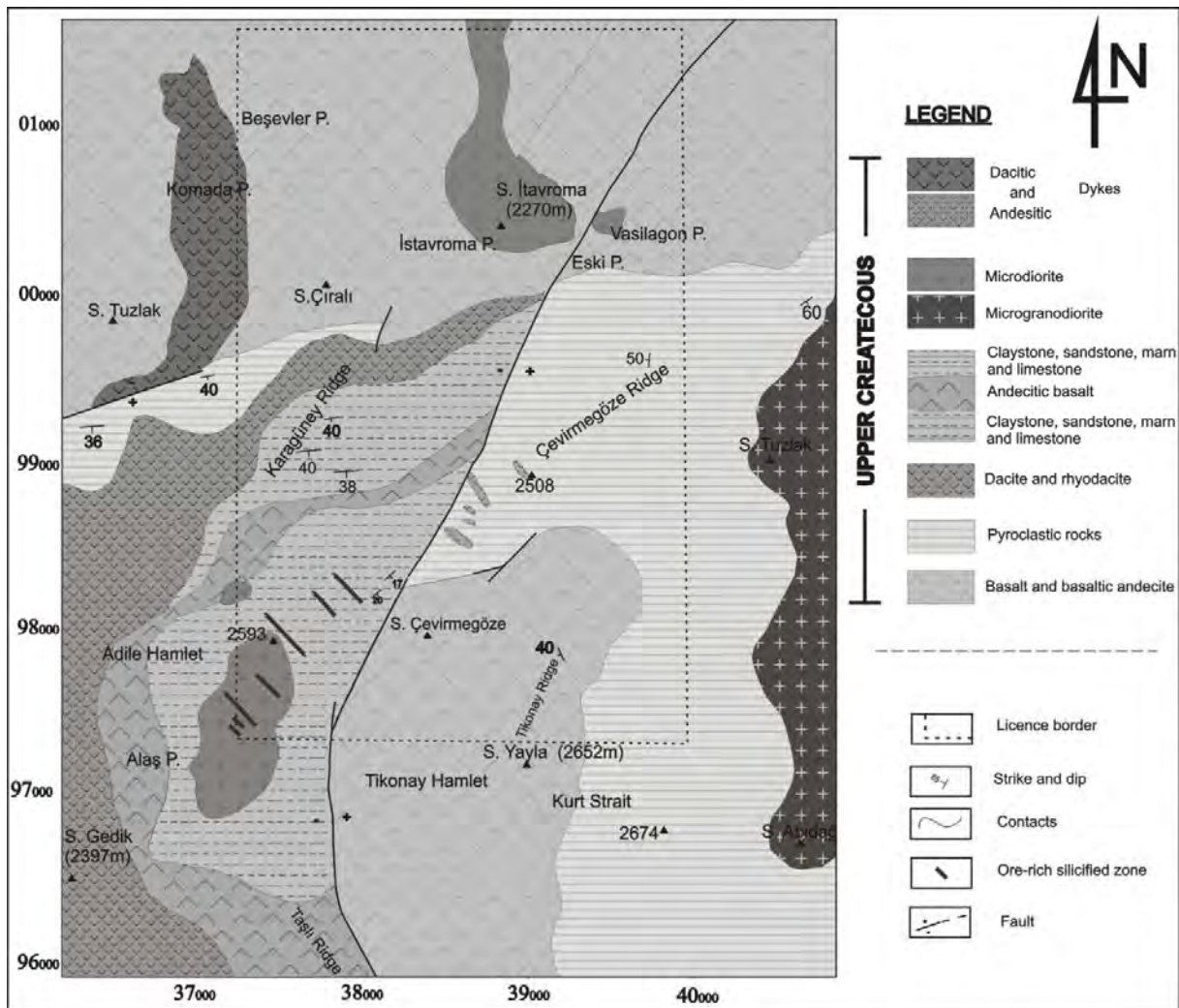
Fig. 2. Geological map of the studied area. The area delimited by the dash line is detailed in Fig. 3
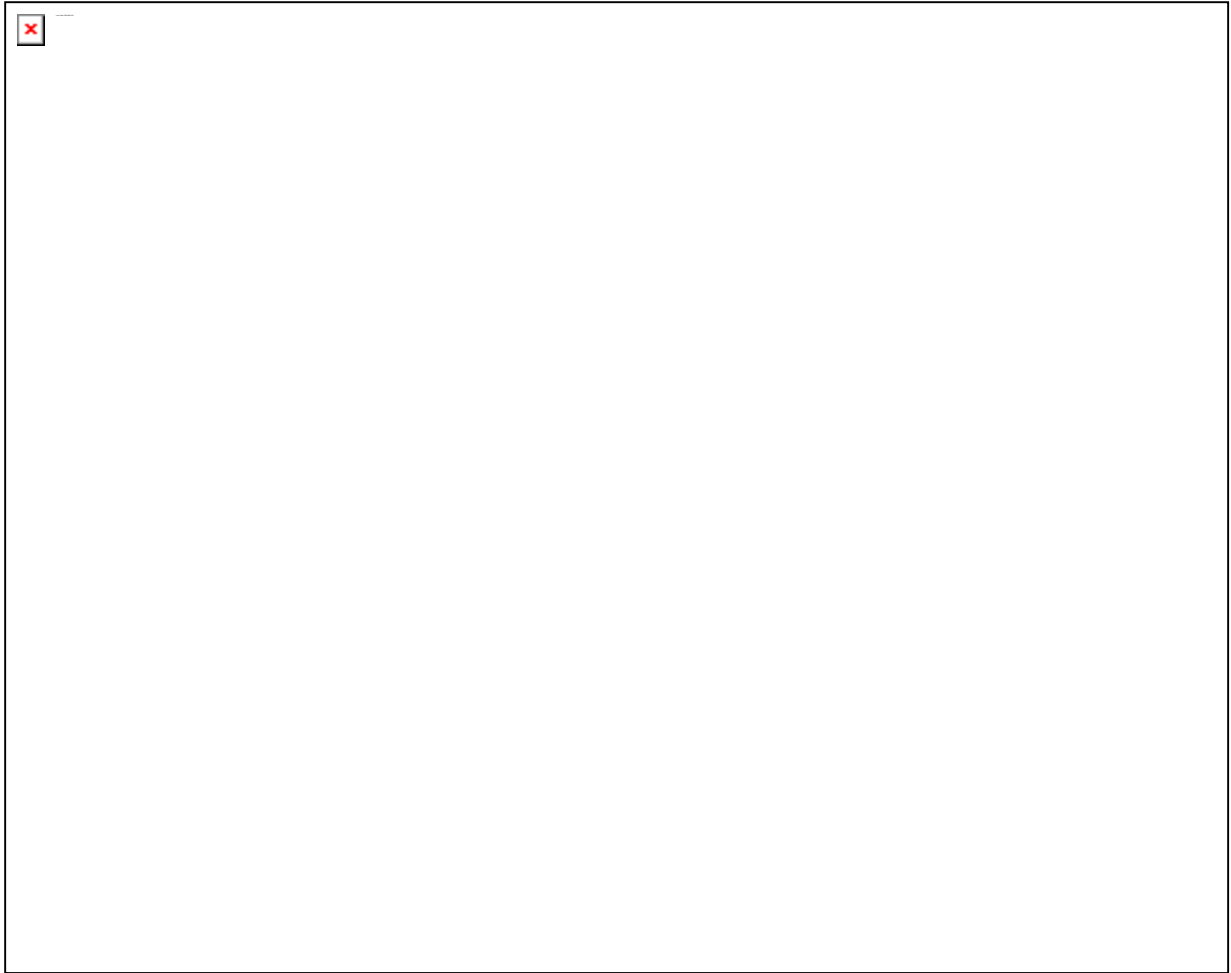
Fig. 3. Geological map of the Adile Hamlet and surrounding area.
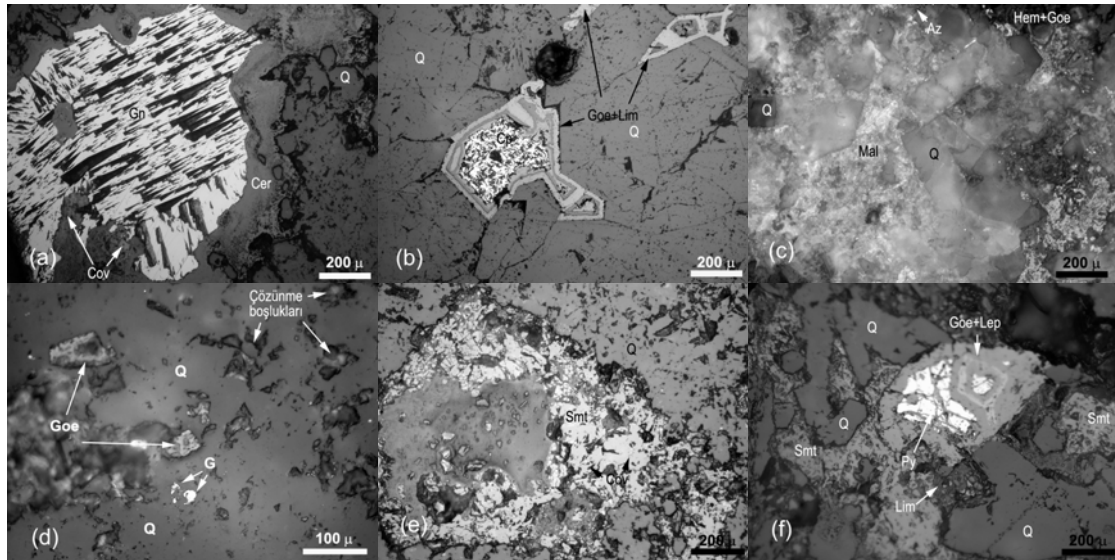
Fig. 4. Ore microscopy images: **(a)** Galena grain (Gn) and its substitution by covellite (Cov) and cerussite (Cer); **(b)** chalcopyrite grain (Cp) in quartz gangue (Q); **(c)** azurite (Az) and malachite (Mal); (d) Gold (G) in quartz (Q) gangue; **(e)** smithsonite (Smt) in highly altered sample; **(f)** fragmented pyrite (Py) with goethite (Goe) and lepidocrocite (Lep).

In this study, the paragenesis was determined in terms of mineral species, abundances, and relations with each other (Fig. 4): Phase I: Galena, sphalerite, pyrite, chalcopyrite, gold. Phase II: Pyrite, chalcopyrite,

gold. Supergene phase: smithsonite, malachite, azurite, covellite, goethite, lepidocrocite, hematite, limonite. Gangue mineral is Quartz. The sequence of mineral formation in the mineralized rocks from the study area is given in the Table 1. According to the aim of the study, 14 test pits were excavated in the investigated area. In every test pits, quartz veins were observed, even very thin. The maximum and minimum content values for the rock samples collected from the test pits are given in the Table 2.

5. Conclusions

Cu-Pb-Zn mineralization in the study area is associated with the calc-alkaline granodiorite intrusion located in the Adile Hamlet surroundings. Granodiorite was exposed to low and/or semi-propylitic alteration. Ore-rich quartz veins were developed by the metal-rich liquids moving throughout the fracture zones from the granodiorite, the granodiorite-sedimentary rock contacts and the fracture system developed in the sedimentary rocks.

In this study, test pits excavated many years ago were investigated and new test pits works were done. The investigation of the spoil piles revealed a paragenesis consisting of galena, sphalerite, pyrite, chalcopyrite, malachite and azurite. This shows that this mineralization is dominantly of Cu-Zn-Pb type. In addition, according to the analytical results, it appears that mineralization can be important in terms of Au contents.

Table 1. Formation phases of the ore-minerals determined in the study area.

	Phase I	Phase II	Supergene
Galena	▬▬▬		
Sphalerite	▬▬▬		
Pyrite	▬▬▬▬▬		
Chalcopyrite	▬▬▬▬		
Gold	▬▬▬▬		
Cerussite			▬▬▬
Smithsonite			▬▬▬
Malachite			▬▬▬
Azurite			▬▬▬
Covellite			▬▬▬
Hematite			▬▬▬
Limonite			
Quartz	▬▬▬▬		

Table 2. Maximum and minimum amounts of some elements identified in 46 rock samples.

Element (ppm)	Cu	Pb	Zn	As	Mo	Ag	Au
Maximum	>10000.0	>10000.0	>10000.0	186.8	39.4	>100.0	7.428
Minimum	190.0	2206.0	163.0	15.1	0.6	1.7	0.018

References
Karslı O., Aydın F., Sadıklar M.B., 2004. Magma Interaction Recorded In Plagioclase Zoning In Granitoid Systems, ZiganaGranitoid, Eastern Pontides, Turkey, Turkish Journal of Earth Sciences,13, 287–305.
Okay A.İ. and Şahintürk Ö., 1997. Geology of the Eastern Pontides. In: Robınson, A.G. (Ed.), Regional and Petroleum Geology of the Black Sea and Surrounding Region, Aapg Memoir, 68, 291–311

GEOLOGY AND ECONOMIC POTENTIAL OF THE AREA BETWEEN SIMAV AND GEDIZ REGIONS (KUTAHYA-WESTERN ANATOLIA)

Barış SEMİZ[1,2], Yahya ÖZPINAR[1], Cahit HELVACI[2]

[1] Pamukkale University, Department of Geological Engineering, TR-20070, Denizli, Turkey
[2] Dokuz Eylul University, Department of Geological Engineering, TR-35160, Izmir, Turkey
(bsemiz@pau.edu.tr, yozpinar@pau.edu.tr, cahit.helvaci@deu.edu.tr)

Abstract This study focuses on the Tertiary rocks, which are well examined in order to assess the potential mineralization of the eastern part of the Simav Graben. In this context, the identification of the stratigraphy of the study area, the 1/25.000 scaled geological mapping and measured stratigraphic sections were carried out, as well as petrographic and geochemical studies on samples. In addition, potential ore deposit areas related to granitic intrusion was studied for the economic importance. As a result, the study area is a host of a number of economic mineral resources, such as alunite, fire opal, coal, zeolite, porphyry-skarn Cu-Mo deposits, sand-gravel, and garnierite, for the first time reported in the Simav Graben.

Key Words: Alunite, Garnierite, Skarn, Cu-Mo mineralization, Economic potential, Simav Graben.

1. Introduction

The study area is located at the eastern part of the E–W trending Miocene Simav Graben, between Simav and Gediz regions in western Anatolia (Figure 1). Numerous studies were conducted in the past on the geology, mineralogy, origin, and reserve of the ore deposits (Akdeniz and Konak, 1979; Ercan et al., 1984; Seyitoğlu et al., 1997; Innocenti et al., 2005; Semiz, 2010). The studies of economic geology in the investigated area were started by Beer (1964), who studied the mineralization of the Şaphane alunites. The first mineralogical studies related to the zeolite exploration in western Turkey showed that clinoptilolite and analcime were the most common minerals in some basins, particularly in the borate-containing deposits (Ataman 1977; Gundogdu et al., 1996; Helvacı and Alonso, 2000). The coal fields located in the Gediz region was studied extensively by the General Directorate of Mineral Resource and Exploration (MTA); Helvacı and Yağmurlu (1995); Karayiğit and Whateley (1997). The economic potential of Simav Graben was documented by Oygur and Erler (2000), based on metallogeny, who mapped the mineralized area. A wide variety of ore deposits occurs along the Simav Graben and they are closely related to two principal tectono-magmatic processes that prevailed during the tectonic development of the western Anatolia (Oygur and Erler, 2000). Later, detailed economical studies were carried out by several workers on subjects such as alunite deposits (Mutlu et al., 2005), zeolites (Snellings et al., 2008; Semiz et al., 2011), fire opal (Hatipoğlu et al., 2010). The aim of this study is to evaluate the economical potential of the investigate area on the basis of available geochemical data.

2. Materials and methods

Geological map of the investigated area was revised at 1/25000 scale over an area of about 1500 km^2 (Figure 1). Detailed geological maps of the same locations were conducted. Thin sections were prepared from rock samples collected from the field. Bulk chemical analysis of 12 samples for major, trace, and rare earth elements (REE) analyses were carried out with fusion inductively coupled plasma (ICP) and fusion inductively coupled plasma-mass spectrometry (ICP-MS) in ACME Laboratories Ltd. Canada. Sample splits of 0.5 g are leached in hot (95°C) Aqua Regia. Larger split size of samples was selected for representative Au analysis.

3. Geology

The basement of the study area is represented by Menderes Massif metamorphic rocks and ophiolitic mélange units of the İzmir-Ankara zone, which were intruded by the Miocene Eğrigöz granitoid. They are structurally overlain by two different volcano-sedimentary successions, separated by an angular unconformity. These are Lower Miocene Hacıbekir Group and Middle Miocene İnay Group. These two units interfinger with volcanic units of different chemical composition. Early Miocene Hacıbekir group that includes sedimentary rocks of Kürtköyü and Yeniköy formations interfingered with the volcanic rocks of the Akdağ volcanics and minor lamproitic flows. The Yeniköy formation is also conformably overlain by the andesitic, dacitic and rhyolitic volcanic rocks of the Akdağ volcanics. The Hacıbekir

---

[2] Corresponding author: Tel: +90-258-2963402, Fax:+90-258-2963382

group is unconformably overlain by the middle Miocene Inay group that is composed of Ahmetler and Ulubey formations, Güzüngülü volcanics and basalts. The Güzüngülü volcanics are composed of andesitic lavas and pyroclastic rocks. The İnay Group is unconformably overlain by the Plio–Quaternary Asartepe formation, which is composed of coarse grained detrital deposits. All these units are unconformably overlain by the recent travertine and alluvia (Fig. 1).
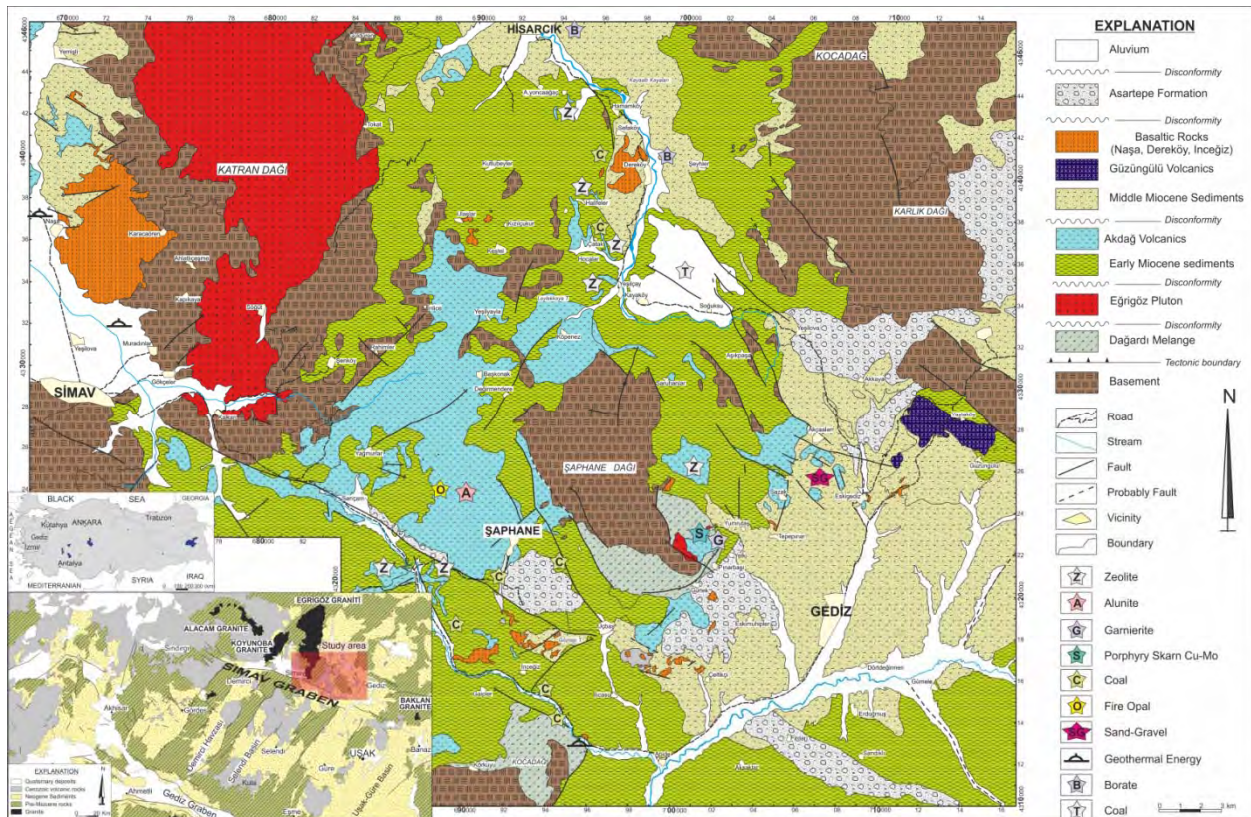

Fig. 1. Geological map of the study area with the location of the various mineral resources mentioned in the study (Modified by Akdeniz and Konak, 1979).

4. Mineral and energy resources

The Simav Graben is a host of a number of economic mineral resources, although there are no detailed and accurate data and information about the location and extent of these deposits.

4.1 Mineral resources

4.1.1 Alunite Şaphane alunite deposit is one of the epithermal deposits in the Simav Graben, western Anatolia. Mining operation of alunite deposits in the Şaphane area goes back to the Roman period. Alunite was one of the most important mining products of that period. Currently, a total of 30,000 tons of alunite is produced annually by the Dostel Company Ltd.; most of it issued to meet the demands of domestic industry. However, the deposit is currently not mined due to low K_2O grades (Mutlu et al., 2005). According to Mutlu et al. (2005), the Şaphane alunite deposit is closely associated with rhyolitic tuffs of Middle Miocene (12 to 13 Ma) age. Advanced argillic alteration level consists of alunite, quartz and kaolinite and is located at the top of the hydrothermal system. This zone changes downwards to an argillic alteration zone that is mostly composed of smectite, illite, kaolinite, calcite and pyrite. The composition and isotope analyses indicate that the alunite formation is nearly coincident with the volcanism and reveal a magmatic origin of sulfur in the deposit.

4.1.2 Fire opal Fire opal has been extracted in the past from mines in Karamanca, east of the Simav, about 10 kilometers northwest from Şaphane vicinity (Kütahya), and mining activity stopped in 1980s. The deposit is mined by the Lydians in ancient times in Turkey, and that it was resumed by the Genoeses about 550 years ago. German companies mined fire opal from the galleries and fracture zones during World War I. Millions of tons of rhyolitic waste can be seen today as evidence of past episodes of intense mining (Hatipoğlu et al., 2010). According to Hatipoğlu et al. (2010), the fire opals are observed in colors of red, orange, yellow and white and fill the vesicles in rhyolite. Fire opal size changes from few

34

millimeters up to few centimeters and displays round and elliptical shapes. By the geochemical studies it is determined that the red and orange color of fire opals come from their Fe content. It is understood from the chemical analyses results of orange and green colored opal dendrites that orange color comes from Fe, Mn and Ti elements and green color comes from Ni and Cr elements.

4.1.3 Coal Coal occur as a thin lens in the roadside in the north of the Ilıca spa, west of the Dereköy and north of the Çatak (Gediz) and in the Kepez hill and Simav road (Şaphane). Coal has been extracted in the past from mines in the Şaphane vicinity, and although mining activity stopped in 1980s, there is still significant mineral reserves awaiting exploitation. According to Karayiğit and Whateley, (1997), most Miocene coals in Turkey are of sub-bituminous to lignite rank. The coal fields in the Gediz area in the western part of Turkey contain mainly high sulphur coals of bituminous rank. The results of the proximate analyses as well as total sulphur analyses and calorific values on an air-dried basis show on average 1.2% moisture, 22.9% ash, 34.6% volatile matter, 6.9% total sulphur contents and 5850 kcal·kg^{-1} calorific value. X-ray powder diffraction studies of the coal samples on an air-dried basis show quartz, pyrite and calcite to be the dominant minerals; kaolinite, hydromuscovite, dolomite, gypsum, iron sulphate hydrate and rarely illite/smectite and feldspar occur in smaller amounts.

4.1.4 Zeolite Another mineral of socio-economic significance is zeolite. Zeolites were found in the locations of Karacaderbent (Şaphane), Köpenez, Halifeler, Yeşilçay, Çatak, Yoncaağaç (Hisarcık) (Helvacı et al., 1993; Gündoğdu et al., 1996) and Saphanedağı (Gediz), in the eastern part of the Şaphane Mountain, western Anatolia, Turkey (Semiz et al., 2011). The zeolitic tuffs are white and pale green, with the primary phase consisting of glass shards and minor occurrences of pumice clasts, feldspar, quartz, and biotite crystals. Glass shards in the vitric tuffs are replaced by zeolite minerals. Petrography and X-ray diffraction show that tuffs consist mainly of the clinoptilolite-heulandite, analcime, and mordenite. Quartz, sanidine, cristobalite and biotite were also detected as secondary minerals (Semiz et al., 2011). According to Semiz et al. (2011), clinoptilolite is the predominant zeolite and occurs as well-developed prismatic crystals associated with K-feldspar. Clinoptilolite was replaced by authigenic alkali feldspar. Heulandite (mean of Si/Al <4) occurs rarely and it was only seen in the Şaphanedağı and Çatak tuffs. Analcime (mean of Si/Al ~2.7) is commonly associated with quartz and K-Feldspar and rarely with clinoptilolite (Kopenez and Saphanedağı locations). Both clinoptilolite and analcime occur within pyroclastic flows of the same stratigraphic unit.

4.1.5 Garnierite Garnierite is among the most important industrial minerals of the supergene nickel deposits. Mine geologists use the term "garnierite" for the pale green, bluish or dark green Ni-rich silicate minerals that occur in many Ni-laterite deposits. Actually, garnierite is a general name for the Ni-Mg hydrosilicates that usually occur as an intimate mixture that commonly includes two or more of the following minerals: serpentine, talc, sepiolite, smectite, and chlorite (Gleeson et al., 2004). In the Simav Graben, garnierite was determined for the first time in this study. They have a grade of >10000 ppm nickel and 488-1487 ppm cobalt (Table 1). Mineralization is formed by the lateritization of rocks containing trace amounts of nickel, such as peridotites, because it is developed over the ultramafic rocks of ophiolitic mélange.

4.1.6 Cu-Mo mineralization The Pınarbaşı district is one of the sulfide deposits in the Simav Graben where the formation of porphyry-skarn Cu-Mo deposits has a close genetic link with a late phase in the evolution of the granitoid body/bodies (Oygur and Erler, 2000). The mineralization in the study area occurs as pirometasomatic type in the contact zone between the intrusive body/bodies and the limestone, and as disseminated and stockwork types in the calc-alkaline magmatic rocks. The contact between limestone and Pınarbaşı granite is commonly affected by silicification. According to the studied samples, major ore minerals are pyrite, chalcopryrite and magnetite. Primary manganese, bornite and secondary malachite, azurite, limonite, hematite accompany those minerals. Pınarbaşı samples (C1, C2, C3) were analyzed but did not reveal important Au contents. The average contents of Cu and Mo are 33.7 and 40.9 ppm, respectively. It was determined that the most important mineralizations are associated with the contact zone of the limestone with Pınarbaşı granite (Table 1). Taşlık samples (M7, M8) consist of Cu (>10000 ppm) mineralization.

4.1.7 Sand and gravel In the south of the study area, sand and gravel are the most widely extracted and commercially exploited mineral resources along the Gediz River. Also, granulated aggregates used for the

most buildings in the Usak and Gediz areas were supplied from sand-gravel quarries located in the Gediz River basin in Turkey. In the study area, Ahmetler formation is suitable for sand and gravel mining. Sand and gravel particles are eroded fragments of rock formations, thus, their range in mineralogical composition is as variable as the rocks from which they are derived. The rock fragments in sand and gravel from the area are made of gneiss, quartzite, schist, limestone and granite. Sand and gravel are used primarily for aggregate. The most common use of sand and gravel is as construction aggregate in Portland-cement concrete and asphaltic concrete.

Table 1. Geochemical analyses (ppm) of the ore deposits in the study area.

Samp N.	C 2	C 3	C 4	M 2	M 3	M 4	M 5	M 6	M 7	M 8
Location	Pınarbaşı	Pınarbaşı	Pınarbaşı	Pınarbaşı	Pınarbaşı	Pınarbaşı	Pınarbaşı	Pınarbaşı	Taşlık	Taşlık
Mo	106.4	1.1	15.2	0.8	0.9	1.3	3.2	18.1	2.6	8.7
Cu	10.4	46.9	43.8	12.9	12.2	12.8	6.4	58.2	>10000.0	6539.7
Pb	27	64.3	129.2	5.4	3.6	2.5	17.4	211	50.3	105.6
Zn	12	65	89	13	14	33	62	1258	239	3266
Ag	0.1	0.1	0.2	<0.1	<0.1	<0.1	<0.1	3.1	7.4	3.8
Ni	2.6	1.7	6.5	687.8	924.9	2095.1	>10000.0	>10000.0	471.4	356.5
Co	14.6	3.7	5.3	42.5	58	95.8	1478.7	488.1	32.1	16.6
Mn	44	62	302	1527	1121	1538	941	3776	60	698
Fe	4.66	2.26	5.24	3.25	2.38	5.31	3.72	24.81	4.55	17.63
As	25.2	27.9	42.7	8	5.3	34.7	1083.5	>10000.0	127.7	1084.9
U	3.3	1.3	4	0.3	0.3	0.5	4.3	5	2.4	4.4
Au	12.2	50.2	158	4.4	34.6	1.8	8.8	60	28.7	406
Th	13.5	12.7	12.5	<0.1	0.2	<0.1	<0.1	0.1	0.3	2.2
Sr	6	8	21	155	148	226	50	41	278	51
Cd	<0.1	<0.1	0.2	<0.1	<0.1	<0.1	0.2	3.3	3.9	67.7
Sb	0.8	0.2	1.6	1	0.2	3.6	59.9	528.7	146	55.5
Bi	1.2	2.8	5.2	<0.1	<0.1	<0.1	<0.1	<0.1	32.5	10.9
V	8	8	9	34	23	29	7	92	10	43
Ca	0.04	0.11	0.75	24.89	28.84	19.62	3.86	21.89	0.11	1.93
P	0.025	0.028	0.164	0.002	0.003	0.002	0.003	0.038	0.013	0.051
La	20	22	18	2	3	2	<1	3	<1	2
Cr	3	4	6	870	1102	1700	436	823	34	109
Mg	0.21	0.08	0.2	4.58	2.42	7.42	2.26	0.39	0.05	0.16
Ba	11	55	21	13	11	23	57	289	79	852
Ti	<0.001	<0.001	0.001	0.001	<0.001	0.002	<0.001	<0.001	<0.001	<0.001
B	2	3	3	<1	<1	<1	<1	<1	<1	<1
Al	0.85	0.66	0.7	0.31	0.4	0.51	0.09	0.13	0.36	1.3
Na	0.013	0.026	0.01	0.002	0.001	0.002	<0.001	0.001	0.001	0.002
K	0.35	0.37	0.37	<0.01	0.01	<0.01	<0.01	0.04	0.05	0.11
W	0.1	<0.1	<0.1	0.4	0.7	6.7	0.7	6.7	<0.1	0.2
Hg	<0.01	<0.01	0.02	<0.01	0.01	0.28	3.11	19.46	3.45	4.5
Sc	0.7	1.2	0.9	6.7	9.3	8.7	2.9	9.2	1.3	3.5
Tl	0.4	0.3	0.3	<0.1	<0.1	0.5	19.9	73.8	0.6	2.3
S	4.15	1.64	2.27	<0.05	<0.05	<0.05	<0.05	<0.05	0.67	0.07
Ga	2	2	1	<1	2	1	1	3	<1	2
Se	10.8	1.4	2.5	<0.5	<0.5	1.1	<0.5	0.8	<0.5	0.7

4.1.8 Light-weight concrete. In recent years, numerous studies have been conducted on natural construction materials and their engineering applications, both in Turkey and in the rest of the world. In addition to aggregates derived from natural deposit of sand and gravel and from crushing of quarry rocks used for producing concrete, tuff aggregates could be used for lighter concrete as puzzolan. Tuffs in the Şaphane area, despite their high porosity and low compressive strength, can be used to form both concrete and/ or satisfactory natural building stones. The tuffs are essentially vitritic and vitritic-crystal tuffs with varied proportions of pyroclasts, pyrogenetic and secondary minerals. These tuffs can be used as light-weight concrete aggregates.

4.1.9 Limestone: At the Yeşilova and Soğuksu areas, limestone deposits occur, being extracted from the limestone quarry in the past, for the manufacture of lime.

4.2. Energy resources

The Simav Graben area has a potential for the geothermal resources. Geothermal energy is an alternative energy resource, since it has low CO_2 emission and it is renewable and sustainable. Potential for geothermal energy exists at several known sites in the region, although they are not yet explored. Potential sites include the hot springs at Eynal, at Çitgöl in Simav District and at Abide in Gediz District. Local heating system in Simav has been supplied by geothermal energy.

5. Conclusions

Our field examination of the mineral and energy resources discussed in this article revealed that Simav Graben has a significant amount of commercially viable reserves. When alunite professionally mined, hundreds of millions of dollars of alunite rough could be produced. The future prospects for commercial development appear to be excellent. Zeolite occurrences in the volcano-sedimentary and pyroclastic rocks have an economically important potential. Zeolite deposits could be explored after detailed investigations. The study of the porphyry Cu-Mo deposits in terms of detailed geological and geochemical investigations will contribute to the regional development. In the region, production of the building insulation materials (briquette) with pumice-rich tuffs will provide to new job opportunities. The use of geothermal energy in the greenhouses can contribute to the revival of the agriculture.

Acknowledgments

References

Akdeniz N. and Konak N., 1979. The setting of the metabasic and metaultramafic rocks and the rock units in the region of Simav, Menderes Massif, Bulletin of the Geological Society of Turkey, 22, 175-184. (In Turkish).

Ataman G., 1977. Zeolite occurrences *in* west Anatolia, Bulletin for Earth Sciences, 3-1. 85-94. (In Turkish).

Ercan T., Satır M., Günay E., Savaşcın M.Y., 1984. Regional interpretation of the Cenozoic volcanism from Simav and the surroundigns. Bulletin of the Mineral Research and Exploration. 97/98, 86-101. (In Turkish).

Gleeson S.A., Herrington R.J., Durango J., Velázquez C.A. 2004. The mineralogy and geochemistry of the Cerro Matoso S.A. Ni laterite deposit, Montelíbano, Colombia. Economic Geology, 99 1197-1213.

Gündoğdu M.N., Yalçın H., Temel A., Clauer N., 1996. Geological, mineralogical and geochemical characteristics of zeolite deposits associated with borates in the Bigadiç, Emet and Kırka Neogene lacustrine basins, Western Turkey. Mineralium Deposita, 31, 492-513.

Hatipoğlu M., Babalık H., Chamberlain S.C., 2010. Gemstone deposits in Turkey. Rocks & Minerals, 85, 124-132.

Helvacı C., Stamatakis M., Zagouroğlou C. Kamaris J., 1993. Borate minerals and related authigenic silicates in northeastern Mediterranean Late Miocene continental basins. Explor. Mining Geol., Vol. 2, No. 2, 171-178.

Helvacı C. and Alonso R.N., 2000. Borate deposits of Turkey and Argentina; a summary and geological comparison. Turkish Journal of Earth Sciences, 24, 1-27.

Helvacı C. and Yağmurlu F., 1995. Geological setting and economic potential of the lignite and evaporite-bearing Neogene basins of Western Anatolia, Turkey. Isr. J. Earth Sci., 44, 91-105.

Innocenti F., Agostini S., Vincenzo G. Di., Doglioni C., Manetti P., Savaşcın M.Y., Tonarini S., 2005. Neogene and Quaternary in Western Anatolia: Magma sources and geodynamic evaluation, Marine Geology, 221, 397-421.

Karayiğit A.I. and Whateley M.K.G., 1997. Chemical characteristics, mineralogical composition and rank of high sulphur coking coals of Middle Miocene age in the Gokler coal field, Gediz, Turkey. From Gayer, R. & Pesek, J. (eds), 1997, European Coal Geology and Technology, Geological Society Special Publication No. 125, 115-130

Mutlu H., Sariiz K., Kadir S., 2005. Geochemistry and origin of the Şaphane alunite deposit, Western Anatolia, Turkey, Ore Geology Reviews, 26, 39-50.

Oygur V. and Erler A., 2000. Metallogeny of the Simav Graben (Inner-Western Anatolia, Turkey). Bulletin of the Geological Society of Turkey, 43-1, 7-19. (In Turkish)

Semiz B., 2010. Mineral-chemistry of Ilicaksu Lamproitic dykes from Gediz region, western Anatolia, Abstracts with Programs, GSA Denver Annual Meeting USA, Session No. 33 Paper no. 33-27.

Semiz B., Schroeder P.A., Özpınar Y., 2011. Zeolitization of Miocene tuffs the Saphane – Gediz – Hisarcık regions, Kutahya-western Anatolia, (Turkey). Euroclay 2011. Antalya. p. 232.

Seyitoğlu G., Duncan A., Geoff N., Scott B., 1997. The evolution from Miocene potassic to Quaternary sodic magmatism in western Turkey: implications for enrichment processes in the litospheric mantle. Jour. of the Volc. and Geoth. Res. 76, 127-147.

Snellings R., Haten van T., Machiels L., Mertens G., Vandenberghe N., Elsen J., 2008. Mineralogy, geochemistry and diagenesis of clinoptilolite tuffs (Miocene) in the central Simav graben, Western turkey, Clays and Clay minerals, 56-6, 622-632.

RELATIONSHIPS BETWEEN CRUSTAL FAULTS, SHALLOW MAGMATIC CHAMBER AND NEOGENE PORPHYRY CU-AU SYSTEMS AT VOIA, METALIFERI MTS., ROMANIA

Ion BERBELEAC[1*], Vlad RĂDULESCU[1], Elena-Luisa IATAN[2], Mădălina VIŞAN[1]

[1]Institute of Geodynamics of the Romanian Academy, 19-21 Jean-Louis Calderon St., Bucharest-37, Romania, R-020032, Tel: +021.317.2126 ion.berbeleac@geodin.ro; ionberbeleac@gmail.com; danamadalina@yahoo.com.

[2] University of Bucharest, Faculty of Geology and Geophysics, 6 Traian Vuia St., Bucureşti, sector 2, Romania, luisaiatan@yahooo.com

Abstract The Voia area is situated in south part of Golden Quadrilateral, Metaliferi Mountains, Western Romania. In a very narrow area ($\sim 1 km^2$) from this region Magnetotelluric Sounding (MTS) data, partially checked with 18 exploration diamond drillings, have been identified a set of three crustal fault, two E-W and one NE-SW which were the major channels for Neogene magmas and related fluids rich in Cu, Au, Ag, Pb and Zn. The E-V faults are the hosts of three low-grade porphyry epithermal Cu – Au and epi - mesothermal Au-Ag, Pb, Zn, Cu systems. These systems are superimposed on a complex and poly-stage hornblende $\pm$ biotite quartz andesite – quartz porphyry microdiorite intrusions, probably Sarmatian in age (12-11 Ma ?). According to exploration drillings the porphyry Cu - Au systems are developed below 150-300m (<0.1% Cu) and are known down to 1200 m depth (0.5 – 0.6% Cu, $\sim$ 0.6 g/t Au) in the deepest drilling (e.g. no 19). The shape of these intrusions is stocks-like with large lateral extents. The high-sulphidation (HS) alteration is present until 700 - 800m down where, the dominant veins mineral assemblage (pyrite - marcasite – gypsum-clay minerals $\pm$ chalcopyrite, magnetite, base metal sulfides gradually superposed with probably younger low-sulphidation (LS) mineral assemblage (native gold-base metal sulfides-carbonates-quartz $\pm$ anhydrite (e. g. drilling no 17, vein m. 964 – 964.30 = 87 g/ t Au, this means $\sim$ 306 below the sea level. In porphyry system, gold is associated with chalcopyrite. The andesitic – microdioritic intrusions have deep roots at about 2 - 2.5 km in the upper parts of shallow magmatic chambers. The sizes and forms of these magmatic chambers have been especially influenced by the old thrusting planes, a fact that explains their forms and sizes.

Keywords: crustal faults, shallow magmatic chamber, Neogene mineralizations, Voia, Metaliferi Mountains.

1.Introduction

The Voia area is situated in southwestern part of the Golden Quadrilateral (GQ), Metaliferi Mountains (MM), South Apuseni Mountains (SAM). It lies at ca. 4 km northeast of the Hondol-old mining center (Fig.1). Within upper part of this Miocene volcanic area, in the 70's and 80's of last century, two state companies, ISEM and IPEG Deva, later MINEXFOR Deva, carried out 18 exploration diamond drillings (EDD), and later, in 2003, the Institute of Geodynamic of Romanian Academy undertook 29 Magnetotelluric Soundings (MTS) (Berbeleac et al, 2003, unpubl.). The target of these works was to investigate a large zone of advanced argillic alteration and related structure and mineralization. This paper is a review of selected available data, details can be found in Ghitulescu and Socolescu (1941), Ianovici et al., (1976), Berbeleac, (1975, 2003), Berbeleac et al. (1985, 2003, (unpubl.), 2010), with emphasis on the results obtained of 29 MTS and 18 EDD.

2. Regional setting

The Tertiary geotectonic evolution of the south MM, in the Voia area is shown by a continuous tectonic regime associated to main deformations happened within Tisza block (Csontos, 1995, in Seghedi, 2004) and Transylvanide unit (Sandulescu, 1984). A successive compression - extension events occurred along the contact between South Carpathians and SAM – South Transylvania Fault systems (Sandulescu, 1984) and Halmagiu - Brad - Sacaramb Basin. As a consequence of these events, the basement crystalline schists and / or ophiolites and their Mesozoic and Lower - Middle Miocene cover deposits underwent great varieties of deformations (faulting, rifting and graben-like small pull-apart basins) all or partially caused by rapid (14-12 Ma) Tisza block clockwise rotation ($\sim 60^0$ C, Panaiotu et al., 1998, in Seghedi, 2004). This setting was favorable for development of the Miocene (14-7.4 Ma) - Pliocene (1.6 Ma, Rosu et al., 2004, Seghedi, 2004) dominant andesitic, calc-alkaline, partial adakitic-like volcanism (Seghedi et al., 2004) and Miocene related mineralizations.

3. Geology of the study area

The upper part of Voia valley is located within the Paleogene Voia graben (VG) structure (Fig.1, 2) which is a Cenozoic rifting system belonging to Halmagiu – Brad – Sacaramb Basin (HBSB), and related to active basin of back-arc continental margins. At the surface in the Voia area there are lava flows and intrusions of Sarmatian - Pannonian Sacarâmb and Cetras hornblende, biotite ± pyroxene K quartz andesite types (12.4-10.27 Ma, Rosu et al., 2004), as the products of Coasta Mare (10.35 ±0.43 Ma), Geamana, Paua (12.40 ± 1.04 -10.27 ± 0.64), Momeasa, Buha, Cetras (11.7 ± 0.5 Ma) and Macris volcanoes (Berbeleac, 1975, 2003), further, from younger to older following (Fig. 1, 2): a) thee Badenian - Sarmatian andesitic volcano-sedimentary formation; b) the Upper Badenian (?) bedded layers of andesitic - dacitic massive lapilli-ash tuffs (hybrid rocks, Berbeleac et al., 2010); c) the Paleogene Fata Baii volcano-sedimentary Formation; d) Upper Jurassic- Lower Cretaceous limestones and flysch formations (Ardeu nappe); e) the Eo-Cretaceous intrusions; f) the Upper Jurassic-Lower Cretaceous sedimentary rocks (Ardeu nappe); g) the Middle Jurassic ophiolites and Late Jurassic calc-alkaline island arc volcanic rocks (Drocea - Techereu nappe) and h) probably, the crystalline schists. Towards the depth, these formations and tuffs are well developed; and are intruded by three successive Sarmatian calc-alkaline rocks of Voia subvolcanic bodies (VSB): being built from hornblende ± biotite quartz andesite – quartz porphyry microdiorites (Barza type), hornblende – biotite quartz andesite – quartz porphyry microdiorites (Arsitei Hills type, Porcurea, Berbeleac, 1975), both syn-ore, and hornblende andesites, post ore; The VSB is a complex structure with poly-stage evolution. The Porcurea andesitic intrusion outcrops on the right slope of Macris Valley (Fig. 1), post-ore hornblende andesite appears as small dike, along NW-SE fault; the rest of VSB and related mineralizations, porphyry epithermal Cu-Au, pyrite (Au) skarn and epi-mesothermal Au-Ag-Pb-Zn-Cu are hidden.
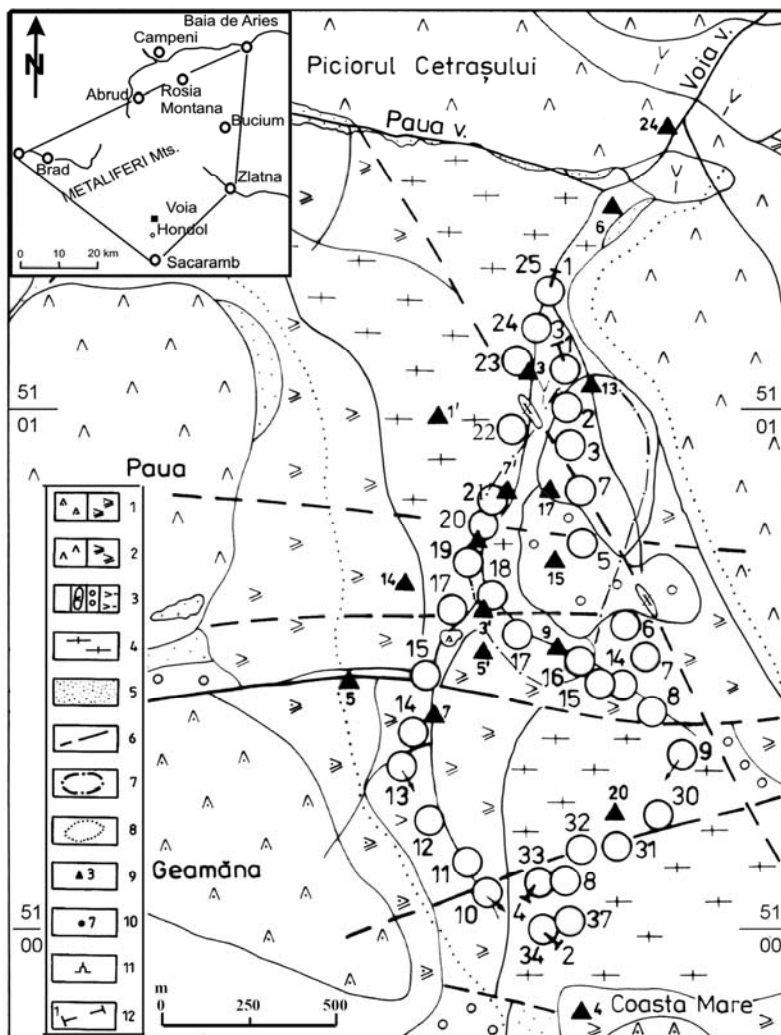

Fig. 1. Geological map of Voia area.
1. Hornblende, biotite, quartz ± pyroxene andesite (Cetras type, 11.7±0.5 Ma): a. intrusion; b. lava flows; 2. Hornblende, quartz ± biotite, pyroxene andesite (Sacarâmb type, 12.4 ± 1.04 Ma): a. intrusion; b. lava flows; 3. a. Hornblende, quartz andesite ± biotite, pyroxene (Barza + Arsita (Porcurea) types (12.4 ±1.2 Ma); b. hornblende andesite (dike, Barza type); c. pyroclastics hornblende andesite; d. Badenian tuffs (hybride rocks); 4. Badenian - Sarmatian volcano-sedimentary formation; 5. Fata Baii Paleogene molasse; 6. Fault; 7. Surface projection limit of porphyry Cu-Au mineralization; 8. Approximate limit of advanced argillic alteration; 9. Diamond drill; 10. MTS; 11. Gallery; 12. Cross-section**.**

4. Methodology of research and field work conditions

The Voia deep structural image is the result of field mapping, laboratory studies and processing and interpretation of 29 MTS and 18 EDD. Field measurements have been carried out with ADU-06 station using the LF1 and LF2 frequency bands (Radulescu, in Berbeleac et al., 2003, unpubl.). For each MTS the maximum resistivity values have been processed and modeled using the acquisition by MAPROS soft and IPI-MTS inversion soft. The MTS have been performed on three lines situated in upper part of Voia Valley, from which only 1 and 2 were chosen for interpretation data (Fig. 2 a, b). The MTS survey covered a surface of 1 km^2 (Fig. 1).
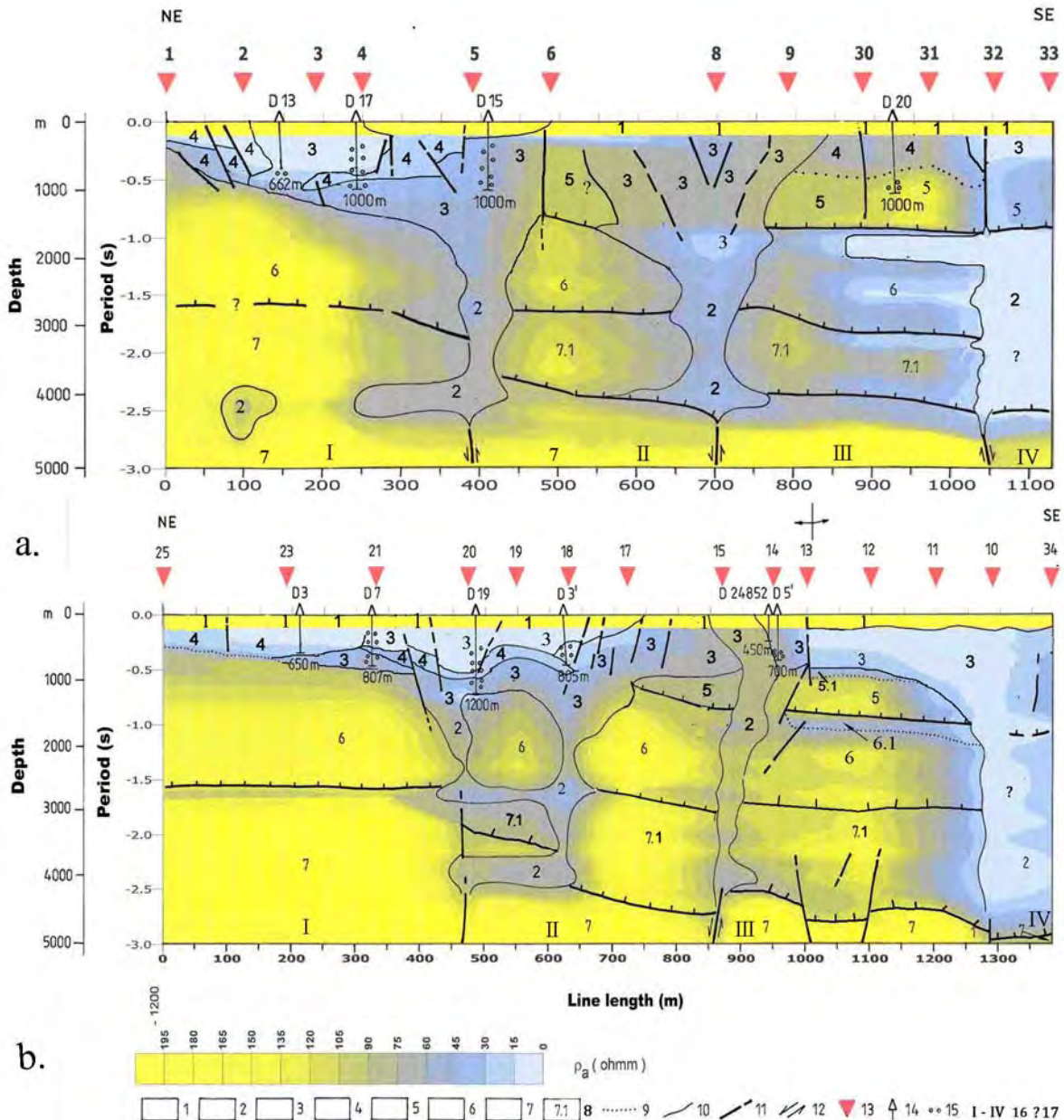

Fig. 2: Geologic cross-section with interpretation of resistivity values along line 1 (a) and 2 (b). 1. Dominant Badenian-Sarmatian volcanogenic-sedimentary Fm. + Fata Baii Fm; 2. Shallow magmatic chambers (dominant intrusive rocks); 3. Voia subvolcanic bodies (porphyry types); 4. Dominant Badenian – Sarmatian, Badenian and Paleogene (Fata Baii molasses) volcano-sedimentary formations, inclusive Lower Cretaceous sedimentary formatione; 5. Upper Jurassic - Lower Cretaceous sedimentary formations (dominant limestones) - Ardeu nappe; 6. Ophiolites + island arc calc-alkaline rocks (Drocea-Techereu nappe); 7. Baia de Aries (nappe) crystalline formation; 8. Biharia nappe; 9. Unconformity boundary; 10. Nappe; 11. Fault; 12. Sense of movement; 13. MTS; 14. Drill; 15. The Cu-Au mineralization in drill; 16. I-IV tectonic blocks; 17. unknown unit.

The field work conditions have been the followings: a) 45^0 -5^0 slope angles; b) the ground slopes had electrical sensors situated at W and E of lines 1 and 3 and NE of line 2; c) the soil thickness was 1-2m and under it a very pronounced iron cap and d) 60-175m the distance between MTS. Total length of the lines was about 2,800m and 550 h the total measurement time and 5000m the investigation depth. Through processing data have been obtained: 1) theoretical and measurement curves of resistivity and phase after N-S direction and at 0.01″-3.00″ period of seconds; 2) the average values of resistivity, the thickness and the depth for each line and sounding and 3) the inversions for each sounding. The drills have been vertically drilled (diamond drillings), roughly in a 100x100 m network with 450-1200 m depths, totalizing about 15,000m.

5. Results

The analysis of the resistivity values distribution for each MTS and their cumulate values for each line (cross-section), together with field mapping and EDD data, allow us to emphasize the followings (Fig. 2 a, b): a) the depth structural image of Voia area, in contrast with others Tertiary volcanic centers from Romania, shows a direct relationship and temporal transition from the deposition of porphyry epithermal Cu - Au, Ca - Mg skarns and epi-mesothermal Au - Ag - Pb - Zn - Cu systems with shallow magmatic chambers (SMC); b) a set of three CF which pass 5 km in depth, two E-W and other NE-SW- probably the master fault - and old thrustings (Drew, 2005) controlled the magmas uplift, the configuration and poly-stage evolution of SMC and the eastern margin of HBSB and the small VG - a pull-apart basin: c) the CF have been the main conducts for magmas and related ore fluids rising and their architecture allowed us to divide the area into four mini-blocks noted I to IV; d) in general, has been established the lithology of each block on 5km depth; the discovery a "blind" low-grade porphyry epithermal Cu – Au, HS and LS systems, consisting of three Sarmatian andesite poly-stage bodies, in which the contents increase towards the depth from < 0. 1% Cu, at 100 – 200 m below surface, to 0.5 – 0.6% Cu, ~ 0.6 g/t Au, in the deepest drilling (e. g., D no 19) and an epi-mesothermal Au-Ag, Pb, Zn, Cu vein systems, rich in native gold (D no 17, m 960 - 960. 30). The shape of these intrusions is stocks-like with large lateral extents.

6. Discussion

The Voia Valley represents a very complex structure which mainly consists of a small tectonic and thermal subsidence basin-like graben and pull apart basin cross-cut by crustal faults hosts of SMC and VSB porphyry epithermal Cu-Au low-grade HS and LS systems and LS epi-mesothermal Au-Ag-Pb-Zn-Cu systems (330-360^0 C =T_H of sphalerite fluid inclusions, Berbeleac et al., 1987), the both systems seem to be related to Barza and Porcurea andesite-quartz porphyry diorite intrusion types. In fact, this activity seems to continue with other two periods and systems: Macris (Sacarâmb, LS, Au-Ag-Pb-Zn-Cu (Te?) and Cetras (As-Au-Ag-Pb-Zn-Cu) system (Udubasa et al., 1982). According to Sillitoe (1998, in Cooke et al., 2005) five ideal conditions are necessary for formation porphyry copper deposits: 1) the compression impedes magma ascent to upper crust; 2) the formation of SMC; 3) the fractionation of magmas and due to their inability to erupt the generation of large volumes of magmatic-hydrothermal fluids took place; 4) the compression which can form at the roof of large magma chamber and 5) rapid uplift and transport of magmatic fluids and the deposit formation. All these keys can explain the direct connection between CF / SMC / porphyry system in Voia structure. Concerning tectonic micro-blocks and their lithology we point out that this supports discussions, especially regarding the blocks no III and IV, in the last the ophiolites seems to be absent.

7. Conclusions

The Voia area is a very complex Miocene structure which consists of seven andesitic volcanoes situated in a circular area of ~ 5km^2 and three subvolcanic andesite – quartz porphyry microdiorite and related porphyry epithermal Cu-Au, pyrite - Ca - Mg skarns and epithermal Au-Ag-Pb-Zn-Cu systems. The roots of VSB are within SMC hosted by three CF. This area can be considered of high economic potential.

References

Berbeleac I., 1975. The Petrographic and Metallogenetic Study of Valisoara (Porcurea), Metaliferi Mountains. Anuarul Institutului Geologic si Geofizic, Ph.D. Thesis, XLVI, 189 p., Bucharest

Berbeleac I., 2003. Time-Space geodynamic evolution of Tertiary magmatic and metallogenetic activity in South Apuseni Mountains, Romania. Studii si Cercetari de Geofizica, 41, p. 19-56, Bucharest.

Berbeleac I., Zamarca Alla, David Margareta, Tanasescu I., Berinde N., 1985. The porphyry copper deposit at Voia, Metaliferi Mountains. Dari de Seama, Institutul de Geologie si Geofizica, vol., LXIXX / 2, p. 5-26 Bucharest.

Berbeleac I., Lazar C., Anastase S., 1987. Gold Occurrences from Voia, Metaliferi Mountains. Buletinul Universitatii Bucuresti, p.19-31, Bucharest.

Berbeleac I., Radulescu V., Visan M., 2003. Deep structure of Voia area, Metaliferi Mountains. Unpublished Report, Institute of Geodynamics, Romanian Academy. Bucharest.

Berbeleac I., Zugravescu D., Radulescu V., Iatan Elena-Luisa, 2010. Deep Neogene volcanic structure and related mineralizations from Voia area, Metaliferi, Romania. Seventh National Symposium on Economic Geology "Mineral Resources of Charpathians Area", Baia Mare. Romanian Journal of Mineral Deposits, 84, p. 38-40, Bucharest.

Cooke R. D., Hollings P., Walshe J. L., 2005, Giant Porphyry Deposits: Characteristics, Distribution, and Tectonic Controls. Economoc Geology, vol. 100, 5, p. 801-818.

Drew J. L., 2005, A tectonic model for the Spatial Occurrence of Porphyry Coppper and PolymetallicVein Deposits – Applications to Central Europe. Scientific Investigations Report 2005-5272, U. S. Geological Survey, 36 p.

Ghitulescu T., P, Socolescu M., 1941. Ètude géologique et miniére des Monts Mètalifères. Anuarul Institutului Geologic al Romaniei, XXI, p.181- 463, Bucharest.

Ianovici V., Borcos M., Bleahu M., Patrulius D., Lupu M., Dimitrescu R., Savu H., 1976, The Geology of Apuseni Mountains (In Romanian), Editura Academiei Romane, 631 p., Bucharest.

Rosu E., Seghedi I., Downes H., Alderton D.H.M., Szakacs A., Pecskay Z., Panaiotu C., Panaiotu C.E., Nedelcu L. 2004. Extension-related Miocene calc-alkaline magmatism in the Apuseni Mountains, Romania: Origin of magmas. Schweizerische Mineralogische und Petrographische Mitteilungen 84, p. 153–172.

Sandulescu M., 1984. Geotectonics of Romania (In Romanian). Editura Tehnică, 334 p., Bucharest

Seghedi I., 2004. Geological evolution of the Apuseni Mountains with emphasise on the Neogene magmatism a review. In: N.J. Cook & C.L. Ciobanu (Eds.), 2004, Au-Ag-telluride Deposits of the Golden Quadrilateral, Apuseni Mountains, Romania, Guidebook of the International Field Workshop of IGCP project 486, p. 5-23, Alba Iulia, Romania.

Seghedi I., Downes H., Szakács A., Mason P.R.D., Thirlwall M.F., Rosu E., Pécskay Z., Márton E., Panaiotu C., 2004. Neogene - Quaternary magmatism and geodynamics in the Carpathian-Pannonian region: a synthesis. Lithos 72: 117-146.

Udubaşa G., Istrate Gh., Vălureanu M., 1982. Metallogeny of Coranda – Hondol, Mtaliferi Mountains. (in Romanian) Dari de Seama IGR, LXVII/2 (1979-1980), p. 197-232, Bucharest.

NEOGENE GOLD MINERALIZATION OCCURRENCES IN VOIA AREA, METALIFERI MOUNTAINS, ROMANIA

Ion BERBELEAC[1], Mădălina VIŞAN[1], Elena-Luisa IATAN[2]

[1]Institute of Geodynamics of the Romanian Academy, 19-21 Jean-Louis Calderon St., Bucharest-37, Romania, RO-020032, Tel: +021.317.2126; ion.berbeleac@geodin.ro; ionberbeleac@gmail.com; danamadalina@yahoo.com.

[2] University of Bucharest, Faculty of Geology and Geophysics, 6 Traian Vuia st., Bucureşti, sector 2, Romania, luisaiatan@yahooo.com.

Abstract Three crustal faults are hosts of shallow magmatic chambers and a complex polystage subvolcanic andesite- porphyry quartz diorites and related porphyry epithermal Cu-Au, pyrite-Ca-Mg skarns and epi-mesothermal Au-Ag-Pb-Zn-Cu system. According to drills data and laboratory studies, in vertical scale, the alteration-mineralization mineral assemblages belong to two zones: HS products in upper part (300-500m) where, dominantly are present the advanced and intermediate argillic alterations with sulfide-sulphate veins (pyrite, marcasite, minor base metal sulfides, Fe oxides, gypsum, anhydrite and alunites, vuggy quartz). All pyrite-anhydrite veins and pyrite substitutions are poor in gold; from 500-1200 m the HS mineral assemblages gradually decrease in favor of IS and LS products characterized by a coexistence of LS assemblages (sericite-illite, chlorite, adularia, calcite, carbonates, ± anhydrite, native gold, base metal sulfide veins) very rich in gold, with IS assemblages (anhydrite, quartz, iron oxides, chalcopyrite, pyrite). The IS and LS assemblages overprint the HS mineral associations, the result being a transition zone characterized by mineral assemblages rich in gold like HS as quartz-anhydrite-pyrite-chalcopyrite-iron oxides and/IS+LS as carbonates, quartz, native gold, pyrite, base metal sulphides.

Keywords: high-low sulphidation, Neogene, porphyry epithermal Cu-Au, epi-mesothermal Au-Ag-Pb-Zn-Cu, Voia

1. Introduction

Voia area is situated in central southern part of the Golden Quadrilateral, Metaliferi Mountains (MM), at about 6 km north-west of Săcărâmb. In this area, 18 drills and 29 Magnetotelluric Soundings (MTS) have been achieved by MINEXFOR Deva, and respectively, the Institute of Geodynamics of Romanian Academy (Berbeleac et al., 2003). This paper is a synthesis concerning the gold from known Neogene mineralizations of Voia area.

2. Regional setting

The Tertiary geotectonic evolution of the MM, in general, and surrounding Voia area, in particular, has been especially controlled by rapid Tisza-Dacia clockwise rotation (14-12 Ma, ~60^0, Panaiotu et al., 1998, in Seghedi, 2004). Successive compression-extension events occurred along the contact between South Carpathians and MM, among the consequences being the South Transylvania Fault systems and Halmagiu-Brad-Sacaramb Basin with their subsidiary rifting, faulting, and graben-like small pull-apart basins, the Neogene volcanic and metallogenic activity.

3. Geology of the study area

The Voia area belongs to the Săcărâmb-Cetras-Cordurea Miocene volcano-tectonic alignment (Berbeleac, 1975). At the surface it consists of: 1) two Sarmatian (12.4-10.27 Ma, Rosu et al., 2004, in Seghedi 2004) hornblende-biotite ± pyroxene quartz andesite (Cetras type) and hornblende ± biotite-pyroxene quartz andesite (Săcărâmb type) as intrusions and lavas, proceeded from Cetras, Buha, Momeasa, Paua, Geamana, Coasta Mare and Macris volcanoes; 2) the Badenian-Sarmatian andesitic volcaniclastic and volcanogenic-sedimentary formation, Paleogene Fata Baii volcano-sedimentary formation. Toward depth, the intrusions of Voia subvolcanic bodies (VSB), the Lower Cretaceous-Upper Jurassic limestones (Ardeu Nappe), the Middle Jurassic ophiolites and Upper Jurassic island arc volcanic rocks (Drocea-Techereu Nappe) and probably Baia de Aries and Supragetic crystalline schists are present. A set of three crustal faults (CF), two E-W, one NE-SW cuts the structure and they are hosts of Shallow Magmatic Chambers (SMC) and VSB with related porphyry epithermal Cu-Au, pyrite (Au)-Ca-Mg skarns and epi-mesothermal Au- and Ag-Pb-Zn-Cu. The VSB represents a complex polystage subvolcanic structure composed of three individual bodies, in upper part probably in connection, occurred on about 600 m in the right slope of Macris Valley. These bodies consist of syn-ore hornblende ± biotite quartz andesite - quartz porphyry microdiorites (Barza type), hornblende-biotite quartz andesite - quartz porphyry microdiorites (Arsitei Hills type, Porcurea, Berbeleac, 1975), and post-ore hornblende andesites. The intrusion roots are probably at 2-2.5 km below the surface where they are directly connected with SMC.

4. Gold in Voia mineralizations

In Voia area, gold is present in all types of the identified mineralizations: porphyry epithermal Cu-Au, epi-mesothermal carbonate veins with gold base metal sulfides, quartz veins with pyrite-chalcopyrite-magnetite ± hematite ± anhydrite veins, anhydrite veins with base metal-sulfosalts, anhydrite veins with pyrite, anhydrite ± quartz veins with pyrite ± magnetite, vuggy quartz (silica residue) and gold poor pyrite veins and impregnations in porphyry systems (Table 1).

Although, these types of mineralizations have been previously described (Berbeleac et al., 1985, 1987), the following remarks will be presented, with respect to the gold (Table 1): 1) in porphyry copper system the gold and copper average contents in drill no 19, m 750-1190 = 0.2612 g/t and 0.315 % Cu and in collective concentrate (laboratory test) are 14.8 g/t Au and 30 g/t Ag (Au:Ag =1:2); 2) in porphyry systems gold is concentrated in chalcopyrite (no 7, 19, 37) of pyrite-chalcopyrite-magnetite-hematite-quartz assemblage from late potassic stage. The major amount of gold from chalcopyrite dominantly seems to be submicroscopic; 3) pyrites of anhydrite veins from early potassic stage ± phyllic alteration are relatively poor in gold (no 1-6; 8-14), while the highest gold contents are present in pentagonal dodecahedron pyrites (no 33, 38, 39) of pyrite-chalcopyrite-magnetite ± hematite-quartz assemblage from late potassic stage ± phyllic alteration; 4) pyrites of anhydrite veins with magnetite seem to be poor in gold (no 29, 28, 15, 11, 8); 5) carbonate vein with gold-bearing base metal sulfides intercepted by drill no 17, m 960.00-960.30, is the richest ore in gold.

The andesitic host rock contains sericite, chlorite, calcite, quartz, clay minerals, adularia and minor anhydrite; chloritization is dominant and increases outwards the vein. The drilling from the surface to depth crossed on 700 m hornblende-biotite quartz andesite (Porcurea type) with first 200-300 m highly argillized and further chloritization is prevalent. The interval between m 700-1000 frequently contains occurrences of porphyry microdiorite; the porphyry epithermal systems occur between m 750-1000. The vein have a zone with the maximum thickness of 5 cm, massive ore consists of native gold, pyrite, sphalerite, galena, chalcopyrite, calcite, minor quartz and anhydrite. The main features of these minerals are as follows: pyrite shows scarce cubic crystals; usually it appears fissured, veined, corroded and / or replaced by subsequent minerals (Fig. 1b). Sphalerite is the most common and abundant base metal sulfide. It occurs as coarse-grained aggregates. Some of the grains show, in place, zonal and exsolution chalcopyrite bodies (1-10μm) sometimes are oriented along of crystallographic planes of sphalerite (Fig.1c, d). Galena occurs as fine to medium-grained aggregates. It is frequently associated with native gold, sphalerite and chalcopyrite (Fig.1a). Chalcopyrite occurs as fine globular or irregular exsolutions blebs within sphalerite. It fills the fissures and contacts between minerals and frequently is associated with galena and native gold (Fig. 1a). Native gold appears as fine inclusions in ore minerals (5-20 μm). Large aggregates of native gold (>50 μm) appear at mineral limits and along the fissures (Fig.1a-d). Visible gold grains have been observed in calcite. The color of gold is bright "golden" yellow. The Au:Ag ratio in base metals sulphide ore is 5:1. This suggests that native gold had formed at relatively high temperature which is in agreement with the homogenization T of fluid inclusions from sphalerite of 330-360^{0}C (Berbeleac et al., 1984) and 6) ore vuggy quartz as centimeter-decimeter blocks are known in south part of Geamana Hill. These blocks are the silica residue resulted from most acid-altered rocks. They have dark colors and spongious texture. Fine pyrite aggregates are visible within voids. The gold content is ~ 2g/t.

5. Discussion and conclusions

In Voia area the most important results obtained through drilling and magnetotelluric exploration works can be summarized, such as: 1) a new structural image point out by SMC, the VSB and the CF - the main conducts of magmas and related ore fluids in their way to surface; 2) the existence of VSB consisting of three Neogene andesite-porphyry microdiorite bodies and related porphyry epithermal Cu-Au, Py-Ca-Mg skarns and epi-mesothermal Au-Ag-Pb-Zn-Cu systems and 3) the Voia mineralizations are genetically and spatially related to VSB systems and belong to HS and IS+LS alteration styles and show a vertical zonality: HS products in upper part (300-500m) where, dominantly are the advanced and intermediate argillic alterations with sulfide-sulphate veins (pyrite, marcasite, minor base metal sulfides, Fe oxides gypsum, anhydrite and alunites). All pyrite-anhydrite veins and pyrite substitutions are poor in gold; from 500-1200 m the HS mineral assemblages gradually decreasing in favor of IS+LS products characterized by sericite (illite), chlorite, adularia, calcite, carbonates, native gold, base metal sulfide ± anhydrite, iron oxides. The IS assemblages are overprinted on HS mineral association, the result being a transition zone characterized by mineral assemblages rich in gold like HS as quartz-anhydrite-pyrite-chalcopyrite - iron oxides and / or IS as quartz-native gold-pyrite-base metal sulphides.

Table 1. The gold contents of some minerals from Voia Neogene mineralized structure

No	Drill No. /meter	Mineral/texture	Veins + veinlets cm. /mineral assemblage	Rocks / alteration types	Au g/t
1	D1 / 591	Coarse grn. py	~1/py-anhy	Sandstone/inter argil	0.015
2	D7 / 358	Coarse grn. py	~1-2/py±anhy	Agl./ inter argil	0.045
3	D7 / 358	Coarse grn. py	1-2/py-anhy	Agl./ inter argil	0.075
4	D9 / 640	Coarse grn. py	~0.5/py-anhy	H-qtz-an/ Phyl.	0.028
5	D9 / 786	Coarse grn. py	~0.5/ py-anhy	H-bio-qtz-an/Phyl	0.148
6	D9 / 787	Coarse grn. py	~0.5/py-cp-mt-he-qtz-anhy	H-bio-qtz-an /Phyl-K	0.205
7	D9 / 815	Coarse grain cp	1-2/py-mt-he±cp-anhy	Qtz-pmd /Phyl-K	60.413
8	D9 / 817	Coarse grn. py	1-2/py±mt-anhy	Qtz-pmd /Phyl-K	0.059
9	D9 / 824	Coarse grn. py	1-2/py-qtz-anhy	Qtz-pmd /Phyl-K	0.072
10	D9 / 877	Coarse grn. py	1-2/py ±mt-anhy	Qtz-pmd /Phyl-K	0.342
11	D9 / 885	Coarse grn. py	1-2/py ±mt-anhy	Qtz-pmd /Phyl-K	0.233
12	D9 / 919	Coarse grn. py	1-2/py-anhy	Qtz-pmd /Phyl-K	0.055
13	D9 / 927	Coarse grn. py	1-2/py-anhy	Qtz-pmd /Phyl-K	0.012
14	D9 / 1030	Coarse grn. py	1-2/py-anhy	Qtz-pmd /Phyl-K	0.033
15	D9 / 1071	Coarse grn. py	1-2/py±mt-anhy	Qtz-pmd /K	0.976
16	D9 / 1184	Coarse grn. py	1-2/py-anhy	Qtz-pmd /K	1.190
17	D9 / 1082	Coarse grn. py	1 -2/py-anhy	Qtz-pmd /K	1.683
18	D9 / 984	Fine grn cp	<0.5/cp-mt-anhy	Qtz-pmd /K	12.870
19	D9 / 750-1190	Concen. cp			17.485
20	D9 / 750-1190	Concen. py			4.286
21	D9 / 750-1190	Concen. mt			0.170
22	D14 / 249	Coarse grn. py		Tuff / argil	0.257
23	D14 / 579	Coarse grn. py	<0.5/py-anhy	H-bio-qtz-an / inter.argil	0.014
24	D17 / 539	Coarse grn. py	<0.5/py-anhy	H-bio-qtz-an /pr	0.891
25	D17 / 911	Coarse grn. py	<0.5/py-anhy	H-bio-qtz-an / pr	0.141
26	D17 / 964	Coarse grn. py	31/cb-qtz±anhy-gold-py-bms	H-bio-qtz-an /pr	162.076
27	D17 / 964	Coarse grn. sph	31/cb-qtz ±anhy-gold-py-bms	H-bio-qtz-an /pr	450
28	D17 / 997	Coarse grn. py	<0.5 cm/py±mt-anhy	H-bio-qtz-an /pr	0.489
29	D19 / 415	Coarse grn. py	1cm/py±mt-anhy	H-bio-qtz-an / inter argil	0.028
30	D19 / 542	Fine grn mt	<0.5/py-cp-mt-chl-anhy	H-bio-qtz-an / pr	0.028
31	D19 / 704	Coarse grn. py (penta. dodec.)	3cm/py-anhy	Sandstone /hornfels	0.375
32	D19 / 764	Coarse grn. py	<0.5/py-qtz-anhy	Sandstone /hornfels	0.194
33	D19 / 920	Coarse grn. py (penta. dodec.)	0.1cm/py-cp±mt-anhy	H-bio-qtz- an / K	2.948
34	D19 / 966	Coarse grn py	0.5/py-cp-mt-he-qtz	H-bio-qtz- an/Phyl-K	0.255
35	D19 / 050+1022	Coarse grn py (penta. dodec.)	1/py-cp-mt-he-qtz	H-bio-qtz- an / K	1.857
36	D19/1050	Medium grn py	0.1-0.3/cp-mt±py-qtz	H-bio-qtz- an / K	0.460
37	D19/928 +1119	Medium grn cp	0.2/py-cp-mt-he-qtz	H-bio-qtz- an /Phyl-K	22.025
38	D19/1118	Coarse grn py (penta. dodec.)	0.1-0.2/py-cp-mt±he-qtz	H-bio-qtz- an /Phyl-K	3.829
39	D19/1150	Coarse grn py (trape. dodec.)	0.1-0.2/py-cp-anhy	H-bio-qtz- an /Phyl-K	0.22 3
40	D17/960.00-960.30	Coarse grn Au-bms	300/py-sph-gn-cp-cb-qtz-ad	H-bio-qtz- an /Phyl-K	87.00
41	D17/960.00-960.30	Medium grn py	300/py	H-bio-qtz- an /Phyl-K	510.281
42	D17/960.00-960.30	Coarse grn sph	300/sph	H-bio-qtz- an /Phyl-K	162.076

Abbreviations: Agl = andesite agglomerates; H-qtz-an = hornblende quartz andesite; H-bio-qtz- an = hornblende biotite quartz andesite; pmd = porphyry quartz microdiorites. Alterations: inter argil = intermediate argillic K=potassic; Phyl = phyllic; pr = propylitic. Minerals: ad=adularia; anhy = anhydrite; bio = biotite; cb = carbonates; cp = chalcopyrite; chl= chlorite; gn = galena; he = hematite; mt = magnetite; py = pyrite; qtz= quartz; sph = sphalerite. Crystal forms: penta = pentagonal; dodec = dodecahedron; trape=trapezoidal; grn= grain; concen=concentrate.
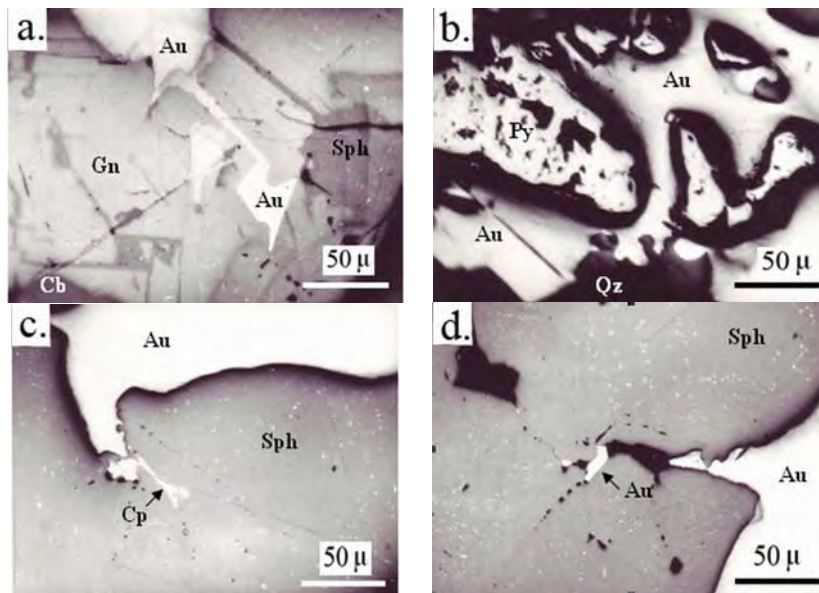
Fig. 1. Photomicrographs showing the relationships between native gold and pyrite, sphalerite, galena and chalcopyrite in vein from D no 17, m 960-00 - 960.30 (reflected light).
1a. Fissure fills with native gold and chalcopyrite in galena; 1b. Anhedral pyrite grains cemented by native gold; 1c. Fissures with native gold and chalcopyrite in sphalerite and 1d. Coarse aggregate of sphalerite with chalcopyrite exsolution bodies and a fissure deep penetrated in sphalerite filled with native gold and gangue.

Acknowledgements

References

Berbeleac I., Zamarca Alla, David Margareta, Tanasescu I., Berinde N., 1985. The porphyry copper deposit at Voia, Metaliferi Mountains. (in Romanian) Dari de Seama, Institutul de Geologie si Geofizica, vol., LXIXX / 2 (1982), 5-26. Bucharest.

Berbeleac I., Lazar C., Anastase S., 1987. Gold Occurrences from Voia, Metaliferi Mountains. (in Romanian) Buletinul Universitatii Bucuresti, 19-31, Bucharest.

Berbeleac I., Radulescu V., Visan M., 2003. Deep structure of Voia area, Metaliferi Mountains. (in Romanian) Report. Unpublished, Institute of Geodynamics, Romanian Academy. Bucharest.

Seghedi I., 2004. Geological evolution of the Apuseni Mountains with emphasis on the Neogene magmatism a review. In: N.J. Cook & C.L. Ciobanu (Eds.), 2004. Au-Ag-telluride Deposits of the Golden Quadrilateral, Apuseni Mountains, Romania. Guidebook of the International Field Workshop of IGCP project 486: 5-23, Alba Iulia, Romania.

THE TEMPORAL AND SPATIAL EVOLUTION OF MINERALIZATION CARRYING FRACTURE SYSTEM IN THE VALEA MORII DIORITE INTRUSION (APUSENI MTS.)

Tivadar Hunor Kun[1], Ferenc Molnár[1], István Márton[2], Gabriella Kiss[1], Dan Filipescu[3], Zsolt Veres[3]

[1]Depart. of Mineralogy, Inst. of Geography and Earth Sciences, EötvösLoránd University Budapest (ELTE), 1117 Budapest, Pázmány Péter sétány 1/C, tivadar.kun@gmail.com, 0036-308-746-807 (HU); 0040-752-270-668 (RO)
[2]Department of Geology, Babeş-Bolyai University, str. Mihail Kogalniceanu nr.1, 400084 Cluj-Napoca, Romania
[3]S.C. European Goldfields S.R.L. - Deva Gold S.A., str. Principala 89 C, Certeju de Sus, Romania

1. Introduction

The Valea Morii prospect, which has been in the focus of our research, is located in the southern part of the Apuseni Mountains, where Miocene calk-alkaline intrusive and volcanic units host numerous porphyry Cu–Au and epithermal Pb-Zn (Ag-Au) mineralization (Neubauer et al., 2005). The Valea Morii mineralization can be interpreted as a part of the 12.5-10 Ma old Barza Magmatic Complex along the Brad-Musariu-Valea Morii belt, with high gold endowment (Roşu et al., 2004; Kouzmanov et al., 2007). Mineralogical and structural data for the fracture systems of the Valea Morii diorite intrusion was collected and analyzed, in order to define mineral paragenetic sequences resulted by the different porphyry and epithermal mineralization stages, as well as the temporal and spatial evolution of the fracture system and hydrothermal alteration processes.

2. Methods

The hydrothermal veins in a homogenous environment always appear to be perpendicular to the minimal main stress direction (Tosdal and Richards, 2001). In deformed rocks, which are rich in cracks, the fluid flows are influenced not only by the present stress field, but also by the older generation of cracks and fractures. The presence or missing of hydrothermal vein system has an influence on the type of the mineralization. For this reason, geometrical analyses of veins may result in important information about the mineralization style. High grade-low volume hydrothermal ore deposits are usually characterized by a few veins, whereas ore deposits with low metal grades but large volumes usually contain many well-connected veins (Cox et al., 2001). Following these arguments, both mineralogical and geometrical analysis of the fracture systems of the Valea Morii porphyry mineralization was carried out. Data have been collected from the pit walls of the existing open pit at Valea Morii and from the VMSDD001 and VMSDD002 drill cores recently obtained by the SC European Godlfields SRL exploration company.

For data collection along the pit wall we followed the method presented by Benkó et al. (2008; also see Fig. 1): (1) from a chosen starting point, a horizontal base line was taken through the wall section; (2) all of veins crossing the base line were characterized according to the following parameters: the distance from the starting point of the base line, the dip and dip direction, the thickness, the extension and vein type/texture; and finally (3) the base line strike at the veins crossing points were measured and the rock type and alteration of the host rock was described. The same measurements were completed on the half drillcores, but in that case it was not possible to define the exact orientation and extension of the structures; the angle between the veins and the drill core axis was analyzable only (Fig. 2). Therefore, some of the statistical parameters independent from the dip-direction and angle of the veins and mineralogical-textural and wall rock alteration characteristics of veins from the half drill cores could be used only for comparison to data collected in the open pit.
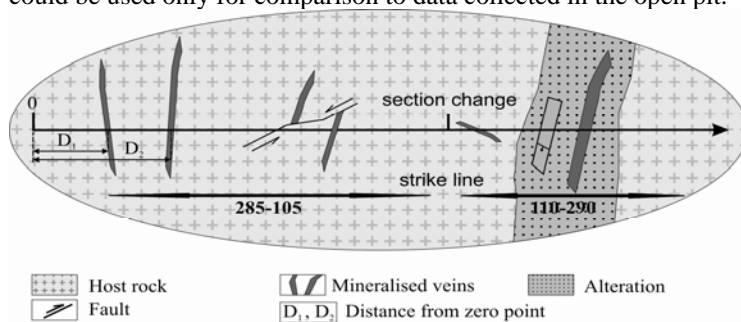

Fig.1. Data collection method along the base line on the pit wall (Modified after Benkó et al., 2008).
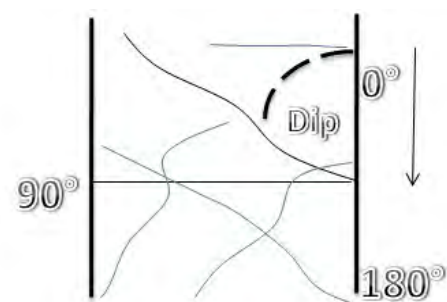
Fig. 2. Structural data collection on the drill core (VMSD001).

In order to convert the vein data into numbers and to correlate them between their different types, fractal analysis was performed on the collected data. The measured data was integrated in two plots: staircase plot and cumulative frequency of vein thickness plot. The staircase plot shows the cumulative vein thickness versus the distance along the base line. The gradient of a staircase plot is a measure of the extensional strain accommodated by a vein array and the irregularity of the curve is a measure of the heterogeneity of the strain (Gillespie et al., 1999). The cumulative frequency of vein thickness plot illustrates the vein thickness versus their cumulative frequencies on log-log axes. Straight lines on this plot, as provided by the fractal/power-law models, indicate a power-law relationship, according to the form ($N_t \propto t^{-D_m}$) where N_t is the cumulative number and D_t is the slope of the line. The physical

meaning of higher D_t values is the higher abundance of the relatively thin veins. Log- normal or negative exponential distributions give curved lines on this plot. The absolute values of these plots in the power-law models are, at 0.75, slightly higher than the ideal value of 0.7. Although the frequency distributions of these models are perfectly power-law, the equivalent cumulative frequency distributions are slightly curved and over-steepened at high thicknesses, providing a higher slope (Gillespie et al., 1999).

3. Intrusive phases and hydrothermal processes at Valea Morii prospect

The Valea Morii prospect is situated about 12 km southeast from Brad, in the eastern part of the Barza Magmatic Complex. The Barza Magmatic Complex is a part of the Zarand-Brad Basin and it is built up by Sarmatian-Pannonian volcanic and subvolcanic rocks. In the region of Barza, the Neogene volcanism has started with the eruption of the Barza type andesite (containing amphibole and pyroxene) lavas and pyroclastics (Borcoş et al., 1977), after this has appeared the first extrusive to intrusive quartz content andesitic stocks continued by several dioritic and microdioritic intrusive bodies. In the area of Valea Morii, the underlying Jurassic basalts and Upper Cretaceous sediments are covered by middle-Miocene volcano-sedimentary rocks, intersected by several magmatic intrusions. The Valea Morii porphyry mineralization is hosted by a quartz-dioritic intrusion (QDI). This QDI is cut by a later quartz-microdiorite (LQMI) and late coarse-grained porphyry dykes (CGP). The QDI shows equigranular to coarse-grained-texture, and contains plagioclase, amphibole and quartz as major rock forming minerals. The LQMI is characterized by equigranular fine-grained texture with pyroxene, amphibole and quartz as major minerals. The CGP is characterized by coarse-grained porphyry texture, with significant amphibole content. Along the contact of QDI and LQMI, an intrusive breccia can be observed in the Valea Morii open pit, where the matrix is formed by LQMI and the rounded clasts are representing the potassic altered QDI. Both diorite types are cut by various quartz-sulphide veins and characterized with various types of hydrothermal alteration. The porphyry Cu-Au type mineralization occurs in veinlets with magnetite-quartz-chalcopyrite, quartz-chalcopyrite and pyrite-chalcopyrite compositions (Fig. 3).The intrusions are also cut by a later vein system, which is filled up by banded, and drusy quartz and carbonate and Pb-Zn sulphides. The hydrothermal fluid/rock interaction produced potassic, propylitic, argillic and sericitic alteration zones during the formation of the Valea Morii mineralization. The potassic and propylitic alteration is characteristic in the whole QDI, however intense argillic and sericitic hydrothermal alteration is restricted to the zones of epithermal veins that cut through the porphyry mineralization assemblage. Thin (~1cm) sericitic alteration halo characterizes the late porphyry veinlets filled by sulphides.

4. Hydrothermal alterations related to the ore forming processes

The original rock texture is well preserved within the potassic and propylitic alteration zones of the QDI. The rocks in the potassic alteration zones are silicified as well, and are characterized with grayish-greenish color and dense sets of veinlets. These veins are filled with biotite, magnetite, chalcopyrite, pyrite and whitish-grayish quartz. The propylitic alteration is present in the internal and also in the marginal parts of the dioritic bodies and is overprinting the potassic alteration. In the propylitic intrusive rocks, three different mineral associations were identified: (1) chlorite-calcite ± clay minerals, (2) albite-epidote-chlorite ± calcite and (3) chlorite-epidote-calcite. The first mineral association appears to be present in the outer part of the ore-body, while the second and third mineral associations occur near the central part of the ore-body. The latter overprints the potassic alteration. High pyrite, chalcopyrite and magnetite content is also typical to these zones. In the zones of argillic alteration, along the epithermal veins, the primary texture of the rock has been destroyed and the rock texture is now defined by the newly formed mineral association. The clay minerals occur in knots and irregular shaped bodies and replace the products of the previous potassic and/or propylitic hydrothermal alteration and also the rock forming minerals. The rock also lost its original texture along the zones of sericitic alteration. This alteration type can be clearly distinguished from the argillic alteration, because of its higher quartz content and thus the characteristically more competent appearance. This alteration is expressly significant along the epithermal veins. At the end of the hypogenic (potassic-propylitic) alteration processes, the Cu-Au ore zone is ripped up by hydrothermal and tectonic brecciation, which was followed by the appearance of Zn-Pb sulphides and significant concentration of Au and Ag in the epithermal veins.

5. Mineralized fracture systems of the Valea Morii prospect

Based on the mineral paragenesis and the cross cutting relationships of the veins, nine types of veins were defined within the Valea Morii mineralization, using the nomenclature of Gustafson and Hunt (1975; A, B and D types) and Arancibia and Clarck (1996; M type). The different vein types and their crosscutting relationships are represented by drill core photos presented on Fig.3.

The strip log of the VMSDD001 hole (Fig. 4) shows the relationship between the host intrusives, the relative distribution of the metal (Au, Cu, Zn) concentrations and the abundance of the different vein types. Based on these plots, the following conclusions can be drawn concerning the vein distribution and the different mineralization stages:

- The abundance of the early porphyry M, A1, A2 and A3 veins correlate well with the Au and Cu grades of the porphyry mineralization;
- The QDI porphyry host all vein types, however the M-type veins are lacking from the LQMI body, while M, A1, A2 and A3 veins are lacking from the CGP body. This suggest a well-defined temporal relationship for the different

- The Au(ppm)/Cu(%) ratio is ~1 for the early M- and A-type veins, however significant Au enrichment can be observed for the late porphyry veins (A3, D1, D2);
- Epithermal veins introduce significant Au and base metal (Zn) mineralization into the system.
- An analysis was carried out on the structural measurements of the observed veins of the pit walls, too. The results suggest that the main stress field changed slightly during the different stages of the mineralization (Fig. 5): - A1 and A2 veins show commonly NNW-SSE strike;
- A3 and A4 veins are generally distributed along NNW-SSE and NNE-SSW striking fracture systems;
- D1 and D2 veins were formed along NE-SW striking fracture systems;
- Late epithermal veins show E-W strike-orientation.

Structural measurements (angle between the plan represented by individual vein and the core axis) on drill cores also suggest variation of the stress field, however absolute directions cannot be related to this data as the measurements were not obtained on oriented cores.

Two groups of the collected data were selected for fractal analyses according to the host rocks of veins. (Fig. 6). The staircase plots (fig 6A and 6B) show the correlation between the measurements on the pit wall and on the drill cores. The plots suggest the heterogeneity of the deformation: it can be observed, that the veins in the QDI are denser then in LQMI, however in the LQMI the veins are more clustered than in the QDI. The cumulative frequencies of vein thicknesses plots (Fig 6C. and 6D) suggest that the veins from the same groups have fractal potential and they fractal dimensions are unique.


M - magnetite, grayish, very thin, unsettled;

A1 - quartz, gray, massive;

A2 - quartz, gray, massive (symmetrical dark band on the edge of the fill);

A3 - quartz, white, massive;

A4 - sulphide fill, whitish yellow, massive

D1 - quartz, sulphides, massive, selvage sericitic alteration halo;

D2 - quartz, white, coarse grained, massive;

Ep - quartz, white, drusy, alteration halo (epithermal);

AEp - quartz, white, brownish, argillic alteration along veins (epithermal);

Fig. 3. Graphical representation of selected veins and their cross-cutting relationships in the drill core of the VMSD001 hole: **A** – 2.45m – cross-cutting relationships between early magnetite (M) and quartz (A2, A3 and A4) veins; **B** – 43.60m – quartz-sulphide (D1) veins with sericitic alteration halo; **C** – 11.35m – cross-cutting relationships of A2, A3 and A4 veins; **D** – 70.70m – late coarse grained quartz of vein (D2).
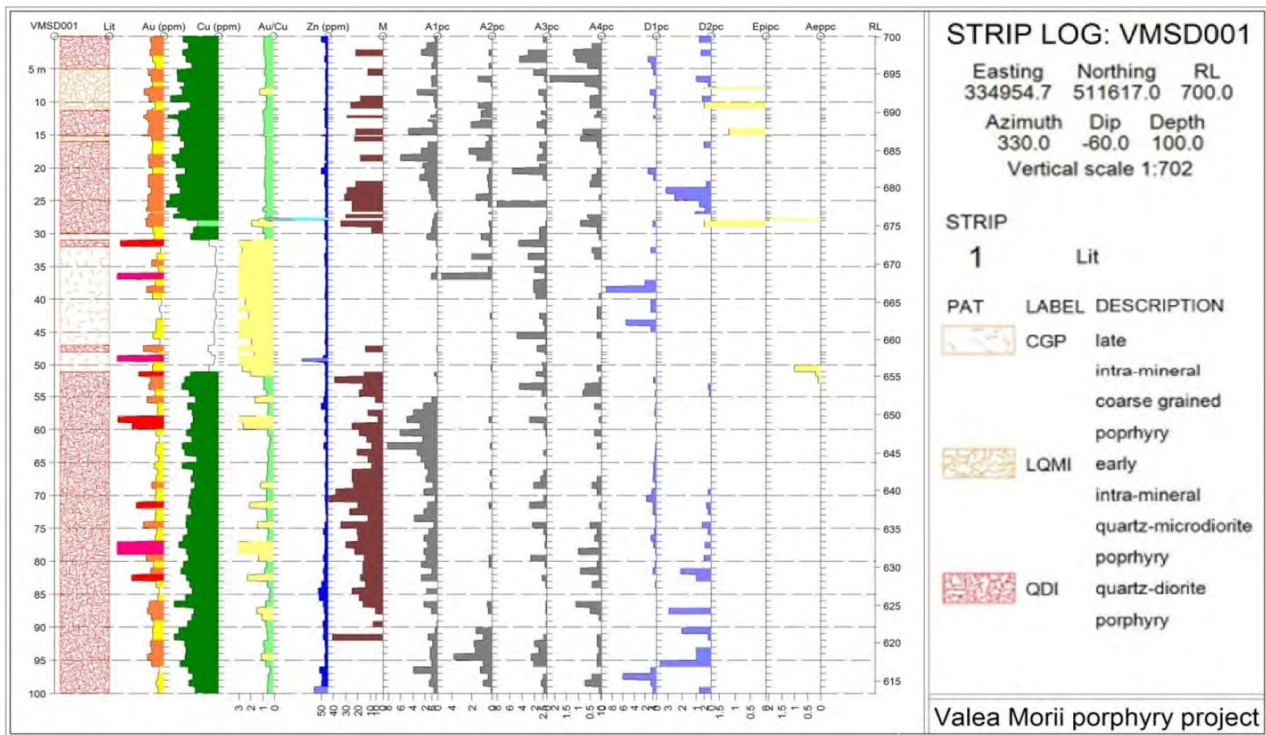
Fig. 4. Strip log of the VMSD001 drill core. The relative distribution of the Au, Zn and Cu assay data is based on the systematic (1 m based) sampling carried out by the European Goldfields SRL and the analytical results reported by the Gura Roşiei ALS – Minerals Division laboratory. Vein abundances (in percentage per meter basis) are based on the drill core logging of the recent study.
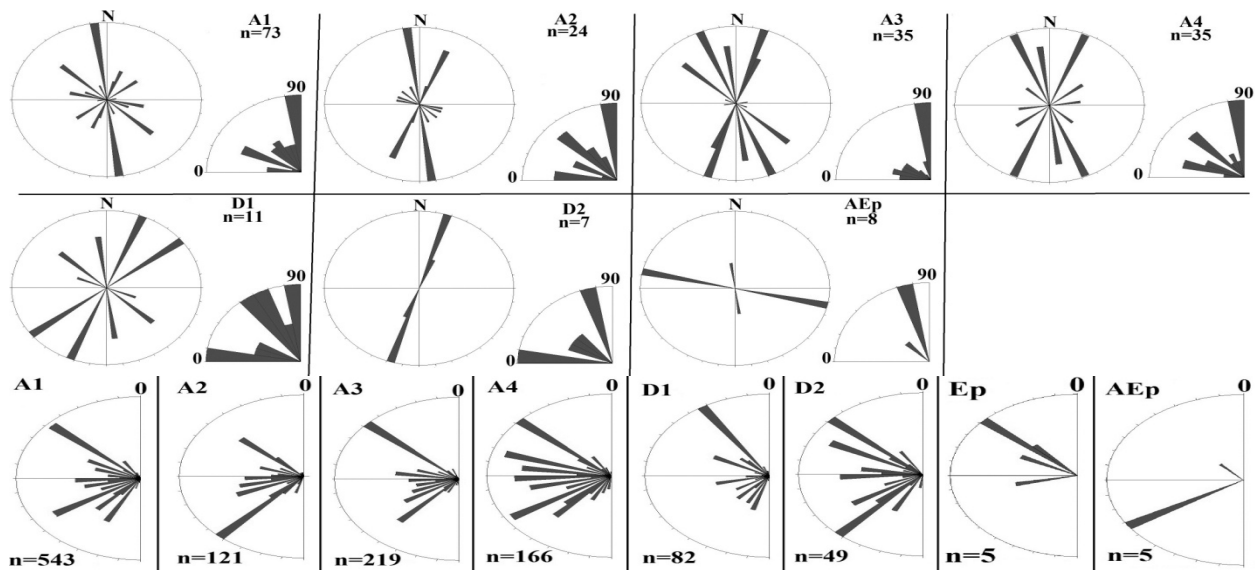

Fig. 5. Stereoplots representing the veins measured on the pit wall (dip direction, dip) and the semicircles are representing the veins measured on the VMSD001 drill core (only angle between the plan represented by the vein and the core axis).

6. Conclusions

Several intrusive and hydrothermal stages of the Valea Morii mineralization were defined. The early QDI porphyry hosts all veins types formed during the porphyry and epithermal mineralization stages. The LQMI porphyry intruded after the formation of M-type porphyry veins, while the intrusion of CGP porphyry followed the main porphyry mineralization stage. Early A-type porphyry veins are associated with potassic, sericitic and propylitic alteration and they carry Au and Cu mineralization with a metal budget close to Au (ppm)/Cu (%) ~1. All intrusive bodies were cut by late epithermal veins associated with argillic and sericitic alteration and high Au and Zn grades. The distribution of vein orientations show that the main stress field evolved during porphyry mineralization, initially forming NW-SE striking veins and later NE-SW striking veins. The epithermal veins formed along E-W striking structures. The different vein types are also distinguished by their unique fractal dimensions.
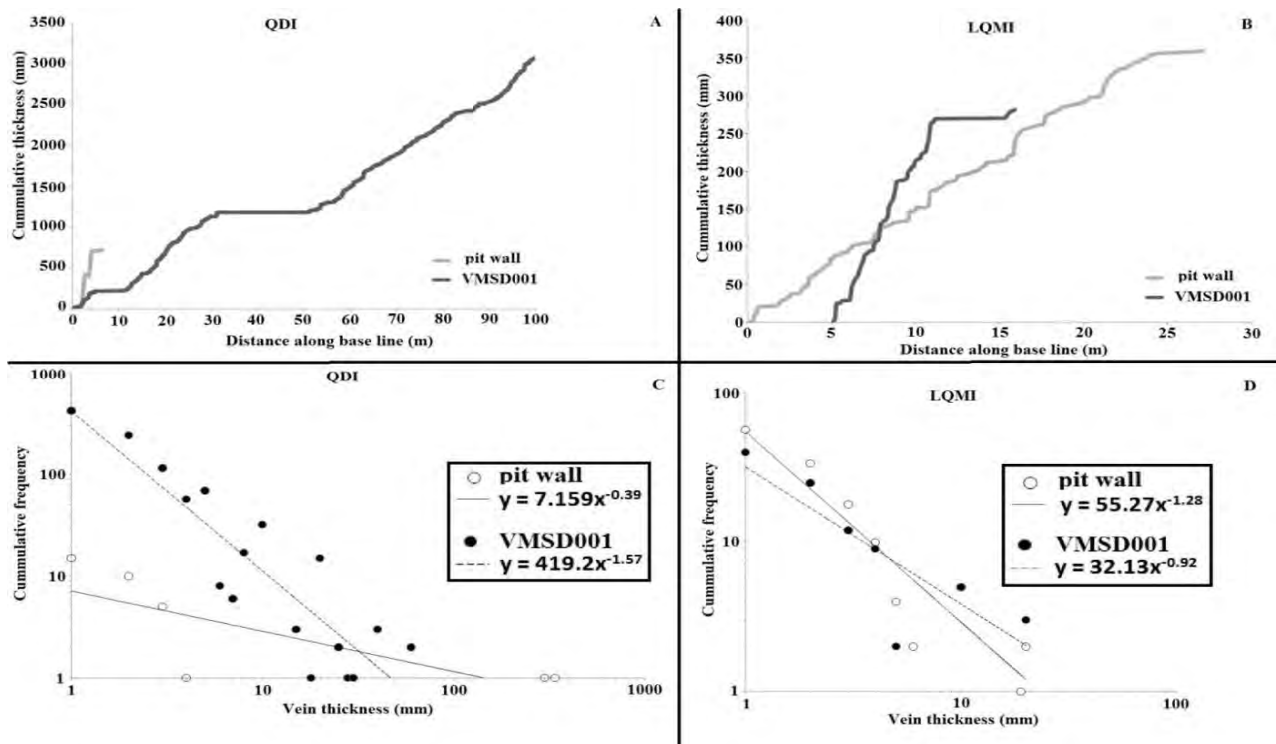
Fig. 6. Staircase plots (A, B) and cumulative frequency plots (C, D) of the measured data.

References

Arancibia O.N. and Clark A. H., 1996. Early magnetite-amphibole-plagioclase alteration-mineralization in the Island Copper porphyry copper-gold-molybdenum deposit, British Columbia. Economic Geology, 91, 402-438.

Benkó Zs.,Molnár F., Lespinasse M., 2008. Application of studies on fluid inclusion planes and fracture systems in the reconstruction of the fracturing history of granitoid rocks I: Introduction to methods and implications for fluid-mobilization events in the Velence Hills. Bulletin of the Hungarian Geological Society (Földtani Közlöny) 138/3, 229-246.

Borcoş M., Berbeleac I., Gheorghiţă I., Bratosin I., Colios E., Zămîrcă A., Anastase S., Verdeş G., Stănescu I., 1977. Geochemical remarks on the ValeaMorii porphyry copper deposit (The Metaliferi Mountains). Proceedings of the Geological Institute of Romania, 2. Ore deposits (Dări de seamă ale şedin elor, 2. Zăcăminte), 64, 17-36.

Cox S. F., Knackstedt M. A., Braun J., 2001. Priciples of structural control on permeability and fluid flow in hydrothermal systems. Reviews in Economic Geology, 14, 1-22.

Kouzmanov K., von Quadt A., Peytcheva I., Harris C.R., Heinrich C.A., Roşu E., Ivascanu P.M., 2007. Miocene magmatism and ore formation in the South Apuseni Mountains, Romania: New genetic and timing constrains. Proceedings of the Ninth Biennial SGA meeting, Dublin 2007, 865-868.

Gillespie P. A., Johnston J. D., Loriga M. A., McCaffrey K. J. W., Walsh J. J., Watterson J., 1999. Influence of layering on vein systematic in line samples, Geological Society Special Publication no.155: Fractures, Fluid Flow and Mineralization, p. 35-56.

Gustafson L. B. and Quiroga J., 1975. The porphyry copper deposit at El Salvador, Chile. Economic Geology, 90, 2-16.

Neubauer F., Lips A., Kouzmanov K., Lexa J., Ivăşcanu P., 2005. Subduction, slab detachment and mineralization: The Neogene in the Apuseni Mountains and Carpathians. Ore Geology Reviews, 27, 13-44.

Roşu E., Seghedi I., Downes H., Alderton D.H.M., Szakács A., Pécskay Z., Panaiotu C., Panaiotu C.M., Nedelcu L., 2004. Extension-related Miocene calk-alkaline magmatism in the Apuseni Mountains, Romania: Origin of magmas. Swiss Bulletin of Mineralogy and Petrology (Schweizerische Mineralogische und Petrographische Mitteilungen), 84, 153-172.

Sillitoe R.H., 2010. Porphyry copper systems. Economic Geology, 105, 3-41.

Tosdal R. M. and Richards J. P., 2001. Magmatic and Structural on the Development of Porphyry Cu±Mo±Au Deposits. Reviews in Economic Geology, 14, 157-181.

METALLOGENIC CONSIDERATIONS IN NW POIANA RUSCĂ MOUNTAINS (ROMANIA)

George TUDOR

Geological Institute of Romania, 1, Caransebeş Street, Bucharest, Romania, george.tudor@igr.ro

Abstract. The studies done by the author in NW Poiana Ruscă Mountains contributed to the clarification of the geological structure and lithology related to the mineral occurrences from this area. The evolution of the study area took place in various tectono-magmatic conditions shown by overlapping of different petrogenetic and metallogenetic processes in the same zones, with the accumulation of specific mineral resources. The most important contributions concern the porphyry copper system of the Rozalia Valley (Gladna Montană) intrusion, the reporting for the first time of the Cu-Ni mineralization from Nădrag and the evidence of the greater extent of the already known occurrences of barite from Tomeşti and aragonite from Luncani.

1. Geological setting

The area in discussion is situated in the Southern Carpathians, in the western part of Poiana Ruscă massif, where the crystalline basement begins to be transgressively covered by the Neogene sedimentary deposits. The geological constitution is heterogeneous, comprising sedimentary, eruptive and metamorphic rocks (Fig. 1).

In the crystalline formations, based on the intensity and conditions of metamorphism, are distinguished mesometamorphic and epimetamorphic rocks, assigned to two metamorphic units separated differently from the previous models (Tudor, 1996).

Mesometamorphic rocks are assigned to a group metamorphosed in the PT conditions of the amphibolite facies, according to the following reasons: the most widespread rocks are represented by micaschists with chlorite and muscovite witch have resulted from retromorphosed micaschists with biotite and muscovite and gneisses. In these rocks, quartzites with kyanite and staurolite were identified, as well as pegmatite veins with microcline, orthoclase and quartz. These features are quite different from the structural and petrographic features of the epimetamorphic from Padeş Group.
Metamorphic rocks (considered as belonging to Padeş and Ghelar groups) contain four lithostratigraphic formations separated on lithological and geometric criteria.

The western area of Poiana Ruscă massif was the host for the formation of numerous eruptive rocks bodies (plutons or dykes), which show an intense tectono-magmatic activity. Mafic rocks have been separated (gabbros, theralites), accompanied by ultramafic (peridotites) and intermediate (monzonites, quartz monzonites, syenites) rocks, with an alkaline character and represent the effects of evolution in an intracontinental rift that preceded the oceanic spreading. In the same area occur also eruptive rocks with specific characters for subduction zones, formed in the closure process of the ocean, represented by Laramian magmatic rocks (granodiorites, tonalites, porphyric granodiorites, dacites, andesites, rhyolites).

2. Metallogenic considerations
2.1 Premetamorphic mineralization
2.1.1 Cu-Ni (+Pt, Pd) mineralization from Nădrag.

The Cu-Ni mineralization, reported for the first time by Tudor (1996) and Tudor (2010) occurs in the basal zone of metamorphosed ultramafic rocks (in tremolite-antigorite schists) from meso-metamorphosed unit. Metallic minerals (20-40 % of total) form nests, schliren or matrix in the ultramafic rock, with silicates in intersitial spaces, which form the "spinifex" texture of rock (tremolite, antigorite).

The ore mineral assemblage consists of Fe, Ni and Cu minerals, in the order of crystallization: magnetite, pentlandite, pyrrhotite, chalcopyrite and sphalerite with secondary minerals such as hematite, limonite, pyrite, bravoite and malachite (almost 50 % is Fe oxides from oxidation zone). Electron microprobe analysis showed that Pd and Pt are associated with pentlandite.

Given the existing data and views on the genesis of the same type of mineralization, e.g., Kambalda, Western Australia (Gresham and Loftus, 1981) can be considered the formation of mineralization by gravity separation of immiscible liquids in ultrabasic lava flows. In subsequent phases mineralization was transformed during the regional metamorphism.

Fig. 1 Mineral resources map form NW Poiana Ruscă Mountains.
(1 – travertine, 2 – aragonite, 3 – iron ore accumulations, 4 –Pb-Zn +-Au hydrothermal mineralization, 5 – porphyry copper, 6 – Ba-F-Pb-Cu epithermal mineralization, 7 – Fe oxides mineralization, 8 – Zn-Pb-Fe – volcano – sedimentary mineralization, 9 – Cu-Ni +- Pt, Pd metamorphosed mineralization).

2.1.1 Zn, Pb and Fe mineralization from Bordaru zone.

The indications of mineralization represented by the limonite presence extend along the ridge Bordaru (on a length of about 1000 m) and south of it. There are two mineralized formations: the formation with pyrite + magnetite + quartz + muscovite ± chalcopyrite, sphalerite and formation with sphalerite, galena + pyrite + marcasite.

The first formation was studied in blocks from dumps of old galleries, whose distribution shows that the mineralized bodies have a minimum thickness of 0.5 m and the total thickness of the mineralized horizon is 40-50 m. In the superficial zone, the primary ore is entirely oxidized, forming a large "iron hat" with a thickness of about 45 m. Primary mineralization consists of alternating layers of siderite, pyrite, magnetite, pyrite and muscovite. Host rocks are quartz-feldspatic rocks with retromorphism processes.

The second mineralized formation is characteristic for the zone from the right side of the Bordaru Creek (first reported by Hurezeanu, 1976). The mineralization consists of bands or nests with sphalerite, galena and pyrite (+ marcasite, anglesite, cerusite and goethite) and is concordantly located in a sequence of muscovite, carbonate-muscovite and quartz - feldspatic schists. The constituent elements of the mineralization and host rocks and also the spatial separation of the two types of ore, come to support the hypothesis that the genesis is of vulcanogen-sedimentary type (Kuroko type), linked to a possible acid volcanism. In subsequent metamorphic processes, ore bodies were budinated and folded, the metallic minerals undergoing various transformations.

2.1.2 Fe mineralization associated with epimetamorphic basic rocks.

The research done on Fe mineralizations from Tomeşti area (Bega Luncanilor Valley) showed three types of mineralizations: lenses with concentrations of magnetite and hematite, magnetite dissemination areas in basic rocks and quartzites with hematite.

Lenses of magnetite ± hematite were investigated in the past with mining works and drilling. Ore bodies are small (tens of meters in length and 1-3 m in thickness) and occur on Ursului, Drujii and Moghi Valleys. The mineral association consists of quartz, magnetite, hematite, chlorite, calcite, dolomite, sericite and rutile.

Magnetite lenses tens of meters-thick developed in basic rocks were sometimes observed in the area, in numerous tributary valleys from the Bega Luncanilor Valley basin. Disseminated mineralizations consist of magnetite, sometimes associated with ilmenite (or leucoxene) and chlorite.

The quartzites with oligist (itabirite) occur in several areas of Ursului Valley basin. The rock consists of quartz and oligist, magnetite, sericite and rutile.

Judging by the new data obtained on the metamorphic rocks from Luncani it can be considered that the Fe mineralizations are genetically related with basic volcanic rocks formed in the geosyncline basins created by the opening of rift zones (Upper Proterozoic rift system). The basic lavas released variable quantities of Fe^{2+}, Mn, Cu, Ti and silica in the aquatic environment, which led to the accumulation of iron mineralization associated with silica gels. The folding and regional metamorphism led to a readjustment of the mineralizations.

2.2 Post-metamorphic mineralization
2.2.1 Ba, F, Pb, Cu epithermal mineralization from Tomeşti.

The Ba-Cu-Pb-F mineralization that occurs east of the Tomeşti locality was investigated in the past with mining works and drilling. The main occurrence is the vein from Scaun hill, where on a length of 200 m were crops out a mineralization of galena, chalcopyrite and tetrahedrite, with a large mass of gangue minerals (quartz, barite, fluorite, calcite, dolomite, siderite, sericite and witherite).

The research conducted north of Scaun hill (Tudor, 1996; 1990) led to the discovery of new barite occurrences associated with galena and cerussite. This research also led to the separation of five mineralized formations: a) barite +/- witherite + galena (+/- silver) +/- tetrahedrite +/- fluorite + quartz, with secondary minerals represented by anglesite, cerussite and malachite; b) tetrahedrite + quartz + calcite, with secondary minerals represented by malachite, azurite, cuprite, native copper, covellite; c) barite +/- witherite + galena + quartz + siderite, with secondary minerals on galena (anglesite and cerussite); d) fluorite + galena + quartz + sericite, with secondary minerals represented by anglesite and malachite; e) quartz + galena, with secondary minerals represented by anglesite and cerussite.

The mineralization from Tomeşti occurs as veins arranged along NE-SW oriented fractures or on the associated smaller fractures. The distribution of sulfides is irregular, more constant being the presence of barite. There is a permanent association of mineralization with siliceous rocks (three generations of quartz associated with different types of mineralizations), formed by the action of hydrothermal solutions. In general, copper mineralizations are located lateral to the area where barite occurs. The absolute age determination with Pb-Pb method on three samples of galena from the Tomeşti mineralization showed ages of 300-340 Ma (Krautner et al., 1973).

The current data lead to the consideration of epigenetic hydrothermal genesis, probably related to basic alkaline rocks formed together in an Upper Paleozoic intracontinental rift. The source for metals is in the mantle, but it can take into account washed elements from crust and migrated on fractures.

2.2.2 Rozalia porphyry copper system (Gladna Montană).

The Rozalia magmatic intrusion generated in the apical zone a porphyry copper system, in a tectonic node area (at the intersection of NE-SW, NNE-SSW and WNW-ESE oriented fractures, reactivated in the Laramian tectono-magmatic phase). Granodiorite, tonalites, andesites and dacites were separated (Tudor 1991a and Tudor 1996).

The mineralogical study of altered rocks has found a zonality in the occurrences of new formed minerals. This zonality, in which the transitions are progressive, is the following starting from center: biotite, potassic feldspar, sericite, chlorite, sericite-argillic, actinolite and propylitic. It created a ring band, which follows the general form of the system, composed of metamorphic and igneous rocks, intensely hydrothermal altered and mineralized, often with breccia structures.

Also there is a zonality for metallic minerals with polystadial forming, corresponding to each area of hydrothermal alteration. The host rocks are both igneous rocks and metamorphic rocks highly transformed. The metallic mineral zones from the center to out are: chalcopyrite + molybdenite + pyrite, secondary magnetite + chalcopyrite + molybdenite + pyrrhotite + marcasite, pyrite + chalcopyrite + molybdenite + marcasite, pyrite, sphalerite + galena + / - Au.

The Laramian tectono-magmatic activity, contained within a succession of tectono-magmatic processes, determined the arrangement of its products, resulting from a subduction process currently situated in the same area, which overlaps riftogenous old fractures. The tectonic node found south of Gladna Montana has been a major access way for calc-alkaline magmas. The consolidation of magmas took place in the subvolcanic domain, resulting a granodioritic body, with a porphyry copper system formed in the upper part, like in Lowell and Guilbert's model (Lowell and Guilbert, 1970).

2.2.3 Pb-Zn +/- Au hydrothermal mineralization (Gladna Montană).

This type of mineralization is represented by small veins with sphalerite - galena - pyrite from the propylitic dacites from Vingl Creek, limonite zone with high contents of Pb, Zn, As and Ag in the Bănița Valley and Pb-Zn mineralization from Talianul Valley. The last was first time reported by Tudor (1991b) in an old mining dump located in the upper basin of the Talianul Valley.

About the mineralization from Talianul Valley, by mode of occurrence and the high volume of mineralized rock, it can be said that it occurs as a stockwork situated in an intensely fractured zone at the intersection of fractures. Host rocks are represented by chlorite - muscovite schists. Metallic and gangue minerals deposited by hydrothermal solutions are found as impregnations and small veins and, sometimes, as stripes conformable with the schistosity of the country rocks. The paragenesis consists of pyrite, pyrrhotite, sphalerite, galena, chalcopyrite, marcasite, Au tellurides (nagyagite and calaverite, determined by microscope with composition measured by electron microprobe) and native Au. Gangue minerals are quartz and carbonates (ankeritic dolomite). Superficial alteration formed limonite, malachite, covellite and Pb and Zn carbonates.

2.2.4 Aragonite from Luncani

Accumulations of aragonite located in carbonate rocks, were formed during the Quaternary from the mobilization calcium carbonate and its precipitation as aragonite.

The best known area is east of Lucian, at about 500 m southwest of the Nimanu Peak. This was previously exploited with small mining works, on an area elongated NW-SE, with a length of 60 m. Tudor (1996) revealed new areas of aragonite occurrence, represented by large outcrops or blocks (right hand side of the Bega Valley, Ştefania Valley, Lupului Valley).

2.2.5 Iron accumulation with uncertain genesis.

South-east of Luncani locality small accumulations of iron ore occur, containing limonite (rolled or rough blocks of siliceous rocks with limonite and manganese oxide with very different sizes, in association with blocks made up of white quartzites blocks, spongy siliceous rocks or metamorphic schists), operated by small pits in the past (Ştefania Valley, left side of Lupului Valley, Lupului hill, left side of Ludwig Valley, left side of Topla Valley, upper side of Brăcinaru and Olaru valleys. Mureşan (1973) considered these accumulations of limonite as continental sedimentary deposits with Albian age, including them in the so-called "Poeni formation".

3. Conclusions

The tectono-magmatic activity from western Poiana Ruscă Mountains is characterized by the overlapping of several cycles that have evolved in a very large interval of time. The main milestones that led to the establishment of the variety of geological settings were: identification of new mineralizations in areas with rocks metamorphosed under the greenschist and amphibolite facies PT conditions, achievement of a new tectono-magmatic development based on petrographic and petrochemical characteristics of igneous rocks, detection of new tectonic elements and new types of mineralization.

A feature is that the study area evolved in various geotectonic settings that followed a cyclical pattern. Thus, for each specific stage there are certain types of mineralizations, in conjunction with certain types of igneous rocks. The mineralizations from the study area correspond to different stages of geological evolution, which are in the same areas due to cyclical tectono-magmatic events and major tectonic movements.

References

Berghes Ş., Berghes M., Tudor G., 1988. The Padeş series kyanite in the Poiana Ruscă unit (in Romanian). Studii şi cercetări de geologie, geofizică, geografie, seria Geologie, 33, 23-28. Bucharest.

Chivu C., Serafimovici V., 1967. Contributions to the knowledge of geology and tectonics of the Romîneşti-Gladna Montană (Poiana Ruscă de NV) region (in Romanian), Dări de seamă ale şedinţelor Comitetului de Stat pentru Geologie, 3, 5-14. Bucharest.

Hurezeanu E., Bordea R., 1976. On the polymetallic mineralization from Bordaru-Dîmbul cu fier (Nădrag), Munţii Poiana Ruscă (in Romanian), Dări de seamă ale şedinţelor Institutului de Geologie şi Geofizică, 63/2, 27-33. Bucharest.

Krautner H., Krautner F., Muresan M., Muresan G., 1969. Stratigraphy and evolution of magmatism, metamorphism and tectonics of the crystalline formations Poiana Ruscă massif (in Romanian), An. Com. Stat. Geol., 37, 179-264. Bucharest.

Krautner H., Muresan M., Iliescu V., Minzatu S., Vijdea E., Tanasescu A., Ioncica M., Andar A., Anastase S., 1973. Devonian-Lower Carbonifer in epimetamorphic rocks from Poiana Ruscă (in Romanian), Dări de seamă ale şedinţelor Institutului Geologic, 59/4, 5-63. Bucharest.

Lowell J.D., Guilbert J.M., 1970. Lateral and vertical alteration mineralization zoning in porpyry ore deposits, Econ. Geol., 65, 373-408.

Maier O., Solomon I., 1967. Metaporphosed igneous rocks of the western part of Poiana Ruscă massif (Nădrag-Hăuzeşti) (in Romanian), Studii şi cercetări de geologie, geofizică, geografie, series Geologie, 12/1, 159-170. Bucharest.

Mureşan M., 1973. Epimetamorphic formations from NV part of the Poiana Ruscă massif (in Romanian), Anuarul Institutului de Geologie şi Geofizică, 42, 7-337. Bucharest.

Papiu C.V., 1956. Geological research on the northwestern part of the Poiana Rucă massif (in Romanian), Dări de seamă ale şedinţelor Comitetului Geologic, 40, 135-149. Bucharest.

Tudor G., 1990. Magmatites and mineralizations associated with the intracontinental paleorift from the Româneşti-Gladna Română zone (Poiana Ruscă mountains) (in Romanian), Studii şi cercetări de geologie, geofizică, geografie, seria Geologie, 35, 33-41. Bucharest.

Tudor G., 1991a. The Gladna Montană igneous intrusion (Poiana Ruscă Mountains) – generationg a porphyry copper mineralization (in Romanian), Studii şi cercetări de geologie, geofizică, geografie, seria Geologie, 36, 9-17. Bucharest.

Tudor G., Tudor R., 1991b. Polymetallic – gold mineralization from Gladna Montană (Poiana Ruscă Mountains) (in Romanian), Analele Ştiinţifice ale Universităţii "Al. I. Cuza" Iaşi, 37, Series IIb, Geologie, 61-64. Iaşi. Bucharest. Bucharest.

Tudor G., 1996. Magmatites and mineralizations from western part of the Poiana Ruscă massif (in Romanian), Ph.D. Thesis, "Al. I. Cuza" University, Iaşi. Bucharest.

Tudor G., 2010. Cu-Ni mineralization from Nădrag-Poiana Ruscă Mountains (Romania), Romanian Journal of Mineral Deposits, 84, Special Issue, 126-128. Bucharest.

THE RĂSCOALA FE-MN METAMORPHIC DEPOSIT, SEBEŞ MTS., ROMANIA

Paulina HÎRTOPANU[1*], Nikita V. CHIUKANOV[2], Gheorghe UDUBAŞA[1], Ion HÎRTOPANU[1]

[1] University of Bucharest, Romania, *paulinahirtopanu@hotmail.com
[2] Institute of Problems of Chemical Physics, Russia

Abstract. The Răscoala Fe-Mn deposit is a metamorphic carbonate-silicate-oxide Fe-Mn ore. The complex studies (optically, X-ray, microprobe, wet chemical and IR analyses) enriched its mineralogy.
Were determined minerals unknown here until now: rhodochrosite, Mn-fayalite, spessartine, as well as anhydrous alkali amphibole and kinoshitalite, new occurrences in Romania.

Key words: Fe-Mn metamorphic ore, magnetite, rhodochrosite, Mn-fayalite, spessartine, anhydrous alkali amphibole, kinoshitalite, magnetite.

1. Geological setting

The Răscoala Fe-Mn deposit (RD) is localized in the South East of Sebes Mts, South Carpathians, Romania. Geologically, the RD is situated in the middle part of metamorphic Sebes-Lotru Series, represented by a complex of plagiogneisses, micaschists, quartzites and amphibolites. In the South proximity of RD and below the above-mentioned complex, there are quartz-feldspar rocks and microcline rich amphibolite. In the South and NW, in the highest areas (Magura Hill, Cioaca Peak) there is the upper metapelitic complex, which is predominantly made up of garnet, kyanite, staurolite micaschists. Generally, the occurrences of Mn rocks in the whole Sebes Mts, are usually localized in this last complex, but the RD has an atypically position being positioned in the middle of the plagiogneisses complex. The intensity of metamorphism in the Răscoala area belongs to sillimanite zone, in the proximity of the kyanite+staurolite/sillimanite zone, which has a large development in the North area (Fig.1). Known so far as un Fe deposit, and improperly called „schists with magnetite" or „pyroxenic limestone with magnetite" (Savu, 1955), the RD is actually a carbonate-silicate oxides Fe-Mn ore, similar to the Razoare deposit, Preluca Mts, East Carpathians, Romania. Our research carried out on its mineralogy has shown some new Mn minerals, unknown until now or wrongly determined. The RD has a lens-like form, concordant with the host rock, having the same NV-SE orientation, and with a dip of 45^0 towards SSV. In the beginning, the RD was explored with mine works by ISEM (1950-1953) and it was established that the ore lens has a 23m length, 0.8m thickness and 9m depth. The Fe-Mn ore has a banded texture, consisting of an alternation of rhodochrosite, magnetite, fayalite and spessartine bands, sometimes magnetite alternates with a black anhydrous alkali amphibole (Fig. 2).
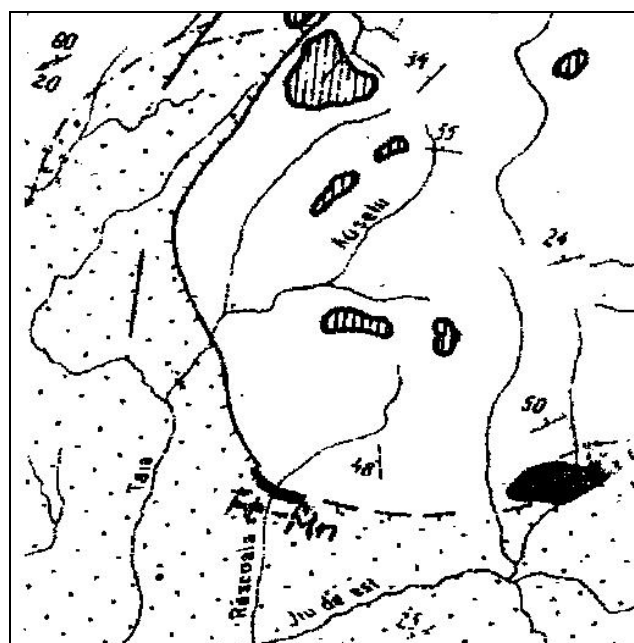

Fig. 1 The geological sketch map of RD: sillimanite zone (points), staurolite+kyanite area (empty) with islands of kyanite rocks (with vertical hachure), synkinematic granite (crossed lines hachure) and the Fe-Mn lens (black) (Hîrtopanu, 1994).
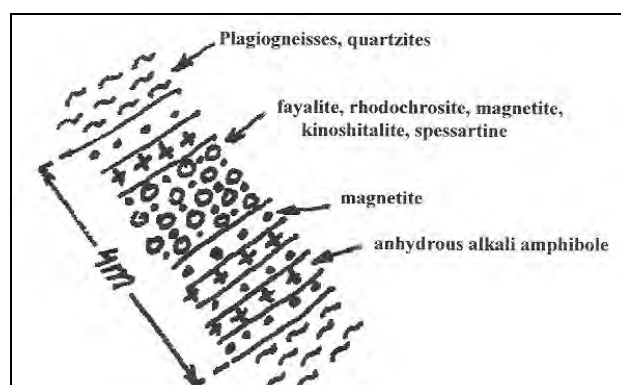

Fig. 2. The sketch of RD outcrop: banding of magnetite, fayalite + rhodochrosite + spessartine + kinoshitalite + magnetite and anhydrous alkali amphibole in plagio-gneisses and quartzites rocks.

2. Mineralogy

From the mineralogical point of view, RD is a Mn-Fe carbonate-oxide-silicate type. Generally, in a Mn carbonate background, silicates and oxides develop. Besides magnetite, new minerals for RD were determined, unknown until now here, namely **rhodochrosite, Mn-fayalite, spessartine, anhydrous alkali amphibole, kinoshitalite, apatite, pyrite, monazite, molybdenite, graphite and gold.**

2.1 The rhodochrosite, $MnCO_3$, develop as big grains up to 2cm in diameter. The rhodochrosite is the mineralogical background, and has two varieties, grey (Rg) and rose (Rr), undistinguished from the chemically point of view. (Table 1).

The calculation was made in base 6 O, being 12 negative charges. The crystallochemical formulae of rhodochrosite correspond to samples Rr, respectively Rg are:

$(Al^{3+}_{.01}Fe^{3+}_{0.010}Fe^{2+}_{0.118}Mn^{2+}_{1.687}Mg^{2+}_{0.111}Ca^{2+}_{0.136})_{\Sigma=2.092}C^{4+}_{1.958}O_3$,

$(Al^{3+}_{.00143}+Fe^{3+}_{0.029}Fe^{2+}_{0.132}Mn^{2+}_{1.541}Mg^{2+}_{0.123}Ca^{2+}_{0.152})C^{4+}_{1.993}O_3$
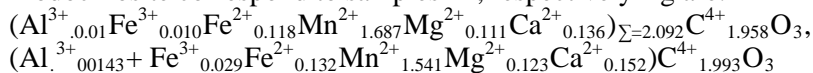
Table 1. The wet chemical analysis of rhodochrosite, samples Rr and Rg.

	Rr	Rg		Rr	Rg
TiO_2	0	0			
Al_2O_3	0.22	0.31	Al^{3+}	0.010	0.014
Fe_2O_3	0.34	1.03	Fe^{3+}	0.010	0.029
FeO	3.68	4.23	Fe^{2+}	0.118	0.132
MnO	51.95	48.85	Mn^{2+}	1.687	1.541
MgO	1.95	2.21	Mg^{2+}	0.111	0.123
CaO	3.32	3.81	Ca^{2+}	0.136	0.152
K_2O	0.04	0.04	$K+$	0.002	0.002
Na_2O	0.04	0.020	$Na+$	0.003	0.001
P_2O_5	0.08	0.08			
H_2O	0	0			
CO_2	37.40	39.20	C^{4+}	1.958	1.993
Fe_2O_3	4.43	5.73			
total					
Cations				4.035	3.987
Charges				12.000	12.000

Table 2. The wet chemical analyses of Mn-fayalite, sample Ro.

Oxides		Cations	
SiO_2	16.940	Si^{4+}	1.106
TiO_2	0.408	Ti^{4+}	0.016
Al_2O_3	0.439	Al^{3+}	0.030
Fe_2O_3	3.322	Fe^{3+}	0.109
FeO	20.187	Fe^{2+}	0.663
MnO	19.702	Mn^{2+}	0.658
MgO	1.562	Mg^{2+}	0.118
CaO	2.323	Ca^{2+}	0.106
K_2O	0.058	K^+	0.003
Na_2O	0.030	Na^+	0.002
Cations			2.811
Charges			8.000

2.2 The Mn-fayalite, $(Mn,Fe)SiO_4$, forms isolated grains in rhodochrosite ore or monomineral grain aggregates. The X-ray and IR analyses confirmed the presence of this mineral in RD, being the second mineral in the occurrence, after magnetite. The wet chemical analyses on the RD olivine (Table 2) show a high FeO content than that of ferriferous tephroite (with cca 10-15% FeO) in the rest of the Sebes massif. In contrast with the Mn-fayalite at Razoare, Preluca Mts, the RD olivine has a higher MnO content, being an intermediary term between this and the Fe tephroite at Pravat (Sebes Mts).

The calculation was made in base 4O (8 negative charges). The crystallochemical formula corresponds to $(Al_{.003}\;Fe^{3+}_{0.109}Fe^{2+}_{0.663}Mn^{2+}_{0.658}Mg^{2+}_{0.118}Ca^{2+}_{0.116})_{\Sigma=1.697}(Ti^{4+}_{0.016}Si^{4+}_{1.106})_{\Sigma=1.122}O_4$. The participation of component terms (%wt), fayalite, tephroite and forsterite in RD olivine is Fa 46.085, teph=45.723, forst=8.193, respectively. The X-ray analyses on RD fayalite gave the same intermediary term between fayalite and tephroite, with following cell parameters: $a_o=4.852\pm0.003$Å, $b_o=10.581\pm0.003$ Å, $v_o=314,29\pm0.07$ Å^3.

2.3 The spessartine, $Mn_3Al_2(SiO_4)_3$, occurs in big grains with cm dimensions. In terms of macroscopic colour the RD spessartine has 3 varieties: red (R_1), rose (R_2) and yellow orange (R_3). Their chemical composition determined by wet chemical method, are given in Table 3.

The corresponding crystallochemical formulae of the spessartine, R1, R2, R3 respectively, were calculated in base of 12 oxigens (24 negative charges):

$(Al_{.1.881}\;Fe^{3+}_{0.258}Fe^{2+}_{0.503}Mn^{2+}_{2.105}Mg^{2+}_{0.086}Ca^{2+}_{0.236})_{\Sigma=5.069}(Ti^{4+}_{0.004}Si^{4+}_{2.927})_{\Sigma=2.931}O_4$

$(Al_{.1.860}\;Fe^{3+}_{0.291}Fe^{2+}_{0.448}Mn^{2+}_{2.126}Mg^{2+}_{0.080}Ca^{2+}_{0.138})_{\Sigma=4.923}(Ti^{4+}_{0.005}Si^{4+}_{2.965})_{\Sigma=2.970}O_4$

$(Al_{.1.860}\;Fe^{3+}_{0.727}Fe^{2+}_{0.00.}Mn^{2+}_{2.033}Mg^{2+}_{0.075}Ca^{2+}_{0.209})_{\Sigma=4.914}(Ti^{4+}_{0.037}Si^{4+}_{2.906})_{\Sigma=2.943}O_4$
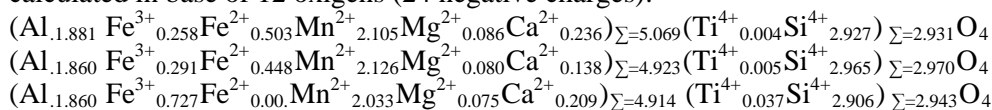
The spessartine R1 and R2 (red and rose, respectively) samples have no chemical differences between them, but the R3 spessartine (orange yellow) sample looks very different. It has no almandine term but contains an andradite term higher than spessartine R1 and R2. The R3 spessartine is younger and its presence indicates high oxidation conditions in the evolution of the Fe-Mn ore.

Table 3. The wet chemical composition of spessartines, sample R_1, R_2 and R_3

Oxides	R_1	R_2	R_3		R_1	R_2	R_3
SiO_2	35.430	35.500	35.900	Si^{4+}	2.927	2.965	2.906
TiO_2	0.060	0.080	0.600	Ti^{4+}	0.004	0.005	0.037
Al_2O_3	19.320	18.900	18.870	Al^{3+}	1.881	1.860	1.800
Fe_2O_3	4.150	4.630	11.930	Fe^{3+}	0.258	0.291	0.727
FeO	7.280	6.980	0	Fe^{2+}	0.503	0.448	0
MnO	30.090	30.060	29.650	Mn^{2+}	2.105	2.126	2.033
MgO	0.700	0.640	0.620	Mg^{2+}	0.086	0.080	0.075
CaO	2.760	1.540	2.410	Ca^{2+}	0.236	0.138	0.209
K_2O	0.010	0.040	0.030	$K+$	0.001	0.004	0.003
Na_2O	0	0	0.060	$Na+$	0	0	0.009
Total	99.710	98.370	100.070	Cations	8.001	7.957	7.800
				Charge	24.000	24.000	24.000
				Al tetr.	0.073	0.035	0.094
				Al oct.	1.807	1.825	1.707
				alm	17.160	17.218	0
				spess	71.836	75.101	87.749
				pyr	2.941	2.814	3.229
				andr	0.411	0.548	4.105
				gross	7.652	4.319	4.918

2.4 Anhydrous alkali amphibole, $KNaCa_2(Fe,Mg,Mn)(FeAl)Ti(SiO_4)O_{22}$.

In the rich magnetite area of the lens ore, an amphibole of black macroscopic colour having a pegmatoid development appears. Its grains could have a length of a few cm. In transmitted light, it has a greenish colour, with a weak pleochroism (Fig. 3). The wet chemical composition of this amphibole is presented in Table 4. It is a very rare amphibole term, because it has neither (OH), nor H_2O. It is an anhydrous rare amphibole term and its identity should be resolved soon.

The crystallochemical formula of anhydrous amphibole, calculated in base $22O^-$ (44 negative charges) is:
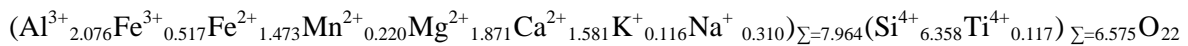
Table 4. The wet chemical composition of anhydrous alkali amphibole, sample Ra.

Oxides		Cations	
SiO_2	46.20	Si^{4+}	6.358
TiO_2	1.13	Ti^{4+}	0.117
Al_2O_3	12.80	Al^{3+}	2.076
Fe_2O_3	4.99	Fe^{3+}	0.517
FeO	12.80	Fe^{2+}	1.473
MnO	0.19	Mn^{2+}	0.220
MgO	9.12	Mg^{2+}	1.871
CaO	10.72	Ca^{2+}	1.581
K_2O	0.66	K^+	0.116
Na_2O	1.16	Na^+	0.310
H_2O, OH	0		
Total	99.770		
Fe_2O_3 total	19.21		

$$(Al^{3+}_{2.076}Fe^{3+}_{0.517}Fe^{2+}_{1.473}Mn^{2+}_{0.220}Mg^{2+}_{1.871}Ca^{2+}_{1.581}K^+_{0.116}Na^+_{0.310})_{\Sigma=7.964}(Si^{4+}_{6.358}Ti^{4+}_{0.117})_{\Sigma=6.575}O_{22}$$
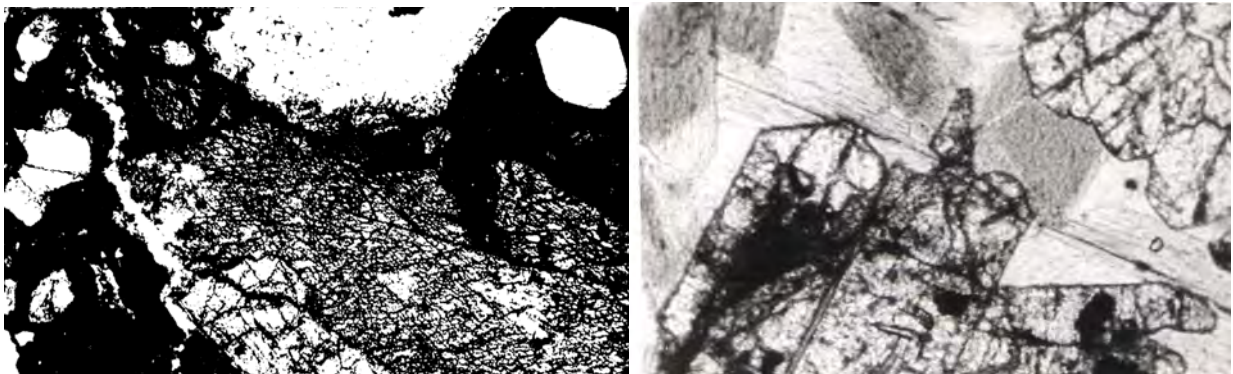
Fig 3. Anhydrous amphibole (centre, right, corner), monazite (white, bottom middle, stuck on amphibole) magnetite (black), rhodochrosite (white, top, middle) and apatite (white, enclosed in magnetite, left and right top corner) (left image); Mn-fayalite (prisms, bottom), spessartine (corner, top, right) and kinoshitalite (vein, top, left and centre toward bottom right).

2.5 The kinoshitalite, $(Ba,K)(Mg,Mn,Al)_3(Si,Al)_4O_{10}(OH,F)_2$, a rare mica mineral was determined, optically, with X-ray and IR analyses, and also with wet chemical analyses (Table 5). It occurs as a second mineral, having a centimetric to decimetric vein appearance. Its macroscopic grains have a black

colour. In transmitted light, the kinoshitalite has a green colour, weak pleochroism and a beautiful birefringence colours, different from that of common micas. It belongs to a late phase of metamorphism, being probably contemporary with yellow orange spessartine (sample R3). By IR spectrum, this mineral corresponds to kinoshitalite.

Table 5. The wet chemical composition of kinoshitalite, sample Rf.

Oxides		Cations	
SiO_2	40.900	Si^{4+}	2.892
TiO_2	0.600	Ti^{4+}	0.032
Al_2O_3	13.100	Al^{3+}	1.092
Fe_2O_3	2.230	Fe^{3+}	0.119
FeO	14.080	Fe^{2+}	0.883
MgO	13.460	Mg^{2+}	1.410
CaO	0.400	Ca^{2+}	0.030
BaO	3.00	Ba^{2+}	0.321
K_2O	4.710	K^+	0.425
Na_2O	0.370	Na^+	0.051
H_2O	2.890	H^+	1.363
F	2.730	F^-	0.610
Total	100.30	Cations =	7.995
Charges			21.390
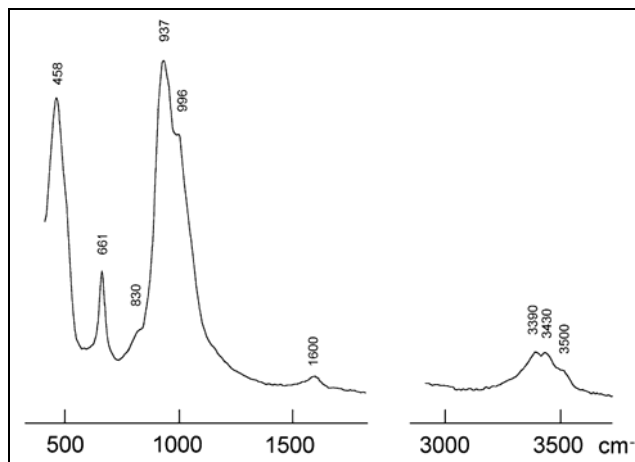
Fig. 4. IR spectrum of Rascoala kinoshitalite; the band at $1600cm^{-1}$ indicates the presence of H_2O molecules.

The calculation was made in base of 12 Oxygens, that is (O+F+OH), resulting the following crystallochemical formula $Al^{3+}_{1.092}Fe^{3+}_{0.119}Fe^{2+}_{0.883}Mn^{2+}_{0.137}Mg^{2+}_{1.410}Ca^{2+}_{0.030}Ba^{2+}_{0.321}K^+_{0.425}Na^+_{0.051}(F^-_{0.610}OH)_2$. Also, the empirical formula of kinoshitalite was determined by microprobe in two points:
$(Ba^{2+}_{0.97}K^+_{0.07}Mg^{2+}_{1.76}Fe^{2+}_{0.92}Mn^{2+}_{0.32})Si^{4+}_{2.13}Al^{3+}_{1.82}Fe3+_{0.05}O_{10}(OH,F)_2$, and
$Ba^{2+}_{0.91}K^+_{0.08}(Mg^{2+}_{1.74}Fe^{2+}_{0.93}Mn^{2+}_{0.30}Al^{3+}_{0.03}(Si^{4+}_{2.22}Al^{3+}_{1.78}O_{10})(F,OH)_2$

The kinoshitalite substitutes the Mn fayalite, appearing as a texture where the corroded Mn fayalite grains, float" in a kinoshitalite mass.

2.6 The magnetite, $Fe^{2+}O.Fe^{3+}_2O_3$, was determined optically, and with chemical and X-ray analyses. The cell parameter was calculated from X-ray data, $a_o=8.396Å\pm0.006Å$, being nearly pure (theoretic value is 8.396Å).

The accessory minerals, like **apatite, monazite, xenotime, thorite, graphite and gold**, which occur as mm grains or less, are mainly associated with magnetite, anhydrous alkali amphibole and kinoshitalite.

3. Genesis. The Rascoala Fe-Mn ore has been metamorphosed in almandine amphibolite facies when the first mineral association was formed under reduction conditions. It consists of Mn-fayalite-rhodochrosite-magnetite-spessartine-apatite-anhydrous amphibole-graphite. In a second evolution stage of ore the second generation of spessartine (yellow orange with Fe^{3+} and without Fe^{2+}) and kinoshitalite, were formed in a high oxidation environment. It is thus an oxidized association.

References
Hîrtopanu I., 1994. Polymetamorphic evolution of the Sebes-Lotru Series, South Carpathians, as a result of the aluminium silicate-bearing metapelites study. Rom.J.Petrology 76A (special issue), p.1-104.
Savu H., 1955. Unpubl. geological report. Geological Institute of Romania, Bucharest.

A COMPARATIVE STUDY OF THE MAIN
DEPOSITS WITH HIGH ECONOMIC VALUE OF VOLCANIC TUFFS
CONTAINING NATURAL ZEOLITE FROM ROMANIA

Mihai GHIȚĂ[1]*, Viorel BĂDILIȚĂ[1], Florentin STOICIU[1], Ioan DENUȚ[2], Cornelia LUPU[1], Luminița MARA[1], Victoria SOARE[1]

[1]National Institute of Research and Development for Non-ferrous and Rare Metals, 102 Biruintei Blvd., Pantelimon, Ilfov, RO-077145, *mihai86ghita@yahoo.com
[2]Tech. Univ. Cluj Napoca, North Univ. Center Baia Mare, 62A Dr. Victor Babes Street, 430083, Baia Mare

Abstract Volcanic tuffs with clinoptilolite (CLN) active zeolite phase's content are both the most abundant and most commonly used natural zeolite in Romania. This work aim to gain an overview and an analysis of the textural and chemical compositional of the main commercial and undeveloped volcanic tuffs deposits from Romania covering a wide range of geological environments. Tuffs samples with different CLN amounts were characterized by X-ray diffraction (XRD), optical microscopy, X-ray fluorescence methods and chemical analyses. For this study samples from nine volcanic tuffs deposits have been characterized and analyzed. The results show a wide range of the CLN content (between 15-90%) closely related to the geological environments. All the samples show a real potential for industrial use intimately related to textural and structural properties.

Keywords: volcanic tuffs, clinoptilolite, zeolite, Romanian deposits, mineralogical characterization

1. Introduction

Natural zeolites are volcanic sedimentary minerals composed primarily of alumosilicates. These minerals have a three –dimensional crystal lattice, with loosely bounds cations, capable of hydrating and dehydrating without altering the crystal structure (Mumpton, 1999).

It is known that the CLN zeolite has a large cation exchange capacity (CEC) and pore spaces, and has many applications such as gas absorption, odor control, water filtration for municipal and residential building waters and aquariums, agricultural use (e.g. additive in animal foods, soil amendments, etc.), and many others.

The physical structure of CLN consists of the three-dimensional arrangements of SiO_4 and AlO_2 tetrahedra consisting of a network or interconnected tunnels and cages. In the crystal lattice the tetravalent silica ions are replaced by trivalent aluminum and the resulting negative charge balanced by cations. The more aluminum ion replacement, the greater is the capacity for cation absorption. Thus the Si/Al ratio, which varies from 2.7 to 5.2 for CLN, and cation content, determine the properties and industrial use of the natural zeolites. The free volume of CLN network structure is closely related to the volume of the cations. This blocking effect can be changed by different chemical treatment for increase the absorption capacity of zeolite closely related to the nature of cages from zeolite structure, a function of the Si/Al ratio of CLN phases.

Samples studied were taken from the following deposits of volcanic tuffs: Slanic Prahova (Prahova), Ocnele Mari (Valcea), Bunesti-Govora (Valcea), Racos (Brasov), Mirsid (Salaj), Barsana (Maramures), Calinesti (Maramures), Dopca (Brasov) and Matau (Arges).

2. Analytical methods

All analyzes presented in this article were undertaken at the National Institute of Research and Development for Non-ferrous and Rare Metals (INCDMNR-IMNR).
Chemical Analyses were performed using the FAAS, ICP-OES and gas methods.
X-Ray Powder Diffraction was carried out on a Bragg-Brentano Bruker D8 Advance diffractometer, using the Bruker DIFFRACplus BASIC software (2006) and the ICDD database PDF-2 release 2006. X-ray diffraction data were carried out in the 2θ range from 4 to 74 degrees, 0.02 degrees step size and 3 sec time per step with CuKα radiation at 40 kV and 40 mA. Cukβ radiation was removed by SOL-X detector.
Microscopical Analyses were performed using an AXIO IMAGER.A1m with polarized light.

In the case of the impurities analysis (ppm level) **X-ray Fluorescence (XRF)** elemental analysis method was used which require no sample preparation. A portable X-MET-3000TXR spectrometer and Hewlet – Packard (HP) iPAQ personal data assistant (PDA) for software management and data storage have been used.

3. Results

This paper presents the results for some of the analyzed samples, as follows: T2- Slanic Prahova, T3- Ocnele Mari, T6- Bunesti- Govora, T8- Racos, T11- Mirsid, T14- Calinesti, T15- Dopca, T17- Barsana, T18- Matau.

Chemical Analyses of the considered samples revealed the compositions showed in Table 1. *X-ray Fluorescence* shows for the analyzed samples the composition presented in Table 2. The results of semi quantitative *X-Ray Diffraction* phase analysis are summarized in Table 3 and Fig. 1.

Table 1. The results of chemical analyses for the selected samples

Element %/ Code	T2	T3	T6	T8	T11	T14	T15	T17	T18
Si	35.1	31.6	33.7	30.4	30.9	31	28.3	30.7	30.2
Al	6.1	6.12	6.5	7	6.55	6.3	6.2	6.6	7.3
Na	1.01	1.84	1.84	0.98	0.29	2.93	1.69	2.9	1.88
K	1.65	1.91	1.64	1.71	2.02	1.36	1.56	1.62	1.67
Ca	4.53	6.38	6.47	1.7	1.74	0.86	1.96	0.87	1.48
Fe	0.87	1.5	1.88	0.79	0.52	1.06	1.56	1.03	1.32
Mg	0.37	0.58	0.52	0.44	0.52	0.36	1.12	0.25	0.64
H_2O	3.1	5.2	2.96	6.51	6.82	4.91	8.22	5.66	4.71
LOI	12.7	13.1	10.0	13.5	15.1	12.2	16.1	12.3	11.3
Si/Al	5.75	5.17	5.19	4.34	4.72	4.92	4.56	4.65	4.14
R (Si:(Si+ Al+Fe))	0.83	0.81	0.8	0.8	0.81	0.81	0.78	0.8	0.87

Table 2. The results of chemical analyses for selected samples

Code/ Element ppm	Fe	Ca	Ti	Sr	Ba	Mn	Zr	Sn	Sb	Zn	Pb
T2	8529	15432	520	962	612	136	175	125	97	18	25
T3	12330	28828	892	190	522	268	97	113	95	40	42
T6	14618	15918	1378	362	583	155	205	124	110	42	19
T8	6118	14863	456	299	394	14	107	153	102	8	12
T11	4431	18335	930	385	565	-	90	115	70	28	12
T14	8758	6564	391	170	468	241	95	135	91	16	16
T15	15257	16766	881	101	438	872	131	149	113	49	45
T17	7880	5967	715	195	596	407	94	146	109	41	12
T18	13727	11873	1232	681	421	254	199	116	99	35	32

Table 3. Semi quantitative X-Ray diffraction phase analysis [% wt.] of volcanic tuffs samples

Compound Name	*Formula*	*PDF Reference*	*T17*	*T3*
Clinoptilolite	$(Na,K,Ca_{0.5})_6(Al_6Si_{30}O_{72})(H_2O)_{24}$	01-072-7919 (N)	84	2
Quartz	SiO_2	00-046-1045 (*)	5	17
Cristobalite	SiO_2	01-089-3607 (C)	2	
Plagioclase	$(Na,Ca)Al(Si,Al)Si_2O_8$	01-083-1939 (*)	4	12
Calcite	$CaCO_3$	00-005-0586 (*)	-	20
Biotite	$K(Mg,Fe^{2+})_3(Al,Fe^{3+})[(Al,Si)_3O_{10}](OH)_2$	01-080-1110 (*)	5	-
Muscovite	$KAl_2(AlSi_3O_{10})(OH)_2$	01-082-0576 (*)	-	15
Clinochlore	$(Mg,Fe^{2+})_5Al(Si_3Al)O_{10}(OH)_8$	01-089-2972 (I)	-	8
Glass	SiO_2 - based		-	26
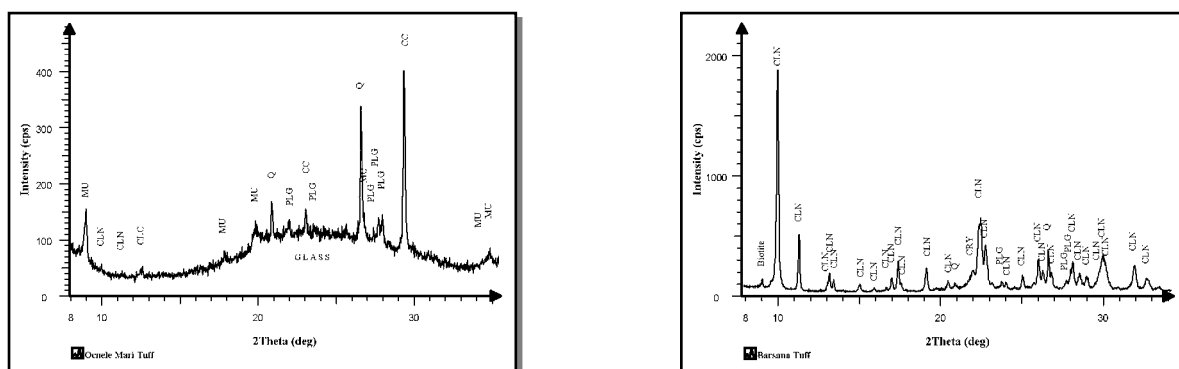
Fig. 1. X-Ray diffraction phase analysis volcanic tuffs from T3 (A) and T17 (B). Legend: Clinoptilolite – CLN, Quartz – Q, Cristobalite – CRY, Plagioclase – PLG, Calcite – CC, Biotite – Biotite, Muscovite – MU, Clinochlore – CLC, Glass – GLASS.

Microscopic Analysis revealed, for the studied samples, the compositions showed by the Fig. 2-5 (Anastasiu, 1977):
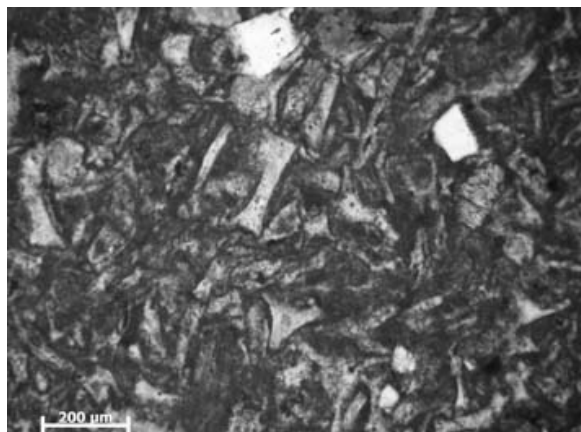

Fig. 2. T2 Sample, NII, transmitted light. Glass, plagioclase feldspar, backed by diatoms (silica minerals) and foraminifera ($CaCO_3$).
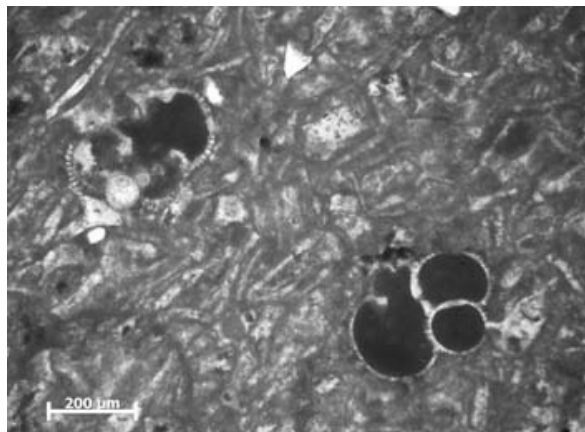

Fig. 3. T2 Sample, NII, transmitted light. Glass, plagioclase feldspar, backed by diatoms (silica minerals) and foraminifera ($CaCO_3$).
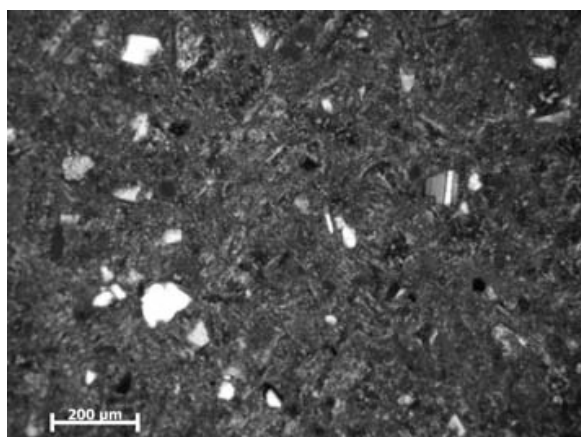

Fig. 4. T14 Sample, N+, transmitted light. Glass, plagioclase feldspar, biotite, quartz, calcite
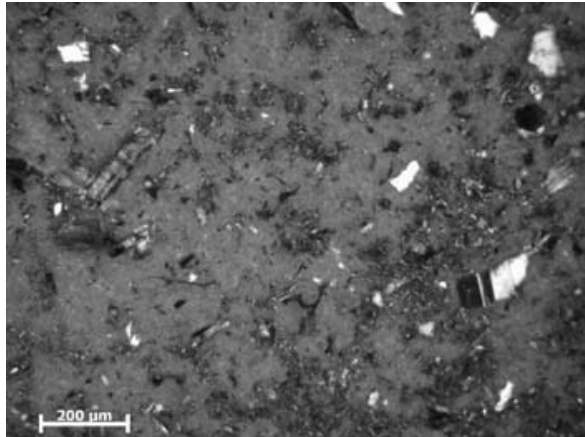
Fig. 5. T18 Sample, N+, transmitted light. Glass, plagioclase feldspar, biotite, cristobalite

4. Discussions

SiO_2 and Al_2O_3 content in clinoptilolite and unaltered glass by halmyrolisis were included in the value of 64.7 to 78% and from 11.5 to 12.6%. SiO_2 content shows a narrow range, and Al_2O_3 content was higher in samples with higher content of clinoptilolite compared with unaltered volcanic glass. As a result, the ratio ($SiO_2/Al_2O_3 = 5.3$) was slightly lower in samples with a high ratio of unaltered volcanic glass ($SiO_2/Al_2O_3 = 6.25$).

Cationic composition in the analyzed samples was markedly higher in samples with dominant CLN composition, they are richer in K (K = 1.7 to 2.02%) compared with samples containing mostly unaltered volcanic glass (K = 1.49 to 1.65%).

Cation selectivity of CLN showing a preference for K to Ca and Na plays an important role in the concentration of K in CLN during the formation of CLN from volcanic glass during hydrothermal transformations.

It also makes clear that in terms of calcium content in the analyzed samples they clearly differ depending on the area of origin. In samples from the Transylvanian Basin, rich in CLN in tuffs cemented with Ca, they were not enriched in Ca during their transformation, suggesting that CLN cation exchange composition was not changed, unlike samples of South Carpathians, that have a much higher concentration in Ca. Apparently, CLN cation exchange composition, once formed, is relatively stable

63

over time and difficult to change even in conditions when calcite is precipitated on the surface of CLN crystals.

5. Conclusions

The results show a wide range amounts of the active zeolite phase CLN, distinguishing thus the tuffs located in Transylvanian basin from those in sub-Carpathian regions (15 to 90%wt.)

In all analyzed samples halmyrolisis process has been observed. CLN is the dominant species for Slanic Prahova, Bunesti-Govora, Racos, Mirsid, Calinesti and Barsana samples, and in the rest of samples the dominant species are the silica minerals.

The industrial potential application of Romanian volcanic tuffs, closely related to the amounts of CLN natural zeolite active phases, suggests the following potential use: materials construction (for tuffs with low CLN contents), and other applications (e.g. agriculture, domestic animal diets, waste waters treatments, gas purification, etc.) for tuffs with high CLN content.

References

Anastasiu N., 1977. Minerale si roci sedimentare – Determinator. Editura Tehnica, Bucharest.

Mumpton F., 1999. La roca magica: Uses of natural zeolites in agriculture and industry. Proceedings of the National Academy of Sciences of the U.S.A., 96, 3463–3470.

SURFACE MINING OF USEFUL SOLID MINERAL, NON-METALLIFEROUS AND NON-COMBUSTIBLE SUBSTANCES IN HUNEDOARA COUNTY

Mihai MARINESCU[1*], Roxana FECHET[2], Doru ANGHELACHE[3]

[1]University of Bucharest, Faculty of Geology & Geophysics, #6 Traian Vuia Street, Sect.2, code 020956, Bucharest, Romania. E-mail: mmar54@yahoo.com.

[2]CEPROCIM S.A., #6 Preciziei Blvd, Sect. 6, cod E 062232, Bucharest, Romania. E-mail: roxana_fechet@hotmail.com

[3]Nitro Nobel Group, #7 Aviatorilor Blv, Sect. 1, Bucharest, Romania. E-mail: doru.anghelache@nitro-nobel.ro

Abstract. From ancient times and until nowadays, a great number of mineral substances have been exploited in Hunedoara county, from metalliferous (well-known in Metalliferous Mountains and Poiana Rusca) to non-metalliferous ones, especially those used as building materials, present on whole country territory. In the most cases, exploitation of ore deposits has been carried out by quarries and open pits. This dominant trend of surface exploitation is still continuing. This paper is reviewing these exploitations.

Keywords: Hunedoara county, surface exploitation, quarries, open pits, mineral deposits.

1. Geographical and geological aspects regarding Hunedoara County
1.1. Geographical considerations

From geographical point of view, Hunedoara county is situated in the area of intersection between Apuseni Mountains (Bihor and Metalliferous Mountains, northwards to Mureş river and Poiana Ruscă Mountains in the south) and South Carpathians (Sureanu-Sebeşului Mountains, Tarcu Mountains, Retezat Mountains, Parâng Mountains, Vilcan Mountains). Between Bihor Mountains and Metalliferous Mountains there is Brad Depression; between Poiana Ruscă Mountains, Retezat Mountains and Şureanu Mountains there is Haţeg Depression; between Retezat Mountains, Vilcan Mountains, Şureanu Mountains there is Petroşani Depression. From the east to west, it is crossed by Mureş river that flows through a depressionary corridor.

1.2. Geological considerations

Hunedoara county has a complex geological structure (Mutihac et al., 2007), depending on the geostructural unit to which it belongs to: Apuseni Mountains (South Apuseni Mountains subunit) at north of Mureş and South Carpathians in the south of the above-mentioned river, flowing through a tectonic depression, sometimes with horst aspect.

Southern Apuseni Mountains consist of crystalline schists (Rapold island), Mesozoic sedimentary rocks (limestones, conglomerates, gritstones, marls, clays), ophiolitic magmatites (rhyolites, diorites, diabases, gabbros), Laramic magmatites (granodiorites) and Neogene (dacites, andesites, basalts and some pyroclastics). Among them, Metalliferous Mountains are famous for non-ferrous and precious metals deposits.

South Carpathians consist of Danubian Autohtonous/Realm (massifs of Parâng, Vilcan, Retezat, Tarcu) and Getic Realm (Massifs of Godeanu, Şureanu, Poiana Rusca). In their constitution there are crystalline schists (also migmatites, pegmatites, amphibolites, limestones and crystalline dolomites, marbles), meso- and epimetamorphic rocks, interwoven with granitoids and serpentinites, on top of which there are Jurrasic and Cretaceous sedimentary rocks (especially limestones, gritstones, conglomerates).

In Brad depression there are different rocks, clays, pyroclastics, marls, tuffs and sands formed during the Badenian − Pannonian. Petroşani depression is filled up with Eocene-Oligocene formations (conglomerates), Upper Oligocene − Aquitanian (marl complex with 25 layers of coal), Burdigalian (conglomerates) and Sarmato-Pliocene formations (gravel). In Haţeg depression, there were accumulated Paleogene formations (conglomerates, gritstones, clays), Badenian-Sarmatian (conglomerates, gritstones, marls, limestones) and Pannonian formations (sands, gravel, boulders, clays). On Mureşului Corridor, there are important quaternary sand, gravel, boulders deposits that are mined by numerous open pits.

Some ore deposits distinguished in Hunedoara county, from coal to dimension stones, from ferrous to non-ferrous minerals (gold, gold-silver, copper, polymetallic, bauxite, rare and dispersed elements) as well as non-metalliferous ores and industrial minerals, all of these have been or are still exploited.

2. Mining of mineral substances in the course of time in Hunedoara County
2.1. Place of Hunedoara County within surface mining context of non-metalliferous and non-combustible solid mineral substances in Romania

In the course of time, in Hunedoara County, several surface mining activities as well as in all counties of the country took place (Marinescu, 2003; Mihailescu and Grigore, 1981). In Table 1 it can be seen the number of quarries and gravel plants that were identified within the first ten most important counties from this point of view.

Table 1. Number of surface mining activities known in the main ten counties of Romania

No.	COUNTY	QUARRIES & PITS
1.	Hunedoara	235
2.	Tulcea	202
3.	Constanta	182
4.	Maramures	162
5.	Cluj	151
6.	Arad	148
7.	Covasna	134
8.	Suceava	127
9.	Brasov	123
10.	Bihor	120

Table 2. Number of known mineral substances surface exploited in the main ten counties of Romania

No.	COUNTY	NUMBER OF EXPLOITED MINERAL SUBSTANCES
1.	Hunedoara	30
2.	Arad	28
3.	Caras - Severin	26
4.	Cluj	23
5.	Maramures	20
6.	Harghita	19
7.	Tulcea	19
8.	Mehedinti	18
9.	Alba	17
10.	Bihor	17

With a number of 235 of surface of mining activities, Hunedoara County occupies by far the first place. We mention that this table does not contain, due to lack of information, the number of domestic mining through which the inhabitants insured the necessary of minerals, especially ones used as building materials.

Analysis of number of solid, non-metalliferous and noncombustible minerals, exploited at the surface in Romania, along time, place Hunedoara County on the first place, closely followed by Arad County. Situation for the first ten most important counties in Romania from this point of view can be seen in Table 2.

2.2. Allotment of mining activities per day in Hunedoara County, on types of mineral substances

As it has been presented before, in Hunedoara County, 30 solid non-metalliferous and noncombustible mineral substances have been extracted in the course of time, by means of 235 known surface mining activities. (Parvu et al. 1977).

Limestone has been extracted in over 53 surface mining sites: Pietroasa, Baldovin, Bretea Mureseana, Banita 1, Banita 2, Boiu, Boz, Brad, Buces, Folt, Fornadia, Pestera – Petrosani 1, Pestera – Petrosani 2, Taia – Petrila, Rosia – Petrila, Racastia, Salistioara, Valisoara, Zaicani, Ardeu, Banpotoc, Barasti, Geoagiu Bai, Ohaba-Ponor, Pestera – Ardeu, Rasculita, Troita, Craciunesti, Vulcan, Paroasa, Pojoga 1, Pojoga 2, Valea Valisoara (much more), Pestera Bolii – Pestera (Petrosani), Pribeagu, Boholt, Magura Feredeului – Magulicea (Baita Craciunesti), Rapoltu Mare, Pestisu Mare, Seicani, Valea Bradului – Bucuresci, Sanatoriului – Geoagiu, Magura Feredeului – Pestera Baita, Magura Baitei – Pestera Baita, Pestera – Prihodiste, Roscani I, Roscani II, Teliuc I – Teliucul Inferior, Teliuc II – Teliucul Inferior, Teliuc III – Teliucul Inferior, Stanjeasca – Vata de Jos, Vatisoara – Vata de Jos, Jugastru – Cata de Jos.

Sand and gravel have been extracted in the following 43 open pits: Criseni – Calan, Balastiera I – Harau, Balastiera II – Harau, Balastiera III – Harau, Saulesti I, Saulesti II, Folt, Turdas, Vorta, Carastau, Rasca, Tebea, Vata de Jos, Geoagiu, Iscroni, Balata, Harau I, Harau II, Harau III, Ludesti, Nalativad, Det, Drumul Schiopului, Cioplea, Plopi, Rusi, Strei – Calan, Strei – Sangeorgiu, Roscani, Vata de Sus, Bretea Romana – Rusi, Gura Streiului, Ilia – Ilteu, Saulesti – Simeria, Baiesti, Saulesti – Simeria, Simeria Veche – Gura Streiului, Balata – R Mures, Dobra – R Mures, Pricaz - R Mures, Santuhalm, Bretea – Strei, Turdas – Folt.

Andesite has been extracted in the following 20 quarries: Branisca, Bretea Mureseana, Caraci, Cozia 1, Cozia 2, Gurasada (La Stean), Coltu Pietrii – Lesnic, Ormindea, Pietroasa – Deva, Rapoltu Mare, Rasca, Tisa, Uroiu, Gura Morii – Criscior, Valea Arsului – Criscior, Cozia – Miscovet, Valea Balului, Mihaileni, Deva, Sub Stean – Godhatea.

Sand has been extracted in quarries or open pits in: Baru Mare, Cigmau, Deva, Mihalt, Orastie, Simeria, Ilia, Hasdat I, Hasdat II, Hasdat III, Hasdat – Nadas, Islaz – Baia de Cris, Nadastia de Jos, Sarmizegetusa, Padurea Brad – Brad, Nadas – Hasdat, Grindu I – Ohaba Streiului, Grindu II – Ohaba Streiului, Tunel – Zlasti.

Crystalline limestone that appears in various areas, has been extracted from over 17 quarries: Bontarul de Sus, Ghelar, Livezeni, Nandor, Vulcan, Alun, Boiu, Bunila, Carpinis, Luncani, Sanatoriul Geoagiu, Valea Bobalna – Geoagiu (more quarries), Roscani I, Roscani II, Boz, Craciuneasa – Govajdia, Terlea – Govajdia.

Common clays have been obtained in the quarries: Petros, Magura Bolesti, Baru Mare, Lupeni, Crivadia, Hula-Turdas, Islaz-Baia de Cris, Sancrai – Calan, Chiscadaga, Turdas, Bicau – Branisca.

Gypsum was exploited in the quarries: Rasca, Romos, Vaidei, Calanu Mic – Sancraiu, Dealul Varului – Chimindia.

Dolomite and dolomitic limestone have been exploited in 10 quarries: Hunedoara, Teliucu Mic (quarry on Metallurgic Plant), Teliuc I, Teliuc II, Teliuc III, Craciuneasa, Zlasti, Bania, Tulea and Valea Cernei. **Basalt** productions have been obtained in the quarries: Sacamas, Magura – Sarbi, Pietrelor – Birtin, Herepea, Magura - Sarbi - Branisca, Zam, Lunca, Lesnic.

Travertine productions have been achieved in more than 7 quarries: Banpotoc – Carpinis (from certain sources it results that this is the only area there have been over 9 quarries in the course of time, but we have not enough information), Geoagiu I – Geoagiu Bai, Geoagiu II – Groagiu Bai, Rapoltu Mic, Carpinis, Geoagiu, Marjaria – Carpinis, whereas, **the grit stone** has been exploited in exactly 7 locations: Sacamas, Stanija, Buitur, Bozes, Ardeu, Bacainti and Calnic.

In 6 open pits the **gravel** has been mined (Hunedoara, Geoagiu de Jos, Deva, Orastie, Balastiera de Jos – Geoagiu, Balastiera de Sus - Geoagiu) and the **gypsum** in 5 quarries (Romos, Vaidei, Rasca, Calanu Mic – Sancraiu, Dealul Varului - Chimindia), as well as **quartzite** (Gambrinus – Petrosani, Sasa – Izvor, Livezeni, Gambrinus – Petrosani, Gruneti - Petrosani).

In 4 surface mining sites each, there have been extracted: **grit stone and conglomerate** (Bobalna, Boiu, Bozes, Stanija) and **talc** (Cerisor, Lelese – Cerisor, Lelese – Cerisor Vest, Cerisor – Lelese Vest). **Bentonite** has been exploited at Poieni – Gurasada, Devuta – Gurasada, Mihailesti – Dobra and **marble** at Alun, Barastii Iliei and Luncani.

In two quarries there have been exploited the following mineral substances: **diabase** (Zam I, Zam II), **ornamental andesite** (Dl Magura – Almasu Sec, Pietroasa), **dolerite** (Cazanesti I, Cazanesti II), **marl** (Alesd, Prisloape - Pui) and **andesitic tuff** (Deva, Bacia). From a single quarry there have been extracted **calcite** (Cazanesti – V. Ponor), **quartz** (Siglau - Uricani), **dacite** (Sacaramb), **diorite** (Birtin), **gneisse** (Calnic), **granite** (Raul de Mori) and **basaltic tuff** (Birtin).

Table 3. Situation of mining licenses for Hunedoara county in 2011

NAME OF QUARRY OR OPEN PIT	MINERAL SUBSTANCE	ECONOMIC ENTITY
Valea Arsului - Criscior	Industrial or building andesite	Carpat Agregate S.A. Bucuresti
Pietroasa	Ornamental andesite	Marmosim S.A. Simeria
Chiscadaga	Common clay	Carpatcement Holding S.A
Crivadia	Common clay	Macon SRL Deva
Magura Sarbi -Branisca	Basalt	Carpat Agregate S.A. Bucuresti
Zam	Basalt	Carpat Agregate S.S. Bucuresti
Gurasada Poieni	Bentonite	Bega Minerale Industriale S.A. Aghiresu
Baita Craciunesti(Magura Feredeului)	Limestone	Carpatcement Holding S.A
Pojoga	Industrial and building limestone	Carmeuse Holding SRL
Cazanesti-Valea Ponor	Calcite	Gabbro Minnerale
Siglau-Uricani	Quartz	Novacuart SRL
Calanul Mic - Sancrai	Gyps	Carpatcement Holding SA
Simeria Veche-Gura Strei I	Sand and gravel	Pomponio S.A. Alba Iulia
Baiesti	Sand and gravel	Consmin S.A. Petrosani
Simeria-Uroi	Sand and gravel	CCCF S.A. Deva
Folorat	Sand and gravel	Directia Judeteana de Drumuri - Deva
Saulesti - Simeria	Sand and gravel	Macon SRL Deva
Uroi	Sand and gravel	Directia Judeteana de Drumuri - Deva
Carpinis	Travertine	Marmosim S.A. Simeria
Geoagiu	Travertine	Marmosim S.A. Simeria

Table 4. Situation of mining permits for Hunedoara county, in 2011

NAME OF QUARRY OR OPEN PITS	MINERAL SUBSTANCE	ECONOMIC ENTITY
Roscani	Industrial and building limestone	Danut si Cornelia Agregate SRL Dobra
Homorod 2	Sand and gravel	Vespa System SRL
Lesnic 2	Sand and gravel	Riviera Prod Com SRL Vetel
Totia	Sand and gravel	Casito Transimpex SRL Pestisu Mic
Turdas amonte	Sand and gravel	Acomin S.A. Cluj-grupul santier Deva
Paroasa-Campu lui Neag	Industrial and building limestone	CCCF S.A. Bucuresti - F.D.P. Timisoara
Lapusnic	Sand and gravel	Autosenna SRL
Sacel 4	Sand and gravel	CCCF-Drumuri si Poduri Timisoara SRL Bucuresti
Homorod 1	Sand and gravel	Vespa System SRL
Rapolt Uno	Sand and gravel	Numero Uno Texport SRL filiala Geoagiu
Simeria Veche III	Sand and gravel	Pomponio S.A. Alba Iulia
Folt	Sand and gravel	CIF S.A. Deva
Sacamas	Sand and gravel	Drupo SRL Deva
Streisangeorgiu	Sand and gravel	Drupo SRL Deva
Carpinis Nord 1	Travertine	Silva Forte SRL Deva
Valea Balului	Industrial or building andesite	Minvest Deva
Dealul Socolul Mic	Industrial or building andesite	Minvest Deva
Mihaileni	Sand and gravel	Socot S.A. Tg. Mures
Harau Iaz Piscicol	Sand and gravel	Damida Special Construct SRL
Simeria	Sand and gravel	Best Master SRL
Bretea Maceu	Sand and gravel	Hidroconstructia S.A. Bucuresti
Folt	Sand and gravel	Get Tomexplor SRL Simeria
Insula Pod Gelmar	Sand and gravel	Drumuri & Poduri S.A. Deva
Pod Gelmar aval	Sand and gravel	Tcind S.A. Orastie
Branisca Bozu	Sand and gravel	Agro Tab Com SRL Deva
Fata Teiului	Industrial or building andesite	Teod Energy SRL Stanija
Turdas aval	Sand and gravel	Alex Beton Vily SRL Turdas
Cigmau 3/2	Sand and gravel	Vespa System SRL

3. Current situation of mining

This year, in Hunedoara county, a number of 11 mineral substances are exploited on surface through 48 quarries and open pits. The exact situation of these, regarding the location, extracted mineral substance and the economic entity that performs the mining is presented in Table 3 (for mining licenses) and Table 4 (for mining permits) [1980 – 2011. Exploitation data. National Agency for Mineral Resources (NAMR), Bucharest].

4. Conclusions

Long and very complex geologic evolution of the rock complexes within the Hunedoara county has led to formation of numerous deposits of different mineral substances, many of which are at the surface or in shallow depth. Having in view the surface of the county (Hunedoara is one of the 7 largest counties in Romania), with numerous population, and significant economic development (which determined an increased request of mineral products), the surface mining of mineral substances in this county has increased (a number of 235 identified quarries and gravel pits, that extracted a number of 30 non-metalliferous and noncombustible mineral substances). Their real number is great, having in view at the same time the minerals on which there is no information in specialized literature.

References

Marinescu M., 2003. Management and marketing in geology (in Romanian). Vol. 1.Publishing House of the Bucharest University, 196 pp., Romania

Mihailescu N., Grigore I., 1981. Mineral resources for construction materials (in Romanian). Ed. Tehnica (Technical Publ. House), Bucharest, 422 pp., Romania

Mutihac V., Stratulat M.I., Fechet R.M., 2007. The Geology of Romania (in Romanian). Editura Didactica si Pedagogica, Bucharest, 249pp, Romania.

Mutihac V., Mutihac G., 2010. The Geology of Romania within the Central-East-European Geostructural Context. Editura Didactica si Pedagogica, Bucharest, 690 pp., Romania.

Parvu G., Mocanu Gh., Hibomschi C., Grecescu A., 1977. Useful Rocks in Romania (in Romanian). Ed. Tehnica (Technical Publ. House) Bucharest, 412 pp., Romania.

*** 1980 – 2011. Exploitation data. National Agency for Mineral Resources (NAMR), Bucharest.

MARBLE – BETWEEN TRADITION AND CURENT USE

Gabriela-Silviana MARICA

Geological Institute of Romania, Caransebes street no.1, Bucharest, sector1
silviana.marica@gmail.com, (+40)21 3060458, Fax (+40)21 3181326

1. Introduction

Currently building stone rightfully regains the natural charm of the building where the growing market requirement is that beauty together with endurance.

Analyses and studies in recent years have realized that size to develop and supported the concept of sustainable development in relation to economic and social development of society. Bear in mind so that this development is inconceivable in the absence of natural resources.

Marble as non-renewable natural resource due to its outstanding characteristics, can be characterized in many material respects as of the time. No other material has such a great variety of issues, from natural matrix or color ventures. Marble has in the eyes of the beholder three essential characteristics: quality, durability, design. They talked a lot of sometimes about "intelligent" stone or natural material that is a building designed to resist even for hundreds of years.

The so-called time "*patina"* refers primarily to marble and limestone rocks and is one of its most valued attributes. The global economic competition and the context of the need for uniform behavior of building this "*patina*" is searching including new constructions.

This paper is a summary of laboratory and field work undertaken in recent years, particularly with reference to the buildings with marble and limestone rocks cover.

2. From Romans to modern time

Stone processing occupation can be regarded as a leading approach to auras dark ages until early this century. Gothic art, made as a strong expression of power through its features marble proved as expression of traditional classical works that can be a permanent example for today's buildings. (Fig.1)

An inimitable example is the Milan Cathedral, where *Candoglia marble* was used for hundreds of indoor and outdoor decorations as well as fine quality vertical sharp stone.

Since the beginning of Christianity in particular, for the vast majority of religious buildings marble was used for the construction of exterior walls, stairs and floor tiling and polished marble especially for interior products.

From the commercial point of view, that includes not only marble strictly speaking –the crystalline rock which petrography was incurred by recrystallization of carbonate rocks, but also dolomites and limestones, rocks with a wide range of colors and decorations. The largest deposits of marble in the world are in Italy, running from Alps to Sicily.

Fig. 1. The Parliament Palace in Budapest, built from marble.

Marble is still currently playing an important role in outer facades of urban buildings, tourist and monumental, being suitable for any of the internal and external architecture, as the buildings Finlandia Hall from Helsinki, Finland and the Amoco Building from the USA. These buildings proved special problems of installation and durability of marble. Finlandia Hall in Helsinki was covered with marble using fixed installation, which later proved unstable, detaching tiles due to stone expansion and requiring replacement of stone of the entire surface. Fixed installation is not good for marble.

Dimension stone production and processing industry, especially the marble industry is one of the most dynamic industries. Marble was the most efficient building material with an upward trend that will continue in the coming years. Italy held for long time the leadership in building stone, but nowadays China has come forward and covers 19% of the global market.

3. Geological-economic conditions at Ruschița and not only

From ancient Roman aqueducts and paved with indigenous stone to the Sarmizegetusa city, built of Bucova marble and Uroiu andesite, marble – especially the Ruschita marble- show a spectacular spread in Romania, in construction and monumental buildings.

Clearly, white or pink with grey, Ruschita marble has become the most popular in Romania and is currently brand of 12440/2008 European standard of natural stone, with others ornamental stones in Romania.

Ruschita marble deposit is located in northern part of Caras Severin County, 10 kilometers northwest of the village Rusca Montana. In the areas where the marble develops, the relief is rugged with steep walls and deep valleys (Fig. 2).

Fig. 2. Old Ruschița quarry with steep wall over 100 m high.

Between 1884-1960, the exploitation of Ruschita marble was from an inverted bell-shaped quarry, thus forming Ruschita Old Quarry that reached a depth of 130 meters. In 1960, operating platforms have been opened and form the present quarry. Exploitation is made by horizontal slices, strips down and longitudinal.

White marbles current level is present in the central part of this quarry. As development, it becomes more homogeneous thick marble in terms of colors, predominantly white milky color. Level of pink marble is located south of white marble level, appearing in the form of strips. Podeni and Ruschita marble are the most used construction rocks from Romania. They were used to build the House of Free Press, Institute of Agronomy, Institute of Architecture, Royal Palace, Telephone Palace, Palace of Parliament. Also from Ruschita marble were built the Parliaments of Vienna and Budapest (Fig.1) and the baths of the Palace of the Sultan from Brunei.

Characteristics of Ruschita marble determined in accredited laboratory on specific specimens of natural stone are presented in Table 1.

Table 1. Characteristics of Ruschița marble.

Characteristics	U M	Values
Apparent density	Kg/dmc	2.70-2.72
Water absorption	%	0.12-0.21
Porosity	%	0.37-0.74
Compressions strength	N/mmp	85-96
Resistance to wear	g/cmp	0.62-0.71

Another white marble statuary from Romania is Sohodol marble, Alba County. The color is white, sometimes yellow venatura due to iron oxides. Sohodol marble has a granoblastic structure and massive texture. The size of calcite crystals reach 2.5 cm. Marble has good mechanical properties (Table 2), also physical, decorative properties and high strength, being used in many buildings.

Table 2. Characteristics of Sohodol marble.

Characteristics	U M	Values
Apparent density	Kg/dmc	2.70-2.72
Water absorption	%	0.06-0.45
Porosity	%	0.3-0.6
Compression Strenght	N/mmp	60-110
Compression Strength after frost	N/mmp	56-93
Resistance to wear	g/cmp	0.37-0.43

4. Buildings quality with marble and limestones

Marbles and limestone have been used over time as interior and exterior tiles for large buildings, but also capitals, columns, ornaments, decorations. Carrara white marble and the vast majority of white marbles are best known for the impressive sculptures of Renaissance artists.

Railings, capitals, plinths, fireplaces, stairs (Fig. 3) modern tilings combined with other types of marble, have given special celebrity to Ruschita marble, especially for interior decorations.

Today there are older buildings and works and later plated on the outside with Ruschita marble, who although proving a particular aesthetic can be combined with artistic touch despite bad behavior and degradation of the stone due

Fig. 3. Railing and stairs made of Ruschiţa marble.

external agents and inappropriate use type of stone. This was proved by the famous Finlandia Hall and the Amoco Building cases, but also for example in solar watch from Piaţa Sf. Gheorghe (St. George Market) in Bucharest that has been restored after a major breakdown.

Marble and limestone are not resistant to acids, limestone is also resistant to salt due to their composition consisting of light mineral (carbonate minerals). For public environment is recommended honing surface or polished surface, which resists wear but can quickly become slippery. A flat or cut with diamond may be a good choice. Marble of good quality, according to its functions, means durability and dark granules that can win a beautiful *patina* over time.

Table 3. The required physical and mechanical characteristics of natural stone.

Uses of natural stone products	Required physical and mechanical characteristics of natural stone								
	Density	Porosity	Compression Strength	Frost resistance	Resistance to bending	Elasticity modulus	Coefficient of linear expansion	Resistance to weathering	Knoop microhardness
Exterior finishes									
Interior vertical finishes									
Pavements outside									
Horizontal interior finishes									
Stairs									
Coatings and decorations									

Notes: = little importance; = average importance; = great importance

Marble is still playing currently an active role in outer facades of urban construction, touristic buildings or monuments, but was net surpassed in the last two decades by the presence of hard rocks on the market: granite, labradorite, serpentinite, of different varieties and colors, which were required for most new buildings. Due to this aspect, where there is marble works, conservation works and maintenance are necessary.

Large amount of marble and others calcareous stones are still required due their qualities: the permanence of technical and aesthetic properties, the technical advantage of thermal and electrical insulation and ease of maintenance.

Applications of marble create a treatment that is required to work a few years after its installation on the outside, facing architects with technical issues. For this reason, especially in the context of global warming and pollution, increasingly higher volatile compounds and acid emissions in the large cities, more facades of recent constructions are made up of metamorphic and magmatic rocks.

The relationship between destination sites of marble and calcareous rocks products and the required physical-mechanical characteristics are presented in Table 3. The table shows the particular importance of several characteristics, especially of frost resistance in finished and external paving, but also the internal paving.

5. Concluding remarks

Marble is a non-renewable resource and can be called *material of time* due to its characteristics, especially time "patina". Many monumental buildings, including the Parliament Palace in Budapest and Milan Cathedral are built of marble, especially Italian, but also from Romania.

Ruschita marble deposit located in Caras Severin County is the largest in Romania with its two varieties of marble white and pink of very good quality.

Fixed installation for exterior is not good for marble. Today there are recent constructions plated with marble which proved a bad behavior over time due to poor resistance to acids and whether. For the exterior finishes and pavements of particular importance are the following characteristics: frost resistance, bending, hardness and weather resistance.

RAW MATERIALS USED FOR THE PHOSPHATE FERTILIZER PRODUCTION IN ROMANIA - NEW RADIOMETRIC DATA

Aurora Măruța IANCU (CARAVEȚEANU)[1], Delia-Georgeta DUMITRAȘ[1], Ştefan MARINCEA[1], Adriana ION[1], Essaid BILAL[2], Maria Angela ANASON[1]

[1] Department of Mineralogy, Geological Institute of Romania, 1 Caransebes St 012271, Bucharest, Romania, aurash83@yahoo.com

[2] Ecole Nationale Supérieure des Mines de Saint Etienne, UMR6425, CNRS, France

Abstract Uranium, thorium and potassium were measured by low background gamma spectrometry in natural apatites used as raw materials in the phosphate fertilizer industry. The results confirmed that the phosphates of sedimentary origin (i.e. the samples from Jordan and Morocco) have higher concentrations of uranium (98-119 ppm) and lower concentrations of thorium (21-31 ppm), while phosphates of magmatic origin (i.e., Kola Peninsula, Rajasthan) are thorium-richer (40-117 ppm) and uranium-poorer (24-35 ppm).

Key-words: phosphates, uranium, thorium, sedimentary, magmatic

1. Introduction

The nature of phosphate fertilizer produced by sulfuric acid attack and the nature of phosphogypsum as technogenic by-product are directly determined by the type of the phosphate ore used for the production of phosphoric acid. The phosphate ores used in the industry of phosphate fertilizers are generally of sedimentary origin, rarely of igneous origin and exceptionally of metamorphic origin. Sedimentary phosphates (phosphorites), represent about 85 % of the phosphate rock used for the production of phosphoric acid (Habashi, 1980), which is also the case of the producers in Romania.

In fact, the composition and quality of the base phosphate ores clearly indicates their genesis. In most of the phosphate deposits, apatite is the main P-bearing mineral (Lehr and McCleallan, 1972) and has a relative chemical homogeneity. The mineralogy is rather simple, the main constituent of the deposits being apatite-(OH) in the case of the sedimentary ores and apatite-F in the case of the magmatic ones.

2. Methods

The determination of uranium, thorium and potassium by low background gamma spectrometry with HPGe detector is a simple and nondestructive method that requires a simple preparation of the simple. The method allows the selective determination of uranium, thorium and potassium, up to very low limits (under 0.1 ppm). The Gamma spectrometric equipment used for analysis included a DSPEC jr. 2.0 device, with 16684 channels, digital multi-channel analyzer, HPGe detector model GEM-25 pop-top (relative detection efficiency of 26 %, resolution ranging from 1.8 keV to 1332 keV for Co-60 and 0.8 to 122 keV for the cobalt line in the standard, peak/Compton ratio of 56/1). The device uses electromechanical cooling (X-cooler II), a protection of Pb screen-type and a HPGe detector of ORTEC type.

The gamma spectra of the apatite samples was performed with a standard spectrometric equipment using the following work conditions: the energy calibration was done with Eu-152 and Cs-137 radioisotopes, for the optimal energy range between 50 and 2000 keV, the channel width for measurements was of about 0,5 KeV, the counting time was of 86400 s. Both the samples and the standards were measured under the same conditions of geometry and time.

Radiometric determination was performed on five apatite samples from four different locations namely: two apatite samples from Jordan, one sample from Morocco, one sample from the Kola Peninsula and one sample from Rajasthan (India).
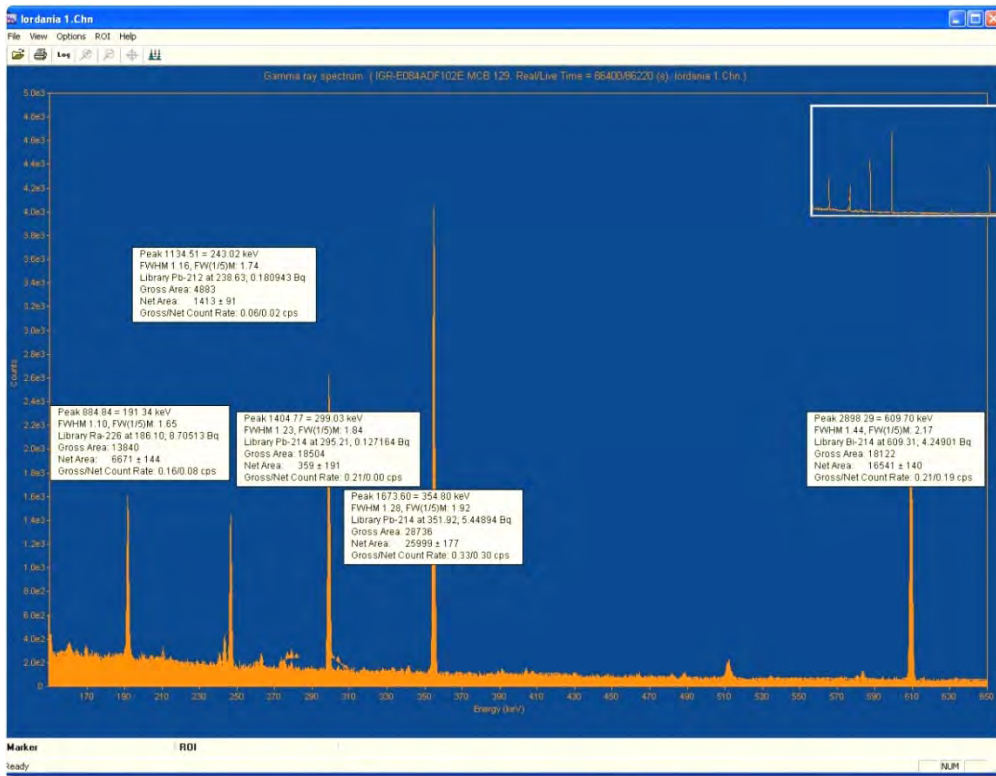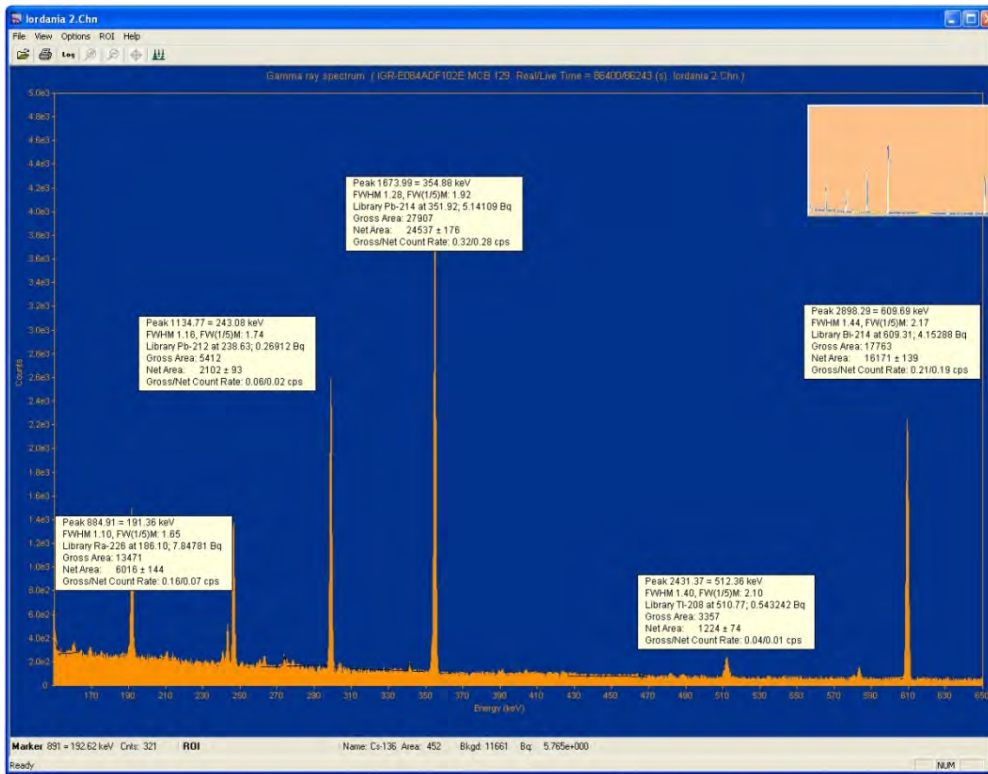
Fig. 1. A.Gamma-ray spectrum of Jordan 1 apatite sample. Note the high content in U-238; **B.** Gamma-ray spectrum of Jordan 2 apatite sample. Note also the high content in U-238; **C**. Gamma-ray spectrum of an apatite sample from Morocco. Note also the high content in U-238.
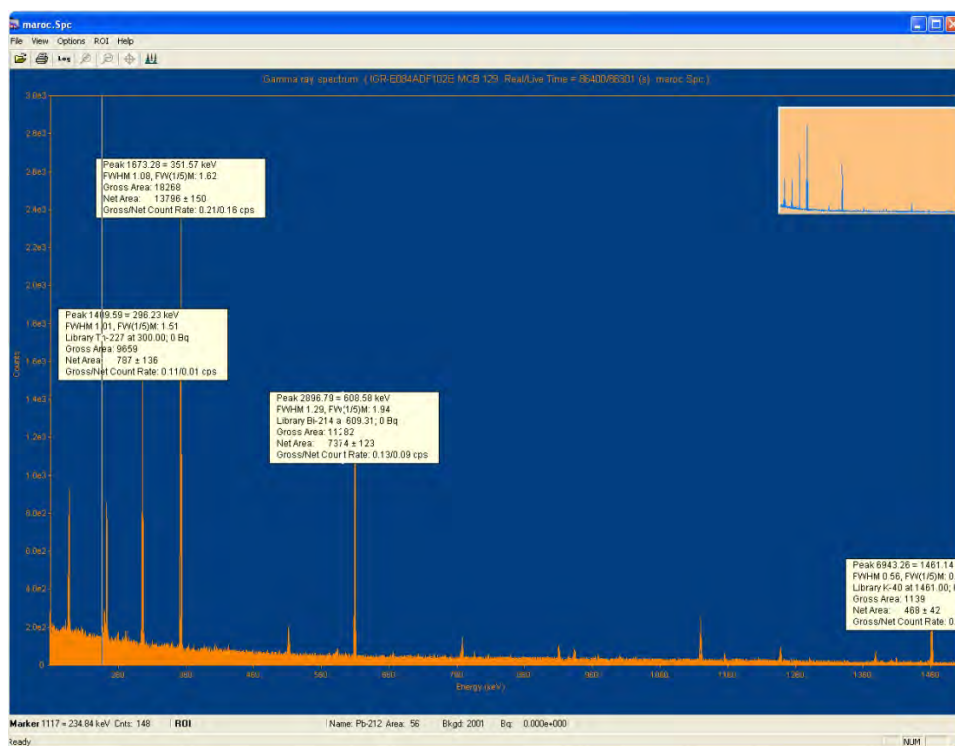
C

Fig. 1. – continued.

3. Results

The results of radiometric analyses on the five apatite samples used in the production of phosphoric acid and phosphogypsum are given in Table 1.

Table 1. Radio isotopes in the apatite samples used for the manufacture of phosphoric acid

Sample location	U-238 (ppm)	Th-232 (ppm)	K-40 (%)
Jordan 1	100.45	30.12	0.023
Jordan 1	119.35	20.75	0.031
Morocco	98.21	31.12	0.12
Kola Peninsula (Russia)	24.12	117.48	0.17
Rajasthan (India)	34.74	40.12	1.04

The resulting gamma ray spectra of the five samples are depicted in Figs. 1 and 2. They are represented in terms of counts (number of pulses/unit time) versus energy.

When the radiation is monoenergetic and its energy is completely absorbed by the detector, the spectrum is represented by a line (theoretical spectrum). In reality, the bands in the experimental spectra are not lines but complex peaks of different extension, because their amplitude is a factor of the fluctuations in the absorption of the radiation of the same energy. Broadening of the bands is amplified by other instrumental factors. The peak shape is similar to a Gaussian curve and the apex location indicates the radiation energy.

4. Conclusions

The radiometric study of the natural apatites used as raw materials in the phosphate fertilizer industry is an easy method for the determination of their origin. Our study confirms that the phosphates of sedimentary origin (i.e. the samples from Jordan and Morocco) have higher concentrations of uranium and lower concentrations of thorium, as proved by the frequency of the radioactive U-238 isotope. Phosphates of magmatic origin (i.e., Kola Peninsula, Rajasthan) are, on the contrary, thorium-rich, as proved by the high contents in Th-232.
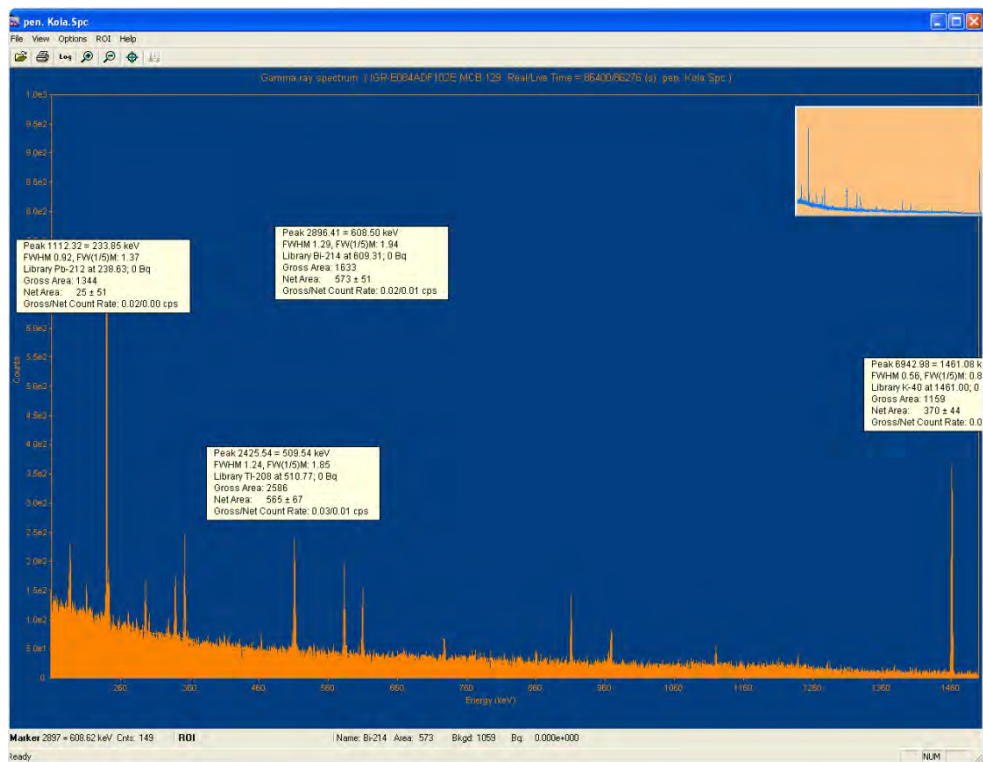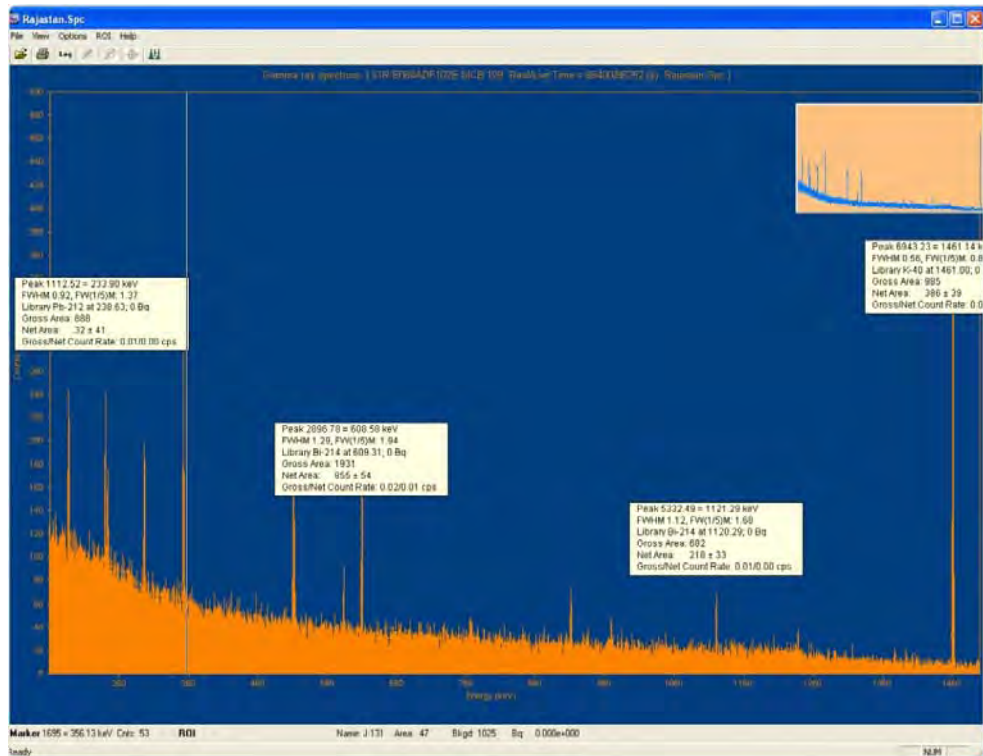
Fig. 2. A. Gamma-ray spectrum of a sample of magmatic apatite from Kola Peninsula. Note the high content in Th-232; **B**. Gamma-ray spectrum of a sample of apatite from Rajasthan. Note also the high content in Th-232, which suggests its magmatic origin.

References

Habashi F., 1980. The recovery of uranium from phosphate rock: progress and problems. In: *Proceedings of the Second International Congress on Phosphorous Compounds*, Boston, MA, 629 pp.

Lehr J.R., McClellan G.H., 1972. A revised laboratory reactivity scale for evaluating phosphate rocks for direct application. *Bulletin Y-43,* National Fertiliser and Environmental Research Center, Muscle Shoals, AL..

GOLD, SILVER AND SILVER CARBONATES IN THE WASTE DUMPS OF THE LEAOTA MOUNTAINS, SOUTH CARPATHIANS

Sorin Silviu UDUBAŞA[*], Gheorghe UDUBAŞA

University of Bucharest, Faculty of Geology and Geophysics, N. Bălcescu Blv. 1, 010041 Bucharest, Romania;
E-mail: *sorin.udubasa@gmail.com, udubasa@geo.edu.ro*

Abstract Among the different types of ores hosted by the Leaota crystalline massif, the most important are the pentametallic ones in the area of Neguleţ and Dăniş Valleys. The mineral association described is large and comprise native gold and silver, (Au, Ag) alloys, as well as native bismuth and other sulfides and some sulphosalts. Material from the Bădeanca 2 adit waste dump has been analysed using several structural techniques (XRD, TEM/SAED, NGR) in order to estimate the transformations suffered by the primary ore minerals in the waste dump. The most interesting findings are the nanometric sized grains of gold as well as the silver carbonates. The nanogold occurs as isolated spheres or as coral-like aggregates; the silver carbonates may represent secondary phases formed during the residence of the material in the waste dump. The use of structural methods in analyzing the waste dump material (and not only) can dramatically increase the number of the mineral species discovered in the area by revealing the nanoscale side of the mineralogy of the waste dump.

Keywords: nanogold, nanosilver, silver carbonates, waste dumps, Leaota Mts.

1. Introduction

The Leaota crystalline massif (LCM) consists of several metamorphic series or groups (Voineşti, Lereşti and Căluşu) and contains and amazingly high number of ore occurrences. The age of the metamorphic rocks and the genesis of the ores is still matter of many debates. The aim of this paper is to present mainly some aspects of the ore genesis and the fate of metals in the waste dumps material as well.

2. Ore deposits in the area

Except the northern part of the LCM (Gibe and Casework Valleys), where the ores are dominantly gold-bearing and mostly related to the thrust plane between the Vainest series (older and with a superior structural position) and the Lereşti series (younger). Associated with this thrust/shear plane, there occur the so-called Albeşti granites, forming slabs of varying size along the sear plane. The role of these granites in the formation of associated ores is still unclear, bringing however, supplementary problems related to the ore genesis.

Most (about 30 of total 40) ore occurrences are concentrated in the central and southern part of the LCM (Fig. 1) and they are very different (as concern the mineral and chemical composition) and no close relation among the nearly situated occurrences can be traced.

The most celebrated (known since the XIXth century) are the pentametallic ores (Co-Ni-Ag-Bi-U) in the areas of Valea lui Neguleţ and Valea Dăniş brooks. A large number of minerals have been described here, including native gold, silver, (Au,Ag) alloys, bismuth. In searching for uranium mineralisations, the adit Bădeanca 2 surely opened not only the U-ores but also the complex ores identified in the neighboring mining works on Dăniş and Neguleţ brooks. By using the data presented by Pop et al. (1983) for the U-ores and by field observations in the time of intense prospecting and exploration in the LCM (1975-1990, see Udubaşa, 1988, 1993, 2000) the relationships among the different ore types has been derived (Fig. 2), i.e. "pure" shear zone related pyrite-copper ores (said by Udubaşa, 1993, to belong to the Tibra-Tincava type), the associated polymetallic (mostly pentametallic) ores, developed on discordant veinlets crossing the shear zone related pyrite-copper ores and finally the U-ores located on discordant faults crossing also the shear plane.
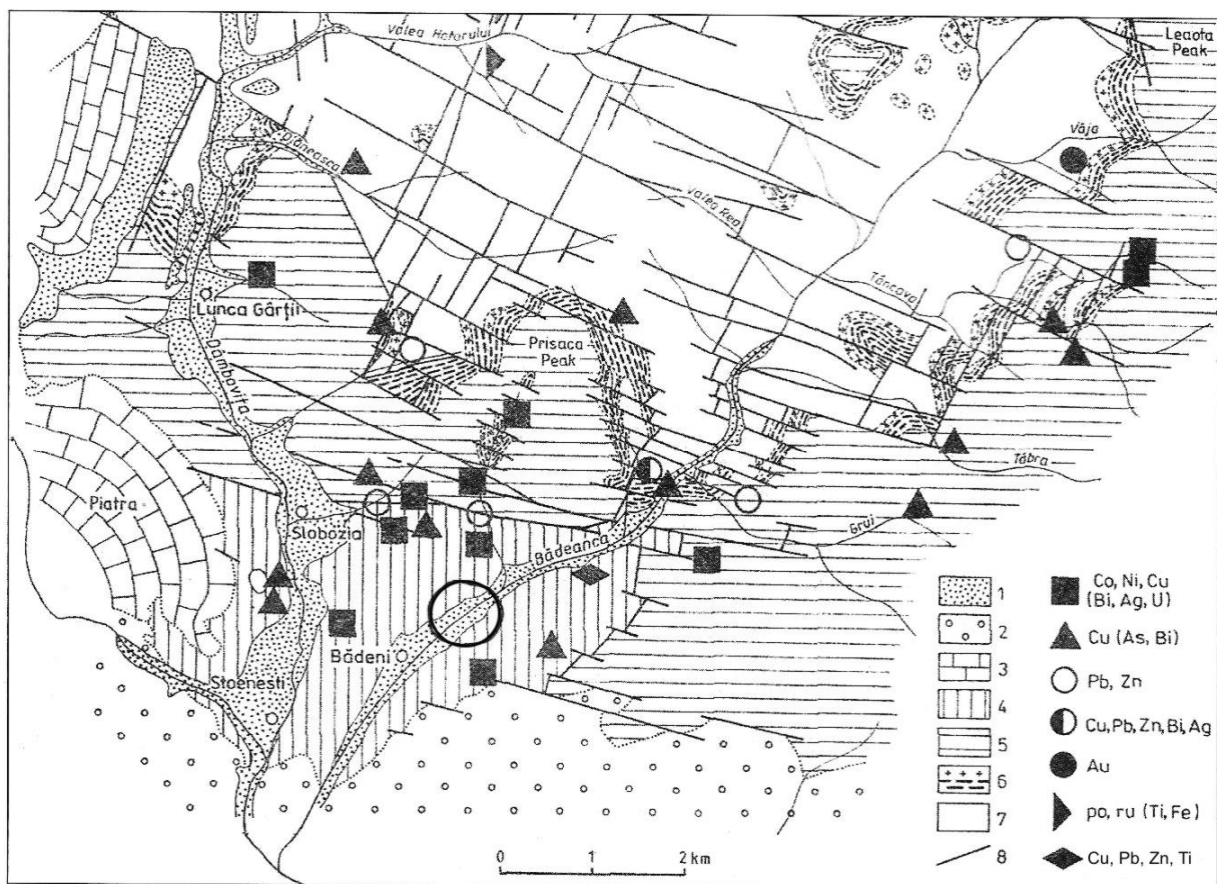
Fig. 1. Geological sketch map of the Leaota Mts. (from Udubaşa, 2000).
1- Quaternary deposits; 2 and 3 – Mesozoic sedimentary deposits: 2- conglomerates, 3- limestones; 4-7 – Leaota metamorphic Group (Late Proterozoic?): 4- Căluşul Formation (quartz-chlorite-sericite schists), 5- Lereşti Formation (partly retrogressed micaschists ± garnet and albite porphyroblasts, gneisses), 6- Bughea amphibolite and Albeşti granite (a rock mixture reminiscent of a pseudo "mini greenstone belt", 7- Voineşti Formation (gneisses, amphibolites ± garnet and pyroxene); 8- Faults. *Great circle – location of the waste dump from Bădeanca 2 adit.*
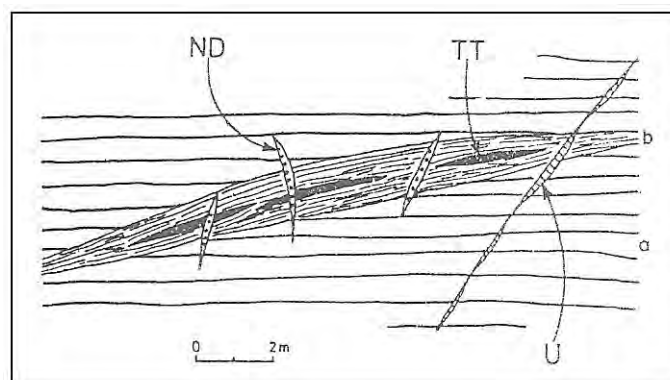
Fig. 2. Relationships between the fahlband-like ores (TT- Tibra-Tincava) + ND (Neguleţ-Dăniş) and the late (Alpine?) uranium mineralization (U – pitchblende-tucholite) in the Leaota Mts. Country rocks are (a) micaschists and paragneisses with (b) sheared counter parts. (From Udubaşa, 1993).

The mineralogy of the various ore types is quite different, although some overlappings seemingly exist (Table 1).

Table 1. Mineral content of some ore types in the southern Leaota Crystalline Massif.

Ore types	Mineral composition
"Pure" shear type - Tibra-Tincava type (TT)	- pyrite, chalcopyrite, pyrrhotite, rutile, titanite, native bismuth, bismuthinite, brookite. - Gangue minerals: quartz, carbonates.
Extended pentametallic type - Neguleț-Dăniş type (ND)	- pyrite, chalcopyrite, galena, arsenopyrite, sphalerite, pyrrhotite, tetrahedrite, bismuthinite, safflorite, wittichenite, nickeline, skutterudite, nickelskutterudite, maucherite, löllingite, stibnite, linneite, vaesite, molybdenite, millerite, rammelsbergite, bornite, polydimite, gersdorffite, emplectite, hodrushite-krupcikite. - native metals: gold, silver, (Au,Ag) alloys, bismuth - secondary minerals: chalcocite, erithrite, annabergite, azurite, marcasite, covellite. - Gangue minerals: quartz, calcite, ankerite, dolomite, chlorite.
Uranium ores (U)	- pitchblende (uraninite), marcasite, pyrite. - Gangue minerals: carbonaceous matter (partly tucholite).

Data sources: Caracas (2006), Petrulian (1936), Poni (1884), Pop et al. (1983), Popescu (1968), Udubaşa (1988, 1993, 2000)

3. Nanomineralogy of the waste dumps

The waste dump of the Bădeanca 2 adit (Fig. 1) has been chosen for investigations as it is the largest in the area and one of the oldest (more than 50 years). By using several structural methods (XRD, TEM/SAED, NGR; for working conditions see Udubaşa et al., 2011) some new minerals were encountered, some of them not previously known. The mineral species identified by these methods in the waste dump of Bădeanca 2 adit are presented in Table 2. First of all is to be mentioned the nanogold (gold grains several nanometers in size) either as isolated spheres or as clusters (coral-like aggregates). In addition, (Au, Ag) alloys with associated nano-lamellae of silver carbonates (α- and β-AgCO$_3$), ferrihydrite, maghemite, plattnerite, cristobalite, pseudobrookite, SiC etc. were identified by using electron diffraction technique. Very interesting is a ring-shaped opaque mineral, identified by NGR as a Mn-rich spinel, presumably formed at the expense of spessartine.

Table 2. Mineral species identified in the waste dump of Bădeanca 2 adit. See Udubaşa et al. (2011) for further details, including the methods of identification.

Gold, gold-silver alloys
α-Ag$_2$CO$_3$, β-Ag$_2$CO$_3$
Quartz, cristobalite, moganite
Maghemite, ferrihidrite, pseudobrookite
Plattnerite, jacobsite (?)
Cattierite, greigite, acanthite, pyrrhotite
SiC (?)
Illite, corrensite, kaolinite

4. Conclusions

By far the most interesting is the nanogold, which represents a good alternative of the "invisible gold". The silver carbonate, presumably have been formed secondarily during the ore residence in the

waste dump. To our knowledge it is the first naturally occurring silver carbonate (both alpha and beta forms).

Adding the nanominerals, the number of the mineral species in the LCM dramatically increased, showing that nanomineralogy can reveal an "unseen" side of the waste dumps mineralogy. In addition, attempts were made to recover metals by using different plants (phytomining), which were mostly successful (Udubaşa et al., 2011).

References
Caracas E.F.R., 2006. Studiul mineralizatiei de Ni, Co, Bi, As din perimetrul Valea Badeanca, sud-vestul masivului Leaota. Unpubl. PhD thesis, Univesity of Bucharest, Romania, 94 p.
Petrulian N., 1934. Les minerais de cobalt de la Valea lui Negulet (Badeni-Ungureni). An. Inst. Geol. Rom. 17.
Poni P., 1884. Mineralele de la Bădenii Ungureni. An. Biur. Geol., II/1, 66-71.
Pop Gh., Buzila Al., Constantinescu P., Hadareanu R., 1983. Date noi privind mineralizatiile de sulfuri din bazinul Vaii Badeanca – masivul Leaota, obtinute prin lucrarile geologice complexe executate in perioada 1977-1982. M.M. Of. Inform. Docum. – Elemente rare si radioactive, II, 42-68.
Popescu Gh., 1968. Asupra prezentei maucheritului in mineralizatiile de nichel de la Badeni (M. Leaota). St. cerc. geol. geofiz. geogr., Geologie, 13/2, 431-435.
Udubaşa G., 1988. Metalogeneza masivului Leaota. C. D. Geol., Bul. Inf. Doc., Geologie, 3, 5-17.
Udubaşa G., 1993. PTX constraints of ore parageneses with some case studies. Rom. J. Mineralogy, 76, part 1, 7-13.
Udubaşa G., 2000. Brookite from Badeanca Valley, Leaota Mts. Rom. J. Mineralogy, 80, 51-60.
Udubaşa S.S., Constantinescu S., Popescu-Pogrion N., Sarbu A., Stihi C., Udubaşa G., 2011. Nanominerals and their bearing on metals uptake by plants. Rev. Roum. Geologie, 53-54 (2009-2020), 47-60.

PRELIMINARY COMPOSITIONAL DATA ON GOLD SAMPLES FROM CETATE HILL, ROŞIA MONTANĂ AND ROATA MINE, CAVNIC ORE DEPOSITS (ROMANIA)

Daniela CRISTEA-STAN[1]*, Bogdan CONSTANTINESCU[1], Daniele CECCATO[2], Claire PACHECO[3], Laurent PICHON[3]

[1]Horia Hulubei National Institute for Nuclear Physics and Engineering, P.O.Box MG-6, RO-077125 Bucharest-Magurele, Romania, E-mail: daniela@nipne.ro, Tel: +40214042349, fax: +40214574440
[2]Università di Padova, Dip. Di Fisica "G. Galilei" and INFN, Laboratori Nazionali di Legnaro, I-35020 Legnaro (Padova), Italy, E-mail: ceccato@lnl.infn.it
[3]Centre de Recherche et de Restauration des Musées de France, CNRS UMR 171, Palais du Louvre, Paris CEDEX 01, France, E-mail: claire.pacheco@culture.gouv.fr, E-mail: laurent.pichon@culture.gouv.fr

Abstract: Very small samples (hundreds of microns) of native gold from Cetate Hill quarry Rosia Montana, Apuseni Mountains and from Roata mine Cavnic (Baia-Mare district) were scanned by micro-PIXE method to determine their elemental composition, Ag/(Au+Ag) ratios, trace elements (Te, Sb) suggesting gold minerals (tellurides) and associated minerals.

1. Introduction

This study was conducted on three samples of native gold (electrum) from Rosia Montana - Cetate Hill, Apuseni Mountains and on five samples from Cavnic-Roata mine (Baia-Mare district) using two X-ray based methods of elemental analysis:
- XRF (X-Ray Fluorescence) excited by an X-ray tube - using the X-MET TX3000 portable spectrometer at NIPNE
- micro-PIXE (micro Proton Induced X-ray Emission) at AN2000 accelerator of Laboratori Nazionali di Legnaro (LNL), INFN, Italy and at AGLAE accelerator of CNRS-Musee du Louvre, Paris, France to obtain information on:
- electrum structure - values of ratio Ag/(Au + Ag)
- presence of gold and silver minerals (tellurides, antimony compounds) – many as micro-inclusions
- presence of gold associated minerals – gangue

2. Geology of the studied areas

Rosia Montana is one of the oldest and most interesting gold deposits in the Metaliferi MTS. with both veins and stockworks developed in highly altered rhyodacites. They locally contain up to 10-20 % adularia. The gold fineness here is quite low (about 500). The associated minerals include many silver-rich sulfosalts such as proustite, pearceite, stephanite, and polybasite. Alabandite, sphalerite, berthierite, and silver-rich tetrahedrite in association with rhodochrosite all represent further gold associates. Gold leaves or moss-like aggregates, as well as crystals as cubes and icositetrahedra can reach several cm in size (Udubasa et al. 2002).

Cavnic deposit (Popescu, 1986) belongs to Baia-Mare mining district, which is located in the eastern part of the Carpathian belt, one of Europe's major metallogenic provinces, extending from Slovakia, Hungary and Ukraine to Romania and including important epithermal gold-polymetallic ore deposits. The Baia-Mare district, with about 15 mines, provides most of Romania's lead and zinc and some gold, silver, copper and antimony (Grancea et al. 2002). The Cavnic deposit is a polymetallic deposit with local Au–Ag enrichments (generally in the upper part of the system) which were selectively mined out in the past.

3. Materials and methods

Analyzed samples are from recovery obtained by Rosia Montana inhabitants from existing on-site landfills of former Cetate hill exploited in quarry mode during 1970-1990 and by Cavnic inhabitants from Cavnic-Roata mine.

To study these samples we used two elemental analysis methods: XRF (Cristea-Stan et al., 2012) – mainly to obtain Ag/ (Au+Ag) ratios and to identify chemical elements from gold-silver and gangue minerals and micro-PIXE emission for more sensitive determination of elemental composition: lower detection limits (because of much higher intensity of the excitation beam) and a much improved lateral

resolution due to the use of micrometer-size beam. Very small samples (hundreds of microns) of geological samples can be scanned by micro-PIXE method to identify especially minor (between 0.1 and 1%) elements and for possible micro-inclusions (micro-areas of different composition from the surrounding material – e.g. rich in tellurium and antimony).

4. Results and discussion

For Cetate - Rosia Montana samples the most important results are:

- using micro-PIXE method at LNL AN2000 accelerator (Boccaccio et al., 1996) we concentrated on the existence of areas rich in silver and antimony which is present in the sample Rosia Montana 1 well illustrated (see Fig. 1) in the maps of element Au, Ag, Sb, Fe, Mn, As, where in the top right you can see an area with silver and antimony, but no gold. GUPIXWIN program indicated for the entire area (approx. 2mm x 2mm) concentrations for these key elements: Au = 18.96%, Ag = 15.41%, Fe = 10.13%. It is clearly seen greater proportion of silver than with regular electrum.

- a point-range (5 μm X 5 μm area) without gold silver area on the back of the sample is presented in Fig. 2. Note the disappearance of gold and the antimony presence, Sb/Ag ratio being 1/5-6, indicating from stoichiometric point of view the existence of stephanite (Ag_5SbS_4). GUPIXWIN program give for this small area of 5 μm X 5 μm following concentrations: Au = 0.17%, 39.69% Ag, Fe = 10.33%, Sb = 6.45% confirming the practical disappearance of gold and silver compounds domination, only pyrite remaining unchanged.
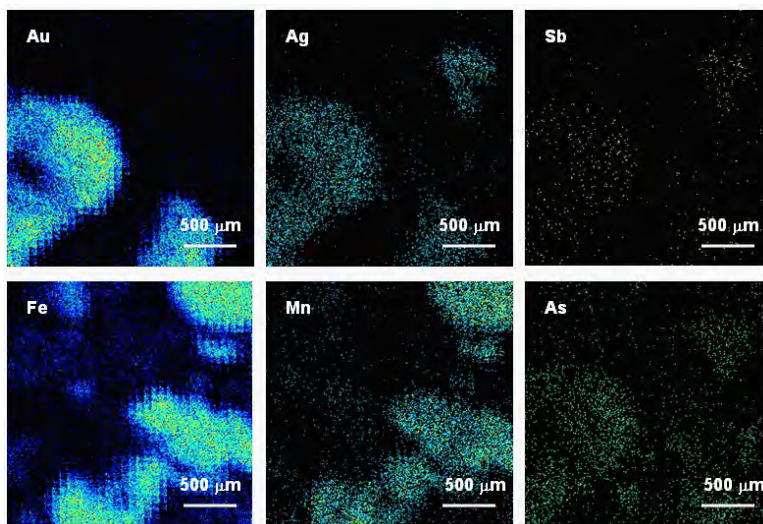
Fig. 1. Rosia Montana 1 - micro-PIXE elemental maps
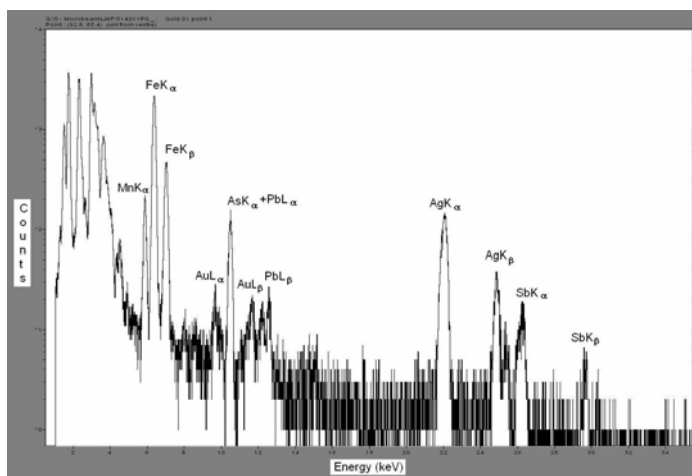
Fig. 2. Rosia Montana 1 - micro-PIXE - point spectrum

For Cavnic-Roata samples, to investigate gold and silver minerals - tellurides and antimony compounds, the most interesting sample (Cavnic-Roata 2) was analyzed by micro-PIXE using a 3 MeV

proton beam at AGLAE accelerator (Maxwell et al., 1989) (3 MeV it is an adequate energy to have a good sensitivity for Sb and Te detection).

We analyzed "points" (areas of approx. 50 microns diameter) located in various regions of the samples. The study was focused on Sb and Te presence and on the variation of Ag/(Au+Ag) ratio values, which characterize electrum's metallogeny (geological provenance) (Shimizu et al., 2001).

For all Cavnic-Roata samples the Ag/(Au+Ag) ratio varies from 0.221 to 0.395. We can consider an average value of 0.27, but big differences remain strong from point to point illustrating electrum's inhomogeneities. Ratio values are significantly lower than those given in (Shimizu et al., 2001) for Cavnic-Boldut - between 0.47 and 0.53, but approaching over Nistru data - 0.25 or rather Herja - 0.36. For a Rosia Montana polished sample (Neacsu et al., 2009) the range of ratio values is between 0.21 and 0.23. An interpretation in terms of electrum metallogeny is required for the future.

One point from the sample Cavnic-Roata 2 (see Fig. 3 a, b) revealed an important presence of tellurium (Te=16657 ppm of the area's total composition), a significant presence of antimony (Sb=2861 ppm) and an increase of silver content (Ag=32.75% versus Au =50.05%), indicating the presence of a silver telluride containing also antimony. The high arsenic content (As=6.64%) could indicate benleonardite - $Ag_8(Sb,As)Te_2S_3$ highlighted in Kremnica, Slovakia (Udubasa et al., 2002) – also in Northern Carpathians Mts. We cannot exclude the presence of a krennerite - $(Au, Ag)Te_2$ enriched in antimony, as revealed in Sacarâmb, Metaliferi Mts. (Shimizu et al., 1999).
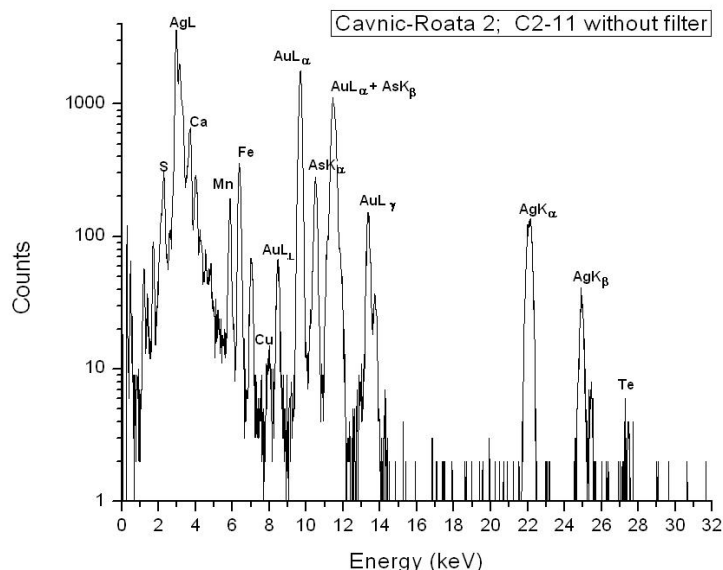
Fig. 3. a. Cavnic-Roata 2, spectrum C2-11-without filter
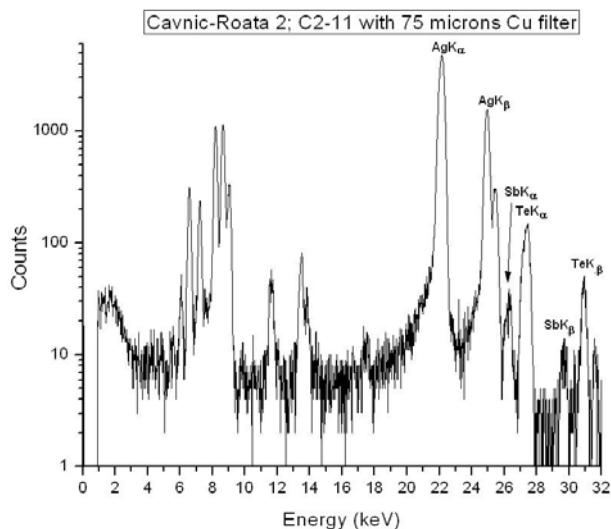
Figure 3. b. Cavnic-Roata 2, spectrum C2-11- Cu filter

To identify undoubtedly the telluride(s) in our samples we intend to perform a micro-mineralogical study using a SEM (Scanning Electron Microscope) associated with EDX (Energy-dispersive X-ray spectroscopy) facility.

References

Boccaccio P., Bollini D., Ceccato D., Egeni G., Rossi P., Rudello V., Viviani M., 1996. LNL AN2000 microprobe system, Nuclear Instruments and Methods in Physics Research B 109, 94-98

Butucescu N., Bonea L., Botnarencu A., Stoicescu G., Stoicescu F., 1963. Gold-silver tellurides mineralization from Baiata-Nistru deposit (Baia Mare) (in Romanian). Revista Minelor 14, 5, 214-221.

Cristea-Stan D., Constantinescu B., Chiojdeanu C., Ceccato D., Pacheco C., Pichon L., 2012. Micro-PIXE and XRF studies on native gold from Cavnic ore deposit (Baia Mare District). Romanian Journal in Physics, 57, 3-4, (in press)

Grancea L., Bailly L., Leroy J., Banks D., Marcoux E., Milesi J. P., Cuney M,, Andre A. S., Istvan D., Fabre C., 2002. Fluid evolution in the Baia Mare epithermal gold/polymetallic district, Inner Carpathians, Romania, Mineralium Deposita 37, 630–647.

Istvan D., Virsescu I., Halga S., Grancea L., 1995. Gold-silver epithermal levels and associations in the eastern area of the Gutai Mts. And in the Varatec Mts. (Firiza-Botiza area), East Carpathians, Romania. Studia Universitatis Babes-Bolyai, Geol XL(1), 195-210

Maxwell J. A., Campbell L. A., Teesdale W., 1989. GUPIX software for X-ray cross sections, Nuclear Instruments and Methods in Physics Research B 43, 218 -225.

Neacşu A., Popescu Gh. C., Constantinescu B., Vasilescu A., Ceccato D., 2009. The geochemical signature of native gold from Rosia Montana and Musariu ore deposits, Metaliferi Mts. (Romania); Preliminary data. Carpathian Journal of Earth and Enviromental Sciences, 4, 1, 49 - 59.

Plotinskaya O. Y., Damian F., Prokofiev V. Y., Kovalenker V. A., Damian Gh., 2009. Tellurides occurrences in the Baia Mare region, Romania. Carpathian Journal of Earth and Environmental Sciences, 4, 2, 89-100.

Popescu Gh.C., 1986. Applied metalogeny and geological prognosis (in Romanian), Partea II-a, Tipografia Universitatii Bucuresti.

Shimizu M., Shimizu M. (Marina), Cioflica G., Jude R., Lupulescu M., Berbeleac I., Kovacs I., (2001). Gold in Romania: chemisty and Alpine metallogenesis, Mineral Deposits at the Beginning of the 21st Century, Piestrzynski et al (eds)

Udubaşa G., Szakall S., Duda R., Kvasnytsya V., Koszowska E., Novak M., 2002. Mineral of the Carpathians, Granit Publishers, Prague.

FLUID AND MELT INCLUSIONS: A PRECIOUS TOOL IN SELECTIVE EXPLORATION STRATEGY

Ioan PINTEA

Geological Institute of Romania, ipinteaflincs@yahoo.com

Motto:
"behind every important mineral there once was a fluid"
(*Hans P. Eugster, 1986*)

1. Introduction

There are many and valuable analytical data released from fluid and melt inclusion study during the last decades in Romania, which can be used as database for the present and further exploration works. PVTX characteristics of fluid phases involved in alteration-mineralization processes are known in epithermal and porphyry copper +/- skarn from Alpine metallogenesis, in metamorphic low- and medium grade fluids or sedimentary brines and hydrocarbons. The main depositional processes are related to fluid phase behavior expressed by mineral occurrences in veins, breccia bodies and lodes or disseminated in pervasive altered subvolcanic stockworks. Inside of these, pulses of boiling or unmixed fluid fluxes deposited monominerals or several associations and parageneses. Many of them were entirely or partially exploited. New extraction techniques beneficiated Au, Ag, Cu, Mo, W, but also other elements used in high - tech electronics, energy or spatial technology such as Cd, In, Ga, Ge, Sn, Tl, Bi, Se, Te,Co, Re, Nb, etc. These are the minor (e.g. Chesu, 1983), trace or rare earth elements always dispersed, but rarely forming individual mineral species. To understand their concentration history it is necessary to know the moment of their entering (and related processes too) in the various magmatic-hydrothermal and metamorphic systems, the associated fluid types and their further evolution. It is known that inside a specific ore deposit body, minor and trace elements were concentrated irregularly, depending on the local tectonics, fluid phase composition and evolution. Consequently, selective exploration strategy would be based upon specific characteristics of these (re)depositional processes and they come out simply by analyzing brine, hydrous silicate melt inclusions (or glassy), immiscible Fe(-S-O) melt, vapor- and liquid-rich fluid inclusions trapped in ore and gangue minerals. The lecture contains also some informative data about gas and liquid hydrocarbons trapped in bedded salt and quartz, which can also be used in exploratory oil, and gas field works in Carpathians.

2. Some selected exploration targets of fluid association in Carpathians

Each deposit and mineral occurrence shown characteristic fluid association related to various internal features of the alteration- mineralization or metamorphic fluid/melt processes, which can be used as "first-order" tools in further exploratory works. Gaseous and hydrocarbon fluid inclusions are common in sedimentary bedded salt and diagenetic black shale (Fig.1.).

2.1 Porphyry copper deposits and occurrences

It was demonstrated that brine inclusion assemblages are the main fluid phase in porphyry copper ± skarn deposits and occurrences in the Alpine metallogenesis (Pintea, 1993a; 2002; Damman et al., 1996; Heinrich et al., 2005; Fig.1.a, b). They are associated with hydrosilicate glass (Th =940 - 1170°C) and aqueous pairs (H_2O-vapor rich +/-CO_2 and H_2O-rich liquid) and also immiscible Fe(-S-O) melt inclusions, generally originated in a metasomatic, magmatic-driven processes (Pintea, 2010; Wilkinson and Cooke, 2011). The saline fluid phases evolved at high T (420 to 1300°C) and estimated P between 0.1 to 12 kb, with salinity from 31 to 89 wt% NaCl equiv. (e.g. Pintea, 1996; 1997; 2009; Fig. 2.). Fluid phase evolution, as seen in fluid and melt inclusion study in Alpine porphyry copper from Romania shown that metasomatic, magmatic - driven processes in potassic, propylitic and phyllic assemblages, and remelted sulfide features are very characteristic (Pintea, 2010). The exsolved magmatic fluid become subtle products as the feedback reaction with crystallizing host rocks proceeds by cooling and decompressing conditions in the endogene related stockworks. Perhaps further experimentally charges would elucidate some of these alterations - mineralizing processes. Endo- and exoskarn contemporaneous or later epithermal events are characteristic in the upper Cretaceous porphyry Cu-Mo (Au) systems. High temperature and high salinity fluid are representative in Miocene porphyry Cu-Au(Mo) overprinted by epithermal high- to low sulfidation types (Fig. 1f). It is mentioned that first attempt for using fluid inclusion as tool in porphyry copper prospecting were published early by Pomarleanu and Intorsureanu (1986).
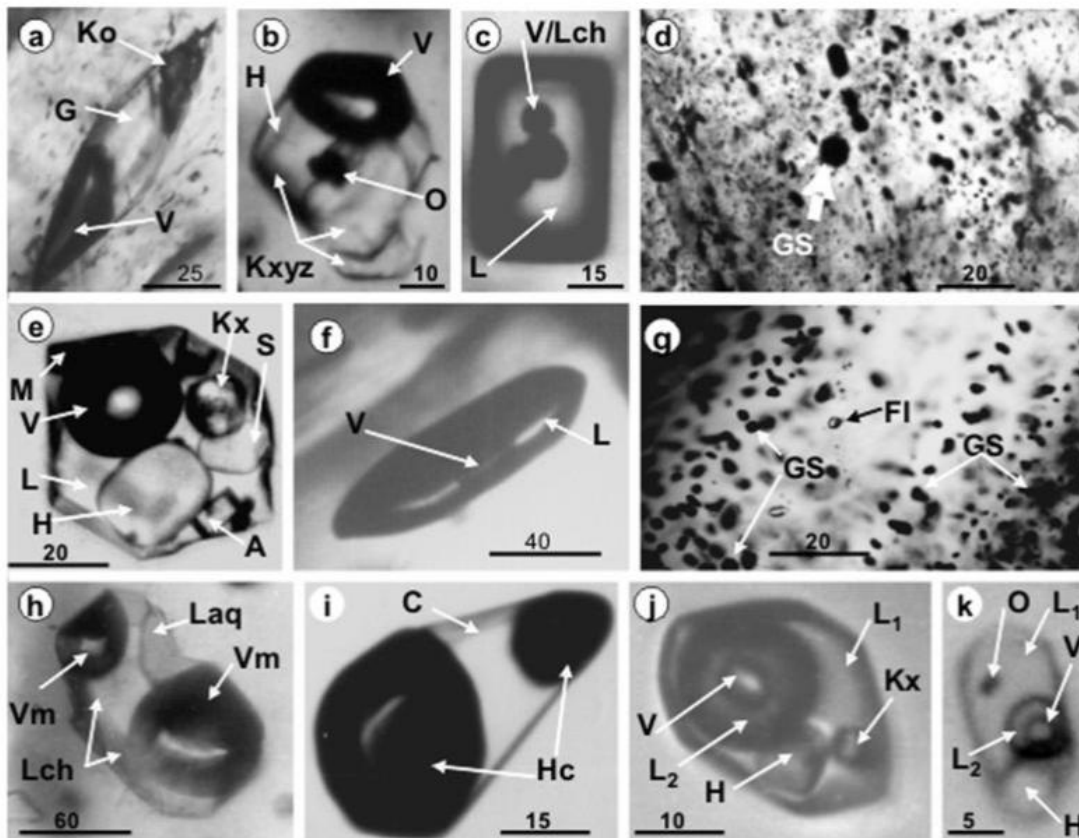
Fig.1. Some specific fluid and melt inclusion types from Carpathians (Romania). **a.** Silicate/carbonate(?) melt inclusion in apatite from high temperature magnesian - skarn from Tibles Mountains with glass (G), vapors (V) and undetermined solid daughter mineral (Ko) at T_{room} conditions; **b.** Liquid-free brine inclusion type from Deva porphyry copper deposit, H-halite, O-opaque, V-vapor, Kxyz - undifferentiated salt and silicate/sulfate daughter phases. For these type of brine inclusions the highest homogenization temperature recorded up to 1300°C, or even higher (Fig.2.) have geological uncertain relevance (Pintea, 1997, 2009). **c.** Vapor bubbles (three) or droplets of liquid hydrocarbons (Lch) in liquid inclusions from Badenian halite in Ocna - Dej bedded salt deposit; **d.** Globular sulfide melt (GS - mainly pyrite) as remelted features in quartz from Rosia Poieni porphyry copper deposit; **e**. Brine inclusion type in miarolitic quartz (often smoky) from Vladeasa granite. V-vapor, M- magnetite, prevailing over hematite in these brine inclusions and could be a "footprint" for IOCG fluid association, L- liquid, H-halite, A-anhydrite, S-sylvite, Kx- undetermined solid daughter phase; **f.** Biphasic fluid inclusion in enargite-luzonite from Rosia Poieni porphyry copper deposit. (microthermometry pers. com., Bailly, 2002: Th= 243 - 290°C, Ws= 3.55 - 21.68 wt% NaCl equiv., n=30). A comprehensive study on fluid inclusion from enargite and pyrite from Rosia Poieni porphyry copper was published recently by Kouzmanov et al., 2010; **g.** Sphalerite globules in metamorphic quartz from Blazna-Guset metamorphic Pb-Zn mineralization (Faget adit, Pintea 1988 unpubl, original sample revised), GS- globular sulfide, FI- fluid inclusion (biphasic L+V type); **h.** Liquid hydrocarbons (Lch), aqueous liquid (Laq) and methane (Vm) in "Maramures diamond" quartz crystal; **i.** Droplets of liquid (?) hydrocarbons (Hc) attached to a solid mineral microinclusion in langbeinite from Tazlau adit in potash bedded salt, C- possible carnalite; **j.** Complex brine-CO$_2$ fluid inclusion in quartz from MoS$_2$-REE mineralization from Jolotca mining district – Ditrau alkaline massif, L$_1$ – liquid aqueous solution, L$_2$- liquid CO$_2$,V- CO$_2$ gas, H-halite, Kx- undetermined solid daughter solid phase- possible a REE mineral; **k**. Multiphase fluid inclusion in metamorphic quartz from Blazna-Guset ore deposit (Faget adit, Pintea, 1988 – original), L$_1$ – aqueous liquid solution, L$_2$-liquid CO$_2$, V-CO$_2$ gas, H-halite, O-opaque. Scale bar in microns.

2.2 Epithermal systems in Eastern Carpathians

Excepting Tibles -Bran - Magura - Neagra (Pintea et al., 1999) and Nistru area (Pintea, unpubl) where a porphyry copper fluid association can be documented by fluid and melt inclusions study and alteration-mineralization features (Damian, 2003), the epithermal systems well-known from Sasar, Valea-Rosie, Herja, Baia Sprie and Cavnic were deposited from aqueous fluids with low salinity (< 26 wt% NaCl equiv. at low T (< 370°C) and low P (< 0.1 kb), none halite daughter crystal being ever reported until now in these famous epithermal ore deposits. Many boiling or reheating pulses could be seen in oscillatory-zoned minerals, which can be related to various alteration facies and parageneses (Grancea, et al., 2002). Although there is still debating if the original fluids were high-, or low - salinity types. Carbonate and sulphate step daughter minerals prevailing in a subsequent mineralization episodes and dawsonite - daughter mineral phase is also present (Pintea, 1995).

2.3 Upper Cretaceous Vladeasa granite

High temperature brines (Th = 420°C to 1070 °C or more, 32 - 74 wt% NaCl equiv., minimum 0.1 to 2.3 kb,) are associated with hydrosilicate melt (Th= 979 - 1069°C) low salinity aqueous +/- CO_2 fluids (Th = 248 - 414°C, 1 - 6 wt % NaCl equiv.) in miarolitic cavities and veins in the orthoclase bearing granite-aplite as magmatic-metasomatic facies (Pintea, 1993b, 1995, Fig. 1.e, plus new microthermometry in this study). This occurrence is typical for barren fluids as a whole.
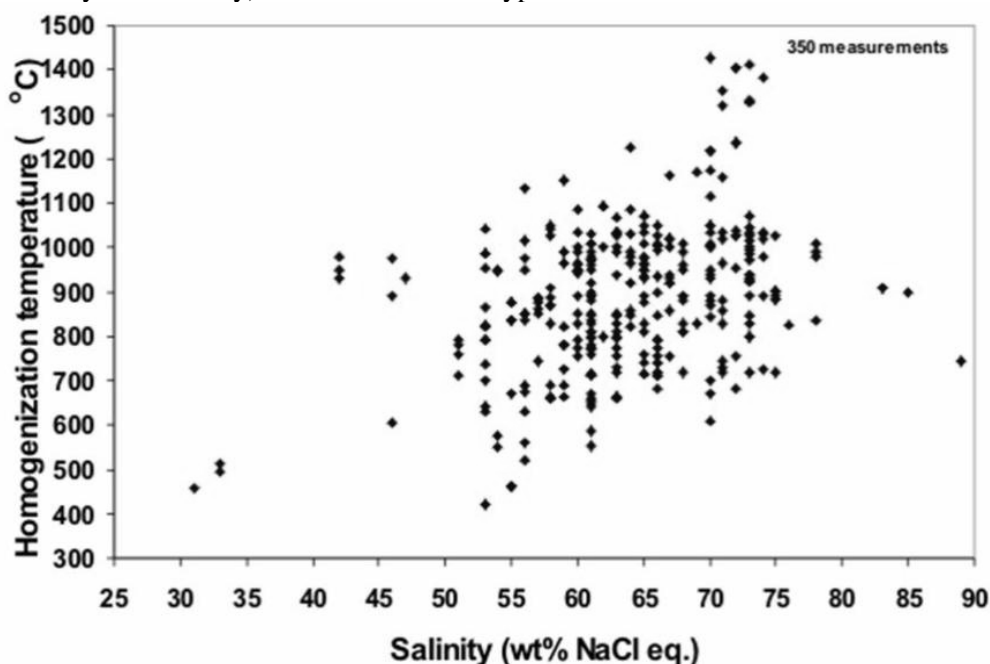
Fig.2. Homogenization temperature (Th) vs salinity (wt% NaCl equiv.) data for brine inclusions assemblages from upper Cretaceous (mainly the lowest values) and Miocene (medium to high values) porphyry copper in Carpathians (modified from Pintea, 2010). In the T-X projection of the H_2O-NaCl system the data points fitted between locus of critical points [extended from the critical point of H_2O T=374.1°C, P=220 bars and the critical point of NaCl, T≈3627°C, P≈ 258 bars with a max P≈ 2500 bars at T ≈ 2000°C (Pitzer, 1984), and the locus of liquid (L)-vapor(V)-halite(H) triple points (from peritectic,T=0.1°C, P=0.004 bar, 26.2 wt% NaCl, to the NaCl triple point, T=801°C and P~1 bar], Bodnar, 2003. The majority of the microthermometric data shown "single phase state" or "L+V" to the measured values, based upon Sowat (re)calculations (Driesner and Heinrich, 2007; Pintea, 2009).

Some hydrothermal quartz veins contain a Fe- rich paragenesis of magnetite-hematite, which can be a "footprint" of **I**ron-**O**xide-**C**opper-**G**old magmatic - related fluid occurrence (Rusk et al., 2009). This is first mentioned here, although in the South Carpathians (Banat) a possible Upper Cretaceous IOCG mineral occurrence was already presumed at Ocna de Fier by Ciobanu and Cook (2004).

2.4 Immiscible sulfide melt associations

Droplets of immiscible Fe (-S-O) melt are characteristic in alpine fertile (Fig.1.d) and barren intrusive and their destruction during magmatic-hydrothermal and/or meteoric fluid interaction could be the main source of ore elements in many ore deposit types (Pintea, 2008a). They seem to be representative for a mafic input (recycling?) during the magmatic evolution in intermediate to shallow magma chambers. Remelting features of sulfide are quite frequent and can concentrate "droppers" mainly in metamorphic ore deposits (e.g. Sparks and Mavrogenes, 2005). It is very possible that they are reheated and transported as partially (re)melted phases by silicothermal fluids, because they trapped brine, fluid and silicate glass remnants (e.g. Nedelcu et al., 2003). For example, a quartz sample collected from the Upper Precambrian Rodna-Guset Pb-Zn mineralization (Faget adit, Pintea, 1988 unpubl) revealed the coexistence of globular sphalerite droplets and complex CO_2 + brine fluids inclusions in the same quartz crystal (Fig 1.g, k). It is suggested that fluid and sulfide (re)melt were in equilibrium at the trapping conditions. Chalcopyrite disease in sphalerite is also emphasized in two occurrences, one from East Carpathians and another from Metaliferi Mountains respectively.

2.5 Ditrău alkaline massif

Two distinctive fluid phase associations can be defined in this alkaline massif, one related to the pneumatolitic-hydrothermal MoS_2-REE mineralization at Jolotca external NW-mining prospect (Pintea,

1991; 1995, Fig. 1.j), and another one in the inner part related to the complex foidic - syenites rocks (Fall et al., 2007). They are vein-type hydrothermal mineralization deposited by complex aqueous + brine + CO_2 rich fluids (Th= 280°C, 30 - 35 wt% NaCl equiv., P= 0.8 - 1.4 kb) in the external part at Jolotca (Pintea, 1991). The second one is a magmatic-metasomatic disseminated system in the inner part, with aqueous low-salinity + brine fluid association (180 - 230°C, 6 - 9.6 wt% NaCl equiv.; 243 - 325°C, 20.5 - 39.8 wt% NaCl equiv.; P = 0.5 - 2.0 kb, Fall et al., 2007). There are some intriguing similarities between this system with the alkalic porphyry Mo(-Nb) - type (Audetat, 2010) and/or porphyry Cu-Au alkalic-type (Panteleyev A., 2005: L03- Mineral deposit profile, British Columbia). A porphyry-style ore was already mentioned in the "Aurora" mining prospect by Hartopanu and Udubasa, 2003.

2.6 Gaseous and liquid hydrocarbons in salt deposits and black shales

Generally, bedded salt minerals contain sea water mother- liquid as primary liquid-rich inclusions (Pintea, 2008b). Secondary trails of gaseous CO_2-CH_4 rich and liquid droplets of hydrocarbons suggest possible gas and oil accumulation or migration underneath (Fig. 1.c, h, i). The famous "Maramures diamond" quartz crystals inherited the PVTX data and phase relation between aqueous, gas and liquid hydrocarbons in the Neocomian-Albian argillaceous black shale from Transcarpathian flysch (e.g. Pintea, 1995, Jarmolowicz-Szulc et al., 2006), Fig.1.h) Microthermometric study recorded for aqueous fluid Th=150 - 250°C, 7 - 8.6 wt% NaCl equiv., 0.5 - 0.9 kb), Th (gas + liquid hydrocarbons) ≈ 60 - 300°C, for carbonic immiscible phases (Pintea, 1995).

3. Conclusions

A selective exploration strategy is proposed based upon fluid and melt inclusions study. The targets are grouped here as followings: **1.** Brines with high salinity evolved at high P-T conditions in porphyry copper and presumed IOCG-related to metasomatic, magmatic driven processes in Banat, East Carpathians and Apuseni Mountains; **2.** Aqueous fluids with low salinity and low P and T are involved in transport and depositional processes from low, intermediate and high sulphidation epithermal alteration-mineralization processes; **3.** Immiscible sulfide/melt features in petrogenetic minerals and (re)melting sulphide features in epithermal, porphyry copper and metamorphic ore deposits processing; **4.** Unique fluid association related to Ditrau alkaline massif as CO_2-rich + brines in the external ring and magmatic and/or metasomatic- related fluids involved in a possible alkalic porphyry system in the inner foidic-sienite stockwork; **5.** Gas and oil fluids migrated in bedded salt and Transcarpathian flysch. All of these fluid phase assemblages and their PVTX properties can be used as data base for tracking the minor and trace element concentration features in the mentioned ore deposits or in new prospecting areas. Migration and further fluid evolution can be evaluated based upon gas and liquid hydrocarbons inclusions content in sedimentary digenesis and anchizone.

References
Audetat A., 2010. Source and evolution of molybdenum in the porphyry Mo(-Nb) deposit at Cave Peak, Texas. Journal of Petrology, 51, 8, 1739-1760.
Bodnar R.J., 2003. Interpretation of data from aqueous-electrolyte fluid inclusions. In I. Samson, A. Anderson, D. Marshall, eds. Fluid Inclusions: Analysis and interpretation, Mineral. Assoc. Canada, Short Course Ser. 32, 81-100.
Ciobanu C.L., Cook N.J., 2004. Skarn textures and a case study: the Ocna de Fier-Dognecea ore field, Banat, Romania. Ore Geol. Rev., 24, 315-370.
Chesu M., 1983. Elemente minore in minereuri neferoase din Romania. Ed. Tehnica, Bucuresti.
Damian F., 2003. The mineralogical characteristics and the zoning of the hydrothermal types alteration from Nistru ore deposit, Baia Mare metallogenetic district. Studia Univ.Babes-Bolyai, XLVIII, 1, 101-112.
Damman A. H., Kars S. M., Touret J. L. R., Rieffe E. C., Kramer J. A. L. M., Vis R. D., and Pintea I., 1996. PIXE and SEM analyses of fluid inclusions in quartz crystals from the K-alteration zone of the Rosia Poieni porphyry-Cu deposit, Apuseni Mountains, Rumania. Eur. J. Mineral. 8, 1081–1096.
Driesner T., Heinrich C., 2007) The system H2O-NaCl. Part I: Correlation formulae for phase relations in temperature-pressure-composition space from 0 to 1000oC, 0 to 5000 bar, and 0 to 1 XNaCl. Geochim.Cosmochim. Acta, 71, 4880-4901.
Eugster P., 1986. Minerals in hot water. Amer. Min., 71, 655-673.

Fall A., Bodnar R.J., Szabo Cs., Pal-Molnar E., 2007. Fluid evolution in the nepheline syenites of the Ditrau alkaline massif, Transylvania, Romania. 95, 3-4, 331-345.

Grancea L., Bailly L., Leroy J., Banks D., Marcoux E., Milesi J.P., Cuney M., Andre-Mayer A. S., Istvan D., Fabre C., 2002. Fluid evolution in the Baia Mare epithermal gold/polymetallic district, Inner Carpathians, Romania. Miner. Deposita, 37, 630-647.

Hîrtopanu P., Udubaşa G., 2003. Mineralogy of a "sacred monster" the Ditrău alkaline massif, East Carpathians (Romania). Studia Univ. Babes-Bolyai Cluj-Napoca, Ser.Geol., Spec.Issue., p.47.

Heinrich C.A., Halter W., Landtwing M.R., Pettke T., 2005. The formation of economic porphyry (-gold) deposits: constraints from microanalysis of fluid and melt inclusions. In: McDonald I., Boyce, A.J., Butler, I.B., Herrington, R.J., and Polya, D.A. (eds)., Mineral Deposits and Earth Evolution. Geol. Soc., London, Spec. Publ., 248, 247-263.

Jarmolowicz-Szulc K., Karwowski L., Dudok I.V., 2006. Marmarosh diamonds - the typical association with the organic matter in the outher Carpathians. Acta Min-Petr., Abstr. Ser., 5, Szeged p.51.

Kouzmanov K., Pettke T., Heinrich C.A., 2010. Direct analysis of ore-precipitating fluids: combined IR microscopy and LA-ICP-MS study of fluid inclusions in opaque ore minerals. Econ. Geol., 105, 351-373.

Nedelcu L., Rosu E., Costea C., 2003. Mineral microinclusions hosted in sulfides of main neogene porphyry copper and epithermal ore deposits of the south Apuseni Mountains, Romania. Acta Mineralogical-Petrographica. Abstr. Ser. 1, Szeged, 78.

Pintea I., 1991. Fluid inclusion studies on quartz crystals associated to the REE and sulphide ore body from Jolotca (NW-Ditrau masiff, Transylvania, Romania). Abstr. ECROFI XI, Plinius no. 5, p. 176, Firenze, Italy.

Pintea I., 1993a. Fluid inclusions evidence to the importance of the hydrous saline melts in porphyry - type ore deposits genesis from Apuseni Mts. (Romania). Terra abstr. suppl. no 1, to Terra Nova, v. 5, p. 481, 1993, EUG VII, Stasbourg, France.

Pintea I, 1993b. Contributions to the study of the fluid inclusions in the miarolitic quartz inclusions in the Draganului Valley. Rom. J. Mineralogy, 76, 1, 23-27.

Pintea I., 1995. Fluid inclusions microthermometry. Some typical examples. Rom. J. Mineralogy, 76, 2, 25-36.

Pintea I., 1996. Fluid inclusions study with special view on fluid phases immiscibility associated to porphyry copper genesis from Metaliferi Mountains. Ph D thesis, Univ Bucharest (in Romanian). 172p.

Pintea I., 1997. The significance of the liquid homogenization temperature in salt melt inclusions. A case study in neogene porphyry copper ore deposits from Metaliferi Mountains (western Romania). ECROFI XIV, Nancy, abstract vol., 266 – 267. Nancy, France.

Pintea I., Udubasa G., Nedelcu L., 1999. Evolution of fluid phases related to a new porphyry copper deposit in Romania:The Tibles massif. In: Proceed. 5th SGA and 10th IAGOD meeting., London Mineral Deposits: Processes to Processing, Stanley et al. (eds), 83-85.

Pintea I., 2002. Fluid inclusions from porphyry Cu-Mo(Au) and epithermal ore deposits from Banat - Mures zone. In Rosu et al., 2002: Alpine Metalogenesis in Carpathian areas, unpubl. IGR report - A3/2002. (in Romanian).

Pintea I., 2008a. Fluid and melt inclusion evidence for succession of magmatic and hydrothermal events from Neogene/Quaternary subduction zone in Carpathians. In Pan-American Conference on research on Fluid Inclusions - In memory of Edwin Roedder, Progr. and abstr. p 47.

Pintea I., 2008b. Liquid inclusions microthermometry in the Badenian halite and actual evaporate salt crust from Romania. 6th National Symp. on Economic Geology, Rocksalt and other nonmetalliferous deposits. Sovata, Abstr. vol., 115-118.

Pintea I., 2009. Still problematic facts on the fate of brines in the alpine porphyry copper systems in Romania. ECROFI XX, Granada (Spania) Abstr. 187 – 188.

Pintea I., 2010. Fluid and melt inclusions evidences for autometasomatism and remelting in the alpine porphyry copper genesis from Romania. Rom. Jour. of Mineral Deposits., 84 Spec. issue, 15 – 18. The 7th Nat. Symp. on Econ. Geol., "Mineral Resources of Carpathians area", 10 - 12 Sept., 2010, Baia Mare.

Pitzer K.S., 1984. Ionic fluids. Journal of Physical Chemistry, 88, 2689-2697.

Pomarleanu V., Intorsureanu I., 1986. Salinity of fluid inclusions of the porphyry copper ore deposits and their significance in geobarometry and prospecting (The Lapusnicu Mare ore deposit-Banat). D.S. Inst. Geol. Geofiz., 70,-71/2 (1983;1984) 1985, 83-95.

Rusk B., Xavier R.P., Monteiro L.V.S., 2009. Compositions of hydrothermal brines that form porphyry-Cu (Mo-Au) and iron oxide copper gold deposits. J.C.U. Newsletter, 13-15.

Sparks H.A., Mavrogenes J.A., 2005. Sulfide melt inclusions as evidence for the existence of a sulfide partial melt at Broken Hill, Australia. Econ. Geol., 100, 773-779.

Wilkinson J., Cooke D., 2011. Enhanced geochemical targeting in magmatic hydrothermal systems. AMIRA P1060. http://www.amira.com.au.

GREEN CRUSTS ON CHROMITE ORE FROM SOUTHERN BANAT REVISITED

Gavril SĂBĂU*, Constantin COSTEA

Geological Institute of Romania, 1 Caransebeş St., RO-02271 Bucharest 32, Romania,
g_sabau@yahoo.co.uk

Abstract Scanning electron microscope investigation of the green coatings on the chromite ores from Southern Banat reveals mainly Cu-dominant minerals of the rosasite group, malachite being the most abundant and followed by glaukosphaerite. Ni-rich assemblages previously described seem to be less widespread in this occurrence, considering also information from recent literature.

Keywords: podiform chromite, pellicular alteration, glaukosphaerite, malachite

1. Introduction

Green crusts along the fractures of massive chromite ore are a feature recognized in most podiform chromite occurrences worldwide. The green alteration rather results from the weathering of the sulfides accompanying the chromite than from chromite itself, and occurs as veneers, encrustations, cavity fillings and botryoidal overgrowth aggregates. After the green crusts mostly formed by zaratite ($Ni_3CO_3(OH)_4 \cdot 4H_2O$) of the classic occurrence at Wood's Chrome mine, Texas, Fulton, PA, known ever since the Dana's System of Mineralogy, many other chromite deposits were found to contain green coatings with a surprisingly diverse mineralogy, from which several new minerals were discovered during the past two centuries.

As a common feature, the green incrustations appeared to be dominantly formed of Ni-bearing hydroxyl-carbonates and hydroxides. In Romania as well, massive chromite occurrences display as a rule the green pellicles along cracks, known especially from the ultramafic rocks of Southern Banat. These occurrences have been only occasionally mineralogically investigated, due to handling difficulties inherent to the structure of the material, namely thin films on the ore surface with finely intergrown minerals.

2. Geological setting and previous investigations

Podiform chromites are scattered inside the mostly serpentinized peridotitic member (dunites, harzburgites) of the Early Paleozoic Tişoviţa Ophiolitic Complex located in the Danubian Units of Southern Banat. Chromite lenses appear between the localities of Eibenthal and Dubova, approximately paralleling the Danube shore, larger concentrations occurring between the Plavişeviţa and Liubotina brooks and NW from Dubova.

The available mineralogical data on the green crusts on chromite refer to the Eibenthal, Goleţu Mare and Lomuri occurrences (last two near Dubova), but the results show limited consistency. After previous works assuming the green crusts to be garnierite, Moţiu (1971) identified at Lomuri the dominant phase of the coatings as a Ni-rich carbonate, on account of the IR-spectrum and chemical behaviour, but failed to obtain a precise determination and assumed zaratite to be closest match to the obtained data. Strusievicz (1995) identified by powder diffraction an assemblage of theophrastite, nimite and hydrotalcite at Goleţul Mare, while Fehér *et al.* (2010) found at Eibenthal rather hydroxil-carbonate minerals of the rosasite group, among which a nickeloan mcguinnessite, but no theophrastite.

3. Description of the studied material

Chromite samples with green coatings were collected from blocks near the Lomuri occurrence (44°37'3"N, 22°12'24"E - WGS84/UTM). The colour of the coatings from this occurrence is generally emerald-green with varying saturation degrees, rarely with a slightly bluish shade in less-intensely coloured pellicles, but never displaying the bright-green to apple-green hues expected from Ni-dominant phases.

The green crusts were scraped down from the chromite substratum and examined under an EDS-scanning electron microscope, in order to observe the fine-grained intergrowth, which do not allow separation and identification of the phases using other methods. The sampled material was found to consist dominantly from Cu-bearing phases, the most abundant being malachite, contrary to the previous findings. Malachite forms cavernous or crystalline aggregates flattened against the walls of the substratum (Fig. 1).
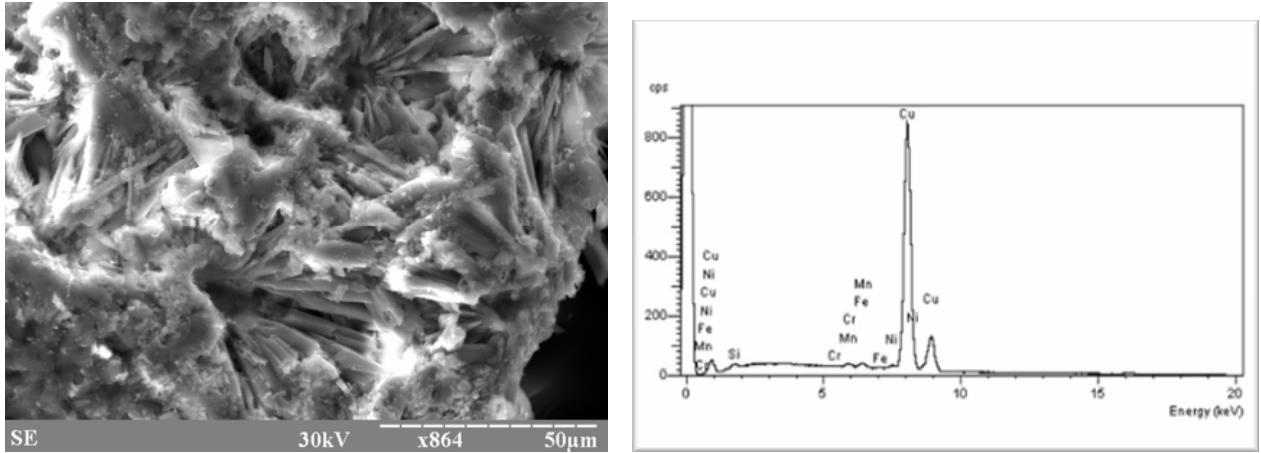

Fig. 1 Malachite coating the chromite ore: A. Cavernous-radiating aggregate, B. Energy dispersive spectrum (EDS) of malachite
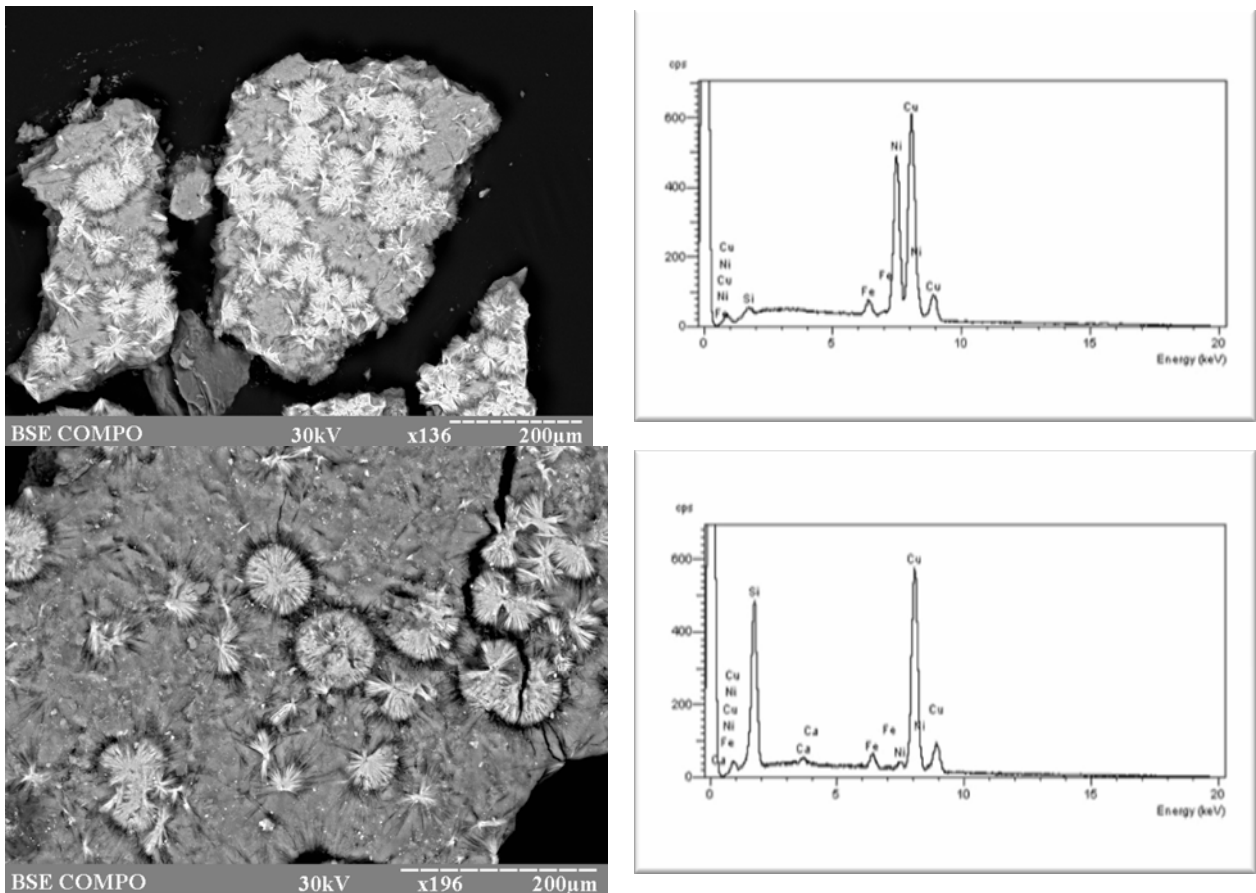
Fig. 2 Composite vein aggregate consisting in glaukosphaerite and chrysocolla: A – Backscattered image of spherulitic glaukosphaerite embedded in chrysocolla (darker), B. EDS of glaukosphearite, C. Detail of the aggregate showing the spheroidal aggregates, D. EDS of host chrysocolla

Malachite forms spongy aggregates, but also well-crystallized intergrowths, partly radiating and partly in parallel bundles (Fig. 1). The energy-dispersive spectrum indicates, together with the morphology and colour, that the dominant phase of the crusts is malachite. Other copper-bearing phases may appear, such as chrysocolla, which can be rather abundant in crusty amorphous aggregates, displaying a "clean" EDS spectrum indicating only Cu and Si, which is distinctive in connection with the habit of the mineral (Fig. 2).

Sometimes the chrysocolla fillings host radiating aggregates building up spherules up to 100 microns across at most, which often are "rattling" in the cavities of chrysocolla, being only partly attached by the tips of the needles to the host cavities. The composition of the spherulites indicates essential Ni besides Cu, and low Fe, which, in connection with the habit and the assemblage allows the identification of glaukosphaerite $(Cu, Ni)_2CO_3(OH)_2$. The mineral was also acknowledged by Koller (*oral. comm.*) in green coatings sampled from Eibenthal, its presence being hereby confirmed. Glaukosphaerite was the only Ni-bearing hydroxil-carbonate identified in the studied samples; the bluish hue of some coatings could also indicate the presence of other rosasite group minerals besides malachite and glaukopsphaerite, but the expected composition is rather more magnesian that Ni-rich, closer to the mcguinnessite identified by Fehér *et al.* (2010). However, the material described by Moțiu (1971) from the same occurrence is a carbonate containing Ni and no Cu, indicating a larger variability of the assemblages coating chromite.

A copper-rich assemblage in the chromite coatings comes as no surprise, as Cu sulfides appear along with Ni sulfides associated to the ultramafic rock hosting the chromite ore. Exceptionally a native copper microfoil was also identified in the pellicular material.

The "green" phases are associated with silicate minerals, especially serpentines, but also chlorites. A remarkable violet mineral appears as scaly aggregates along fissures in chromite. The compositional spectrum shows a magnesium silicate containing Cr and Fe, and no Al, indicating Cr-antigorite (Fig. 3).
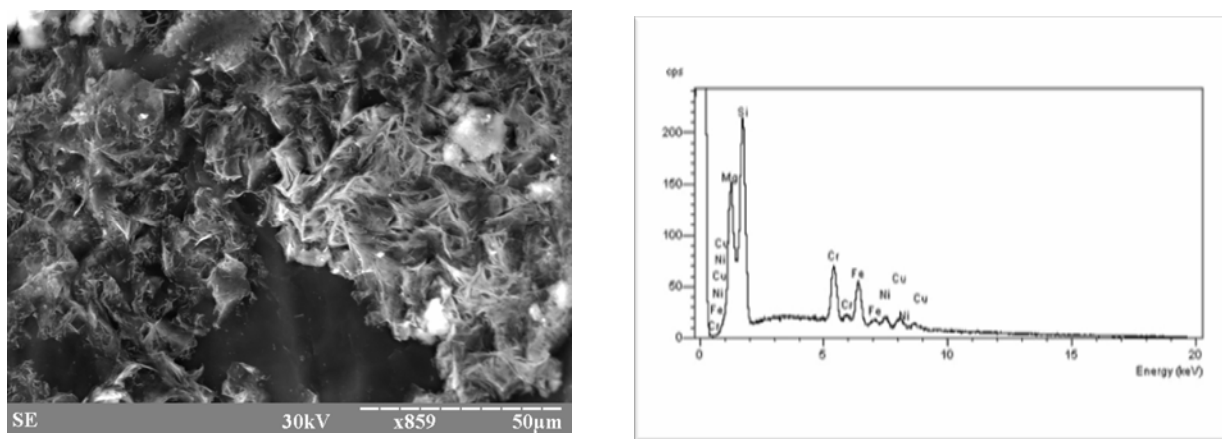
Fig. 3 Scaly Cr-bearing antigorite coating chromite: A. Secondary electron image, B. EDS

4. Conclusions

The mineral assemblage identified in the green crusts coating chromite from Southern Banat contain phases which are not commonly known from similar occurrences, containing Cu-dominant hydroxyl-carbonate minerals from the rosasite group, which are rather more widespread as alterations in Ni-Cu deposits than in chromite ores. On the other hand, nickel secondary minerals such as in the type locality of theophrastite, Vermion Mt., Macedonia (Marcopoulos and Economou, 1981) were described alongside the rosasite-group assemblages, proving an unusually complex composition to this particular occurrence.

References

Fehér B., Szakáll S. and Bigi S., 2010. Ni-rich mcguinnessite from Eibenthal, Romania: an intermediate phase toward a new hypothetical rosasite-group end-member. 20th General Meeting of the IMA (IMA2010), Budapest, Hungary, August 21-27, Abstracts CD, 495

Marcopoulos Th. and Economou M., 1981. Theophrastite, $Ni(OH)_2$, a new mineral from northern Greece. American Mineralogist 66, 1020-1021

Mo iu A., 1971. Prezen a unui carbonat de nichel în serpentinele cromifere din Banat (Notă).Studia Universitatis Babeş-Bolyai, Series Geologia-Mineralogia, Fasciculus 1, 3-9

Strusievicz R. O., 1995. Mineralogical composition of the "Green Crusts" in the Podiform Chromites of the Tişovi a-Iu i Ophiolites (Southern Banat, Romania).Romanian Journal of Mineralogy 76/2, 91-94.

AGES CONSTRAINTS IN PEGMATITE PROVINCE RELATED TO CHARNOCKITIC HOST ROCKS IN MINAS GERAIS, BRAZIL

Fernando Machado de MELLO[1], Essaid BILAL[2*],

1- Universidade Federal Rural do Rio de Janeiro, Brazil (UFRRJ) - fermamll@ufrrj.br
2- École des Mines de Saint-Etienne, Dept. de Géosciences & Environnement-158, cours Fauriel 42023 Saint-Etienne cedex 2, France; *bilalessaid@gmail.com*; Tel/Fax – +33 4 77 42 01 63/ +33 4 7749 9707

Abstract Cambrian-Neoproterozoic granitoids suites in southeastern Brazil are the main host rocks of largest pegmatite field of Brazil, the Eastern Pegmatite Province. The P-Li-Nb pegmatites group represent the richest in precious stones like Beryl, Aquamarine, Topaz and Tourmaline. Two types of pegmatites are characterized by their mineralogical characteristics and tectonic and magmatic relations. The first group formed during compressive event about 582 Ma and the second pegmatite group was formed by cooling of residual melts during the transition to an extensional phase (520-500Ma) of the Brasiliano/Pan-African Orogeny, related to metamorphic rock melts (gneiss migmatite, gneiss) and extensive granite-charnockite emplacement. The new charnokite isotopic data presented here constrain the latest pegmatite genesis at about 500 Ma as its maximum age.

Keywords: Geochronology Pegmatite Charnockite; Brasiliano/Pan-African; Magmatic and Tectonic Relationships; Minas Gerais-Brazil.

1. Introduction

The Neoproterozoic evolution of Northern Mantiqueira Province, Brazil, was characterized by an intense granitic magmatism, associated with a network of continental-scale ductile shear zones, related to a compressive, transpressional and later extensional tectonics. The arc-type structure, which develops over more than 47,500 km^2 in southeast Brazil, links many lithospheric tectonic discontinuities to an abundant and various magmatism. This paper is mainly concerned with geochronological and tectono-magmatic relationships of the Pegmatite Province and the latests magmatic events in that region (Fig. 1). There, the plutonic framework intruded in the Archaean and Paleoproterozoic magmatic and metamorphic basement, has been emplaced during different periods in relation to the geotectonic events and includes important pegmatite fields.

2. Regional setting

The Rio Doce region is located in the northern portion of the Mantiqueira Structural Province (Almeida and Hasuy, 1980), east of São Francisco Craton in the eastern Minas Gerais and northwestern Espirito Santo states. This province is represented by Neoproterozoic mobile belts that surrounded the São Francisco cratonic block and is associated to the Brasiliano/Pan-African Orogeny (600 - 450 Ma). These mobile belts reworked the Archaean-Palaeoproterozoic country rocks (high and low-grade metamorphic rocks of Piedade, Paraíba do Sul and Pocrane Complexes; Juiz de Fora and Neoproterozoic supracrustal sequences of Rio Doce Group) and enabled the intrusion of granitoid plutons and pegmatites. Several rare metals and gem mineral rich pegmatites are related to charnockitic rocks (hypersthene-granitoids).

Petrographic, geochemical and structural features allow the separation of these rocks into pre-, syn-, late and post-tectonic granitoids. The whole emplacement process lasted less than 100 Ma: from 595 Ma for the pre-tectonic granitoids, to 500 Ma for the post-tectonic ones. During this interval, a 45 Ma magmatic quiet period (from 582 to 537 Ma) can also be identified. Detailed field observations and mapping, coupled with petrological and geochemical observations, indicate an important role of the Archaean and Paleoproterozoic crust in the genesis of these granitoids, showing even evidence of some mantle interactions.

3. Pegmatite groups

According to Bilal et al, 2000 there are two main pegmatite groups; the first one is considered the result of fractional crystallization of a syntectonic magmas. Its representative types are leucogranites and P-Li-Be bearing pegmatites. The isotopic ages of these intrusions are estimated at about 582 Ma. Their presence is mainly confined to the area near the cities of Governador Valadares, Teofilo Otoni, Araçuaí, Conselheiro Pena and São José da Safira.
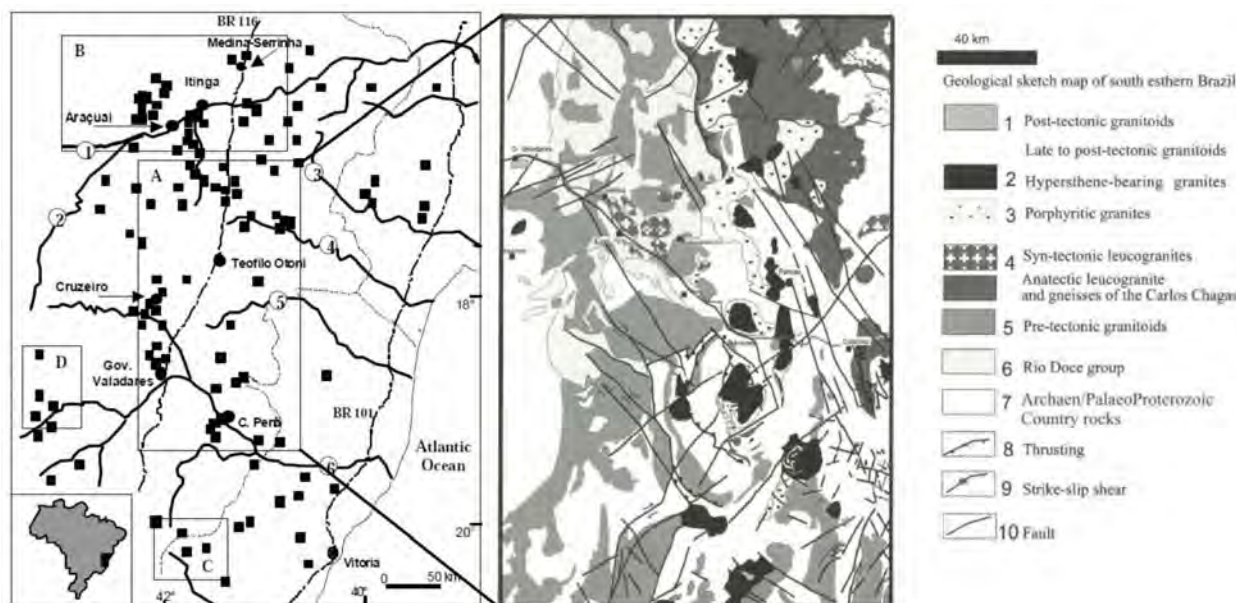
Fig. 1. Distribution fields of pegmatites in southeastern Brazil. Pegmatites from the first group occur in the quadrangles A (Gov.Valadares, Teófilo Otoni, São José da Safira and Galiléia) and B (Araçuai and Itinga). Pegmatites from second group are in quadrangles C (Caparaó, Espera Feliz) and D (Sta Maria de Itabira). Dots: Federal State Boundaries. Roman Numerals: Federal States (I- Bahia; II- Espírito Santo; III- Minas Gerais). Open circles with Arabic numerals: Rivers 1- Jequitinhonha; 2- Araçuai; 3- Itanhém; 4 Mucuri; 5- São Mateus; 6 Rio Doce. BR 116 and 101: Federal Highways. Blacksquares: pegmatites. Black circles: towns. (Pinto C. P. 1997, Bilal E. et al. 1998, 2000a, 2000b, 2001, Mello F.M. and Bilal E., 2004)

The second group was formed during the second phase D2 (520-500Ma) of the Brasiliano metamorphic rock fusion The main pegmatite bodies show outcropping lengths ranging from 150 m up to 1300 m and widths ranging from 10m up to 60 m. They are subvertical bodies striking N10-20°W. The pegmatite outcrops at different topographic levels, ranging from 150 m up to 1100 m into staurolite-garnet schists and paragneisses, concordant and discordant to the Brasiliano structures.

Their internal features are in all of them essentially very similar. They show consistent mineral assemblages arising from an internal zoning around the quartz core. The centimetric tourmaline crystals have been collected from the border and the wall zones (black tourmalines), from the intermediate zones (black, green, blue and pink tourmalines) or even from metasomatic pockets (green, blue and pink to red tourmalines). The schorlitic tourmalines are associated with quartz, muscovite, (K,Na)-feldspar, garnet (almandine-spessartite), columbite-tantalite (Nb>Ta) and prismatic beryl. The elbaitic ones are found together with Na-feldspar (cleavelandite), quartz, amblygonite, spodumene, Li-rich violet micas, morganite, tantalite-columbite (Ta>Nb) and spessartite garnet.

We study many little leucogranite bodies linked to the pegmatites. They are controlled by a previous main compressive deformation phase Dl. Ten individual zircon crystals within leucogranites are dating 579 ± 5 Ma. The very Sr-enriched and Nd-depleted initial ratios ($0.782 \leq {}^{87}Sr/{}^{86}Sr_{(i)} \leq 0.823$ and $-8.2 \leq \varepsilon Nd_{(600)} \leq -7.4$) must be related to an important role of a crustal source. They are linked with Urucum granite (584 ± 2 Ma zircon U-Pb) suite in Galilea region (Nalini et al., 2000). The syn-tectonic magmatic series are related to crustal melting produced by decompression and thermal relaxation (550-700°C and 4-5 kbar). These perphosphorous leucogranites displays porphyritic textures and are characterized by the presence of apatite phenocrystals (2 cm) and P-rich feldspars. They are highly peraluminous (1.07<ASI<1.38) and, vary from the porphyritic granites to the haplopegmatitic facies. Their P_2O_5 contents (0.28 to 1.06 wt%) decrease with increasing SiO_2 (72-75 wt%) can be classified as phosphorus-rich leucogranites. Very high concentrations of P_2O_5 in silicic peraluminous granites are symptomatic of strong differentiation. The MgO/TiO_2 ratio nears 3, which may be compared to the typical granites of crustal origin. In a same way, a decrease of major elements (CaO, Fe_2O_3, MgO, TiO_2) and of trace elements (Zn, V, Sc, Co, Cr, Ni, REE) are observed from the porphyritic granites to the haplopegmatites.

The Galileia suite, with 594 ± 6 Ma zircon U-Pb ages, is related to few pegmatite bodies and is characterized by elongated batholiths trending in the NW-SE and N-S directions associated with high angle shear zone. The batholiths present solid state and magmatic flow foliations and a well-developed

magmatic lineation. Two deformation phases were described: the first was responsible for the development of a solid-state foliation and magmatic flow lineation in the granitic suites and a schistosity and stretching lineation in the country rocks of the São Tomé schist, which hosts, in its foliation planes important pegmatite bodies. The second was responsible for an extensional crenulation cleavage and other associated structures.

4. Charnockites

The charnockites related to pegmatite bodies discussed here belong to a group mainly consisted of balloon-shaped, bimodal, granitic and/or charnockitic to dioritic/noritic intrusions, formed and emplaced in the deep crust (> 25 km). Geochemically, they are high-K and high-Fe calc-alkaline to alkaline with widespread evidence of magma mixing and mingling processes. These bodies are supposed to be the source of residual pegmatites that can host deposits of aquamarine, topaz and quartz crystals. These pegmatites are generally rich in biotite and poor in tourmaline. Lithium minerals are rare or absent. These pegmatites are the source of blue and greenish blue aquamarine, colourless topaz and quartz.

4.1 Charnockites Rb/Sr, U/Th/Pb, U/Pb and Sm/Nd Isotopic Data

Rb-Sr and Sm-Nd isotopic data of hy-granitoids (charnockites) of Aimores Complex (details in Mello, 2000 unpubl.), performed at the CPGeo-USP, Brazil, with a mass spectometer VARIANMAT, model TH-5. The results are showed in Tables 1, 2 and Fig. 2. The granitoids of the Aimores Complex show $\varepsilon_{Sr(500-600Ma)}$ ranging from -5.9 to -8.07 and exhibited initial rates $^{87}Sr/^{86}Sr$ = 0.705-0.708. Sm-Nd data exhibited ε_{Nd} initial values strongly negative, suggesting crustal contribution in the source. The granitoids of the have $\varepsilon Nd_{(0)}$ values ranging from –12.95 to –10.94, and TDM model ages ranging from 1,513.6 to 2,023.7 Ga, suggesting a Meso to Paleoproterozoic sources.

Table 1 - Rb/Sr Results of Aimores Pluton whole rock isotopic analyses.

Sample	Unit	Rb(ppm)	Sr(ppm)	$^{87}Rb/^{86}Sr$	Error	$^{87}Sr/^{86}Sr$	Error
S4	SCh	142.4	339.6	1.215	0.034	0.71756	0.00009
S25	SCp	124.9	332.8	1.087	0.031	0.71686	0.00009
S1	SGG	146.6	75.6	5.644	0.159	0.76548	0.00007
S21	SMGp	71.2	215.5	0.957	0.027	0.71962	0.00009

Table 2- Sm/Nd data from Aimores Pluton.

| Sample	Sm(ppm)	Nd(ppm)	Sm/Nd	$^{147}Sm/^{144}Nd$	Erro	$^{143}Nd/^{144}Nd$	Error	TDM(Ma.)	Factr f	εNd0	εNd500.	εNd600Ma.
S4	12.456	70.273	0.177251	0.1072	0.0004	0.511984	0.00004	1513.6 ± 1 54.8	-0.455	-12.76	-7.05	-5.90
S25	16.551	77.978	0.212252	0.1283	0.0004	0.512077	0.00004	1721.9 ± 65.8	-0.347	-10.94	-6.58	-5.71
S1	7.425	32.659	0.227349	0.1375	0.0005	0.512031	0.00004	2023.7 ± 5 82.1	-0.301	-11.84	-8.07	-7.31
S21	7.936	41.555	0.190975	0.1155	0.0004	0.511974	0.00003	1656.6 ± 43.5	-0.412	-12.95	-7.77	-6.74
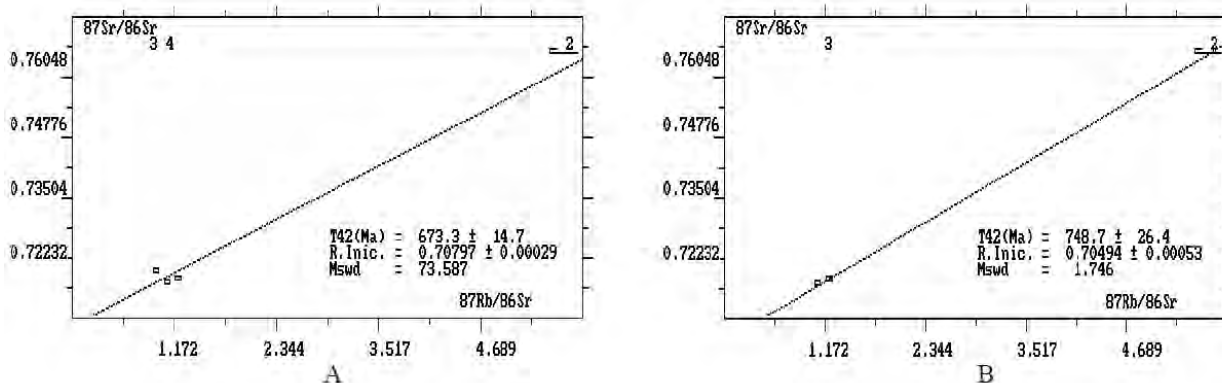
Fig. 2. Rb-Sr Isochron diagram from Aimores granitoids (A) and only for charnockites (B)

The U-Pb-Th monazite ages of two Aimores Complex charnockite samples were calculated from 31 analyses in U, Pb and Th monazite concentrations obtained by electron microprobe on thin sections. The U-Pb-Th determinations on monazites were performed on a Cameca SX100 electron microprobe at the Laboratoire Magmas et Volcans of the University of Blaise Pascal, Clermont-Ferrand (France). Analytical conditions included an accelerating voltage of 15 kV and a beam current of 150 nA. The theoretical basis and associated statistical treatment of data follow the analytical procedure detailed by Montel et al.(1996).

Monazites in hy-granitic rocks of the Aimores pluton yield average U-Th-Pb ages for the first sample of 470 ± 15 Ma; 502 ± 18 Ma and 552 ± 30 Ma, respectively 471 ± 24 Ma, 515 ± 24 Ma and 567 ± 50 Ma for the second one. The whole group taken together gives ages from 445 Ma to 572Ma.

U-Pb isotopic dilution analyses were carried out (Geochron Labs, United States) on separated zircon crystals from one charnockite sample. Fourteen elongated pale-rose zircons were grouped (Z2 in Fig. 3) and one single ablated crystal was analysed (Z1 in Fig. 3).

The zircon crystals are concordant, and indicate an emplacement age (lower intercept) of 498 ± 35.6 Ma.

The monazite and zircon crystals analyses could indicate an age ~500Ma for the charnockite emplacement, thus, maximum age for related pegmatites
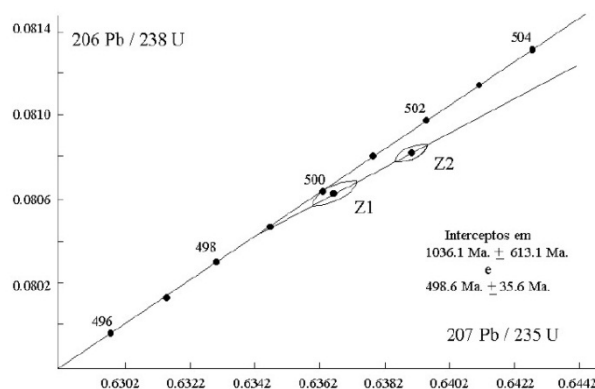
Fig. 3. Concordia diagram for hy-granitoids of Aimores Complex. Z1 represents one single zircon, Z2 a group of 14 zircons. Sample S10.

5. Conclusions

U-Pb isotopic charnockite zircon ages are the more precise. However, U-Pb-Th monazite ages obtained by electron microprobe provide similar ages and constrain these later pegmatites at about 500 Ma, which is in accordance with micas ages obtained by Viana et al. (2003).

References

Almeida F. F. M., Hasui Y., 1984. O Pré-Cambriano do Brasil. Edgar Blücher, S.Paulo, p. 282-307.

Bilal E., Correia-Neves J.M., Fuzikawa K., Horn A.H., Marciano V.R.R.O., Fernandes M.L., Moutte J., Mello F.M., Nasraoui M., 2000. Pegmatites in southeastern brazil. Revista Brasileira de Geociências, S. Paulo, v. 30, n. 2, p. 234-237,

Bilal E., A.H. Horn, H.A. Nalini, J.M. Correia-Neves, A. Giret, K. Fuzikawa, M.L.S. Fernandez, F.M. de Mello, J. Moutte, 1998. Neoproterozoic granitoid suites of Rio Doce Region, Brazil. In: International Conference on Precambrian and Craton Tectonics, Ouro Preto, Brazil, pp.41-43.

Bilal E., A.H. Horn, H.A. Nalini, J.M. Correia-Neves, A. Giret, J. Moutte, K. Fuzikawa and M.L.S. Fernandez, F.M. de Mello, 2000a. The Neoproterozoic granitoid suites in South-easthern Brazil. Special issue Revista Brasileira de Geocience, Vol 30(1), pp.51-54.

Bilal E., A.H. Horn, J. Moutte, 2000b. Zur Mineralogie und chemischen Zusammensetzung der Pegmatite in Ostbrasilien. Münchner Geol. Hefte, Vol. A28, pp. 91-97.

Bilal E., Horn H., Nalini H.A., Correia-Neves J.M., Mello F.M., 2001. Evolução magmatica das suites granitoides proterozoicos do Setor Setentrional Província Estrutural Mantiqueira, Minas Gerais, Espírito Santo, Brasil. Geonomos, VIII,(1-2), 77-86.

Bilal E., J. Cesar-Mendes, J.M. Correia-Neves, M. Nasraoui, K. Fuzikawa, 1998. Chemistry of tourmalines in some pegmatites of São José da Safira area, Minas Gerais, Brazil. Journal of the Czech Geological Society, Vol. 43/1-2, pp. 33-38.

Bilal E., J. César-Mendes, J. Correia-Neves, 1984. Os niobio-tantalatos dos pegmatitos da região de São José da Safira, Estado de Minas Gerais. In: Cong. Bras. Geol., 38, Balneário Camboriú. Bol. Res. Balneário Camboriú, SBG, vol 1, pp. 198-199.

Bilal E., H. Horn, H. Nalini jr., FM. de Mello, J.M. Correia-Neves, A. Giret, J. Moutte, K. Fuzikawa, Fernandes, 2000. The Neoproterozoic granitoid suites in Southeastern Brazil. Revista Brasileira de Geocience, 30 (1) 51-54.

Bilal E., H. Horn, V.R.O.P. Marciano, M.L. Fernandes, J.M. Correia-Neves, K. Fuzikawa, J. Moutte, FM. de Mello, M. Nasraoui, 2000. The Chemsitry of pegmatites in the southeastern Brazil. Special issue of Revista Brasileira de Geocience, 30 (1), 234-237.

César-Mendes J., E. Bilal, J.M.Correia-Neves, A. Giret, 1994. As turmalinas de pegmatitos da região de São José da Safira, Estado de Minas Gerais. In: 38th Cong. Bras. Geol., Balneário Camboriú. Bol. Res. Expand. Balneário Camboriú, SBG, Vol. 1, pp. 204-205.

Mello, F.M., 2000. Litogeoquímica e Química Mineral do Maciço Charnockítico Aimorés-MG. São Paulo: USP, 167p. unpublished Thesis. USP, São Paulo.

Mello F.M. de and Bilal, E., 2004. The perphosphorous leucogranites of the Minas Gerais state, Brazil. Romanian Journal of Mineral Deposits, Vol. 81, pp.140-143.

Montel J.M. ; Foret S., Veschambre, M., Nicollet C., Provost, A., 1996. Electron microprobe dating of monazite. Chemical Geology, 131: 37 53.

Pinto C.P., 1997. "Projeto Leste-MG. Relatorio Integrado CPRM"

Viana R.R., Manttari I., Henjes-Kunst, Jordt-Evangelista H., 2003. Age of pegmatites from eastern Brazil and implications of mica intergrowths on cooling rates and age calculations. Journal of. South. American Earth Science. 16, 493–501.

THE INFLUENCE OF H₂O₂ ON THE OXIDATIVE DISSOLUTION OF IRON SULFIDE

Cristina A. CONSTANTIN*, Mircea PREDA, Paul CHIRIȚĂ
University of Craiova, Department of Chemistry, Calea Bucuresti 107I, Craiova Romania
(cristina.a.constantin@gmail.com; mpredachim@yahoo.com; paulxchirita@gmail.com)
Tel./Fax: 0040251597048

Abstract In this study, we have analyzed the effect of hydrogen peroxide concentration on iron sulfides (FeS_2 and FeS) dissolution in acidic medium at 25ºC. The oxidative dissolution extent was evaluated by measuring the amount of released sulfate. It was found that the rate of iron sulfides dissolution increases when $[H_2O_2]$ increases. The reaction order with respect to oxidant concentration was 1.02 in the case of pyrite and 1.55 in case of FeS, respectively.

Keywords: iron sulfides, oxidative dissolution, hydrogen peroxide

1. Introduction

The dissolution of iron sulfide is of high importance in various natural (acid mine drainage and remediation of mineral wastes) or industrial processes (metal extraction). There are two important categories of natural iron sulfide: 1) iron disulfide (FeS_2) = pyrite and marcasite, and 2) iron monosulfide ($Fe_{1-x}S$) = pyrrhotite, (FeS) = troilite and ($Fe_{1+x}S$) = mackinawite.

The oxidative dissolution of iron sulfides has a serious negative impact on the environment because it produces aggressive species (protons and ferric iron) (Descostes et al., 2004; Chirita and Descostes, 2006) and releases toxic elements incorporated in minerals matrix, like heavy metals and arsenic (Thomas et al., 2001). Hydrogen peroxide is a very powerful oxidant (Chirita, 2004) that easily accepts the electrons released by iron sulfide minerals. In nature, it can appear in rain water. The oxidation of FeS_2 and, respectively, FeS by H_2O_2 in acidic media is characterized by the following over-all reactions.

$$FeS_2 + 7.5H_2O_2 = Fe^{3+}_{(aq)} + 2SO_4^{2-}_{(aq)} + H^+ + 7H_2O \qquad (1)$$
$$FeS + 4.5H_2O_2 + 2H^+ = Fe^{3+}_{(aq)} + 2SO_4^{2-}_{(aq)} + 5H_2O \qquad (2)$$
$$FeS + 0.5H_2O_2 + H^+ = Fe^{2+}_{(aq)} + S + H_2O \qquad (3)$$
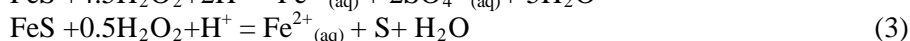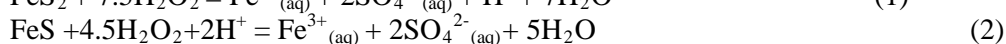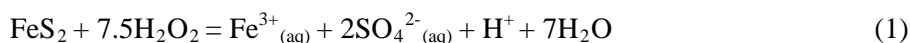
The main objective of this study was the investigation of the effect of hydrogen peroxide concentration on the oxidative dissolution of iron sulfides.

2. Materials and methods

A natural sample of iron disulfide and a synthetic sample of iron monosulfide were used in this study. X-ray diffraction (XRD) showed that the iron disulfide powder is pyrite, and iron monosulfide powder is troilite. The sample of pyrite was treated with a solution of 1 mol·L⁻¹ HNO_3 in order to produce very clean pyrite surface. The troilite powder was several times suspended in ethylic alcohol, vigorously shaked, and decanted in order to remove the fine particles adhering to the larger ones.

The hydrogen peroxide solutions were prepared by adding the necessary volume of reagent grade H_2O_2 (33%) solution to acidic solutions (pH 1.5 in the case of FeS and 2.5 in the case of FeS_2), respectively, immediately before run started. The oxidative dissolution of iron disulfides was followed by monitoring the concentration of released sulfate. Periodically, 20 mL liquid sample was taken from reaction solution with a syringe connected to a 0.4 µm filter. The amount of the dissolved sulfur was determined by turbidimetric method at 420 nm. One hand, the hydrogen peroxide concentrations was varied from 0.1 to 0.5 mol L⁻¹, and, on the other hand, solid to liquid ratio (0.2:250 g:mL) and reaction temperature (25ºC) were kept constant.
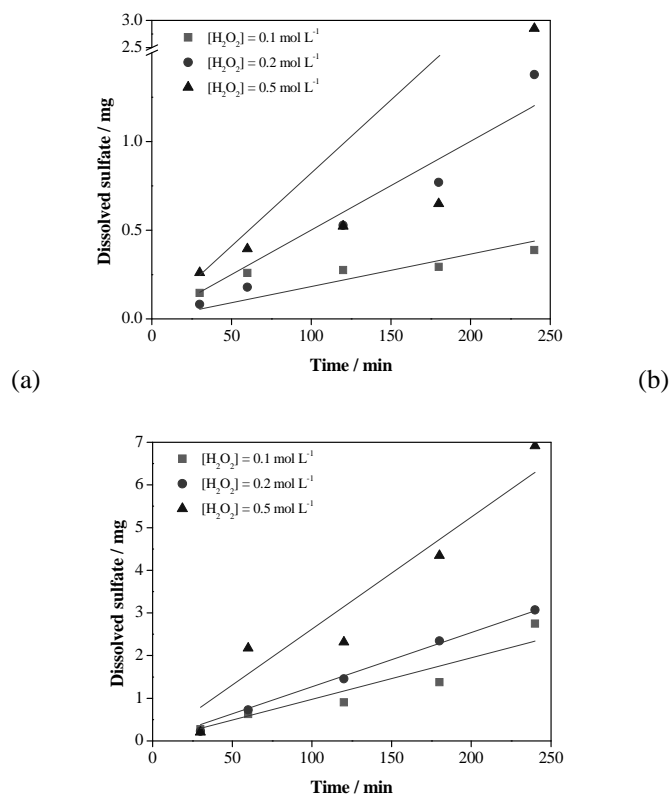
Fig. 1. Dissolution curves of a) FeS_2 and b) FeS.

The reaction orders of iron sulfides oxidative dissolution with respect to oxidant concentration ($[H_2O_2]$) were obtained from the plots of log k versus log $[H_2O_2]$ (Figure 2).
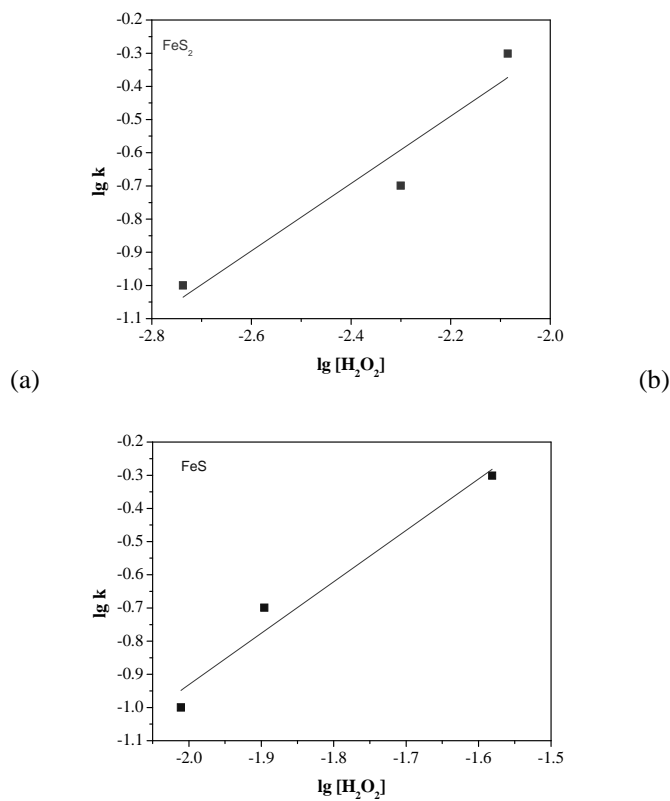

Fig. 2. The plots of log k vs log $[H_2O_2]$ for a) FeS_2 and b) FeS.

3. Results

The dissolution curves of FeS and FeS_2 are presented in Figure 1. As can be seen from this figure, the amount of dissolved sulfur increases when $[H_2O_2]$ increases from 0.1 mol L^{-1} to 0.5 mol L^{-1}. The dissolution rates (k) were determined from the slope of regression lines. The rates of FeS_2 dissolution (the rates of sulfur release from FeS_2 matrix) at initial pH 2.5 increase from 0.14 mg min^{-1} ($[H_2O_2]$=0.1 mol L^{-1}) to 0.38 mg min^{-1} ($[H_2O_2]$=0.1 mol L^{-1}). The rates of FeS dissolution (the rates of sulfur release from FeS matrix) at initial pH 1.5 increases from 0.27 mg min^{-1} ($[H_2O_2]$=0.1 mol L^{-1}) to 6.9 mg min^{-1} ($[H_2O_2]$=0.1 mol L^{-1}).

In the case of pyrite dissolution, the reaction order with respect to $[H_2O_2]$ was 1.01. The same kinetic parameter determined for FeS dissolution was 1.55. Both reaction orders indicate a strong dependence between dissolution rate and oxidant concentration. The stoichiometry of activated complex developed during minerals dissolution can be related to the corresponding reaction order. In the case of FeS the stoichiometry of activated complex is $2FeS·3H_2O_2$, and for FeS_2 it is $FeS_2·1H_2O_2$.

It must be noted that immediately after contact between FeS and H_2O_2 solution it was observed the formation of colloidal sulfur (the milky aspect of solutions). This indicates that the colloidal sulfur is an important reaction product/intermediate of FeS oxidative dissolution. This finding is in good agreement with the literature, where the elemental sulfur is reported to be the main oxidation product of FeS oxidation by dissolved oxygen and an essential reaction intermediate of FeS oxidation by hydrogen peroxide. Colloidal sulfur is formed by the rapid oxidation of H_2S with hydrogen peroxide (Eq. 4).

$$H_2O_2 + H_2S = 2H_2O + S \qquad\qquad (4)$$

H_2S is released by the action of protons on sulfide groups presents at FeS surface (Eq. 5)
.
$$FeS + 2H^+ = H_2S + Fe^{2+} \qquad\qquad (5)$$

When FeS_2 comes in contact with H_2O_2 solutions the supernatant remains clear. This fact suggests that no colloidal sulfur is produced during FeS_2 oxidation with H_2O_2. This is in good agreement with the results of the previous studies (Ciminelli and Osseo-Asare, 1995; Descostes et al., 2004) who show that the main reaction intermediate of pyrite oxidation is thiosulfate, but not elemental sulfur, and the main reaction product is sulfate.

4. Conclusions

The oxidative dissolution of iron sulfide minerals (pyrite and troilite) was investigated in the presence of H_2O_2, at 25°C and in acidic media. It was found that oxidative dissolution of both pyrite and troilite is strongly dependent by oxidant concentration. The reaction orders with respect to $[H_2O_2]$ are 1.55 for FeS oxidative dissolution and 1.01 for FeS_2 oxidative dissolution, respectively. It was observed that the colloidal sulfur is an important reaction intermediate of troilite oxidative dissolution. Instead, the formation of colloidal sulfur was not visible during the oxidative dissolution FeS_2.

References

Chirita P., 2004. Pyrite oxidation by hydrogen peroxide in phosphoric acid solutions. The European Journal of Mineral Processing and Environmental Protection, 4, 203-209

Chirita P., Descostes M., 2006. Anoxic dissolution of troilite in acidic media. Journal of Colloid and Interface Science, 294, 376–384.

Ciminelli V.S.T., Osseo-Asare K., 1995. Kinetics of pyrite oxidation in sodium hydroxide solutions. Metallurgical and Materials Transactions B., 26, 677-685.

Descostes M., Vitorge P., Beaucaire C., 2004. Pyrite dissolution in acidic media. Geochimica et Cosmochimica Acta, 68, 4559-4569.

Thomas J.E., Skinner W.M., Smart R.S.C., 2001. A mechanism to explain sudden changes in rates and products for pyrrhotite dissolution in acid solution. Geochimica et Cosmochimica Acta, 65, 1–12